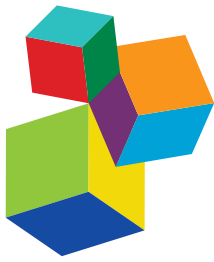


# INTER-CELLULAR ELECTRICAL SIGNALS IN PLANT ADAPTATION AND COMMUNICATION

EDITED BY: Simon Gilroy, Kazimierz Trebacz and Vicenta Salvador-Recatalà

PUBLISHED IN: Frontiers in Plant Science and Frontiers in Physiology



#### Frontiers Copyright Statement

© Copyright 2007-2018 Frontiers Media SA. All rights reserved.

All content included on this site, such as text, graphics, logos, button icons, images, video/audio clips, downloads, data compilations and software, is the property of or is licensed to Frontiers Media SA ("Frontiers") or its licensees and/or subcontractors. The copyright in the text of individual articles is the property of their respective authors, subject to a license granted to Frontiers.

The compilation of articles constituting this e-book, wherever published, as well as the compilation of all other content on this site, is the exclusive property of Frontiers. For the conditions for downloading and copying of e-books from Frontiers' website, please see the Terms for Website Use. If purchasing Frontiers e-books from other websites or sources, the conditions of the website concerned apply.

Images and graphics not forming part of user-contributed materials may not be downloaded or copied without permission.

Individual articles may be downloaded and reproduced in accordance with the principles of the CC-BY licence subject to any copyright or other notices. They may not be re-sold as an e-book.

As author or other contributor you grant a CC-BY licence to others to reproduce your articles, including any graphics and third-party materials supplied by you, in accordance with the Conditions for Website Use and subject to any copyright notices which you include in connection with your articles and materials.

All copyright, and all rights therein, are protected by national and international copyright laws.

The above represents a summary only. For the full conditions see the Conditions for Authors and the Conditions for Website Use.

ISSN 1664-8714  
ISBN 978-2-88945-521-8  
DOI 10.3389/978-2-88945-521-8

#### About Frontiers

Frontiers is more than just an open-access publisher of scholarly articles: it is a pioneering approach to the world of academia, radically improving the way scholarly research is managed. The grand vision of Frontiers is a world where all people have an equal opportunity to seek, share and generate knowledge. Frontiers provides immediate and permanent online open access to all its publications, but this alone is not enough to realize our grand goals.

#### Frontiers Journal Series

The Frontiers Journal Series is a multi-tier and interdisciplinary set of open-access, online journals, promising a paradigm shift from the current review, selection and dissemination processes in academic publishing. All Frontiers journals are driven by researchers for researchers; therefore, they constitute a service to the scholarly community. At the same time, the Frontiers Journal Series operates on a revolutionary invention, the tiered publishing system, initially addressing specific communities of scholars, and gradually climbing up to broader public understanding, thus serving the interests of the lay society, too.

#### Dedication to Quality

Each Frontiers article is a landmark of the highest quality, thanks to genuinely collaborative interactions between authors and review editors, who include some of the world's best academicians. Research must be certified by peers before entering a stream of knowledge that may eventually reach the public - and shape society; therefore, Frontiers only applies the most rigorous and unbiased reviews.

Frontiers revolutionizes research publishing by freely delivering the most outstanding research, evaluated with no bias from both the academic and social point of view. By applying the most advanced information technologies, Frontiers is catapulting scholarly publishing into a new generation.

#### What are Frontiers Research Topics?

Frontiers Research Topics are very popular trademarks of the Frontiers Journals Series: they are collections of at least ten articles, all centered on a particular subject. With their unique mix of varied contributions from Original Research to Review Articles, Frontiers Research Topics unify the most influential researchers, the latest key findings and historical advances in a hot research area! Find out more on how to host your own Frontiers Research Topic or contribute to one as an author by contacting the Frontiers Editorial Office: [researchtopics@frontiersin.org](mailto:researchtopics@frontiersin.org)

# INTER-CELLULAR ELECTRICAL SIGNALS IN PLANT ADAPTATION AND COMMUNICATION

Topic Editors:

**Simon Gilroy**, University of Wisconsin-Madison, United States

**Kazimierz Trebacz**, Maria Curie-Sklodowska University, Poland

**Vicenta Salvador-Recatalà**, Ronin Institute for Independent Scholarship, United States

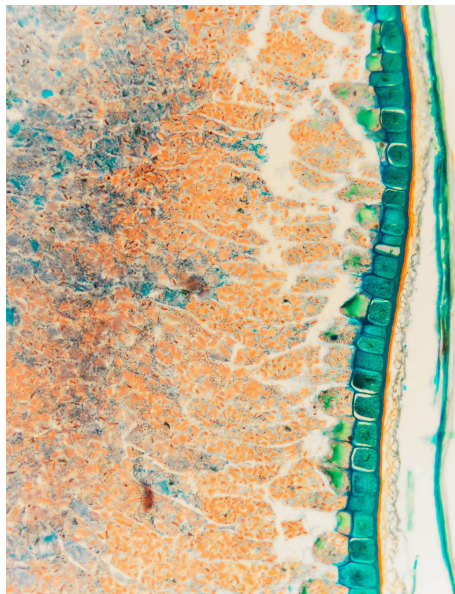


Image: Digital Photo/Shutterstock.com

Plants use the Sun's energy to synthesize the basic biomolecules that make up all the organic matter of all organisms of terrestrial ecosystems, including ourselves. Therefore, understanding their adaptive mechanisms to variations of environmental factors, both biotic and abiotic, is fundamental, and particularly relevant in the current context of rapid climate change. Some of the most important adaptive mechanisms of plants are the electrical and chemical signaling systems for the exchange of information between proximally and distally located cells. These signalling systems allow plants to dynamically coordinate the activities of all cells under a diversity of situations.

In this Research Topic, we present eight articles that bring up new hypotheses and data to understand the mechanisms of systemic electrical signaling and the central role that it plays in adapting the whole plant to different stresses, as well as new findings on intracellular calcium and nitric oxide-based signaling pathways under stress, which could be extrapolated to non-plant research.

**Citation:** Gilroy, S., Trebacz, K., Salvador-Recatalà, V., eds. (2018). Inter-cellular Electrical Signals in Plant Adaptation and Communication. Lausanne: Frontiers Media. doi: 10.3389/978-2-88945-521-8

# Table of Contents

- 05 Editorial: Inter-cellular Electrical Signals in Plant Adaptation and Communication**

Simon Gilroy, Kazimierz Trebacz, Vicenta Salvador-Recatalà

## SECTION 1

### FINE-TUNING ADAPTATION TO ENVIRONMENTAL STIMULI THROUGH ELECTRICAL SIGNALING

- 07 Expression Analysis of Sound Vibration-Regulated Genes by Touch Treatment in Arabidopsis**

Ritesh Ghosh, Mayank A. Gururani, Lakshmi N. Ponpandian, Ratnesh C. Mishra, Soo-Chul Park, Mi-Jeong Jeong and Hanhong Bae

- 20 Electrical Signaling, Photosynthesis and Systemic Acquired Acclimation**

Magdalena Szechynska-Hebda, Maria Lewandowska and Stanisław Karpiński

## SECTION 2

### PHYSIOLOGICAL RELATIONSHIPS BETWEEN DIFFERENT TYPES OF INTER-CELLULAR ELECTRICAL SIGNALS

- 34 The Integration of Electrical Signals Originating in the Root of Vascular Plants**

Javier Canales, Carlos Henriquez-Valencia and Sebastian Brauchi

- 49 Osmotic and Salt Stresses Modulate Spontaneous and Glutamate-Induced Action Potentials and Distinguish Between Growth and Circumnutation in Helianthus annuus Seedlings**

Maria Stolarz and Halina Dziubinska

## SECTION 3

### SYSTEMIC ELECTRICAL SIGNALS CONTRIBUTE TO TOLERANCE OF BIOTIC AND ABIOTIC STRESSES

- 62 Barley yellow dwarf virus Infection Leads to Higher Chemical Defense Signals and Lower Electrophysiological Reactions in Susceptible Compared to Tolerant Barley Genotypes**

Maria K. Paulmann, Grit Kunert, Matthias R. Zimmermann, Nina Theis, Anatoli Ludwig, Doreen Meichsner, Ralf Oelmüller, Jonathan Gershenzon, Antje Habekuss, Frank Ordon, Alexandra C. U. Furch and Torsten Will

- 77 High-Temperature Tolerance of Photosynthesis can be Linked to Local Electrical Responses in Leaves of Pea**

Vladimir Sukhov, Vladimir Gaspirovich, Sergey Misyagin and Vladimir Vodeneev

## SECTION 4

### NEW DATA ON CALCIUM-DEPENDENT INTRACELLULAR SIGNALING UNDER STRESS

- 92** *Calcium and Calmodulin are Involved in Nitric Oxide-Induced Adventitious Rooting of Cucumber Under Simulated Osmotic Stress*

Lijuan Niu, Jian Yu, Weibiao Liao, Jihua Yu, Meiling Zhang and Mohammed M. Dawuda

- 106** *Cytosolic and Nucleosolic Calcium Signaling in Response to Osmotic and Salt Stresses Are Independent of Each Other in Roots of Arabidopsis Seedlings*

Feifei Huang, Jin Luo, Tingting Ning, Wenhan Cao, Xi Jin, Heping Zhao, Yingdian Wang and Shengcheng Han



# Editorial: Inter-cellular Electrical Signals in Plant Adaptation and Communication

Simon Gilroy<sup>1</sup>, Kazimierz Trebacz<sup>2</sup> and Vicenta Salvador-Recatalà<sup>3\*</sup>

<sup>1</sup> Botany, University of Wisconsin-Madison, Madison, WI, United States, <sup>2</sup> Department of Biophysics, Maria Curie-Skłodowska University, Lublin, Poland, <sup>3</sup> Ronin Institute for Independent Scholarship, Montclair, NJ, United States

**Keywords:** ion channel, plant electrophysiology, plant stress, inter-cellular signaling, phloem

## Editorial on the Research Topic

### Inter-cellular Electrical Signals in Plant Adaptation and Communication

Molecular studies suggest that the transition into multi-cellularity took place ~1 billion years ago, after the fungi, animal, and plant lineages had separated (Sanderson, 2003; Peterson and Butterfield, 2005). Although the selective pressures to evolve multi-cellularity are far from understood, comparative studies of two volvocine algae, the colonial *Volvox* and the unicellular *Chlamydomonas* suggest that it was a gradual, multi-step process that involved genetic innovations. Among the first multi-cellularity genes were those that encode extracellular matrix proteins that bind cells together, since *Volvox* has them, but *Chlamydomonas* does not (Prochnik et al., 2010). The increase in cell number and cell types would not have been possible without additional genetic innovations that made it possible for the thousands, millions, and even billions of cells that compose these multicellular organisms to coordinate their activities and cooperate to produce responses to environmental stimuli.

One of the most successful mechanisms to coordinate the activities of distally located cells, tissues, and organs is the electrical impulse, which was first studied in frogs in the 1790s by Galvani and Volta (Galvani, 1791; Pera, 1992). Similar, yet slower electrical impulses were also described in plants a century later by (Burdon Sanderson, 1873), although their relevance was not recognized immediately, being regarded as an anecdotal feature limited to a few exotic species. It is now accepted that most, if not all, plants routinely use electrical and chemical signals that quickly bring into communication distally located cells, yet most aspects of these signals' underlying mechanisms still remain mysterious. With the purpose of promoting this under-researched area of biology and fostering a dialogue between the different perspectives from which it is studied, we invited a diversity of scientists who work on molecular, cellular, and systemic aspects of inter-cellular signals, to contribute their work to this Research Topic. The result is this volume, which contains a diversity of review and original research articles that bring new ideas and elements for reflection, and expand the state-of-the-art of inter-cellular electrical and chemical phenomena, from the ion channel (Ghosh et al.), to the cellular scale (Huang et al.; Niu et al.), and systemic perspectives (Stolarz and Dziubinska; Paulmann et al.).

The review by Szechynska-Hebda et al. set forth an interesting hypothesis to explain the propagation of light-induced systemic electrical signals that involves cellular structures in chloroplasts named "stromules." Stromules are membrane extensions that connect different chloroplasts, and are proposed to operate as electrical platforms that allow the propagation of these light-related signals. Also in this review, the authors discuss a crosstalk between electrical signaling, as well as calcium and ROS waves, phytohormones, gene expression, and pressure changes in the xylem. In addition, they discuss the genetic basis of the electrophysiological responses to plant

## OPEN ACCESS

### Edited and reviewed by:

John Hancock,  
University of the West of England,  
United Kingdom

### \*Correspondence:

Vicenta Salvador-Recatalà  
vicenta.salvador@ronininstitute.org

### Specialty section:

This article was submitted to  
Plant Physiology,  
a section of the journal  
Frontiers in Plant Science

**Received:** 19 March 2018

**Accepted:** 26 April 2018

**Published:** 15 May 2018

### Citation:

Gilroy S, Trebacz K and  
Salvador-Recatalà V (2018) Editorial:  
Inter-cellular Electrical Signals in Plant  
Adaptation and Communication.  
*Front. Plant Sci.* 9:643.  
doi: 10.3389/fpls.2018.00643

illumination, focusing on genes that encode ion channels and membrane transporters that are behind these responses.

A hypothesis and theory article by Brauchi and collaborators also emphasize the genetic bases plant electrophysiological phenomena, in this case of the inter-cellular signals between different cell types, specifically between vascular and non-vascular cells (Canales et al.). Interestingly, *in-silico* analyses of tissue-specific expression of various ion channels have led them to suggest that long- and short-distance systemic electrical signals use different cellular routes. Further, they propose a working model for understanding the cellular pathways and mechanisms by which electrical signals travel from the stimulated peripheral areas to the input region of the phloem, and from the phloem to peripheral cells in effector tissues, one that requires the participation of both the apoplast and plasmodesmata.

Niu et al. demonstrate the involvement of nitric oxide (NO), Ca<sup>2+</sup> and calmodulin (CaM) in adventitious root formation, which is an important aspect of plant strategy to alleviate osmotic stress. They propose a complex molecular mechanism that involves sequenced activation of NO, Ca<sup>2+</sup>/CaM signaling pathways leading to protection of the photosynthetic apparatus and stimulation of the antioxidant defense system. In another study that also focuses on Ca<sup>2+</sup> signaling pathways, Huang et al. ask how subcellular compartmentation of the Ca<sup>2+</sup> signal may play a role in imposing specificity on signaling response systems. By targeting a heterologously expressed Ca<sup>2+</sup> binding protein to buffer Ca<sup>2+</sup> changes in specific subcellular locales, they show that nuclear and cytosolic Ca<sup>2+</sup> changes are independently regulated. However, when assaying downstream events such as alterations in gene expression, changes in both compartments are shown to be required for the complex coordinated responses to osmotic and salt stresses.

Here, Stolarz and Dziubinska bring new light into the classical problem of the sunflower's circumnutation movement, a phenomenon driven by ion and water fluxes, with a study

that clarifies the connections between action and spontaneous potentials and glutamate-induced potentials. A different study by Paulmann et al. shows an indirect yet relevant contribution of the phloem's role as an electrical signaling network to determine the susceptibility of barley to viral infection. By altering the phloem's anatomy, the virus blocks the electrical message that would alert of its presence.

Two research articles show new findings that underscore an unsuspected degree of sophistication of the plant electrical responses to environmental stimuli. On one hand, in their report of a new, protective role of local electrophysiological responses over the photosynthetic process under high temperature stress, Sukhov et al. show significant electrophysiological responses of pea leaves to increases of only 1°C above the background temperature. On the other hand, Ghosh et al. show that plants can consistently distinguish between touch and sound vibration. Both research articles support the notion that plants are much more sensitive to external stimuli than previously thought, and respond to these with strong and finely tuned responses. In the first case (Sukhov et al.), in the form of variation potentials that propagate between cells; in the second case (Ghosh et al.), by increasing or decreasing the expression of similar yet distinct mechanosensitive ion channels.

All together, the articles included in this Research Topic bring new theory and data to this exciting research area that hopefully will spark future studies that help us to understand how these rapid communication systems aid plants in overcoming their lack of mobility in the complex, dynamic, and often hostile environments in which they thrive.

## AUTHOR CONTRIBUTIONS

All authors listed have made a substantial, direct and intellectual contribution to the work, and approved it for publication.

## REFERENCES

- Burdon Sanderson, J. S. (1873). Note on the electrical phenomena which accompany stimulation of the leaf of *Dionaea muscipula*. *Proc. R. Soc.* 21, 495–496.
- Galvani, L. (1791). *De viribus Electricitatis*. The International Centre for the History of Universities and Science (CIS), Università di Bologna.
- Pera, M. (1992). *The Ambiguous Frog: The Galvani–Volta Controversy on Animal Electricity*. Oxford: Princeton University Press.
- Peterson, K. J., and Butterfield, N. J. (2005). Origin of the Eumetazoa: testing ecological predictions of molecular clocks against the Proterozoic fossil record. *Proc. Natl. Acad. Sci. U.S.A.* 102, 9547–9552. doi: 10.1073/pnas.0503660102
- Prochnik, S. E., Umen, J., Nedelcu, A. M., Hallman, A., Miller, S. M., Nishii, I., et al. (2010). Genomic analysis of organismal complexity in the multicellular green alga *Volvox carteri*. *Science* 329, 223–226. doi: 10.1126/science.1188800

Sanderson, M. J. (2003). Molecular data from 27 proteins do not support a Precambrian origin of land plants. *Am. J. Bot.* 90, 954–956. doi: 10.3732/ajb.90.6.954

**Conflict of Interest Statement:** The authors declare that the research was conducted in the absence of any commercial or financial relationships that could be construed as a potential conflict of interest.

Copyright © 2018 Gilroy, Trebacz and Salvador-Recatalà. This is an open-access article distributed under the terms of the Creative Commons Attribution License (CC BY). The use, distribution or reproduction in other forums is permitted, provided the original author(s) and the copyright owner are credited and that the original publication in this journal is cited, in accordance with accepted academic practice. No use, distribution or reproduction is permitted which does not comply with these terms.



# Expression Analysis of Sound Vibration-Regulated Genes by Touch Treatment in *Arabidopsis*

Ritesh Ghosh<sup>1</sup>, Mayank A. Gururani<sup>2</sup>, Lakshmi N. Ponpandian<sup>1</sup>, Ratnesh C. Mishra<sup>1</sup>, Soo-Chul Park<sup>3</sup>, Mi-Jeong Jeong<sup>3</sup> and Hanhong Bae<sup>1\*</sup>

<sup>1</sup> Department of Biotechnology, Yeungnam University, Gyeongsan, South Korea, <sup>2</sup> Department of Biology, College of Science, United Arab Emirates University, Al Ain, United Arab Emirates, <sup>3</sup> National Institute of Agricultural Sciences, Rural Development Administration, Wanju, South Korea

## OPEN ACCESS

### Edited by:

Vicenta Salvador Recatala,  
Ronin Institute, USA

### Reviewed by:

Heidi M. Appel,  
University of Missouri, USA

Elizabeth Haswell,  
Washington University in Saint Louis,  
USA

### \*Correspondence:

Hanhong Bae  
hanhongbae@ynu.ac.kr

### Specialty section:

This article was submitted to  
Plant Physiology,  
a section of the journal  
*Frontiers in Plant Science*

Received: 14 October 2016

Accepted: 18 January 2017

Published: 31 January 2017

### Citation:

Ghosh R, Gururani MA,  
Ponpandian LN, Mishra RC,  
Park S-C, Jeong M-J and Bae H  
(2017) Expression Analysis of Sound  
Vibration-Regulated Genes by Touch  
Treatment in *Arabidopsis*.  
*Front. Plant Sci.* 8:100.  
doi: 10.3389/fpls.2017.00100

Sound vibration (SV) is considered to be a mechanical stimulus which gives rise to various physiological and molecular changes in plants. Previously, we identified 17 SV-regulated genes (SRGs) which were up-regulated by SV treatments in *Arabidopsis*. Here, we analyzed the expression pattern of similar genes after an exposure of 500 Hertz at 80 decibels, for various time periods. Simultaneously, we confirmed the SV-mediated expression of these genes under lighted condition as many of them were reported to be dark-induced. For this, we designed an improved SV treatment chamber. Additionally, we checked the electrolyte leakage (EL), photosynthetic performance and expression of mechanosensitive (MS) ion channel genes after 5 days of SV treatment in the illuminated chamber. EL was higher, and the photosynthetic performance index was lower in the SV-treated plants compared to control. Seven out of the 13 MS ion channel genes were differentially expressed after the SV treatment. Simultaneously, we checked the touch-mediated expression pattern of 17 SRGs and 13 MS ion channel genes. The distinct expression pattern of 6 SRGs and 1 MS ion channel gene generate an idea that SV as a stimulus is different from touch. Developmental stage-specific expression profiling suggested that the majority of the SRGs were expressed spatiotemporally in different developmental stages of *Arabidopsis*, especially in imbibed seed, seedlings and leaves.

**Keywords:** sound vibration, touch, mechano-stimulus, MS ion channel, electrolyte leakage, photosynthesis

## INTRODUCTION

Sound vibration (SV) is considered to be a mechanical stimulus which can create the thigmomorphogenetic response in plants (Telewski, 2006). Available evidences suggest that the interaction between SV and plants is relevant both in ecological as well as environmental context. For instance, the phenomenon of 'Buzz Pollination' has been noted in number of plant species which indicates the ecological relevance of SV. Buzz-pollinated plants release pollen from anthers only at a particular frequency produced by bee's buzz (De Luca and Vallejo-Marin, 2013). Similarly, plants' responsiveness to environmental sound has been shown recently. Pretreatment with vibrations caused by chewing sound of caterpillar has been noted to elicit plant defense against herbivore (Appel and Croft, 2014). This advocates the relevance of natural SV in plants' defense. In addition, several other plausible environmental significance of SV has been discussed by Mishra et al. (2016). Taken together, it is amply clear that like other physical factors SV is ecologically and/or environmentally significant to plants.

Experimentally, previous studies have shown the various effects of synthetic single frequency SV on plants (Hassanien et al., 2014). SV has the ability to alter antioxidant activities, calcium flux, sugar and ATP contents, hormonal modulation and plasmalemma architecture in plants (Mishra et al., 2016). SV-induced antioxidant (like- catalase, superoxide dismutase, and ascorbate peroxidase) activity was noted in chrysanthemum seedlings and hazel cells (Xiujuan et al., 2003; Safari et al., 2013). Increased ATP content in the SV-treated *Actinidia chinensis* callus suggests that SV can alter the energy metabolism (Xiaocheng et al., 2003). SV-induced changes in levels of phytohormones (like- auxin, cytokinin, and salicylic acid) were previously reported in *Arabidopsis* plant, *Chrysanthemum* callus, and protocorm-like bodies of *Dendrobium* (Bochu et al., 2004; Wei et al., 2012; Ghosh et al., 2016). Besides that, beneficial effects of SV were noted in terms of disease resistance, crop yield, callus regeneration and plant growth (Hassanien et al., 2014). A growing body of recent evidence suggests the existence of sophisticated molecular mechanisms for SV perception and signal transduction in plants. Despite this, however, there exists a huge gap in our understanding regarding the SV-mediated molecular alterations in the cellular milieu, which is a prerequisite to gain insight into SV-mediated plant development. Necessitated by this, we had previously investigated the global transcriptomic and proteomic changes in *Arabidopsis thaliana* upon treatment with SV of five different frequencies (250, 500, 1000, 2000, 3000 Hz) with constant amplitude to bridge this gap (Ghosh et al., 2016). Several genes were noted to be differentially expressed after SV treatment, and it was noted that 500 Hz for 1 h has maximum impact on cellular processes in *Arabidopsis*. Additionally, 17 genes were further confirmed by real-time PCR analysis, which are termed as SV-regulated genes (SRGs).

Another well-known mechanical stimulus which alters the physiology of plants at various levels is touch. Touch-mediated growth retardation, calcium spiking, reactive oxygen species generation, hormonal modulation and gene expression were previously reported (Braam, 2005; Chehab et al., 2011). It has been demonstrated that repetitive touch treatment can prime plants, which subsequently alter the plant defense against fungal pathogen and herbivore (Chehab et al., 2012). Previously, we hypothesized that SV and touch share some common mechanosensitive (MS) signaling events, as many of the touch-regulated genes were induced by SV (Ghosh et al., 2016). Therefore, it was concluded that touch-mediated expression profiling of SRGs is necessary to strengthen this idea. In the present study, we investigated the expression of SRGs after the touch treatment. Simultaneously, we checked the expression pattern of similar genes after exposure of 500 Hz for various time periods, and investigated their transcript levels in various developmental stages. Additionally, we have designed an improved SV treatment chamber, and cross-confirmed the SV-mediated expression of SRGs in lighted conditions. Simultaneously, this chamber was used to investigate the effect of long-term SV treatment on physiological responses like electrolyte leakage (EL) and photosynthesis.

It was hypothesized that plant MS ion channels have important roles in mechanical stress perception and signaling

(Monshausen and Haswell, 2013; Mishra et al., 2016). In plants, broadly, three major groups of MS ion channels were reported: MS channel of small conductance-like (MSL), Mid1-complementing activity family (MCA) and Piezo (Monshausen and Haswell, 2013). MSLs in *Arabidopsis* are homologous to *Escherichia coli* MS channel of small conductance (MscS) protein which provides the rapid release of osmolytes from cells in response to the increased membrane tension. MCA and Piezo belong to the putative stretch-activated  $\text{Ca}^{2+}$ -permeable channels. Various electrophysiological, pharmacological and molecular-genetic analyses identified the importance of MSL9, MSL 10 and MCA1 for mechanosensitive activity in *Arabidopsis* (Nakagawa et al., 2007; Haswell et al., 2008). Additionally, the functions of MSLs in various biological processes, like-chloroplast shaping, cell death signaling, and pollen germination, were previously reported (Haswell and Meyerowitz, 2006; Veley et al., 2014; Hamilton et al., 2015). Here, we investigated the expression level of MS ion channels after 5 days of continuous SV treatment. Simultaneously, we checked the transcript levels of these MS channel genes after repetitive touch treatments for 5 days.

In summary, we investigated the expression of 17 SRGs and 13 MS-ion channel genes after SV and touch treatments. Simultaneously, we have checked the developmental stage-specific expression pattern of 17 SRGs. In addition, EL and photosynthetic performance were analyzed to check the SV-mediated physiological response after the long exposure.

## MATERIALS AND METHODS

### Plant Materials and Growth Condition

*Arabidopsis thaliana* (Col-0 ecotype) seeds were placed in pots containing artificial soil (Punong, Korea) and stratified for 2 days in the dark at 4°C for homogenous germination. Subsequently, pots were transferred to the growth room and seedlings were allowed to grow under continuous light ( $\sim 150 \pm 10 \mu\text{mol m}^{-2} \text{s}^{-1}$ ) at  $22 \pm 1^\circ\text{C}$ . The growing seedlings received supplements with nutrients (Bio-nex, Korea) mixed in water at every 3-day interval.

### SV Treatment under Dark Conditions

Twenty-day-old *Arabidopsis* plants were transferred to a sound-proof chamber and subjected to 500 Hz at 80 dB (adjusted manually) for four different time periods (10, 30 m, 1 and 2 h) including the 1 h treatment as analyzed previously (Ghosh et al., 2016). A 1 h treatment was included for further confirming the stringency of our results. Control plants were kept in a similar chamber without SV treatment. The sound-proof chamber was customized by Korea Scientific Technique Industry (Korea) according to Jeong et al. (2008). This sound-proof chamber was not equipped with a light source and temperature controller. Sound intensity of the growth room, as recorded by a sound intensity meter TES-1350A (Pusung, Korea), was noted to be  $75 \pm 2$  dB. The sound intensity within the chamber was recorded to be 40 dB. The Adobe Audition version 3.0 software (USA) was used for generation of single frequency sound. After the

SV treatment, rosette samples were harvested for quantitative real-time PCR (qRT-PCR) analysis.

## SV Treatment under Lighted Condition

Thirteen-day-old plants were covered with a transparent plastic dome to protect them from mechanical perturbation caused by direct air flow within the plant growth chamber. Two sides of the dome were cut manually to make a big hole, and placed perpendicularly to the air flow channel. Additionally, eight small holes were made on the top of the dome for gentle aeration. Plants covered by the dome were placed on a thick sponge cushion within the chamber to reduce the effect of mechanical vibration of the compressor. This set-up was maintained for 2 days under continuous light ( $\sim 150 \pm 10 \mu\text{mol m}^{-2} \text{s}^{-1}$ ) at  $22 \pm 1^\circ\text{C}$  within the growth chamber for the plants to get acclimatized. The plant growth chamber was equipped with a speaker (Sammi, Korea) and provision for watering from outside. A schematic diagram of this specialized plant growth chamber has been shown in Supplementary Figure S1. After the acclimatization, 1 h SV treatment (500 Hz,  $100 \pm 1 \text{ dB}$ ) was given under continuous illumination. The intensity of background noise within the chamber was  $82 \pm 2 \text{ dB}$ . Control plants were acclimatized under similar condition without SV treatment. For long-term SV treatment, 15-day-old plants were transferred to this specialized plant growth chamber and treated continuously for 5 days. Plants were regularly watered upto 18 days. After 5 days, rosette leaves from 20-day-old SV-treated plants were harvested and used for the expression analysis of MS ion channel genes, EL and photosynthesis. Two independent experiments were performed by swapping the chambers between control and treatment (indicated as set 1 and 2 in the figures) to normalize the chamber effects and add more precision in our data. For a better representation of treatment method, a schematic diagram has been shown in **Figure 1**.

## Touch-Mediated Expression Profiling of SRGs and MS Ion Channel Genes

Gentle touch treatment was given to the 18-day-old plants in the growth room, as mentioned previously (Lee et al., 2005); 3–4 mature rosette leaves per plant were gently bent back and forth (four times) manually, and the samples (all touched and untouched leaves in a rosette) were harvested at 5, 15, 30 m and 1 h after the touch treatments. The control sample was harvested before the touch treatments. For long-term treatments, the 15-day-old plants were repeatedly touched (twice per day at 10 h interval) for 5 days. After 5 days, rosette leaves (both touched and untouched) from 20-day-old touch-treated plants were harvested and used for the expression analysis of MS ion channel genes. At the same time, 20-day-old untouched plants were harvested as control sample. Two independent experiments with long-term touch treatments were performed and results for both have been shown (indicated as set 1 and 2 in the figures).

## Developmental Stage-Specific Samples Collection

Rosette leaves (two types, young and mature), cauline leaves, young flowers (green and unopened buds) and mature flowers (white and fully opened), were harvested from 23-day-old plants. Samples from four different developmental stages (root, stem, young green pods and matured green pods) were harvested from 35-day-old plants. Ripening pods (fully developed and yellowish green in color) were collected from 38-day-old plants. Fifty to 100 seeds were washed twice, followed by soaking in water, and kept at  $4^\circ\text{C}$  for 2 days in dark. Imbibed seeds were subsequently transferred to the growth room under light for 10 h before harvesting. For the seedling sample, seeds were surface-sterilized and placed on plates containing 1 × Murashige and Skoog (MS) salts and 0.4% phytagel (Sigma, USA), pH5.8. Subsequently,

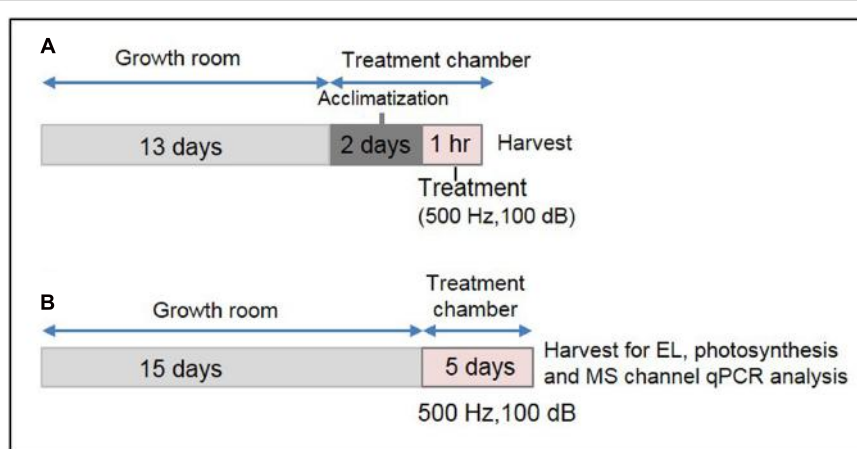


**FIGURE 1 | Experimental set-up for SV treatment under lighted condition and the sample harvest strategy. (A)** Schematic representation of 1 h SV treatment. Thirteen-day-old plants were acclimatized in the specialized plant growth chamber. Five-hundred hertz (Hz) was applied to *Arabidopsis* for 1 h with 100 decibel (dB) sound intensity. Two separate experiments were carried out with chamber swapping and whole experiment was carried under continuous light condition. **(B)** Schematic representation of SV treatment for continuous 5 days. Fifteen-day-old plants were exposed to 500 Hz at 100 dB. After 5 days samples were harvested for electrolyte leakage (EL), photosynthetic parameter and MS ion channel qRT-PCR analyses.

plates were kept at 4°C for 2 days in dark before transferring them to the growth room. Seeds were allowed to germinate, and 5-day-old seedlings were harvested.

## Quantitative Real-Time PCR (qRT-PCR) Analysis

Total RNA from an *Arabidopsis* rosette was extracted with the RNeasy Plant Mini kit (Qiagen, USA) and treated with DNase I (Qiagen) according to the manufacturer's instruction. cDNA was prepared with 1 µg RNA, using GoScript Reverse Transcription system (Promega, USA), as per manufacturer's instructions. cDNA was diluted 10-fold before using as a template for qRT-PCR analysis. qRT-PCR was performed using Mx3000P qPCR system (Agilent, USA) and LF Taq qPCR SYBR Mix (LPS Solution, Korea). Primer details of SRGs are available in Ghosh et al. (2016). Primer details of MS ion channels are available in Supplementary Table S1. At1g13440 (*GAPDH*) gene encoding glyceraldehyde-3-phosphate dehydrogenase was used as an internal control. We noticed the low coefficient of variation of *GAPDH* across SV treatments with various Hz at constant amplitude (Supplementary Table S2), which indicates relatively stable expression levels. Furthermore, Duncan's multiple range test also indicated that there was no significant difference between  $C_T$  values of *GAPDH* in different Hz treatment at  $P$ -value 0.05.  $C_T$  values for all genes of interest ( $C_{T.GOI}$ ) were normalized to the  $C_T$  values of *GAPDH* ( $C_{T.GAPDH}$ ) for each replication [ $\Delta C_T = (C_{T.GOI}) - (C_{T.GAPDH})$ ] as suggested previously (Schmittgen and Livak, 2008). Relative transcript levels of each gene were calculated with respect to *GAPDH* (% relative expression to *GAPDH*) using  $2^{-\Delta C_T}$  value [ $2^{-\Delta C_T} \times 100$ ] and plotted in the graph (Schmittgen and Livak, 2008). To isolate RNA from other developmental stages, a similar protocol was followed. RNA from imbibed seeds was isolated using the cetyltrimethylammonium bromide (CTAB) method as mentioned previously (Ghosh et al., 2012). Mean values and standard errors were obtained from four biological replicates.

## Measurement of Relative EL

Relative EL was measured as previously described by Cao et al. (2007), with slight modifications. Three to five matured rosette leaves per plants were cut, weighed ( $\sim 0.1$  g) and washed with deionized water. Cut leaves were fully submerged in 20 ml of deionized water and shaken gently in a shaker incubator for 6 h (at 23°C, 140 rpm). Subsequently, the electrical conductivity (C1) was measured by a conductivity meter (Cond 3110, Incli.Teta Con@ 325, 2CA101, Germany). Later, the samples were boiled for 15 m in a water bath, following which the samples were allowed to cool to normal temperature. Conductivity was measured again for the second time (C2). Finally, relative EL was calculated using C1/C2.

## Measurement of Photosynthetic Parameters

Photosynthetic parameters were measured as previously described by Gururani et al. (2015). The maximum quantum

of yield of photosystem II photochemistry ( $F_v/F_m$ ) and performance index (PI) were measured using a Pocket PEA chlorophyll fluorometer (Hansatech, UK) in darkness-adapted plants. Furthermore, the chlorophyll-a fluorescence transients recorded in the darkness-adapted control and SV-treated *Arabidopsis* plants were analyzed by the so-called JIP-test (Strasser and Tsimilli-Michael, 2001) to study their structural and functional parameters that indirectly quantify the photosynthetic behavior of the experimental plants. The data are represented in the form of a radar plot which exhibits the calculated average values of the photosynthetic parameters of the control and SV-treated *Arabidopsis* plants. The measurements were taken with 5–7 matured rosette leaves per plants, and the average and standard error of means were calculated from 12 individual plants.

## RESULTS

### Expression Pattern of SRGs after SV Treatment for Various Time Periods

*Arabidopsis* plants were treated with 500 Hz SV for four different time periods: 10, 30 m, 1 and 2 h. Plants were exposed to SV under darkness in a specialized sound-proof chamber, and control plants were kept in a similar chamber without SV. Broadly, the SRGs were down-regulated after short exposures (10 and 30 m), and up-regulated after long exposures (1 and 2 h) of SV (Figure 2). The overall expression pattern was bell-shaped: started with low expression at 10 m, followed by highest expression at 30 m or 1 h, and reduced again at 2 h. On the basis of the up-regulation pattern, we can categorize genes into two groups: (1) genes which were up-regulated either at 1 or 2 h (*CML38*, *TPS8*, *BT5*, *RZPF34*, *LHCB2*, *At3g07350*, *At2g44500* and *At2g20670*), and (2) the ones which were up-regulated at both time points (*CYP76C6*, *MPK11*, *MYB77*, *RAV1*, *KMD1*, *DREB26*, *HSPRO2*, *At1g76600* and *At1g25400*).

### Cross-Confirmation of SV-Regulated Genes' Expression under Light Condition

Darkness-mediated up-regulation of 14 out of 17 genes was noted previously (Lee et al., 2005), which is summarized in Supplementary Table S3. Cross-talk between light/dark transition and SV treatment could be the reason for initial down-regulation (at 10 and 30 m) of SRGs (Figure 2). Therefore it was necessary to confirm SRGs' expression under lighted condition. For this purpose, plants were exposed to 500 Hz for 1 h under lighted condition in a specialized plant growth chamber (Figure 1A). Similarly, to reduce the effect of movement of plants from growth room to chamber, we acclimatized the plants in the chamber for 2 days prior to SV exposure (Figure 1A). Experiments under lighted condition also confirmed the SV-mediated induction of these genes (Figure 3). Besides that, repeating the experiments with chamber-swapping conditions (marked as set 1 and 2) also confirmed the reproducibility of the set-up for future research.

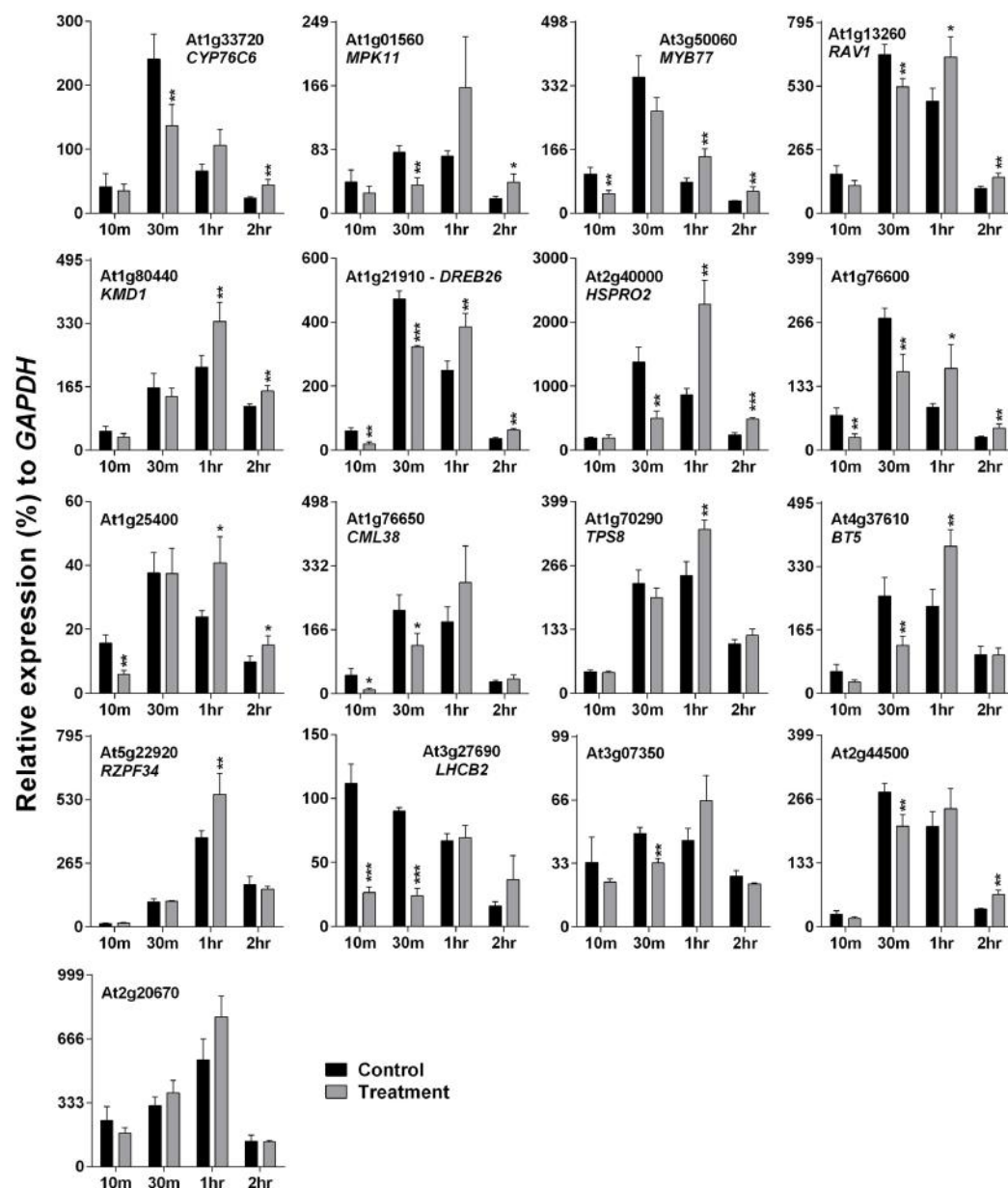


**FIGURE 2 | Quantitative real-time PCR analysis of SV-regulated genes after exposure to 500 Hz for various time periods.** Expression of each gene in the *Arabidopsis* exposed to SV (gray) was compared with control (black). The time (10, 30 m, 1 and 2 h) indicates the duration of SV exposure in the sound-proof chamber. Intensity of the 500 Hz SV was manually set to 80 dB. Error bar indicates the standard error of means from four biological replications. *P*-value ranges are marked by asterisks: \*\*\**P* < 0.01, \*\*0.01 < *P* < 0.05, \**P* < 0.1.

## Touch-Mediated Expression Profiling of SRGs

Previously, it was hypothesized that SV and touch share some common mechanosensitive (MS) signaling events (Ghosh et al., 2016). Therefore, touch-mediated expression profiling of SRGs is necessary to elucidate their similarities and/or dissimilarities at the molecular level. Touch treatment resulted in up- and down-regulation of 11 and 4 genes, respectively, out of the 17 SRGs (Figure 4). On the basis of the expression pattern,

we categorized these genes into four distinct groups: (1) genes that were highly up-regulated at 15 m (eight in no; *At1g76600*, *DREB26*, *HSPRO2*, *BT5*, *MYB77*, *At1g25400*, *At2g44500* and *RAV1*), (2) those which were down-regulated at 5 m and 1 h, but up-regulated at other time points (*CML38*, *CYP76C6* and *MPK11*), (3) the ones down-regulated at each time point (*At3g07350*, *At2g20670*, *KMD1* and *RZPF34*), and (4) genes without any specific trend, but down-regulated at some time points (*TPS8* and *LHC2*).

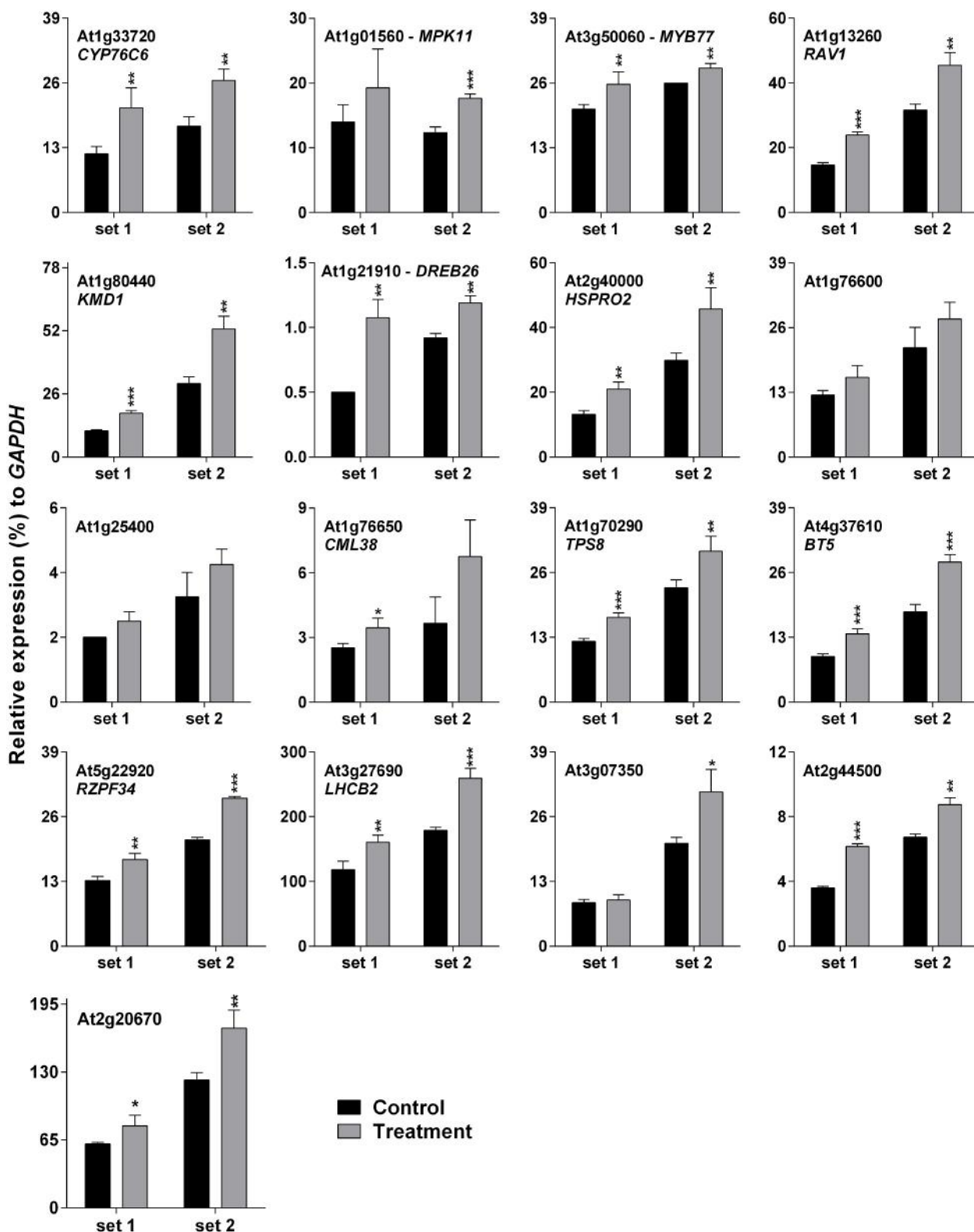


**FIGURE 3 | Quantitative real-time PCR analysis of SV-regulated genes under lighted condition.** Expression of each gene in the *Arabidopsis* exposed to a 500 Hz SV for 1 h (gray) was compared with control (black). Intensity of the 500 Hz SV was 100 dB. Set 1 and 2 indicate the two independent experiments with chamber swapping between control and treatment. Error bar indicates the standard error of means from four biological replications. *P*-value ranges are marked by asterisks: \*\*\**P* < 0.01, \*\*0.01 < *P* < 0.05, \**P* < 0.1.

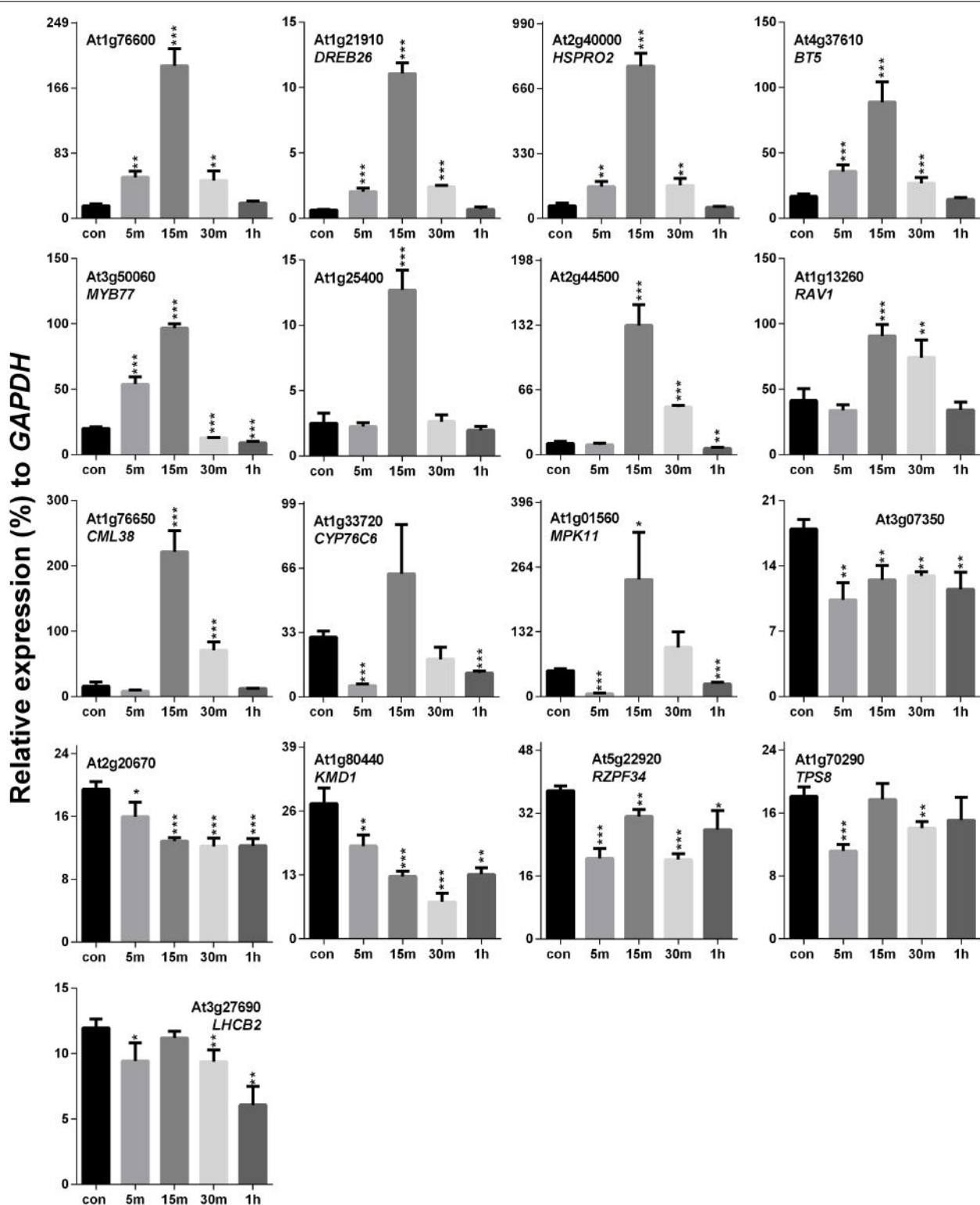


**FIGURE 4 | Quantitative real-time PCR analysis of SV-regulated genes after touch treatment.** The time (5, 15, 30 m and 1 h) indicates sample harvesting time after touch treatment. The control sample (black) was harvested before the touch treatment. Error bar indicates the standard error of means from four biological replications.  $P$ -value ranges are marked by asterisks: \*\*\* $P < 0.01$ , \*\* $0.01 < P < 0.05$ , \* $P < 0.1$ .

## Developmental Stage-Specific Expression Pattern of SRGs

Thirteen different samples were analyzed by qRT-PCR, which are as follows: root, stem, leaves (four types; caudine, young, mature, and senescence), flowers (two types; young and mature), pods (three types; young, mature, and ripening), imbibed seeds and seedlings (Supplementary Figure S2; Supplementary Table S4). On the basis of high expression pattern, we categorized these genes broadly into four groups: (1) genes that were restricted in one developmental stage (*MYB77* in imbibed seed and *At3g07350* in seedlings), (2) genes that were restricted in one tissue type (*LHCB2* and *CYP76C6* in leaves), (3) highly expressed genes in two to three developmental stages (*CML38*, *HSPRO2* in imbibed seeds and senescent leaves; *KMD1* in seedlings and senescent leaves; *At2g20670*, *DREB26* in seedlings and leaves; *At1g25400* in young and senescent leaves; *TPS8* in imbibed seeds, seedlings and senescent leaves; *At1g76600* in imbibed seeds, mature leaves and senescent leaves) and (4) highly expressed genes in more than three developmental stages (*At2g44500*, *RZPF34*, *MPK11*, *RAV1*, and *BT5*). However, statistically highest expression of some genes from group 2 to 4 were observed in the following developmental stages: imbibed seeds (*CML38*, *HSPRO2* and *TPS8*), seedlings (*KMD1*, *At2g20670*, *DREB26*, *RZPF34*, and *BT5*), young leaves (*CYP76C6*, *LHCB2*, *DREB26* and *RAV1*) and senescent leaves (*At1g25400*, *At1g76600*, and *MPK11*).

## Assessment of Changes in EL and Photosynthetic Machinery in the SV-Treated Plants

Electrolyte leakage and photosynthetic parameters were analyzed to check the SV-mediated physiological response after 5 days of long exposure. EL is a measurement for the ionic loss through the plasma membrane caused by external stimuli (Cao et al., 2007). Higher EL was observed after 5 days of SV treatment compared to control (Figure 5A). Simultaneously, two photosynthetic parameters were measured: (i) *Fv/Fm*, which indicates the quantum efficiency of photosystem II and (ii) PI, which shows the PI for energy conservation from excitation to the reduction of PSI end acceptors. PI was significantly reduced after 5 days of SV treatment compared to control, though no significant change was observed in *Fv/Fm* (Figure 5B). The comparative diurnal behavior of nine critical biophysical PS II characteristics in control and SV-treated plants is presented as a radar plot in Figure 5C. All data were normalized to the reference (control plants) and each variable at reference was standardized by giving it a numeric value of 1. All variables were deduced from the JIP-test analysis. Any deviation in these parameters relative to their control values represents a change in the PSII efficiency and it has been used earlier in numerous studies (Smit et al., 2009; Gururani et al., 2015). The parameter ABS/RC indicates the total absorption of PSII antenna chlorophylls per active reactive center (RC), while ET<sub>0</sub>/RC reflects the transport of electrons to the photosynthetic electron transport chain per active PSII-RC. The trapping of an excited photon by the RCs leads to the reduction of quinone, and since at time zero, the RCs are considered open, the maximal trapping of excited photons

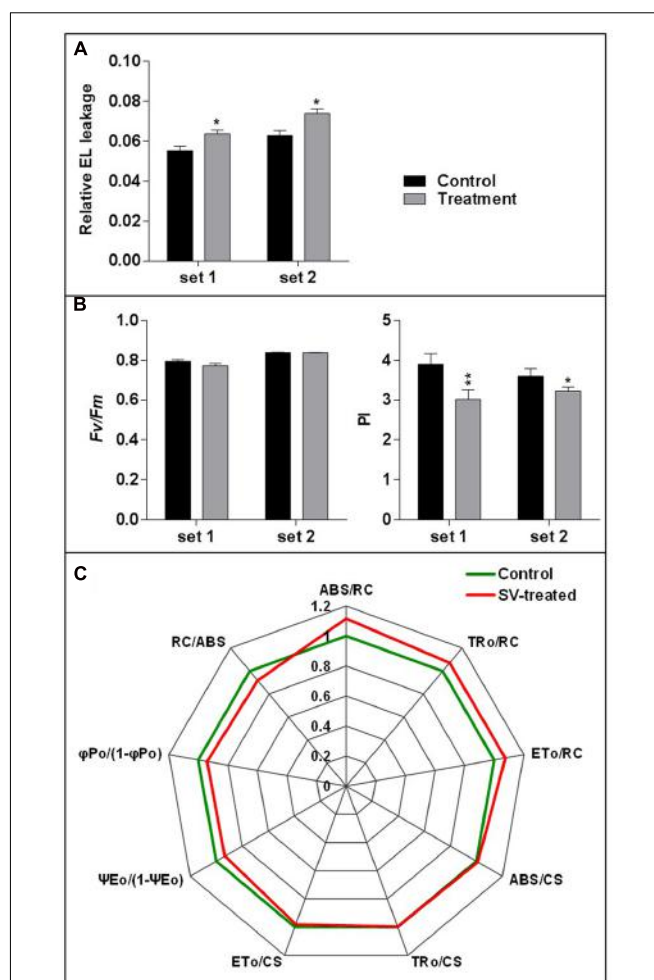


**FIGURE 5 | Measurement of relative electrolyte leakage and photosynthetic parameters.** (A) The relative electrolyte leakage of leaves was measured after 5 days of SV treatment ( $n = 10$ ). (B) Similarly, maximum quantum yield of photosystem II photochemistry ( $Fv/Fm$ ) and performance index (PI) were measured after 5 days of SV treatment ( $n = 12$ ). Black and gray colors indicate control and SV-treated plants, respectively. Set 1 and 2 indicate the two independent experiments with chamber swapping. Error bar indicates the standard error of means. Asterisks indicate the level of significance as determined by  $t$ -test (\*\* $0.01 < P < 0.05$ , \* $P < 0.1$ ). (C) Radar plot with a series of parameters derived from JIP-test analyses of the fast OJIP transients exhibiting the differences in the structure and function of the photosynthetic apparatus in control (green) and SV-treated (red) *Arabidopsis* plants. The OJIP-test used in this study, delineates the maximal energy fluxes for the following photosynthetic events- absorption (ABS), trapping (TR<sub>0</sub>), and electron transport (ET<sub>0</sub>) in the energy cascade quantified by the fluxes per cross section (CS) and per reaction center (RC) in SV-treated plants compared to those of control plants. Any marginal difference in these parameters between SV-treated and control plants is seen as a change in primary photochemistry of PSII. ABS/RC, light absorption flux (for PSII antenna chlorophylls) per RC; TR<sub>0</sub>/RC, trapped (maximum) energy flux (leading to Q<sub>A</sub> reduction) per RC; ET<sub>0</sub>/RC, maximum electron transport flux (further than Q<sub>A</sub>) per PSII RC; ABS/CS, absorbance of photons per excited CS, TR<sub>0</sub>/CS, trapped energy flux per excited CS; ET<sub>0</sub>/CS, maximum electron transport flux (further than Q<sub>A</sub>) per excited CS; ψEo, efficiency/probability for electron transport (ET), i.e., efficiency/probability that an electron moves further than Q<sub>A</sub> at  $t = 0$ ; φPo, maximum quantum yield for primary photochemistry at  $t = 0$ ; RC/ABS, density of reaction centers per PSII antenna chlorophyll. Data are mean  $\pm$  SE ( $n = 4$ ,  $P$ -value for comparison of treatments:  $<0.05$ ).

per RC can be represented as  $TR_0/RC$ . The increased value of ABS/RC, ET<sub>0</sub>/RC and TR<sub>0</sub>/RC in SV-treated plants suggested that the absorption and trapping flux of photons, as well as the electron transport per active RCs was higher in these plants compared to those in control plants. Notably, a concomitant increase in ABS/RC is seen as an increase in the apparent size of the antenna rather than a structural increase in the antenna size of a biochemical complex (Strasser et al., 2004; Smit et al., 2009; Redillas et al., 2011). Next, the phenomenological energy fluxes per excited cross-section (CS) for absorption (ABS/CS), trapping (TR<sub>0</sub>/CS) and electron transport (ET<sub>0</sub>/CS) were calculated. We found that the amount of chlorophyll per leaf area of the tested samples was either similar or marginally higher than the control plants after 5 days of SV treatment. The parameter  $\Psi E_0/(1 - \Psi E_0)$  which indicates the efficiency of a trapped exciton to transport an electron into the photosynthetic electron transport chain was recorded to be lower in SV-treated plants than in control plants. Reduced values of  $\Psi E_0/(1 - \Psi E_0)$  with increasing salt concentration in wheat plants and in cold-stressed turf grasses have been reported earlier (Mehta et al., 2010; Gururani et al., 2016). Similarly, the maximum yield of primary photochemistry  $\varphi Po/(1 - \varphi Po)$  where  $\varphi Po = TR_0/ABS$  was also recorded to be lower in SV-treated plants compared to that in control plants, SV treatment negatively influenced these parameters after 5 days of SV treatment. This could perhaps be corroborated with the reduced PI values in SV-treated plants (**Figure 5B**). PI is an indirect indicator of the vitality of plant samples where a reduced vitality is expressed in terms of reduced PI values. However, earlier studies have indicated that since electron flux is used in both carbon metabolism and other biochemical pathways, PI values are only indirectly related to the net photosynthesis (Bussotti et al., 2007). PI essentially includes three photosynthetic parameters: (1) the density of reaction centers (RC/ABS); (2) the quantum yield of primary photochemistry of PSII ( $\varphi Po = TR_0/RC$ ), and (3) ability to feed electrons into the photosynthetic electron transport chain between PSII and PSI ( $\Psi_0 = ET_0/TR_0$ ) (Strasser and Tsimilli-Michael, 2001; Bussotti et al., 2007).

## Expression Analysis of MS Ion Channels after SV and Touch Treatment

Higher EL in SV-treated plants can be caused by the modulation of membrane integrity or alteration of channel activity. Therefore, expression analysis of MS ion channels after SV treatment could be interesting. Herein we investigated the expression pattern of 13 MS ion channels after 5 days of SV treatment which are as follows: *MSLs* (1–10), *MCAs* (1 and 2) and *Piezo*. Among them, seven genes had a similar expression pattern between chamber swapping experiments. Four genes (*MSL3*, *MSL4*, *MSL7* and *MSL8*) were up-regulated, and three genes (*MSL10*, *MCA2* and *PIEZO*) were down-regulated in the SV-treated plant (**Figure 6**). Simultaneously, we checked the expression of MS ion channels after touch treatment for comparing two mechanostimuli: SV and touch. Four genes (*MSL3*, *MSL7*, *MSL9* and *MCA2*) were up-regulated by 5 days of touch treatments in two independent experiments (**Figure 7**).

Among them, *MSL3* and *MSL7* had similar up-regulation patterns between touch treatment and SV treatment, but *MCA2* showed an opposite expression pattern: down-regulated after SV treatment and up-regulated after touch treatment. The rest of the genes which showed inconsistent results between two sets of independent experiments after mechanical stimulation have been shown in Supplementary Figure S3.

## DISCUSSION

The expression pattern of SRGs after exposure to SV for four different time periods in darkness was revealed (**Figure 2**). Up-regulation was observed after long exposure (1 and 2 h) of SV, though the magnitude of expression was reduced at 2 h. Surprisingly, the short exposure (10 and 30 m) of SV down-regulated the genes compared to the control. Previously strong correlation between darkness and touch treatments at transcript level was reported (Lee et al., 2005). More than 50% of touch- and darkness-induced genes were common (Lee et al., 2005). On the basis of our previous report as well, many up-regulated genes were common between touch and SV treatments (Ghosh et al., 2016). Among the SRGs, 14 were already noted to be up-regulated by 30 m of darkness, which are marked in Supplementary Table S3 (Lee et al., 2005). Besides that, nine genes (*MYB77*, *DREB26*, *HSPRO2*, *RAV1*, *MPK11*, *At3g07350*, *At2g44500*, *At1g76600* and *At1g25400*) were common in touch- and SV-mediated induction (Supplementary Table S3). It is reported that both light/dark transition and touch treatments are capable of altering membrane potential in plants (Koselski et al., 2008; Chehab et al., 2011). Besides, we hypothesized that both touch and SV have a common mechanical impact in general (Ghosh et al., 2016). Previously, slight difference in transcript levels of fructose 1, 6-bisphosphate aldolase (*ald*) and rubisco small sub-unit (*rbcS*) genes were noticed after the SV treatment between light- and dark-grown rice plant (Jeong et al., 2008). Collectively, our result generates a strong notion of molecular cross-talk between touch, SV and light/dark stimuli. In the future, a detailed study is needed to establish a strong correlation between these three stimuli.

The sudden transfer of light-grown plants to darkness and exposure to SV could create antagonistic molecular events. Consequently, dark and SV treatment together resulted in initial down-regulation (at 10 and 30 m) of SRGs as compared to the non-competitive dark effect in the control plants (**Figure 2**). Nevertheless, SV exposure for a long time overcame the dark acclimatization and resulted in eventual induction of the SRGs. Simultaneously, movement of plants from growth room to the sound-proof chambers may provoke molecular alteration in plants (**Figure 2**). Hence, it was necessary to confirm the expression of these genes in acclimatized plants by exposure to SV under lighted condition. Swapping experiments in the illuminated chamber confirmed the SV-induced modulation of these genes (**Figure 3**). Additionally, the light-equipped SV treatment chamber proved to be useful for long-term SV treatment in future research. Of course, a gene transcription can be modulated by multiple environmental stimuli. Correlating a gene's expression with a particular stimulus definitely needs

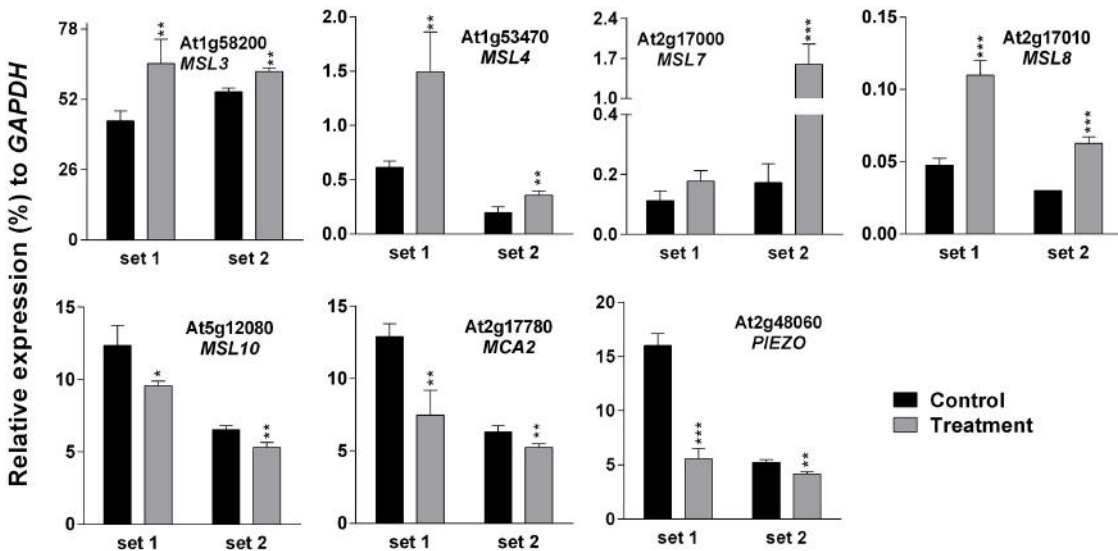


**FIGURE 6 | Quantitative real-time PCR analysis of MS ion channel genes after exposure to SV.** Plants were exposed to 500 Hz SV with 100 dB intensity for 5 days in a specialized plant growth chamber. Expression of each gene in the *Arabidopsis* exposed to SV (gray) was compared with control (black). Set 1 and 2 indicate the two independent experiments with chamber swapping between control and treatment. Error bar indicates the standard error of means from four biological replications. *P*-value ranges are marked by asterisks: \*\*\**P* < 0.01, \*\*0.01 < *P* < 0.05, \**P* < 0.1.

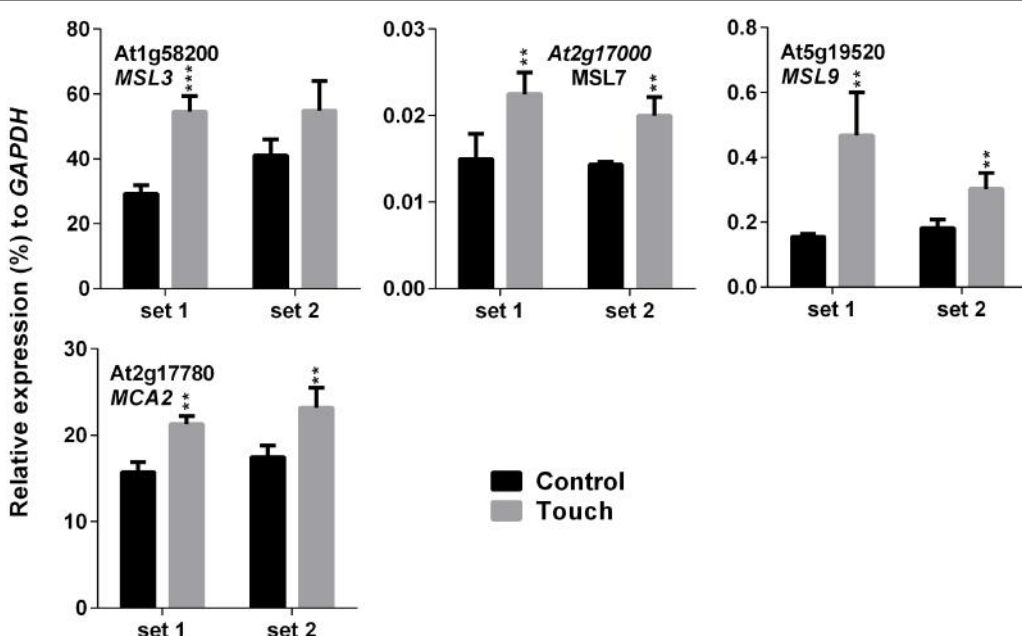


**FIGURE 7 | Quantitative real-time PCR analysis of MS ion channel genes after repetitive touch treatments.** Plants were repeatedly touched for 5 days. Expression of each gene in the *Arabidopsis* treated with touch (gray) was compared with control (black). Set 1 and 2 indicate the two independent experiments. Error bar indicates the standard error of means from four biological replications. *P*-value ranges are marked by asterisks: \*\*\**P* < 0.01, \*\*0.01 < *P* < 0.05.

rigorous study at the molecular level. Therefore, mechanistic investigation in future may shed more lights on the SV-mediated regulation of these genes.

The majority of the SRGs were expressed spatiotemporally (Supplementary Figure S2). Among them, various genes are involved in plant growth and development. SV-mediated plant

growth promotion was observed previously (Hassanien et al., 2014). These genes might have a role in SV-mediated plant growth promotion. KMD1 and DREB26 encode a kelch repeat containing F-box protein and an AP2/ERF family protein, respectively. BT5 protein contains BTB and TAZ domain together. Several members of F-box, BT and AP2/ERF family

are involved in the various processes of plant development (Kuroda et al., 2002; Robert et al., 2009; Krishnaswamy et al., 2011). CYP76C6 is a member of the cytochrome P450 subfamily C. P450s are involved in the phytohormone metabolic process and regulate plant growth and development (Xu et al., 2015). RAV1, an AP2/EREBP (APETALA2) type of TF involves in the flowering and senescence processes (Matias-Hernandez et al., 2014). Besides plant growth promotion, SV can induce the process of seed germination as well (Hassanien et al., 2014). The genes which were highly expressed in imbibed seeds probably have roles in SV-mediated seed germination. MYB77 is believed to interact with auxin response factors (ARFs) and involve in auxin response (Shin et al., 2007). Auxin is a positive regulator of gibberellic acid (GA) response and biosynthesis (Weiss and Ori, 2007); as GA is an important hormone for seed germination, this may be a reason behind SV-mediated enhancement in seed germination.  $\text{Ca}^{2+}$  fluxes are also considered to be crucial players during the germination process (Duval et al., 2002).  $\text{Ca}^{2+}$  binding calmodulin (CaM) has a role in sequestering cellular  $\text{Ca}^{2+}$  to maintain physiological range and avoid cytotoxicity (Duval et al., 2002). Induction of CaM transcripts was observed in pea during seed imbibition and germination (Duval et al., 2002). Therefore, it could be assumed that CaM-like (*CML38*) protein might be involved in similar processes. TPS enzyme converts glucose-6-P to trehalose-6-P, a positive regulator of seed germination (Tsai and Gazzarrini, 2014). Therefore, TPS8 might also be involved in the germination process. Direct correlation of these genes with SV-mediated germination or the developmental process needs detailed study in the future.

To check the effect of long exposure on a plant's physiology, 500 Hz at 100 dB was applied for 5 days in the light-equipped SV treatment chamber and the EL and photosynthetic parameters were checked (Figure 5). Changes in molecular events such as gene expression and changes in photosynthetic efficiency in plants should not be seen as isolated events. Hence, an indirect approach called chlorophyll-a fluorescence analysis was employed to determine changes in the photosynthetic efficiency in SV-treated plants. Data from these studies indicated a significant change in the photosynthetic machinery after the plants were exposed to SV treatment for 5 days (Figures 5B,C). Previously, chlorophyll-a fluorescence studies have largely been used to assess the photosynthetic performance and overall physiology of plants under abiotic stresses (Gururani et al., 2013, 2016; Zurek et al., 2014). On the basis of the present data it can be concluded that this indirect approach of evaluating photosynthetic efficiency of plants can also be used in SV-treated plants. Measurement of EL helps to understand the status of plasma membrane integrity, which can be easily affected by external stressors (Cao et al., 2007). Previous studies have shown that SV can alter cell wall and membrane microstructure which leads to a change in tension of the cell membrane (Bochu et al., 2001; Mishra et al., 2016). SV-mediated changes in lipid fluidity and protein secondary structure of plasma membrane were observed in chrysanthemum and tobacco, respectively (Zhao et al., 2002b; Yi et al., 2003). Therefore, it could be assumed that being a pressure wave, SV exerted pressure on cell wall-plasma membrane microstructure and altered its integrity which

resulted in higher EL compared to the control plant. Additionally, SV-mediated changes in the activity of membrane-associated channels may alter the EL. It was previously noted that SV can alter  $\text{K}^+$  channel permeability and  $\text{H}^+$ -ATPase activity in chrysanthemum (Zhao et al., 2002a,c). It was hypothesized that MS ion channels might be involved in the perception of the mechanical signals (Monshausen and Haswell, 2013). The role of MS ion channels for touch sensing was observed in earlier studies (Shepherd et al., 2002; Nakagawa et al., 2007). To check whether SV has any effect on the transcript level of MS ion channels, herein we investigated their expression pattern. The result showed that SV treatment continuously for 5 days up-regulated four genes (*MSL3*, *MSL4*, *MSL7*, and *MSL8*) and down-regulated three genes (*MSL10*, *MCA2* and *PIEZO*) (Figure 6). SV-mediated differential expression of channel genes may be involved in the higher EL, and triggers the downstream signaling processes.

Touch is considered as an external mechanical force like SV. Touch-mediated gene induction pattern was broadly spiking in nature, and was normalized to control level after 1 h (Figure 4). Hence, time points for expression analysis after touch treatments are crucial. Surprisingly, six SRGs (*At3g07350*, *At2g20670*, *KMD1*, *RZPF34*, *TPS8* and *LHCB2*) were not up-regulated by touch at any of the time points. On the other hand, *MCA2* showed the opposite expression pattern after 5 days of SV and touch treatments, i.e., down-regulated after SV treatment and up-regulated after touch (Figures 6 and 7). This variation indicates the difference between two mechanostimuli at molecular level. Therefore, these seven genes could be the interesting candidates to highlight the differences between touch- and SV-mediated molecular responses in future. It has already been noted that the expression of *MSL8* and *MSL9* are mainly restricted in *Arabidopsis* flower and root, respectively (Haswell et al., 2008; Hamilton et al., 2015). In corroboration with this, we also observed very low expression of these two genes compared to other ubiquitously expressed MS ion channel genes (like- *MSL2*, *MSL3*, *MSL5*, *MSL6*, *MSL10*, *MCA1* and *MCA2*). A detailed tissue-specific analysis of MS-ion channel genes after mechanical stimulation can lead to more interesting inferences in future.

## CONCLUSION

SRGs could be regulated by darkness and touch treatments. Both being mechanostimuli, touch and SV may share some common MS signaling events. Besides, the distinct expression pattern of six SRGs and *MCA2* generates an idea that SV is perceived as a stimulus distinct from touch. Certainly, a detailed comparative study is required to elucidate the similarities and dissimilarities between these two mechanostimuli. Additionally, the spatiotemporal expression of SRGs could be linked to SV-mediated growth promotion and germination by extensive research in the future. Induction of chemical defense by chewing sound of caterpillar in *Arabidopsis* and elevated level of polyamine by natural sound in Chinese cabbage (Qin et al., 2003; Appel and Cocroft, 2014) indicate the ecological and/or environmental significance of SV to plants. Corroboratively,

'Buzz Pollination,' a phenomenon where pollen from anthers are released at a particular frequency produced by bee's buzz (De Luca and Vallejo-Marin, 2013), also highlights the environmental significance of SV. Such kind of natural SVs can be the interesting stimulus for extending the plant-acoustic research to molecular level. Therefore, comparative investigation with various ecologically significant SVs in natural photoperiod is required to give impetus to this least explored area of plant science.

## AUTHOR CONTRIBUTIONS

RG performed most of the experiments. LP performed the experiment shown in **Figure 6**. RG and RM analyzed the data. MG analyzed the data shown in **Figure 5C**. RG, S-CP, M-JJ, and HB conceived the idea and designed the experiments. HB

supervised the experiments. RG, MG, RM, and HB wrote the manuscript. All the authors approved the final manuscript.

## FUNDING

This work was carried out with the support of "Cooperative Research Program for Agriculture Science and Technology Development (PJ010497)" Rural Development Administration, Republic of Korea.

## SUPPLEMENTARY MATERIAL

The Supplementary Material for this article can be found online at: <http://journal.frontiersin.org/article/10.3389/fpls.2017.00100/full#supplementary-material>

## REFERENCES

- Appel, H. M., and Cocroft, R. B. (2014). Plants respond to leaf vibrations caused by insect herbivore chewing. *Oecologia* 175, 1257–1266. doi: 10.1007/s00442-014-2995-6
- Bochu, W., Hucheng, Z., Yiyao, L., Yi, J., and Sakanishi, A. (2001). The effects of alternative stress on the cell membrane deformability of *Chrysanthemum callus* cells. *Colloids Surf. B Biointerfaces* 20, 321–325. doi: 10.1016/S0927-7765(00)00181-8
- Bochu, W., Jiping, S., Biao, L., Jie, L., and Chuanren, D. (2004). Soundwave stimulation triggers the content change of the endogenous hormone of the *Chrysanthemum* mature callus. *Colloids Surf. B Biointerfaces* 37, 107–112. doi: 10.1016/j.colsurfb.2004.03.004
- Braam, J. (2005). In touch: plant responses to mechanical stimuli. *New Phytol.* 165, 373–389. doi: 10.1111/j.1469-8137.2004.01263.x
- Bussotti, F., Strasser, R. J., and Schaub, M. (2007). Photosynthetic behavior of woody species under high ozone exposure probed with the JIP-test: a review. *Environ. Pollut.* 147, 430–437. doi: 10.1016/j.envpol.2006.08.036
- Cao, W. H., Liu, J., He, X. J., Mu, R. L., Zhou, H. L., Chen, S. Y., et al. (2007). Modulation of ethylene responses affects plant salt-stress responses. *Plant Physiol.* 143, 707–719. doi: 10.1104/pp.106.094292
- Chehab, E. W., Wang, Y., and Braam, J. (2011). "Mechanical force responses of plant cells and plants," in *Mechanical Integration of Plant Cells and Plants*, ed. P. Wojtaszek (Berlin: Springer), 173–194.
- Chehab, E. W., Yao, C., Henderson, Z., Kim, S., and Braam, J. (2012). *Arabidopsis* touch-induced morphogenesis is jasmonate mediated and protects against pests. *Curr. Biol.* 22, 701–706. doi: 10.1016/j.cub.2012.02.061
- De Luca, P. A., and Vallejo-Marin, M. (2013). What's the 'buzz' about? The ecology and evolutionary significance of buzz-pollination. *Curr. Opin. Plant Biol.* 16, 429–435. doi: 10.1016/j.pbi.2013.05.002
- Duval, F. D., Renard, M., Jaquinod, M., Biou, V., Montrichard, F., and Macherel, D. (2002). Differential expression and functional analysis of three calmodulin isoforms in germinating pea (*Pisum sativum* L.) seeds. *Plant J.* 32, 481–493. doi: 10.1046/j.1365-313X.2002.01409.x
- Ghosh, R., Choi, B. S., Jeong, M. J., Bae, D. W., Shin, S. C., Park, S. U., et al. (2012). Comparative transcriptional analysis of caffeoyl-coenzyme A 3-O-methyltransferase from *Hibiscus cannabinus* L., during developmental stages in various tissues and stress regulation. *Plant Omics* 5, 184–193.
- Ghosh, R., Mishra, R. C., Choi, B., Kwon, Y. S., Bae, D. W., Park, S. C., et al. (2016). Exposure to sound vibrations lead to transcriptomic, proteomic and hormonal changes in *Arabidopsis*. *Sci. Rep.* 6:33370. doi: 10.1038/srep33370
- Gururani, M. A., Ganeshan, M., Song, I. J., Han, Y., Kim, J. I., Lee, H. Y., et al. (2016). Transgenic turfgrasses expressing hyperactive ser599ala phytochrome a mutant exhibit abiotic stress tolerance. *J. Plant Growth Regul.* 35, 11–21. doi: 10.1007/s00344-015-9502-0
- Gururani, M. A., Upadhyaya, C. P., Strasser, R. J., Yu, J. W., and Park, S. W. (2013). Evaluation of abiotic stress tolerance in transgenic potato plants with reduced expression of PSII manganese stabilizing protein. *Plant Sci.* 198, 7–16. doi: 10.1016/j.plantsci.2012.09.014
- Gururani, M. A., Venkatesh, J., Ganeshan, M., Strasser, R. J., Han, Y., Kim, J. I., et al. (2015). In vivo assessment of cold tolerance through chlorophyll-a fluorescence in transgenic zoysiagrass expressing mutant phytochrome A. *PLoS ONE* 10:e0127200. doi: 10.1371/journal.pone.0127200
- Hamilton, E. S., Jensen, G. S., Maksaev, G., Katims, A., Sherp, A. M., and Haswell, E. S. (2015). Mechanosensitive channel MSL8 regulates osmotic forces during pollen hydration and germination. *Science* 350, 438–441. doi: 10.1126/science.aac6014
- Hassanien, R. H. E., Hou, T. Z., Li, Y. F., and Li, B. M. (2014). Advances in effects of sound waves on plants. *J. Integr. Agric.* 13, 335–348. doi: 10.1016/S2095-3119(13)60492-X
- Haswell, E. S., and Meyerowitz, E. M. (2006). MscS-like proteins control plastid size and shape in *Arabidopsis thaliana*. *Curr. Biol.* 16, 1–11. doi: 10.1016/j.cub.2005.11.044
- Haswell, E. S., Peyronnet, R., Barbier-Brygoo, H., Meyerowitz, E. M., and Frachisse, J. M. (2008). Two MscS homologs provide mechanosensitive channel activities in the *Arabidopsis* root. *Curr. Biol.* 18, 730–734. doi: 10.1016/j.cub.2008.04.039
- Jeong, M. J., Shim, C. K., Lee, J. O., Kwon, H. B., Kim, Y. H., Lee, S. K., et al. (2008). Plant gene responses to frequency-specific sound signals. *Mol. Breed.* 21, 217–226. doi: 10.1007/s11032-007-9122-x
- Koselski, M., Trebacz, K., Dziubinska, H., and Krol, E. (2008). Light- and dark-induced action potentials in *Physcomitrella patens*. *Plant Signal. Behav.* 3, 13–18. doi: 10.4161/psb.3.1.4884
- Krishnaswamy, S., Verma, S., Rahman, M. H., and Kav, N. N. (2011). Functional characterization of four APETALA2-family genes (RAP2.6, RAP2.6L, DREB19 and DREB26) in *Arabidopsis*. *Plant Mol. Biol.* 75, 107–127. doi: 10.1007/s11103-010-9711-7
- Kuroda, H., Takahashi, N., Shimada, H., Seki, M., Shinozaki, K., and Matsui, M. (2002). Classification and expression analysis of *Arabidopsis* F-box-containing protein genes. *Plant Cell Physiol.* 43, 1073–1085. doi: 10.1093/pcp/pcf151
- Lee, D., Polisensky, D. H., and Braam, J. (2005). Genome-wide identification of touch- and darkness-regulated *Arabidopsis* genes: a focus on calmodulin-like and XTH genes. *New Phytol.* 165, 429–444. doi: 10.1111/j.1469-8137.2004.01238.x
- Matias-Hernandez, L., Aguilar-Jaramillo, A. E., Marin-Gonzalez, E., Suarez-Lopez, P., and Pelaz, S. (2014). RAV genes: regulation of floral induction and beyond. *Ann. Bot.* 114, 1459–1470. doi: 10.1093/aob/mcu069
- Mehta, P., Jajoo, A., Mathur, S., and Bharti, S. (2010). Chlorophyll a fluorescence study revealing effects of high salt stress on Photosystem II in wheat leaves. *Plant Physiol. Biochem.* 48, 16–20. doi: 10.1016/j.plaphy.2009.10.006

- Mishra, R. C., Ghosh, R., and Bae, H. (2016). Plant acoustics: in the search of a sound mechanism for sound signaling in plants. *J. Exp. Bot.* 67, 4483–4494. doi: 10.1093/jxb/erw235
- Monshausen, G. B., and Haswell, E. S. (2013). A force of nature: molecular mechanisms of mechanoperception in plants. *J. Exp. Bot.* 64, 4663–4680. doi: 10.1093/jxb/ert204
- Nakagawa, Y., Katagiri, T., Shinozaki, K., Qi, Z., Tatsumi, H., Furuchi, T., et al. (2007). *Arabidopsis* plasma membrane protein crucial for  $\text{Ca}^{2+}$  influx and touch sensing in roots. *Proc. Natl. Acad. Sci. U.S.A.* 104, 3639–3644. doi: 10.1073/pnas.0607703104
- Qin, Y. C., Lee, W. C., Choi, Y. C., and Kim, T. W. (2003). Biochemical and physiological changes in plants as a result of different sonic exposures. *Ultrasonics* 41, 407–411. doi: 10.1016/S0041-624X(03)00103-3
- Redillas, M. C. F. R., Strasser, R. J., Jeong, J. S., Kim, Y. S., and Kim, J. K. (2011). The use of JIP test to evaluate drought-tolerance of transgenic rice overexpressing OsNAC10. *Plant Biotechnol. Rep.* 5, 169–175. doi: 10.1007/s11816-011-0170-7
- Robert, H. S., Quint, A., Brand, D., Vivian-Smith, A., and Offringa, R. (2009). BTB and TAZ domain scaffold proteins perform a crucial function in *Arabidopsis* development. *Plant J.* 58, 109–121. doi: 10.1111/j.1365-313X.2008.03764.x
- Safari, M., Ghanati, F., Behmanesh, M., Hajnorouzi, A., Nahidian, B., and Mina, G. (2013). Enhancement of antioxidant enzymes activity and expression of CAT and PAL genes in hazel (*Corylus avellana* L.) cells in response to low-intensity ultrasound. *Acta Physiol. Plant.* 35, 2847–2855. doi: 10.1007/s11738-013-1318-6
- Schmittgen, T. D., and Livak, K. J. (2008). Analyzing real-time PCR data by the comparative C(T) method. *Nat. Protoc.* 3, 1101–1108. doi: 10.1038/nprot.2008.73
- Shepherd, V. A., Beilby, M. J., and Shimmen, T. (2002). Mechanosensory ion channels in charophyte cells: the response to touch and salinity stress. *Eur. Biophys. J.* 31, 341–355. doi: 10.1007/s00249-002-0222-6
- Shin, R., Burch, A. Y., Huppert, K. A., Tiwari, S. B., Murphy, A. S., Guilfoyle, T. J., et al. (2007). The *Arabidopsis* transcription factor MYB77 modulates auxin signal transduction. *Plant Cell* 19, 2440–2453. doi: 10.1105/tpc.107.050963
- Smit, M. F., Van Heerden, P. D. R., Pienaar, J. J., Weissflog, L., Strasser, R. J., and Kruger, G. H. J. (2009). Effect of trifluoroacetate, a persistent degradation product of fluorinated hydrocarbons, on *Phaseolus vulgaris* and *Zea mays*. *Plant Physiol. Biochem.* 47, 623–634. doi: 10.1016/j.plaphy.2009.02.003
- Strasser, R. J., and Tsimilli-Michael, M. (2001). Stress in plants, from daily rhythm to global changes, detected and quantified by the JIP-test. *Chim. Nouv.* 75, 3321–3326.
- Strasser, R. J., Tsimilli-Michael, M., and Srivastava, A. (2004). "Analysis of the Chlorophyll fluorescence transient," in *Chlorophyll Fluorescence: A Signature of Photosynthesis, Advances in Photosynthesis and Respiration*, eds G. C. Papageorgiou and Govindjee (Dordrecht: Springer), 321–362.
- Telewski, F. W. (2006). A unified hypothesis of mechanoperception in plants. *Am. J. Bot.* 93, 1466–1476. doi: 10.3732/ajb.93.10.1466
- Tsai, A. Y., and Gazzarrini, S. (2014). Trehalose-6-phosphate and SnRK1 kinases in plant development and signaling: the emerging picture. *Front. Plant Sci.* 5:119. doi: 10.3389/fpls.2014.00119
- Veley, K. M., Maksaei, G., Frick, E. M., January, E., Kloepper, S. C., and Haswell, E. S. (2014). *Arabidopsis* MSL10 has a regulated cell death signaling activity that is separable from its mechanosensitive ion channel activity. *Plant Cell* 26, 3115–3131. doi: 10.1105/tpc.114.128082
- Wei, M., Yang, C. Y., and Wei, S. H. (2012). Enhancement of the differentiation of protocorm-like bodies of *Dendrobium officinale* to shoots by ultrasound treatment. *J. Plant Physiol.* 169, 770–774. doi: 10.1016/j.jplph.2012.01.018
- Weiss, D., and Ori, N. (2007). Mechanisms of cross talk between gibberellin and other hormones. *Plant Physiol.* 144, 1240–1246. doi: 10.1104/pp.107.100370
- Xiaocheng, Y., Bochu, W., and Chuanren, D. (2003). Effects of sound stimulation on energy metabolism of *Actinidia chinensis* callus. *Colloids Surf. B Biointerfaces* 30, 67–72. doi: 10.1016/S0927-7765(03)00027-4
- Xiujuan, W., Bochu, W., Yi, J., Defang, L., Chuanren, D., Xiaocheng, Y., et al. (2003). Effects of sound stimulation on protective enzyme activities and peroxidase isoenzymes of Chrysanthemum. *Colloids Surf. B Biointerfaces* 27, 59–63. doi: 10.1016/S0927-7765(02)00038-3
- Xu, J., Wang, X. Y., and Guo, W. Z. (2015). The cytochrome P450 superfamily: key players in plant development and defense. *J. Integr. Agric.* 14, 1673–1686. doi: 10.1016/S2095-3119(14)60980-1
- Yi, J., Wang, B. C., Wang, X. J., Chuanren, D., Toyama, Y., and Sakanishi, A. (2003). Influence of sound wave on the microstructure of plasmalemma of chrysanthemum roots. *Colloids Surf. B Biointerfaces* 29, 109–113. doi: 10.1016/S0927-7765(02)00154-6
- Zhao, H. C., Wang, B. C., Liu, B. A., Cai, S. X., and Xi, B. S. (2002a). The effects of sound stimulation on the permeability of  $\text{K}^+$  channel of *Chrysanthemum callus* plasma. *Colloids Surf. B Biointerfaces* 26, 329–333. doi: 10.1016/S0927-7765(02)00008-5
- Zhao, H. C., Wu, J., Xi, B. S., and Wang, B. C. (2002b). Effects of sound-wave stimulation on the secondary structure of plasma membrane protein of tobacco cells. *Colloids Surf. B Biointerfaces* 25, 29–32. doi: 10.1016/S0927-7765(01)00294-6
- Zhao, H. C., Zhu, T., Wu, J., and Xi, B. S. (2002c). Role of protein kinase in the effect of sound stimulation on the PM  $\text{H}^+$ -ATPase activity of *Chrysanthemum callus*. *Colloids Surf. B Biointerfaces* 26, 335–340. doi: 10.1016/S0927-7765(02)00007-3
- Zurek, G., Rybka, K., Pogrzeba, M., Krzyzak, J., and Prokopuk, K. (2014). Chlorophyll fluorescence in evaluation of the effect of heavy metal soil contamination on perennial grasses. *PLoS ONE* 9:e91475. doi: 10.1371/journal.pone.0091475

**Conflict of Interest Statement:** The authors declare that the research was conducted in the absence of any commercial or financial relationships that could be construed as a potential conflict of interest.

Copyright © 2017 Ghosh, Gururani, Ponpandian, Mishra, Park, Jeong and Bae. This is an open-access article distributed under the terms of the Creative Commons Attribution License (CC BY). The use, distribution or reproduction in other forums is permitted, provided the original author(s) or licensor are credited and that the original publication in this journal is cited, in accordance with accepted academic practice. No use, distribution or reproduction is permitted which does not comply with these terms.



# Electrical Signaling, Photosynthesis and Systemic Acquired Acclimation

Magdalena Szechyńska-Hebda<sup>1,2</sup>, Maria Lewandowska<sup>1</sup> and Stanisław Karpiński<sup>1\*</sup>

<sup>1</sup> Department of Plant Genetics, Breeding and Biotechnology, Warsaw University of Life Sciences, Warsaw, <sup>2</sup> The Franciszek Górski Institute of Plant Physiology, Polish Academy of Sciences, Krakow, Poland

## OPEN ACCESS

### Edited by:

Kazimierz Trebacz,  
Marie Curie-Skłodowska University,  
Poland

### Reviewed by:

Vladimir Sukhov,  
N. I. Lobachevsky State University of  
Nizhny Novgorod, Russia  
Sergey Shabala,  
University of Tasmania, Australia

### \*Correspondence:

Stanisław Karpiński  
stanislaw\_karpinski@sggw.pl

### Specialty section:

This article was submitted to  
Plant Physiology,  
a section of the journal  
*Frontiers in Physiology*

Received: 30 June 2017

Accepted: 25 August 2017

Published: 14 September 2017

### Citation:

Szechyńska-Hebda M, Lewandowska M and Karpiński S (2017) Electrical Signaling, Photosynthesis and Systemic Acquired Acclimation. *Front. Physiol.* 8:684.  
doi: 10.3389/fphys.2017.00684

Electrical signaling in higher plants is required for the appropriate intracellular and intercellular communication, stress responses, growth and development. In this review, we have focus on recent findings regarding the electrical signaling, as a major regulator of the systemic acquired acclimation (SAA) and the systemic acquired resistance (SAR). The electric signaling on its own cannot confer the required specificity of information to trigger SAA and SAR, therefore, we have also discussed a number of other mechanisms and signaling systems that can operate in combination with electric signaling. We have emphasized the interrelation between ionic mechanism of electrical activity and regulation of photosynthesis, which is intrinsic to a proper induction of SAA and SAR. In a special way, we have summarized the role of non-photochemical quenching and its regulator PsbS. Further, redox status of the cell, calcium and hydraulic waves, hormonal circuits and stomatal aperture regulation have been considered as components of the signaling. Finally, a model of light-dependent mechanisms of electrical signaling propagation has been presented together with the systemic regulation of light-responsive genes encoding both, ion channels and proteins involved in regulation of their activity. Due to space limitations, we have not addressed many other important aspects of hormonal and ROS signaling, which were presented in a number of recent excellent reviews.

**Keywords:** electrical signal, ion channel activity, plasma membrane, photosynthesis, PsbS overexpression and npq-4

## INTRODUCTION

One of the most critical functions of each organism is a selective sensing of the environment. Ordered flow of electrical currents between cells and organs allows a given organism for universal, rapid, and efficient communication of the external changes. The steady state of plasma membrane electrical potential defines the electric field of each cell. However, external factors induce rapid changes in the membrane potential, and these changes can be transduced in the form of waves: (1) the movement of ions across of plasma membrane and organelle membranes is a driving mechanism for wavy changes of the electric potential, which propagate along the membrane of one cell or organelle, and in turn, determine intracellular electrical activity of the cell and adjust its local metabolism; (2) the short-distance intercellular electrical signaling to maintain specific behavior of the group of the cells; and (3) the long-distance intercellular electrical signal from the site of stimulus perception to distal organs, where it triggers plant-wide responses.

Despite specific differences, the network of electrical signaling is present at almost each level of complexity, from unicellular bacteria and fungi to multi-cellular organisms like plants and animals. In unicellular organisms, cell-to-cell electrical signaling plays a key role in the reproduction and coordination of colony behavior. For example, bacteria *Bacillus subtilis* generates electrical signals mediated by potassium ion channels to direct motility in a biofilm of their own community, to stop reproducing bacteria on colony periphery, and to leave core cells with a sufficient nutrient supply (Humphries et al., 2017). A polarization and dynamic coordination of the electrical signals underlies also the ability of plant cell groups to proliferation, proper morphogenesis, regeneration and orientation (Filek et al., 2002; Yan et al., 2009; Nakajima et al., 2015). Similarly, the bioelectric network of each cell and the bioelectric gradients serve as a kind of pattern memory of animal tissues and organs (Durant et al., 2017). The environmental signals, physical (e.g., light, temperature, humidity, electric fields, wounding), chemical (e.g., nutrients and various substances), and biological (e.g., symbiosis, pathogenesis), can alter local and systemic electrical responses and modify cell division and growth. However, once the connectivity patterns of electrical signaling are disrupted, organisms can no longer follow appropriate morphogenetic and functional pathways (Szechyńska-Hebda et al., 2010; Karpiński et al., 2013; Nakajima et al., 2015).

Probably the most spectacular system involving electrical signaling is the organism-to-organism signaling. Among unicellular bacteria, electrical communication enables cross-species interactions. *Pseudomonas aeruginosa* cells become attracted to the electrical signal released by the *B. subtilis* biofilm (Humphries et al., 2017). In the plant kingdom, the role of electrical signals in organism-to-organism interactions is still highly speculative and largely phenomenological, but there are several pioneering examples of how plant creates and responds to electrical fields. Flowers exhibit differences in the pattern of the electric field, which can be discriminated by bumblebees. When the bumblebee lands on the flower, the electric field changes within seconds and this facilitates rapid and dynamic signaling between flowers and their pollinators (Clarke et al., 2013). *Arabidopsis thaliana* respond to biotic stress agents: *Spodoptera littoralis*, *Myzus persicae*, *Pseudomonas syringae* with plasma membrane depolarization and it was correlated to specific regulation of the wide range of defense genes (Bricchi et al., 2012). Similarly, transition zone of the roots is an area with unusually high levels of electrical activity (Baluška, 2010; Baluška and Mancuso, 2013), and it makes the root apex zone an attractive target of pathogenic and symbiotic organisms (Brenner et al., 2006). There is also the possibility that electric field generated by each growing root might allow electrical signaling among roots of the same or another plant (Schenk and Seabloom, 2010; Garzon and Keijzer, 2011). However, the most extremal example among multicellular organisms, is the usage of electric organs by fish in murky environment to navigate, recognize the species and sex, and as a shocking defense (Gallant et al., 2014). The electric field generated for predatory purposes is up to 500 V or higher.

## SYSTEMIC PROPAGATION OF ELECTRICAL SIGNALS IN PLANTS

All plants generate long-distance electrical signals, and these signals serve for communication and integration of responses in different tissues and organs. The most extensively studied are electrical signals in lower plants, e.g., *Characeae* or in higher “sensitive” plants such as *Mimosa pudica* or *Dionaea muscipula*. However, in “ordinary” plants, a variety of electrical phenomena have also been described. Various treatments can trigger a specific pattern of changes in the plasma membrane electrical potential of *Arabidopsis* (Szechyńska-Hebda et al., 2010), *Vicia faba* (Dziubińska et al., 2003a; Zimmermann et al., 2009), *Triticum aestivum* (Dziubińska et al., 2003b), *Zea mays* (Grams et al., 2007), as well as in tree species like *Salix* (Fromm and Spanswick, 1993), *Populus* (Lautner et al., 2005), and *Persea* (Oyarce and Gurovich, 2010).

The electrical signals induced by external stimulus differ in their spatial and temporal pattern, in mechanism of the activation, and evoked responses. First, local electrical potential (LEP) is a sub-threshold response induced by environmental factors (e.g., light, cold, water status changes, phytohormones, pathogen infection). LEP is not transferred to other parts of a plant, but has an impact on the local physiological status of the cell (Yan et al., 2009; Roux et al., 2014). Second, action potential (AP) is a fast “all-or-nothing” signal, locally generated in the cell after treatment with different stimuli (light/darkness, electrical stimulation, cold, mechanical stimulus), provided that stimulus reaches a certain threshold. Mechanism of AP propagation involves membrane depolarization and subsequent repolarization, depended on passive  $\text{Ca}^{2+}$ ,  $\text{Cl}^-$ , and  $\text{K}^+$  ion fluxes. Activation of potential-dependent  $\text{Ca}^{2+}$  channels is probably the first stage of AP generation. AP propagates to distant organs without loss of amplitude and triggers a systemic response associated with transient changes in gas exchange, carbon assimilation process, respiration rate, reduction in phloem transport, and expression of specific genes. The information within the transmitted signal may be encoded by the shape of a single AP determined by the relative contribution of the ionic conductance; the AP amplitude (in range of 10–80 mV); the frequency of multiple AP signals and refractory period, i.e., the period following the AP when the cell cannot be stimulated (Fromm and Lautner, 2007; Hedrich, 2012; Kupisz et al., 2017). Third, variation potential (VP), also called electropotential wave is a slow signal evoked by local damaging stimulations (wounding, heating, burning). VP signals also consist of transient changes in membrane potential, but they are irregular in shape and longer in duration (the repolarizations is delayed). Amplitude of VP depends on type and intensity of the damaging stimulus. The VP ionic mechanism differs from that underlying APs; it mainly depends on transient P-type  $\text{H}^+$  ATPase inactivation in the plasma membrane. However, passive  $\text{Ca}^{2+}$  influx and  $\text{Cl}^-$  channel activation were also considered to be involved in VP generation. Probably, activation of ligand-dependent (chemical mechanism) or mechano-sensitive (hydraulic mechanism) calcium channels allows  $\text{Ca}^{2+}$  influx,

which in turn triggers both H<sup>+</sup> ATPase inactivation and anion channel activation. Therefore, VP propagation parameters might be under control of a hydraulic waves or/and chemical agent (wound substances). When transmitted systemically to other organs of the plant, VP influences the quantum yield of electron transport through photosystem II, the net CO<sub>2</sub> uptake rate, respiration, jasmonic acid concentration, ethylene emission, gene expression and protein synthesis. Taken together, VPs seems to carry more information than the APs (Stankovic et al., 1997; Vodeneev et al., 2015, 2017; Gilroy et al., 2016). Fourth, system potential (SP) is a self-propagated systemic signal mediated by the apoplastic ions and the plasma membrane H<sup>+</sup>-ATPase. The initial polarity of these voltage-dependent signal is hyperpolarization. In contrast to action or variation potentials, all of the ions (Ca<sup>2+</sup>, K<sup>+</sup>, H<sup>+</sup>, and Cl<sup>-</sup>) are involved in SP propagation, after the voltage change begins. SP does not obey the all-or-none rule but depends on the intensity and nature of the original stimulus (Zimmermann et al., 2009).

Dependently on the type of stimulus and plant species, electrical signals are transferred to distant tissues and organs with different speed. AP velocity has been estimated in range of 4–8 to 70 mm s<sup>-1</sup> for green algae and higher plants, and even up to 400 mm s<sup>-1</sup> in woody plants (Volkov, 2000, 2006; Fromm and Lautner, 2007). VP is always slower than AP; the flaming or wounding of higher plants evoke VP signal, which moves at a speed of 0.5–5 mm s<sup>-1</sup> (Fromm and Lautner, 2007; Chen et al., 2016). The SP propagates at 0.8 to 1.7 mm s<sup>-1</sup> from leaves that had been injured by cutting (Zimmermann et al., 2009). In *Arabidopsis thaliana* different types of the electrical signals can be generated by various stimuli. The repetitive APs together with VP signal can be induced in the leaf by wounding and KCl treatment. After this stimulus, APs propagated in a bidirectional manner (but mostly from the wound to the petiole) with the velocity approx. 0.5–4 mm s<sup>-1</sup>, whereas VP was recorded as an unidirectional slow propagation wave with the velocity 0.22–0.26 mm s<sup>-1</sup> (Favre et al., 2001). Similarly, AP-like depolarization wave was recorded together with the slow depolarization wave corresponding to a VP in the sieve elements, when *A. thaliana* leaves were wounded. The electrical signal propagation had a velocity of c.a. 0.3–2.5 mm s<sup>-1</sup> (Salvador-Recatal et al., 2014). Touch of *A. thaliana* leaves induced only APs, that moved at a speed of 1.3 mm s<sup>-1</sup> (Agosti, 2014). Voltage-elicited APs for *A. thaliana* ecotype Columbia propagated from the stimulus area via the petiole to the central axis of the rosette with velocity ranging from 0.8 to 1.9 mm s<sup>-1</sup>, whereas for the Wassilewskija ecotype the propagation speed was 0.76–0.17 mm s<sup>-1</sup>. Moreover, the results for both ecotypes differed markedly in the general occurrence of APs; 91% plants ecotype Col and only 45% plants ecotype *Ws* responded to electrical stimulation with generation of the APs (Favre and Agosti, 2007). Several seconds of excess light illumination have induced a systemic electrical signal corresponding to VP or SP. This signal has propagated between two different leaves with the speed of 2 mm s<sup>-1</sup>. Switching light off has triggered signals with the speed ~3 mm s<sup>-1</sup> (Szechyńska-Hebda et al., 2010).

The electrical signal transmission in the living system plays the central functional role as it elicits systemic responses in

an unaffected tissue to protect or defend the whole plant from a second occurrence of that same or tightly associated stress. The fact that similar electrical signals appear in response to many different stimuli suggests that stimulus-specific signals are encoded within the spatial and temporal dynamics of these waves. However, they may act as initial, general priming signals, preparing the plant to respond in a more selective way to subsequent, stimulus-specific signals (Choi et al., 2017). In this case, a number of specific mechanisms and signaling systems have been proposed to operate in combination with electric signaling, e.g., calcium and ROS waves; rapid changes in the xylem pressure; the level of photosynthetic products; hormonal circuits; peptide, protein and RNA signals (Shabala et al., 2016). Operating at different timescales, they encode information about the specific nature of a particular stimulus. The [Ca<sup>2+</sup>]<sub>cyt</sub> signals are very rapid, approx. 400 μm s<sup>-1</sup>. The lower steady state Ca<sup>2+</sup> concentration (~100 nM) in comparison to extracellular space and endoplasmic reticulum interior, a large number of Ca<sup>2+</sup> ion channels in cellular membranes, and a broad range of Ca<sup>2+</sup> sensor proteins, all of these factors allow the calcium signal to convey information about the nature and amplitude of external stimuli. Similarly, ROS propagation is relatively fast, approx. 8 cm min<sup>-1</sup> (Miller et al., 2009). AP can induce the formation of free radicals, and ROS are known to be regulators of a broad range of cation and anion channels, thus a cross-talk between electric and ROS signals is quite probable (Shabala et al., 2016). Plants are able to induce very different and specific cell responses by using a small number of ROS molecules. ROS can act directly as “signaling molecules” or indirectly as “secondary products.” Nevertheless, additional aspects of the ROS adjustment during sensing and signaling mechanisms need to be considered: molecule type, its concentration and cellular localization, or a combination of all of these; modulation of ROS signaling by antioxidative enzymatic system, consisting of specific components in different cellular compartments (Szechyńska-Hebda and Karpiński, 2013). Further, the electrical signals can be accompanied by rapid hydraulic signals. The changes in the xylem tension are sensed by mechano-sensory channels directly, or through the lipid bilayer in which the channel resides. Complementary, slower (minutes to hours) transport of water-soluble signaling molecules (e.g. hormones), and sucrose translocation through the phloem (Shabala et al., 2016) can convey an important information about the external stress factors. However, there could be also another scenario and plant strategy to communicate different stimuli and induce the systemic responses to local stress. In some cases, a cross-talk is seen, in which one type of locally applied stress is capable of generating a protective response or acclimation to another type of biotic or abiotic stress (Mühlenbock et al., 2008; Szechyńska-Hebda et al., 2015, 2016a,b; Czarnocka et al., 2017). The environmental factors, like a sudden increase in light intensity, changes in temperature, limitation in water accessibility, or pathogen attack, all of them depress efficiency of CO<sub>2</sub> assimilation due to reduction of stomatal conductance, but do not limit foliar absorption of light energy (Müller et al., 2001; Mullineaux and Karpiński, 2002; Holt et al., 2004; Baker, 2008). It results in the excess excitation energy (EEE) in photosystem II,

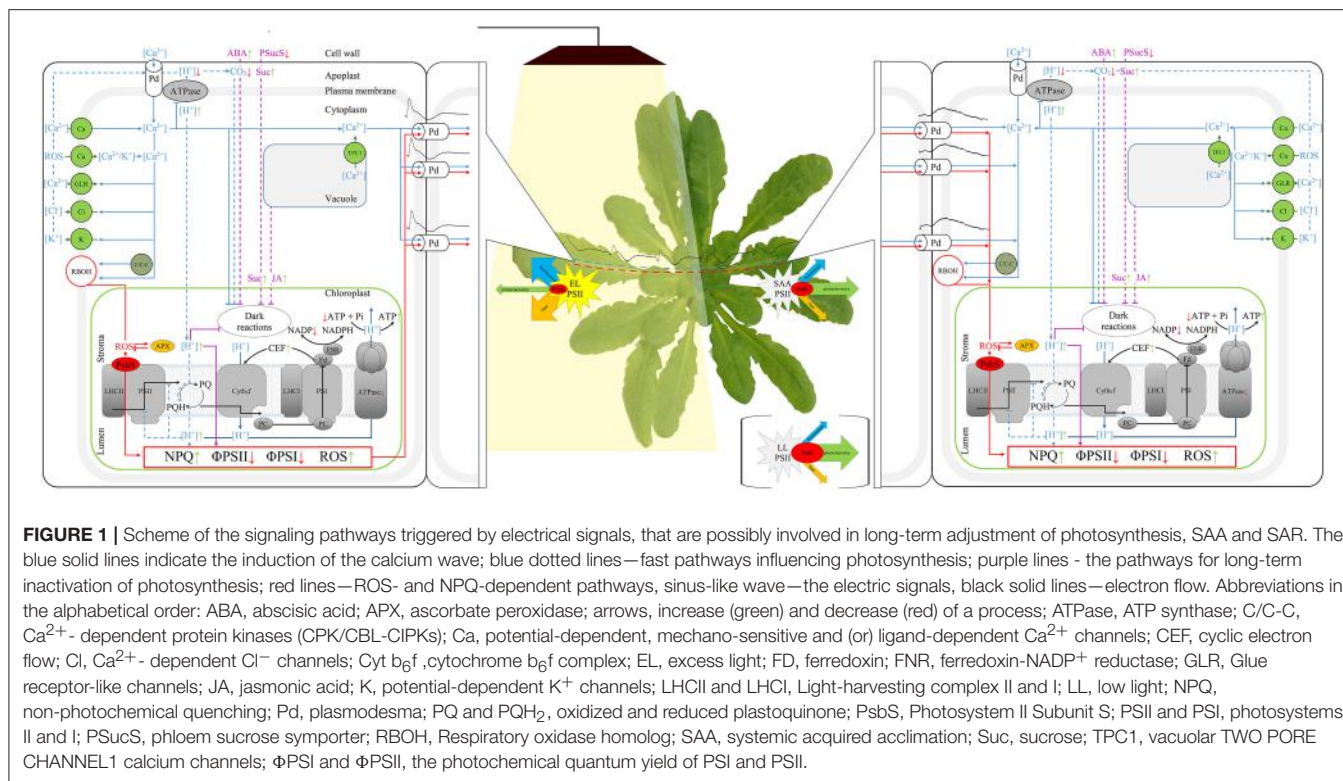
then the changes in redox status of the photosynthetic electron carrier chain (namely the plastoquinone pool) and bursts of ROS, and finally photoinhibition and programmed cell death (PCD) (Mühlenbock et al., 2008; Wituszynska et al., 2013, 2015; Szechyńska-Hebda et al., 2015). EEE-induced cell death is regulated by the same genetic system as the hypersensitive response in disease resistance and the systemic acquired resistance (SAR) (Dangl and Jones, 2001; Mühlenbock et al., 2008). The information about locally induced EEE, unbalanced redox status of the cell, and microlesions is communicated to distant cells and organs via photoelectrophysiological signaling (PEPS), which consists of the electrical waves (with amplitude in range of 10–50 mV, and the nature corresponding to VP or SP), followed with the changes in nonphotochemical quenching, reactive oxygen species (ROS), expression of ASCORBATE PEROXIDASE 2 (Szechyńska-Hebda et al., 2010) and the calcium ( $\text{Ca}^{2+}$ ) wave (Choi et al., 2017). PEPS can affect multiple physiological processes, e.g., respiration, transpiration, changes of ATP content, photosynthesis, transcription and translation of specific proteins, the synthesis of hormones such as ethylene, salicylic acid and jasmonic acid, in the tissues distant from those, which perceives the stimulus (Mühlenbock et al., 2008; Karpiński et al., 2013; Szechyńska-Hebda and Karpiński, 2013; Gilroy et al., 2016). Finally, the adjustment of such signaling components leads to induction of the systemic acquired acclimation (SAA) to abiotic stresses and simultaneously SAR to pathogens (Karpiński and Szechyńska-Hebda, 2010; Baluška, 2013; Karpiński et al., 2013; **Figure 1**).

The plant cells are able to physiologically “memorize” episodes of the EEE and following PEPS, and use this “memorized” information to improve their chances of survival in the future. It was demonstrated that fast development of infection has occurred in *Arabidopsis* plants grown under LL conditions. When the plants were infected prior to the excess light treatment, the bacteria initiated the wide-spread infection process too. However, in plants infected 1, 8 or 24 h after the excess of white or red light incident, bacteria growth was effectively inhibited. A partial exposition of *Arabidopsis* rosette to excess light has also induced the acclimation and defense responses in systemic tissues (Szechyńska-Hebda et al., 2010). Thus, the long-distance systemic signaling of EEE incident has two consequences. Coordination of electrical signals and wave-like changes in NPQ,  $\text{H}_2\text{O}_2$ , *APX1*, *APX2*, and  $\text{Ca}^{2+}$  allows the whole plant to prepare for future challenges, like abiotic and biotic stresses (**Figure 1**). However, one should hypothesize, that changes in the components accompanying the electrical signal allow to differentiate the type of response.

To enable short and long distance electrical signaling to induce SAA and SAR responses, different compartments of the cell and then different cells must be interconnected. At cellular level, chloroplasts can form a cellular network of extended chloroplast envelope membranes, known as stromules, to connect each other, and various organelles (e.g., the nucleus and plasma membrane). Some evidences suggest that this network of stromules is important for signaling and induction of acquired acclimation and resistance. The stromules are formed in response

to light-sensitive redox signals within the chloroplast. Their number increases during the day; after treatment with specific inhibitors of the photosynthetic electron transport (DCMU, 3-(3,4-dichlorophenyl)-1,1-dime-thylurea, DBMIB, 2,5-dibromo-6-isopropyl-3-methyl-1,4-benzoquinone); and as an effect of ROS production, specifically in the chloroplast (Brunkard et al., 2015). Similarly, chloroplasts form stromules during infection or exogenous application of hydrogen peroxide ( $\text{H}_2\text{O}_2$ ) and salicylic acid (SA). Numerous stromules have surrounded nuclei during defense response and these connections correlated with an accumulation of chloroplast-localized NRIP1 defense protein and  $\text{H}_2\text{O}_2$  in the nucleus (Caplan et al., 2015). At intercellular level, AP and VP can propagate through plasmodesmata of the bundle sheath cell layer (Szechyńska-Hebda et al., 2010; Sager and Lee, 2014). The electrochemical potential propagation is effective, provided there is the membranes integrity (plasma membrane and their extension, i.e. the plasmodesmata—plasma membrane of another cell). Indeed, plasmodesmata are highly dynamic intercellular channels in the cell wall, containing, at its axial center the strands of the endoplasmic reticulum that are continuous between cells (Burch-Smith and Zambryski, 2010). Another path of the electrical signal propagation from cell to cell, independent of the PD, is depolarization of the cell plasmamembrane of an adjacent cell without direct connection (Gilroy et al., 2016). In both cases, resistance is too high for electrical waves to travel over distances larger than few neighboring cells. Therefore, other components could be involved, to enable more active electrical signaling, and it is hypothesized, that changes in the photosynthetic electron transport in light-treated chloroplasts are required to electrical signal propagation. If mechanical damage, treatment with  $\text{LaCl}_3$  (inhibitor of ion channels activity) or DCMU were made to the central vein in petiole of a leaf directly exposed to excess light, then such a leaf was not able to communicate SAA by electrochemical signaling. As a consequence, the expression of SAA marker genes (*APX1* and *APX2*) was not changed, and further SAA and SAR were not induced (Mühlenbock et al., 2008; Szechyńska-Hebda et al., 2010).

The chloroplasts in bundle sheath cells of veins have a minor role in the photosynthetic yield of leaves. Instead, they have a unique redox, hormonal and carbon metabolism (Kangasjärvi et al., 2009). Thus, a potential role for chloroplasts, in bundle sheath cell is to participate actively in autopropagation of electrochemical signaling. The relation between the chloroplasts and plasmodesmata-mediated intercellular signal propagation can be further supported by presence of the INCREASED SIZE EXCLUSION LIMIT 2 (ISE2) protein (Burch-Smith and Zambryski, 2010). Careful studies of ISE2-GFP localization reveal that ISE2 is a plastid protein acting as a regulation hub of both, plastid development and spatial organization of the plasmodesmata. The *ise1* and *ise2* mutation results in increased formation of twinned and branched plasmodesmata that facilitate the intercellular transport. Plasmodesmal permeability and remodeling can be also modified by cellular redox status and hydrogen peroxide presence, in both chloroplasts and mitochondria. Further, salicylic acid produced



in chloroplasts, plays a role in closure of the plasmodesma through PLASMODEMATA-LOCATED PROTEIN 5 (PDLP5) (Lee et al., 2011) and in enhancing plasmodesmal complexity (Fitzgibbon et al., 2013). These data add plastid-to-nucleus signaling to plasmodesmata integrity as a critical factor in the plant communication network. Using plasmodesmata in conjunction with a phloem-based transport system, cells can deploy AP long-distance signaling between plant organs (Fromm and Lautner, 2007). Sieve tubes create a low-resistance pathway due to their plate pores and a continuum of plant plasma membranes. The length of a phloem vessel varies from several mm to several m, with diameters in the range from 1 to 100 mm.  $\text{Ca}^{2+}$  permeable channels located in the plasma membrane of the sieve tubes were shown to be associated with propagation of electrical signals induced by biotic and abiotic stresses (for review, see van Bel et al., 2014; Choi et al., 2017). Similarly, xylem participates in VP propagation and together with hydraulic waves it is responsible for systemic responses. Taken together, photosynthesis-dependent co-propagation of the electrical waves, ROS, calcium, and hydraulic waves, is a physiological prerequisite for induction of whole plant acclimation and systemic defense responses (SAA and SAR, Figure 1). SAA and SAR have been studied mainly in the leaves and flowering stems, however, the systemic propagation of signals is not limited to the aerial parts of plants. A role of the electrical signaling in roots was recently proposed. The electric field in the root rhizosphere reach up to  $500 \text{ mV cm}^{-1}$  and this is about two orders of magnitude higher than a threshold for electrotaxis for some soil-dwelling organisms. Thus, the leaf

electric potential resulting from light or temperature fluctuations may propagate down to roots and modify the strength of electric fields in the rhizosphere, affecting the extent of root colonization by plant pathogens (Shabala et al., 2016). Due to the lack of chloroplasts in the root tissues, however, different physiological and molecular mechanism are involved in this signal propagation.

## EXCESS EXCITATION ENERGY AND ELECTRICAL SIGNALING

Chloroplasts and photosynthesis seem to play a key role in triggering of electrical signals and adjustment of the components accompanying this signaling (PEPS). Plants, as sensible organisms, which cannot migrate when environmental conditions change and whose individual organs may experience different stress factors at the same time, need to take a benefit from specific mechanisms to cope with environmental heterogeneity. Many of the stress factors induce the excess excitation energy, over that required for optimal photosynthetic metabolism. In the classical view, the failure to dissipate EEE during stress is damaging to plants and often manifests as chlorosis, bleaching, or bronzing of leaves due to imbalanced metabolism of ROS. However, this could be the most universal system to use energy of the photons absorbed in the excess to improve survival chances of a whole plant (induction of the SAA and SAR). This mechanism has evolved in the photosynthetic organisms, since the light, in this context, is the most powerful

and divergent factor. Quantity and quality of light in a plant canopy, changing day length, or spatial and temporal variations in the amount of radiation useful to photosynthesis, all of them affect plant growth and morphology, which in turn affect competition for light. Light was shown to modulate plant responses to almost all other stress factors (Karpiński et al., 2013). Thus, dynamic response of the plant to transient EEE incidents had an adaptive significance and determine plant Darwinian fitness.

Electrical signal propagation requires functional and photosynthetically active chloroplasts. The excess light triggers specific pattern of changes in plasma membrane electrical potential (**Figure 1**, Szechyńska-Hebda et al., 2010; Białasek et al., 2017). At the same time, local excess light exposure causes a rapid saturation of the photosynthetic reaction centers and their closure. This leads to a reduction in the fraction of energy utilized in photosynthesis, inhibition of the photosynthetic electron transport (photochemical reactions), the subsequent build-up of excess excitation energy in the photosynthetic membrane, and harmful ROS generation (Ruban, 2016). The mechanisms of photosynthetic electron transport and the electrical signaling, were proved to be interrelated. Excess light-triggered changes in plasma membrane potential, and then systemic propagation of the electrical potential were inhibited by DCMU, which prevents reduction of plastoquinone at photosystem II and generates singlet oxygen. The systemic propagation of the electrical signal was also deregulated by DBMIB, which prevents plastoquinol from reducing the cytochrome *b6f* complex, and generates superoxide (Szechyńska-Hebda et al., 2010; Ciszak et al., 2015; Gilroy et al., 2016; Białasek et al., 2017). Similarly, electrical signaling triggered by the excess light, had a reduced amplitude in *cad2* and *rax1* mutant (Szechyńska-Hebda et al., 2010). These mutants have deregulated glutathione synthesis, NPQ, the redox state of the PQ pool, APX2 expression, SAA, and SAR (Ball et al., 2004). The second step of glutathione synthesis in the chloroplasts is important for regulation of APX2 expression, light acclimatory and immune defense responses. Therefore, it is not surprising, that EEE-triggered pattern of the electrical signal in the *apx2-1* recessive mutant was also different, when compared to the wild type plant. Taken together, propagation of the electrical signal as well as other components of PEPS, are directly dependent on the excess energy in chloroplasts and efficiency of photochemical reactions (Szechyńska-Hebda et al., 2010).

Considering above, all factors and mechanisms controlling the local level of the EEE in chloroplasts, other than photochemical reactions, can modify the electrical signaling and PEPS. Nonphotochemical quenching (NPQ) is a process in which light energy absorbed in excess, is dissipated into heat (Demmig-Adams et al., 2014; Ruban, 2016). It requires the trans-tylakoidal pH gradient and the proton sensor protein (PsbS) and prevents ROS generation. Some evidences indicate that NPQ, PsbS protein, H<sub>2</sub>O<sub>2</sub> level, APX2 are interrelated and play an important role in an electrical signal propagation inducing SAA and SAR. First, PsbS is required for SAA and light stress memory in *Arabidopsis* (Szechyńska-Hebda et al., 2010; Ciszak et al., 2015). The wild type rosettes exhibit a

small reduction of fluorescence decay time in leaves directly exposed to excess light and in leaves undergoing SAA in low light conditions. However, recessive *Arabidopsis* mutant *npq4-1* has lost the ability to optimize fluorescence decay time after the excess light episode. It can be concluded that functional PsbS is required for optimization of the absorbed energy, thus quantum-molecular properties of PSII complexes in local and systemic leaves undergoing SAA. Second, PsbS is essential for zeaxanthin-dependent conformational changes in the thylakoid membrane that in turn are necessary for ΔpH-dependent regulation of NPQ (qZ). The lack of PsbS protein and dysfunction of the NPQ process influence the spatial and temporal pattern of the electrical membrane potential (**Figure 2**). Mutant *npq4* had small amplitude of plasma membrane potential after the light switching on and off, whereas plant with the PsbS overexpression (*oePsbS*) had an increased amplitude of membrane potential in comparison to the wild type plants. The kinetics of the electrical response was also different. The hyperpolarization, depolarization and subsequent repolarization of the plasma membrane of *npq4* mutant occurred within 9 min after switching on the light, while within seven and 6 min for wild type and *oePsbS*, respectively. Although, SAA and SAR are triggered by integrated wavy-like changes in the electrical signal, NPQ, H<sub>2</sub>O<sub>2</sub>, and APX2, the role of NPQ in the alternation of a membrane potential seems to be principal. Despite the higher APX2 transcript level has been detected in *npq4* leaves (Szechyńska-Hebda et al., 2010), it did not prevent such considerable changes in electrical potential of its plasma membrane (**Figure 2**). Third, the photoelectrophysiological signaling, wavy-like changes in

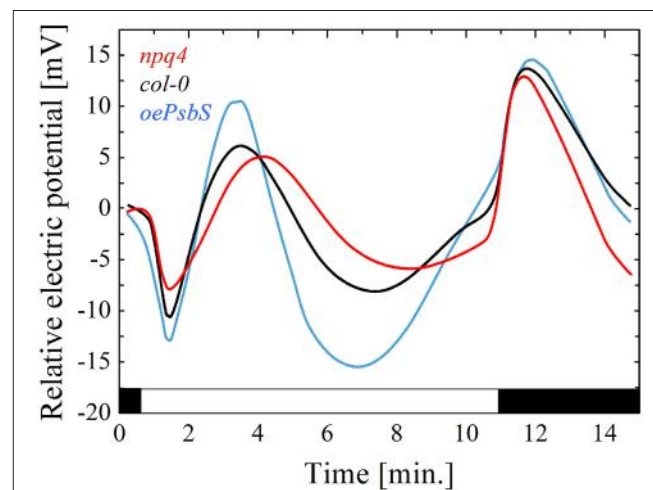


**FIGURE 2 |** The electrical signals generated on the leaf surface in variable light conditions. Relative changes in the plasma membrane electrical potential were recorded for genotypes differing in PsbS protein content: red line, recessive mutant *npq4* devoid of PsbS; black line, WT ecotype Col-0; blue line, overexpressing line of *oePsbS*. Generally, the pattern of electrical signal detected on the leaf surface is reversed, when measured intracellularly. The recording by surface contact electrode detects a mixture of the signals from the three types of cells: guard, epidermal and mesophyll cells, and they can differ in their responses to light.

NPQ and H<sub>2</sub>O<sub>2</sub>, redox status of the glutathione and PQ pools, hormonal circuits (salicylic acid, jasmonic acid, ethylene), and the cellular light “memory” (Mühlenbock et al., 2008; Szechyńska-Hebda et al., 2010; Karpiński et al., 2013) were proposed as the mechanisms coordinating light acclimation (SAA), immune defenses (SAR), photosynthesis, transpiration, and developmental processes in the plants. The optimization of these processes are performed in a way similar to that defined by the algorithm of the cellular automation (Peak et al., 2004). When, leaves have experienced the patchy changes in F<sub>v</sub>/F<sub>m</sub>, NPQ, stomatal aperture, they “calculated” such changes to optimize cellular metabolism in leaves exposed to light and in leaves undergoing SAA.

The electrical signal propagation after the excess light treatment, mechanical wounding, burning, and current stimulation can also inactivate photosynthesis in systemic untreated tissues (Szechyńska-Hebda et al., 2010; Sukhov et al., 2015; Sukhov, 2016). The decrease of the effective quantum yields of photosystem I and II, reduction of CO<sub>2</sub> assimilation rate, increase of NPQ were observed in the first 10–20 min after stimulation (Szechyńska-Hebda et al., 2010; Sherstneva et al., 2015; Sukhov et al., 2015; Sukhov, 2016). The photosynthetic responses were absent, if the electrical signals (PEPS) triggered by EEE do not propagate to systemic tissues or propagate with strongly reduced amplitudes (Szechyńska-Hebda et al., 2010), and it shares similarities with other types of electrical signals and stimuli (Sukhov et al., 2015). The strongest response was observed in the inter-vein area, where the photosynthetically active mesophyll cells are located. However, the photosynthetic changes in the veins were more rapid, thus suggesting the spread of electrical signals *via* the veins into the mesophyll cell (Koziolek et al., 2004; Bialasek et al., 2017). Considering systemic changes in photosynthesis, the AP is less effective than VP. It can result from the restriction of AP spread in phloem without reaching the mesophyll cells, or from the stimulation of stomata opening. In most cases, the systemic photosynthetic response depends linearly on the VP amplitude (Sherstneva et al., 2015), thus the distance from site of stimulus. However, VP have ability to spread even over dead tissues zones and is not restricted in its propagation. Furthermore, VP induces stomata closure (via membrane depolarization, increased Ca<sup>2+</sup> concentration, induction of ABA and JA), negatively influencing photosynthesis (Pavlovic, 2012). Electrical signals arising at the plasma membrane change ionic status of the cell (**Figure 1**). Probable mechanisms of photosynthesis inactivation involve H<sup>+</sup> and (or) Ca<sup>2+</sup> influxes. The reversible inactivation of the plasma membrane H<sup>+</sup>-ATPase during the electrical signals propagation (mainly VP) has an important consequence, i.e., acidification of the cytoplasm and alkalization of the apoplast of plant cells, the extend of which correlates with the VP amplitude (Sherstneva et al., 2015). Electrical signals transmitted to the thylakoid membranes also influence pH gradient at the thylakoid membrane, photoelectrochemical field, the charge separation, recombination reactions in PSII (Koziolek et al., 2004; Bulychev and Kamzolkina, 2006), and energy-dependent NPQ ( $\Delta$ pH-dependent qE) (Krupenina and Bulychev, 2007). However, changes in PSII including an increase

in NPQ may be determined by intensity of the stimuli and thus the parameters of VPs (Vodeneev et al., 2017). Hypothetical mechanism consists of the increase in cytoplasmic Ca<sup>2+</sup> level via opening of plasma membrane Ca<sup>2+</sup> channels and the release of Ca<sup>2+</sup> from intracellular stores. Since, the chloroplast envelope is endowed with a light-dependent Ca<sup>2+</sup> uniport, the accumulation of Ca<sup>2+</sup> in the stroma is ensured. Candidates for the transport across the chloroplast envelope are proteins: ACA1, HMA1, GLR3.4, MSL2/3, and PPF1. The predominant portion of the chloroplastic Ca<sup>2+</sup> can be bound to the negatively charged thylakoid membranes or to calcium-binding proteins, and thus Ca<sup>2+</sup> influx can be linked to photosynthetic electron transport via the membrane potential. Further, the import of Ca<sup>2+</sup> across the thylakoid membrane has been shown to be dependent on a light- or ATP-induced transthylakoid proton. Excess light-induced acidification leads also to reversible release of Ca<sup>2+</sup> from PSII and an inactivation of oxygen evolution gradient (detailed review by Hochmal et al., 2015). The further development of the response can be associated with a decrease in the activity of the dark reactions of photosynthesis (Sherstneva et al., 2015). Accumulation of Ca<sup>2+</sup> in the chloroplast suppresses CO<sub>2</sub> fixation (Pottosin and Shabala, 2016), and K<sup>+</sup> transport is important to these processes. In *Arabidopsis*, TPK3, a member of a tandem-pore K<sup>+</sup> channel family, is localized to the thylakoids. Plants silenced for the TPK3 gene showed lower CO<sub>2</sub> fixation and altered NPQ (Carraretto et al., 2013). Modulation of this channel by natural factors was unexplored, although TPK3 appeared to display a higher activity at high (>100 mM) Ca<sup>2+</sup> (Pottosin and Shabala, 2016). Calcium is also believed to be important for the carbon metabolism by the regulation of several key enzymes, including fructose 1,6-bisphosphatase and sedoheptulose 1,7-bisphosphatase of the reductive pentose phosphate cycle (Hochmal et al., 2015). VP-induced stomata closure increases the HCO<sub>3</sub><sup>-</sup>: CO<sub>2</sub> ratio and decreases CO<sub>2</sub> net uptake into chloroplasts (Pavlovic et al., 2011; Gallé et al., 2013; Sukhov et al., 2016). An increase in the external Ca<sup>2+</sup> concentration has been shown to be crucial for regulating the stomatal aperture in *A. thaliana*. Usually, the closure of stomata *via* an increase of the external Ca<sup>2+</sup> concentration is accompanied by transient and repetitive elevations in [Ca<sup>2+</sup>]<sub>cyt</sub>. Calcium sensor protein CAS is required for proper stomatal regulation in response to elevations of external Ca<sup>2+</sup> through the modulation of cytoplasmic Ca<sup>2+</sup> dynamics (Hochmal et al., 2015). Carbonic anhydrases can mediate the changes in HCO<sub>3</sub><sup>-</sup>: CO<sub>2</sub> ratio in light-dependent manner (Dąbrowska-Bronk et al., 2016). The decrease in the CO<sub>2</sub> flow can also be linked to the changes in abscisic acid accumulation observed during VP generation (**Figure 1**, Sukhov et al., 2016). The decrease in CO<sub>2</sub> assimilation in response to VP was observed in different plants with different extend: 22% of the assimilation under illumination in pumpkin, 55% decrease in the assimilation in pea, decreased by ~100% of the CO<sub>2</sub> absorption under illumination in geranium (Sherstneva et al., 2015). Furthermore, cyclic electron flow could be partially rescued by an increase in the extracellular Ca<sup>2+</sup> concentration and CAS. Cyclic electron flow and qE are interconnected as cyclic electron flow participates in acidification of the thylakoid lumen, which is required for efficient qE. It also interconnects PSI and

$\text{Ca}^{2+}$ -dependent control. Taken together these data underline primary role of calcium in regulation of the photo-protective mechanisms and chloroplast metabolism (Hochmal et al., 2015). It also suggests that photosynthesis and electrical signaling can be regulated/deregulated by the same or at least similar mechanisms in local and systemic tissues (Szechyńska-Hebda et al., 2010).

White, red and blue light stimulated similar temporal pattern of changes in the electrical membrane potential. However, amplitude and speed of the electrical signal can vary with quality of the light, and it suggests that apart from chloroplasts, different photoreceptors (phytochromes, cryptochromes, phototropins) can influence signals propagation in plasma membrane. Several photoreceptors can trigger cytosolic  $\text{Ca}^{2+}$  signals to stimulate changes in photosynthesis, e.g., phototropins in hypocotyls cells (Folta et al., 2003) and phytochromes in caulinema cells (Ermolayeva et al., 1997). Generally, VP and SP are preferably triggered by red light (Okazaki, 2002; Sukhov et al., 2016).

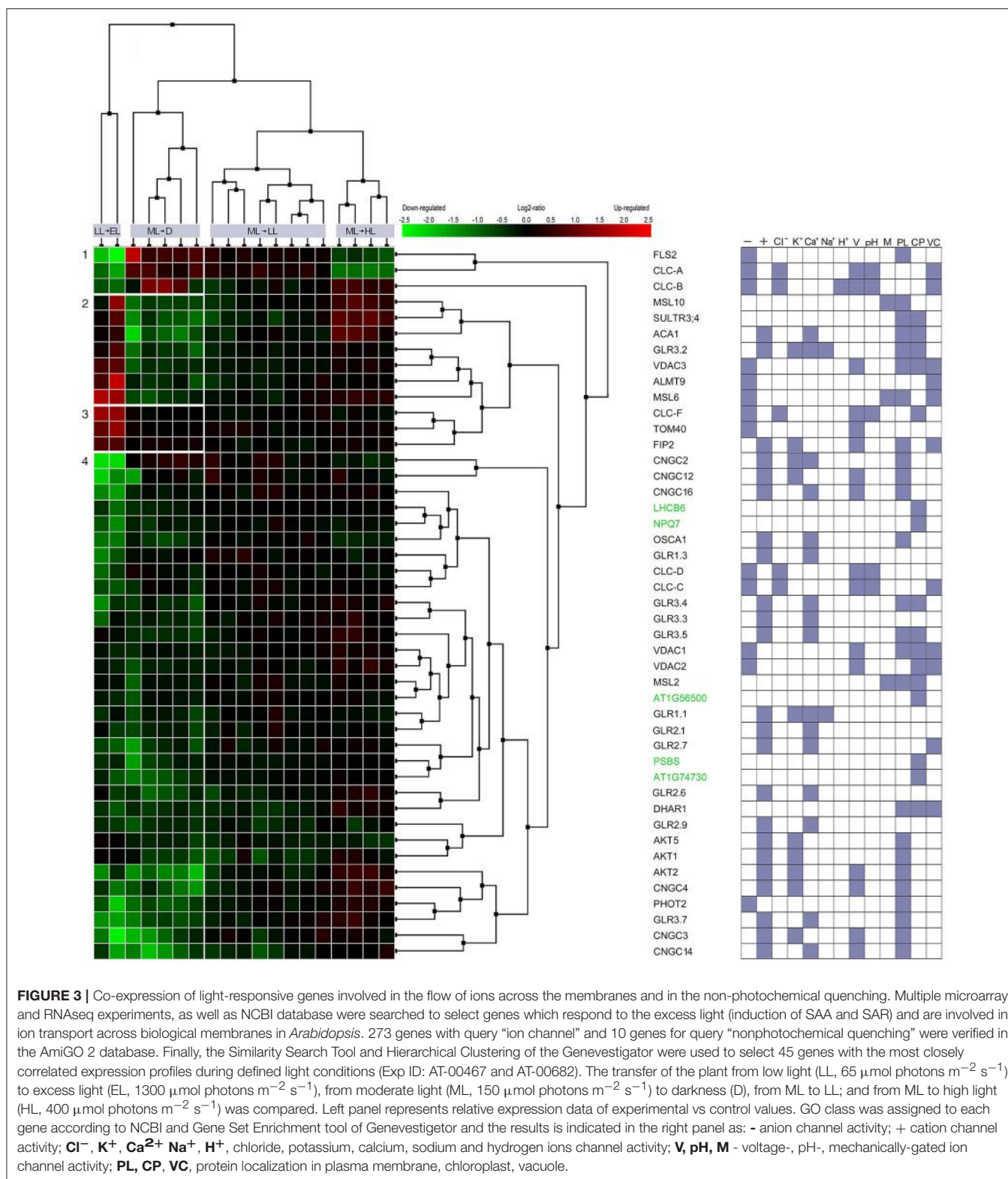
## SYSTEMIC REGULATION OF EXCESS LIGHT-RESPONSIVE GENES ENCODING ION CHANNELS

Approximately 5% of the *Arabidopsis* genome encodes integral membrane transport proteins, classified in 46 families containing ~880 members (Mäser et al., 2001). Some of the ion channels play a key role in the generation and sensing of electrical activity that depends on the light. They are involved in the exchange of the ions between extra-and intracellular space, across plasma membrane. Channels switch between transporting and non-transporting (open and closed) states by a stochastic process referred to as gating, is influenced by a variety of factors (e.g., voltage-, pH-, mechanically-gated) (Spalding, 2000). Many early studies have focused on the changes of membrane electrical potential and its local ionic mechanism during light to dark transition (Jeschke, 1976; Trebacz and Zawadzki, 1985; Trebacz et al., 1989). Although, the design of experiments can influence the pattern of electric signal (Figure 2, Białasek et al., 2017), in most cases, the dark (or low light) to light (or high light) transition results in a short hyperpolarization, followed by a depolarization, and repolarization of membrane (Szechyńska-Hebda et al., 2010). A proton pump,  $\text{K}^+$ ,  $\text{Cl}^-$ , and  $\text{Ca}^{2+}$  ion channels were proposed to participate in the light-induced changes of a membrane potential (Figure 1, Dietrich et al., 2001; Živanović et al., 2005, 2015). The hyperpolarization can result from proton extrusion via the  $\text{H}^+$ -ATPase, an electroenzyme residing in the plasma membrane at high density (Dietrich et al., 2001; Živanović et al., 2005, 2015) as well as from the activity of the voltage-dependent inward rectifying  $\text{K}^+$  channels (Yan et al., 2009). The mechanism of AP depolarization can occur via an influx of  $\text{Ca}^{2+}$  through voltage- or mechanically-gated  $\text{Ca}^{2+}$  channels. The elevated  $\text{Ca}^{2+}$  concentration triggers the sequence of events: activation of voltage-dependent anion channels and the efflux of  $\text{Cl}^-$ , activation of the outward  $\text{K}^+$  channels and  $\text{K}^+$  efflux, gradual inactivation of  $\text{Cl}^-$  channels. The changes in activity of  $\text{K}^+$  and  $\text{Cl}^-$  channels lead

finally to membrane repolarization and its return to level of resting potential. VPs and SPs are rather initiated through a transient inactivation of plasma membrane proton pump  $\text{H}^+$ -ATPase, which causes a slow depolarization of the membrane potential (Fromm and Lautner, 2007). However,  $\text{Ca}^{2+}$ ,  $\text{Cl}^-$ , and  $\text{K}^+$  channel activation might also participate in the process (Sukhov, 2016).

It was suggested that a key component of the electrical waves kinetics and the tissue-specific nature of the spatial patterning of wave transmission may lie in the regulation of its channel activity rather than its gene expression pattern (Choi et al., 2016). However, the induction of vascular genes, i.e., *APX1*, *APX2*, *ZAT10*, can follow almost immediately electrical signal propagation. The exposure of older leaves on the rosette to very high light triggers the signal which moves within 15–30 min via the vasculature toward non-exposed younger rosette leaves (Figure 1), cauline leaves, and the stem of the floral bolt (Szechyńska-Hebda et al., 2010). The induction of EEE, SAA, and SAR marker genes have already been detected within 20–30 min at the same localization on the signal path (Karpiński et al., 1999; Rossel et al., 2007; Szechyńska-Hebda et al., 2010). Moreover, exposure to HL increased the expression of 360 genes and decreased the expression of 247 genes in distal leaves after 30 min (Rossel et al., 2007). In the same way, changes in expression of the genes encoding the ion channels or the proteins regulating ion channel activity take a part of light-dependent mechanism in the plant cells (Figure 3). The differentially expressed genes (in relation to untreated control plants) were detected 30 min after excess light exposure, and 60 min after shift to dark. Interestingly, significant changes in the expression were found, provided the light stress exceed defined threshold. The fluctuations in the range from low light to excess light and from moderate light to darkness have altered 20% of genes toward their induction and 80% of genes toward their suppression. Transfer of the plant from moderate light to low light or high light did not induce considerable changes in gene expression (Figure 3). It suggests analogy with depolarization, which needs to exceed a certain threshold to trigger AP, SAA and SAR (Karpiński et al., 1999; Szarek and Trebacz, 1999; Szechyńska-Hebda et al., 2010).

Genes encoding ion channels critical for the control of long-term responses during excess light fluctuations (that can trigger SAA and SAR) were clustered in several groups. Among the genes in cluster no 1, *FLS2* was down regulated during LL to EL shift and upregulated during ML to D shift. *FLS2* is a plasma membrane receptor-like kinase (RLK), which can recognize a 22-aminoacid residue stretch of the flagellin protein from *Pseudomonas syringae*. *FLS2* is involved in early signaling pathways such as: activation the anion channels (e.g., *SLAH3*) through cytosolic  $\text{Ca}^{2+}$  signals and inhibition the guard cell inward  $\text{K}^+$  channels. The regulation of these channels is important to rapid stomatal closure, thereby retarding pathogen invasion (Zhang et al., 2008; Guo et al., 2014; Deger et al., 2015), but also influencing photosynthesis. *FLS2* complexes with *BAK1* and *BKK1* play a role in the regulation of *AtCLCs* expression (Guo et al., 2014). Indeed, genes encoding *CLC-A*, ion channel protein regulating the outward anion fluxes across the vacuolar membrane (Wege et al., 2014) and *CLC-B*, ion channel protein



mediating  $\text{NO}_3^-/\text{H}^+$  exchange across the tonoplast (von der Fecht-Bartenbach et al., 2010), both were co-expressed with FLS2 (Figure 3, Table 1). They suppression under EL treatment

suggests that SAR (and SAA) induced by EL (Karpiński et al., 1999) would not overlap with FLS2- and CLCs-dependent pathways and resistance. Similarly, genes encoding AtCLC-C and

AtCLC-D, the anion transporters negatively regulating pathogen-associated molecular pattern (PAMP)-triggered immunity (PTI) and stomatal movement (Jossier et al., 2010; Guo et al., 2014), both were down-regulated during fluctuating light conditions (cluster of the genes no 7). In contrast, *CLC-F*, a chloride channel protein, was upregulated during shift to EL (cluster of the genes no 3), but its involvement in light-triggered responses could be related to cellular localization in the chloroplast and Golgi apparatus. Thus, *CLC-F* is rather involved in the second mechanism described below.

Up-regulated genes during plant shift to EL, and down-regulated genes during plant transfer to dark, were clustered into group no 2. Among them, genes encoding MSL10 and two other members of the MSL family (MSL1, MSL6), were found. They are mechanically-gated ion channels, responsible for anion transport, functioning as osmotic safety valves and releasing osmolytes under increased membrane tension. MSL10 is located in plasma membrane and regulates PCD signaling. High-level expression of *MSL10*-GFP in *Arabidopsis* induced small stature, H<sub>2</sub>O<sub>2</sub> accumulation, ROS- and CD-associated gene expression (Maksaev and Haswell, 2012; Veley et al., 2014). A role of MSL1 (SULTR3;4) is diverse. MSL1 participate in sulfate and Pi translocation (Cao et al., 2013), and along with MSL2 and MSL3, controls plastid division and organelle morphology (Haswell et al., 2008; Wilson et al., 2011). MSL6 is located in plasma membrane and plasmodesma, what suggests its role in transportation or signal propagation. Further, two genes involved in calcium transport were found in the cluster no 2. ACA1, a calmodulin-activated calcium channel protein, is the most promising candidate for the calcium import across the inner chloroplast envelope membrane (Carrasco et al., 2016). GLR3.2 (AtGLR2), an intracellular ligand-gated ion channel protein, maintains cellular calcium, potassium, and sodium ion homeostasis. Its deregulation led to Ca<sup>2+</sup> deficiency, hypersensitivity to Na<sup>+</sup> and K<sup>+</sup> ionic stresses, death of the shoot apex, necrosis and deformation of leaves. The promoter of the *AtGLR2* gene was active in vascular tissues, particularly in cells adjacent to the conducting vessels (Kim et al., 2001). Finally, two genes encoding proteins with anion channel activity were upregulated in EL and downregulated in dark. VDAC3, anion channel being the most abundant in plasma membrane (Robert et al., 2012) is involved in the hypersensitive response, regulation of seed germination, and response to cold; whereas ALMT9, is a malate-activated vacuolar chloride channel, having a major role in controlling stomata aperture (De Angeli et al., 2013). This set of genes can be extended with three additional genes encoding proteins with poorly known physiological function. They are clustered into the group no 3, as induced in response to shift from LL to EL, but with the expression unchanged in dark. First, CLC-F, a voltage-gated chloride channel protein, being a component of the outer envelope membrane of chloroplasts (Teardo et al., 2005) or Golgi membranes (Marmagne et al., 2007). Consistent with the plastidial localization of CLC-F, the protein is expressed in leaf etioplasts and chloroplasts, but not in root tissue (Teardo et al., 2005). CLC-F may operate at contact sites, where it may sense voltage and regulate chloride flux into the stroma. Second, TOM40 is exclusively localized

**TABLE 1 |** The genes involved in the flow of ions across the membranes and in the non-photochemical quenching, which expression is graphically presented on Figure 3.

	Gene/product	Gene/product name
1	FLS2	AT5G46330 Leucine-rich receptor-like protein kinase family protein
	CLC-A	AT5G40890 Chloride channel A
	CLC-B	AT3G27170 Chloride channel B
2	MSL10	AT5G12080 Mechanosensitive channel of small conductance-like 10
	SULTR3;4, MSL1	AT3G15990 Sulfate transporter 3;4
	ACA1	AT1G27770 Autoinhibited Ca2+-ATPase 1
	GLR3.2, GLUR2	AT4G35290 Glutamate receptor 2
	VDAC3	AT5G15090 Voltage dependent anion channel 3
	ALMT9	AT3G18440 Aluminum activated malate transporter 9
3	MSL6	AT1G78610 Mechanosensitive channel of small conductance-like 6
	CLC-F	AT1G55620 Chloride channel F
	TOM40	AT3G20000 Translocase of the outer mitochondrial membrane 40
4	FIP2	AT5G55000 Potassium channel tetramerization domain-containing protein
	CNGC2, DND1	AT5G15410 Cyclic nucleotide-regulated ion channel family protein
	CNGC12	AT2G46450 Cyclic nucleotide-gated channel 12
5	CNGC16	AT3G48010 Cyclic nucleotide-gated channel 16
	LHCB6	AT1G15820 Light harvesting complex photosystem II subunit 6
	NPQ7	AT1G65420 Antigen receptor-like protein
	OSCA1	AT4G04340 ERD (early-responsive to dehydration stress) family protein
	GLR1.3	AT5G48410 Glutamate receptor 1.3
	CLC-D	AT5G26240 Chloride channel D
	CLC-C	AT5G49890 Chloride channel C
	GLR3.4	AT1G05200 Glutamate receptor 3.4
	GLR3.3	AT1G42540 Glutamate receptor 3.3
	GLR3.5	AT2G32390 Glutamate receptor 3.5
	VDAC1	AT3G01280 Voltage dependent anion channel 1
	VDAC2	AT5G67500 Voltage dependent anion channel 2
	MSL2	AT5G10490 MSCS-like 2
	SOQ1	AT1G56500 Suppressor of quenching 1
	GLR1.1	AT3G04110 Glutamate receptor 1.1
	GLR2.1	AT5G27100 Glutamate receptor 2.1
	GLR2.7	AT2G29120 Glutamate receptor 2.7
	PsbS, NPQ4	AT1G44575 Chlorophyll A-B binding family protein, Nonphotochemical quenching 4
6	RIQ2	AT1G74730 Transmembrane protein, putative
	GLR2.6	AT5G11180 Glutamate receptor 2.6
	DHAR1	AT1G19570 Dehydroascorbate reductase
	GLR2.9	AT2G29100 Glutamate receptor 2.9
	AKT5	AT4G32500 K+ transporter 5
	AKT1	AT2G26650 K+ transporter 1
	AKT2	AT4G22200 Potassium transport 2/3
	CNGC4	AT5G54250 Cyclic nucleotide-gated cation channel 4
	PHOT2	AT5G58140 Phototropin 2
	GLR3.7/GLR5	AT2G32400 Glutamate receptor 5
	CNGC3	AT2G46430 Cyclic nucleotide gated channel 3
	CNGC14	AT2G24610 Cyclic nucleotide-gated channel 14

to outer mitochondrial membrane and is mainly involved in pore formation, protein targeting and import into mitochondria. However, voltage-gated anion channel activity and ion transport were also considered (Werhahn et al., 2001; Lister et al., 2004). Third, FIP2 is voltage-gated potassium channel located in plasma membrane and vacuole.

Considering localization and function of the above proteins that are induced in EL, but suppressed or unchanged in dark, the tight relations between chloroplasts and plasma membrane, between photosynthesis and long-distance electrical signals propagation, and between SAA and SAR can be assumed (**Figures 1, 3**). Although, the cell is compartmented, there is no doubt that ionic changes in one organelle can influence the others; however, studies clarifying these interrelations are rare. Indirect evidences suggest possible mechanisms. The one of the first response is pH change in both, the cytosol and chloroplast. Hyperpolarization of plasma membrane, induced during EL, can be mediated by H<sup>+</sup>-ATPase activity. H<sup>+</sup>-ATPase was shown to play a main role in VP and SP generation, and participate in AP development (Sukhov, 2016). In chloroplast, EL leads to the generation of a proton motive force (pmf), which comprises a proton gradient ( $\Delta\text{pH}$ ) and a transmembrane electrical potential difference ( $\Delta\Psi$ ). The changes in pH induce fluxes of Cl<sup>-</sup>, K<sup>+</sup>, and Ca<sup>2+</sup> through plasma membrane and chloroplast envelope (**Figure 1**). Ca<sup>2+</sup> dependent Cl channel activation during AP and VP was suggested as the potential mechanism of pH changes in cytosol; and a light-induced anion accumulation in thylakoids, including Cl<sup>-</sup> concentration on the luminal side, was also recorded during shift of the plant to light conditions. Electrical signal-dependent K<sup>+</sup> efflux across plasma membrane could influence the pH, because fixed negative charges can concurrently bind H<sup>+</sup> and K<sup>+</sup>. Similarly, some potassium ion channels of the thylakoid membrane, can modulate the composition of the pmf through ion counterbalancing (e.g., Ca<sup>2+</sup> and H<sup>+</sup>) (Carraretto et al., 2013). Potential-dependent Ca<sup>2+</sup> channels activate AP; and ligand-dependent and mechanosensitive Ca<sup>2+</sup> channel trigger VP. Then, Ca<sup>2+</sup> uptake by energized thylakoids can occur via Ca<sup>2+</sup>/H<sup>+</sup> antiport mechanism. These mechanisms are known to inactivate the Calvin–Benson cycle (**Figure 1**, Lautner et al., 2005; Fromm et al., 2013; Carraretto et al., 2016), by inducing fast and long-term inactivation of photosynthesis (for detailed review refer Sukhov et al., 2016). Altogether, one has to assume that the activity of ion channels localized in chloroplast and plasma membrane is synchronized and the ion channels influence each other as a feedback.

Systemic changes in gene expression (including those genes that are involved in ion channel activity) are an outcome of the electrical signals and transduction of accompanying signaling

components. However, the gene clustering (**Figure 3, Table 1**) indicated clearly, that only part of ion channels is important for mechanisms described above. The upregulation of the genes from cluster 2 indicates them as potential functional candidates and/or markers of long term acclimation (SAA) and defense (SAR). The other genes encoding ion channels are down-regulated (**Figure 3, Table 1**, cluster no 4). They are co-expressed with five genes involved in NPQ responses, i.e., *LHC6*, *NPQ7*, *SOQ1*, *PsbS*, *R1Q2* (**Table 1**, genes marked in green). Without doubt, the electrical signaling is costly. Therefore, probably the most likely explanation is, that in order to establish a favorable energy balance, upregulation of genes directly related to systemic response induction, SAA and SAR, need to be compensated by the down-regulation of genes involved in signaling (effect post-factum).

On a final note, it should be pointed out that unicellular organisms, plants and animals face many of the same problems. The most basic problem to solve is ensuring the energy to life, reproduction, acclimation and defense. To increase the chances of survival and proliferation, organisms at each level of organization need to communicate internal and external factors to adjust energy status in fluctuating environment. The electrical signaling may have evolved in many different ways, however, at the most basic level, the spread of electrical signals is similar and serves as the most universal system for intracellular, intercellular, organ-to-organ and organism-to-organism communication. For plants, solar energy is the basis of functioning. Therefore, integration of electrical signals with additional components that are dependent on energy absorption provides a powerful mechanism that holistically control homeostasis of the plant. Using network of the hyphae of mycorrhizal fungi, plants can even collectively manage absorbed energy and resources, help to survive each other, and regulate homeostasis of the plant community. Therefore, science fiction world presented in James Cameron's Avatar movie seems there is quite close to the real sciences, particularly plant neurobiology.

## AUTHOR CONTRIBUTIONS

The authors made equal intellectual contributions to the work and approved it for publication.

## FUNDING

ML and SK were supported by the Maestro 6 project no UMO-2014/14/A/NZ1/00218, granted by the National Science Centre. MS and SK were granted from PBS3/A9/37/2015 project and from BIOSTRATEG2/298241/10/NCBR/2016 project financed by the National Centre for Research and Development.

## REFERENCES

- Agosti, R. D. (2014). Touch-induced action potentials in *Arabidopsis thaliana*. *Arch. Sci.* 67, 125–138. Available online at: <https://archive-ouverte.unige.ch/unige:48136>
- Baker, N. R. (2008). Chlorophyll fluorescence: a probe of photosynthesis *in vivo*. *Annu. Rev. Plant Biol.* 59, 89–113. doi: 10.1146/annurev.arplant.59.032607.092759
- Ball, L., Accotto, G. P., Bechtold, U., Creissen, G., Funck, D., Jimenez, A., et al. (2004). Evidence for a direct link between glutathione biosynthesis and stress defense gene expression in *Arabidopsis*. *Plant Cell* 16, 2448–2462. doi: 10.1105/tpc.104.022608
- Baluška, F. (2010). Recent surprising similarities between plant cells and neurons. *Plant Signal. Behav.* 5, 87–89. doi: 10.4161/psb.5.2.11237
- Baluška, Ed. (2013). *Long-Distance Systemic Signaling and Communication in Plants* Berlin; Heidelberg: Springer-Verlag.

- Baluška, F., and Mancuso, S. (2013). Root apex transition zone as oscillatory zone. *Front. Plant Sci.* 4:354. doi: 10.3389/fpls.2013.00354
- Bialašek, M., Górecka, M., Mittler, R., and Karpinski, S. (2017). Evidence for the involvement of electrical, calcium and ros signaling in the systemic regulation of non-photochemical quenching and photosynthesis. *Plant Cell Physiol.* 58, 207–215. doi: 10.1093/pcp/pcw232
- Brenner, E. D., Stahlberg, R., Mancuso, S., Vivanco, J., Baluska, F., and van Volkenburgh, E. (2006). Plant neurobiology: an integrated view of plant signaling. *Trends Plant Sci.* 11, 413–419. doi: 10.1016/j.tplants.2006.06.009
- Bricchi, I., Berteia, C. M., Occhipinti, A., Paponov, I. A., and Maffei, M. E. (2012). Dynamics of membrane potential variation and gene expression induced by *Spodoptera littoralis*, *Myzus persicae*, and *Pseudomonas syringae* in *Arabidopsis*. *PLoS ONE* 7:e46673. doi: 10.1371/journal.pone.0046673
- Brunkard, J. O., Runkel, A. M., and Zambrysk, P. C. (2015). Chloroplasts extend stromules independently and in response to internal redox signals. *Proc. Natl. Acad. Sci. U.S.A.* 112, 10044–10049. doi: 10.1073/pnas.1511570112
- Bulychev, A. A., and Kamzolkina, N. A. (2006). Effect of action potential on photosynthesis and spatially distributed H<sup>+</sup> fluxes in cells and chloroplasts of *Chara corallina*. *Russ. J. Plant Physiol.* 53, 5–14. doi: 10.1134/S1021443706010018
- Burch-Smith, T. M., and Zambryski, P. C. (2010). Loss of INCREASED SIZE EXCLUSION LIMIT (ISE)1 or ISE2 increases the formation of secondary plasmodesmata. *Curr. Biol.* 8, 989–993. doi: 10.1016/j.cub.2010.03.064
- Cao, M. J., Wang, Z., Wirtz, M., Hell, R., Oliver, D. J., and Xiang, C. B. (2013). SULTR3.1 is a chloroplast-localized sulfate transporter in *Arabidopsis thaliana*. *Plant J.* 73, 607–616. doi: 10.1111/tpj.12059
- Caplan, L., Kumar, A. S., Park, E., Padmanabhan, M. S., Hoban, K., Modla, S., et al. (2015). Chloroplast stromules function during innate immunity. *Dev. Cell* 34, 45–57. doi: 10.1016/j.devcel.2015.05.011
- Carrasco, L., Teardo, E., Formentin, E., Teardo, E., Checchetto, V., Tomizioli, M., Morosinotto, T., et al. (2013). A thylakoid-located two-pore K<sup>+</sup> channel controls photosynthetic light utilization in plants. *Science* 342, 114–118. doi: 10.1126/science.1242113
- Carrasco, L., Teardo, E., Checchetto, V., Finazzi, G., Uozumi, N., and Szabo, I. (2016). Ion channels in plant bioenergetic organelles, chloroplasts and mitochondria: from molecular identification to function. *Mol. Plant* 9, 371–395. doi: 10.1016/j.molp.2015.12.004
- Chen, Y., Zhao, D.-J., Wang, Z.-Y., Wang, Z.-Y., Tang, G., and Huang, L. (2016). Plant electrical signal classification based on waveform similarity. *Algorithms* 9:70. doi: 10.3390/a9040070
- Choi, W.-G., Hilleary, R., Swanson, S. J., Kim, S.-H., and Gilroy, S. (2016). Rapid, long-distance electrical and calcium signaling in plants. *Annu. Rev. Plant Biol.* 67, 287–307. doi: 10.1146/annurev-arplant-043015-112130
- Choi, W.-G., Miller, G., Wallace, I., Harper, J., Mittler, R., and Gilroy, S. (2017). Orchestrating rapid long-distance signaling in plants with Ca<sup>2+</sup>, ROS and electrical signals. *Plant J.* 90, 698–707. doi: 10.1111/tpj.13492
- Ciszak, K., Kulasek, M., Barczak, A., Grzelak, J., Maćkowski, S., and Karpinski, S. (2015). PsbS is required for systemic acquired acclimation and post-excess-light-stress optimization of chlorophyll fluorescence decay times in *Arabidopsis*. *Plant Signal. Behav.* 10:e982018. doi: 10.4161/15592324.2014.982018
- Clarke, D., Whitney, H., Sutton, G., and Robert, D. (2013). Detection and learning of floral electric fields by bumblebees. *Science* 340, 66–69. doi: 10.1126/science.1230883
- Czarnocka, W., Van Der Kelen, K., Willems, P., Szechyńska-Hebda, M., Shahnejat-Bushehri, S., Balazadeh, S., et al. (2017). The dual role of LESION SIMULATING DISEASE 1 as a condition-dependent scaffold protein and transcription regulator. *Plant Cell Environ.* doi: 10.1111/pce.12994. [Epub ahead of print].
- Dąbrowska-Bronk, J., Komar, D. N., Rusaczonek, A., Kozłowska-Makulska, A., Szechyńska-Hebda, M., and Karpinski, S. (2016). β-carbonic anhydrases and carbonic ions uptake positively influence *Arabidopsis* photosynthesis, oxidative stress tolerance and growth in light dependent manner. *Plant Physiol.* 173, 44–54. doi: 10.1016/j.jplph.2016.05.013
- Dangl, J. L., and Jones, J. D. G. (2001). Plant pathogens and integrated defense responses to infection. *Nature* 411, 826–833. doi: 10.1038/35081161
- De Angeli, A., Zhang, J., Meyer, S., and Martinolia, E. (2013). AtALMT9 is a malate-activated vacuolar chloride channel required for stomatal opening in *Arabidopsis*. *Nat. Commun.* 4, 1804. doi: 10.1038/ncomms2815
- Deger, A. G., Scherzer, S., Nuhkat, M., Kedzierska, J., Kollist, H., Brosché, M., et al. (2015). Guard cell SLAC1 type anion channels mediate flagellin-induced stomatal closure. *New Phytol.* 208, 162–173. doi: 10.1111/nph.13435
- Demmig-Adams, B., Garab, G., Adams, W. III., and Govindjee (eds.). (2014). “Non-photochemical quenching and energy dissipation in plants, algae and cyanobacteria,” in *Advances in Photosynthesis and Respiration 40* (Dordrecht: Springer Science+Business Media), 1–44.
- Dietrich, P., Sanders, D., and Hedrich, R. (2001). The role of ion channels in light-dependent stomatal opening. *J. Exp. Bot.* 52, 1959–1967. doi: 10.1093/jexbot/52.363.1959
- Durant, F., Morokuma, J., Fields, C., Williams, K., Spencer Adams, D., and Levin, M. (2017). Long-term, stochastic editing of regenerative anatomy via targeting endogenous bioelectric gradients. *Biophys. J.* 112, 2231–2243. doi: 10.1016/j.bpj.2017.04.011
- Dziubińska, H., Filek, M., Kościelnik, J., and Trebacz, K. (2003a). Variation and action potentials evoked by thermal stimuli accompany enhancement of ethylene emission in distant non-stimulated leaves of *Vicia faba minor* seedlings. *J. Plant Physiol.* 160, 1203–1210. doi: 10.1078/0176-1617-00914
- Dziubińska, H., Filek, M., Szechyńska-Hebda, M., and Trębacz, K. (2003b). Slow vacuolar channels of non-embryogenic and embryogenic cultures of winter wheat. *Acta Physiol. Plant.* 25, 179–184. doi: 10.1007/s11738-003-0051-y
- Ermolayeva, E., Sanders, D., and Johannes, E. (1997). Ionic mechanism and role of phytochrome-mediated membrane depolarisation in caulonema side branch initial formation in the moss *Physcomitrella patens*. *Planta* 201, 109–118. doi: 10.1007/BF01007695
- Favre, P., and Agosti, R. D. (2007). Voltage-dependent action potentials in *Arabidopsis thaliana*. *Physiol. Plant.* 131, 263–272. doi: 10.1111/j.1399-3054.2007.00954.x
- Favre, P., Greppin, H., and Agosti, R. D. (2001). Repetitive action potentials induced in *Arabidopsis thaliana* leaves by wounding and potassium chloride application. *Plant Physiol. Biochem.* 39, 961–969. doi: 10.1016/S0981-9428(01)01317-1
- Filek, M., Zembala, M., and Szechyńska-Hebda, M. (2002). The influence of phytohormones on zeta potential and electrokinetic charges of winter wheat cells. *Z. Naturfor.* 57, 696–704. doi: 10.1515/znc-2002-7-825
- Fitzgibbon, J., Beck, M., Zhou, J., Faulkner, C., Robatzek, S., and Oparka, K. A. (2013). A developmental framework for complex plasmodesmata formation revealed by large-scale imaging of the *Arabidopsis* leaf epidermis. *Plant Cell.* 25, 57–70. doi: 10.1105/tpc.112.105890
- Folta, K. M., Lieg, E. J., Durham, T., and Spalding, E. P. (2003). Primary inhibition of hypocotyl growth and phototropism depend differently on phototropin-mediated increases in cytoplasmic calcium induced by blue light. *Plant Physiol.* 133, 1464–1470 doi: 10.1104/pp.103.024372
- Fromm, J., Hajirezaei, M. R., Becker, V. K., and Lautner, S. (2013). Electrical signaling along the phloem and its physiological responses in the maize leaf. *Front. Plant Sci.* 4:239. doi: 10.3389/fpls.2013.00239
- Fromm, J., and Lautner, S. (2007). Electrical signals and their physiological significance in plants. *Plant Cell Environ.* 30, 249–257. doi: 10.1111/j.1365-3040.2006.01614.x
- Fromm, J., and Spanswick, R. (1993). Characteristics of action potentials in willow (*Salix viminalis* L.). *J. Exp. Bot.* 44, 1119–1125. doi: 10.1093/jxb/44.7.1119
- Gallé, A., Lautner, S., Flexas, J., Ribas-Carbo, M., Hanson, D., Roeggen, J., et al. (2013). Photosynthetic responses of soybean (*Glycine max* L.) to heat-induced electrical signalling are predominantly governed by modifications of mesophyll conductance for CO<sub>2</sub>. *Plant Cell Environ.* 36, 542–552. doi: 10.1111/j.1365-3040.2012.02594.x
- Gallant, J. R., Traeger, L. L., Volkening, J. D., Moffett, H., Chen, P. H., Novina, C. D., et al. (2014). Nonhuman genetics: genomic basis for the convergent evolution of electric organs. *Science* 344, 1522–1525. doi: 10.1126/science.1254432
- Garzon, P. C., and Keijzer, F. (2011). Plants: adaptive behavior, root-brains, and minimal cognition. *Adapt. Behav.* 19, 155–171. doi: 10.1177/1059712311409446
- Gilroy, S., Bialašek, M., Suzuki, N., Górecka, M., Devireddy, A. R., Karpinski, S., et al. (2016). ROS, calcium, and electric signals: key mediators of rapid systemic signaling in plants. *Plant Physiol.* 171, 1606–1615. doi: 10.1104/pp.16.00434

- Grams, T. E., Koziolek, C., Lautner, S., Matyssek, R., and Fromm, J. (2007). Distinct roles of electric and hydraulic signals on the reaction of leaf gas exchange upon re-irrigation in *Zea mays* L. *Plant Cell Environ.* 30, 79–84. doi: 10.1111/j.1365-3040.2006.01607.x
- Guo, W., Zuo, Z., Cheng, X., Sun, J., Li, H., Li, L., et al. (2014). The chloride channel family gene CLCd negatively regulates pathogen-associated molecular pattern (PAMP)-triggered immunity in *Arabidopsis*. *J. Exp. Bot.* 65, 1205–1215. doi: 10.1093/jxb/ert484
- Haswell, E. S., Peyronnet, R., Barbier-Bryggo, H., and Meyerowitz, E.M. (2008). Two MscS homologs provide mechanosensitive channel activities in the *Arabidopsis* root. *Curr. Biol.* 18, 730–734. doi: 10.1016/j.cub.2008.04.039
- Hedrich, R. (2012). Ion channels in plants. *Physiol. Rev.* 92, 1777–1811. doi: 10.1152/physrev.00038.2011
- Hochmal, A. K., Schulze, S., Trompelt, K., and Hippler, M. (2015). Calcium-dependent regulation of photosynthesis. *Biochim. Biophys. Acta* 1847, 993–1003. doi: 10.1016/j.bbabiobio.2015.02.010
- Holt, N. E., Fleming, G. R., and Niyogi, K. K. (2004). Toward an understanding of the mechanism of nonphotochemical quenching in green plants. *Biochemistry* 43, 8281–8289. doi: 10.1021/bi0494020
- Humphries, J., Xiong, L., Liu, J., Prindle, A., Yuan, F., Arjes, H. A., et al. (2017). Species-independent attraction to biofilms through electrical signaling. *Cell* 168, 200–209. doi: 10.1016/j.cell.2016.12.014
- Robert, N., d'Erfurth, I., Marmagne, A., Erhardt, M., Allot, M., Boivin, K., et al. (2012). Voltage-dependent-anion-channels (VDACs) in *Arabidopsis* have a dual localization in the cell but show a distinct role in mitochondria. *Plant Mol. Biol.* 78, 431–446. doi: 10.1007/s11103-012-9874-5
- Jeschke, W. D. (1976). Ionic relations of leaf cells," in *Encyclopedia of Plant Physiology*, New Series, Vol. 2. Transport in plants II. Part B, tissues and organs, eds U. Liittge and M. G. Pittman (Berlin: SpringerVerlag), 160–194.
- Jossier, M., Kronewicz, L., Dalmas, F., Le Thiec, D., Ephritikhine, G., Thomine, S., et al. (2010). The *Arabidopsis* vacuolar anion transporter, AtCLCc, is involved in the regulation of stomatal movements and contributes to salt tolerance. *Plant J.* 64, 563–576. doi: 10.1111/j.1365-313X.2010.04352.x
- Kangasjärvi, S., Nurmi, M., Tikkanen, M., and Aro, E. M. (2009). Cell-specific mechanisms and systemic signalling as emerging themes in light acclimation of C3 plants. *Plant Cell Environ.* 32, 1230–1240. doi: 10.1111/j.1365-3040.2009.01982.x
- Karpinski, S., Reynolds, H., Karpinska, B., Wingsle, G., Creissen, G., and Mullineaux, P. (1999). Systemic signaling and acclimation in response to excess excitation energy in *Arabidopsis*. *Science* 284, 654–657.
- Karpinski, S., and Szechyńska-Hebda, M. (2010). Secret life of plants: from memory to intelligence. *Plant Signal. Behav.* 5, 1391–1394. doi: 10.4161/psb.5.11.13243
- Karpinski, S., Szechyńska-Hebda, M., Wituszyńska, W., and Burdiak, P. (2013). Light acclimation, retrograde signalling, cell death and immune defences in plants. *Plant Cell Environ.* 36, 736–744. doi: 10.1111/pce.12018
- Kim, S. A., Kwak, J. M., Jae, S. K., Wang, M. H., and Nam, H. G. (2001). Overexpression of the AtGluR2 gene encoding an *Arabidopsis* homolog of mammalian glutamate receptors impairs calcium utilization and sensitivity to ionic stress in transgenic plants. *Plant Cell Physiol.* 42, 74–84. doi: 10.1093/pcp/pce008
- Koziolek, C., Grams, T. E. E., Schreiber, U., Matyssek, R., and Fromm, J. (2004). Transient knockout of photosynthesis mediated by electrical signals. *New Phytol.* 161, 715–722. doi: 10.1111/j.1469-8137.2004.00985.x
- Krupenina, N. A., and Bulychev, A. A. (2007). Action potential in a plant cell lowers the light requirement for non-photochemical energy-dependent quenching of chlorophyll fluorescence. *Biochim. Biophys. Acta* 1767, 781–788. doi: 10.1016/j.bbabiobio.2007.01.004
- Kupisz, K., Dziubińska, H., and Trębacz, K. (2017). Generation of action potential-type changes in response to darkening and illumination as indication of the plasma membrane proton pump status in *Marchantia polymorpha*. *Acta Physiol. Plant.* 39, 82. doi: 10.1007/s11738-017-2378-9
- Lautner, S., Grams, T. E. E., Matyssek, R., and Fromm, J. (2005). Characteristics of electrical signals in poplar and responses in photosynthesis. *Plant Physiol.* 138, 2200–2209. doi: 10.1104/pp.105.064196
- Lee, J. Y., Wang, X., Cui, W., Sager, R., Modla, S., Czummek, K., et al. (2011). A plasmodesmata-localized protein mediates crosstalk between cell-to-cell communication and innate immunity in *Arabidopsis*. *Plant Cell* 23, 3353–3373. doi: 10.1105/tpc.111.087742
- Lister, R., Chew, O., Lee, M.-N., Heazlewood, J. L., Clifton, R., Parker, K. L., et al. (2004). Transcriptomic and proteomic characterization of the *Arabidopsis* mitochondrial protein import apparatus and its response to mitochondrial dysfunction. *Plant Physiol.* 134, 777–789. doi: 10.1104/pp.103.033910
- Maksaei, G., and Haswell, E.S. (2012). MscS-Like10 is a stretch-activated ion channel from *Arabidopsis thaliana* with a preference for anions. *Proc. Natl. Acad. Sci. U.S.A.* 13, 19015–19020. doi: 10.1073/pnas.1213931109
- Marmagne, A., Vinauger-Douard, M., Monachello, D., de Longevialle, A. F., Charon, C., Allot, M., et al. (2007). Two members of the *Arabidopsis* CLC (chloride channel) family, AtCLCe and AtCLCf, are associated with thylakoid and golgi membranes, respectively. *J. Exp. Bot.* 58, 3385–3393. doi: 10.1093/jxb/erm187
- Mäser, P., Thomine, S., Schroeder, J. I., Ward, J. M., Hirschi, K., Sze, H., et al. (2001). Phylogenetic relationships within cation transporter families of *Arabidopsis*. *Plant Physiol.* 126, 1646–1667. doi: 10.1104/pp.126.4.1646
- Miller, G., Schlauch, K., Tam, R., Cortes, D., Torres, M. A., Shulaev, V., et al. (2009). The plant NADPH oxidase RBOHD mediates rapid systemic signaling in response to diverse stimuli. *Sci. Signal.* 2, ra45. doi: 10.1126/scisignal.2000448
- Mühlenbock, P., Szechyńska-Hebda, M., Płaszczyca, M., Baudo, M., Mateo, A., Mullineaux, P. M., et al. (2008). Chloroplast signaling and LESION SIMULATING DISEASE1 regulate crosstalk between light acclimation and immunity in *Arabidopsis*. *Plant Cell* 20, 2339–2356. doi: 10.1105/tpc.108.059618
- Müller, P., Li, X.-P., and Niyogi, K. K. (2001). Non-photochemical quenching: a response to excess light energy. *Plant Physiol.* 125, 1558–1566. doi: 10.1104/pp.125.4.1558
- Mullineaux, P., and Karpiński, S. (2002). Signal transduction in response to excess light: getting out of the chloroplast. *Curr. Opin. Plant Biol.* 5, 43–48. doi: 10.1016/S1369-5266(01)00226-6
- Nakajima, K., Zhu, K., Sun, Y.-H., Hegyi, B., Zeng, Q., Murphy, C. J., et al. (2015). KCNJ15/Kir4.2 couples with polyamines to sense weak extracellular electric fields in galvanotaxis. *Nat. Commun.* 6, 8532. doi: 10.1038/ncomms9532
- Okazaki, Y. (2002). Blue light inactivates plasma membrane H<sup>+</sup>-ATPase in pulvinar motor cells of *Phaseolus vulgaris* L. *Plant Cell Physiol.* 43, 860–868. doi: 10.1093/pcp/pcf099
- Oyarce, P., and Gurovich, L. (2010). Electrical signals in avocado trees. responses to light and water availability conditions. *Plant Signal. Behav.* 5, 34–41. doi: 10.4161/psb.5.1.10157
- Pavlovic, A. (2012). "The effect of electrical signals on photosynthesis and respiration," in *Plant Electrophysiology*, ed A. G. Volkov (Berlin; Heidelberg: Springer-Verlag), 33.
- Pavlovic, A., Slováková, L., Pandolfi, C., and Mancuso, S. (2011). On the mechanism underlying photosynthetic limitation upon trigger hair irritation in the carnivorous plant Venus flytrap (*Dionaea muscipula* Ellis). *J. Exp. Bot.* 62, 1991–2000. doi: 10.1093/jxb/erq404
- Peak, D., West, J. D., Messinger, S. M., and Mott, K. A. (2004). Evidence for complex, collective dynamics and emergent, distributed computation in plants. *Proc. Natl. Acad. Sci. U.S.A.* 101, 918–922. doi: 10.1073/pnas.0307811100
- Pottosin, I., and Shabala, S. (2016). Transport across chloroplast membranes: optimizing photosynthesis for adverse environmental conditions. *Mol. Plant.* 9, 356–370. doi: 10.1016/j.molp.2015.10.006
- Rossel, J. B., Wilson, P. B., Hussain, D., Woo, N. S., Gordon, M. J., Mewett, O. P., et al. (2007). Systemic and intracellular responses to photooxidative stress in *Arabidopsis*. *Plant Cell* 19, 4091–4110. doi: 10.1105/tpc.106.045898
- Roux, D., Catrain, A., Lallechere, S., and Joly, J.-C. (2014). Sunflower exposed to high-intensity microwave-frequency electromagnetic field: electrophysiological response requires a mechanical injury to initiate. *Plant Signal. Behav.* 10:e972787. doi: 10.4161/15592316.2014.972787
- Ruban, A. V. (2016). Nonphotochemical chlorophyll fluorescence quenching: mechanism and effectiveness in protecting plants from photodamage. *Plant Physiol.* 170, 1903–1916. doi: 10.1104/pp.15.01935
- Sager, R., and Lee, J.-Y. (2014). Plasmodesmata in integrated cell signalling: insights from development and environmental signals and stresses. *J. Exp. Bot.* 65, 6337–6358. doi: 10.1093/jxb/eru365
- Salvador-Recatal, V., Tjallingii, W. F., and Farmer, E. E. (2014). Real-time, *in vivo* intracellular recordings of caterpillar-induced depolarization waves

- in sieve elements using aphid electrodes. *New Phytol.* 203, 674–684. doi: 10.1111/nph.12807
- Schenk, H. J., and Seabloom, E. W. (2010). “Evolutionary ecology of plant signals and toxins: a conceptual framework,” in *Plant Communication from an Ecological Perspective*, eds F. Baluska and V. Ninkovic (Heidelberg; Dordrecht; New York, NY: Springer), 1867–9048.
- Shabala, S., White, R. G., Djordjević, M. A., Ruan, Y. L., and Mathesius, U. (2016). Root-to-shoot signalling: integration of diverse molecules, pathways and functions. *Funct. Plant Biol.* 43, 87–104. doi: 10.1071/FP15252
- Sherstnevá, O. N., Vodeneev, V. A., Katicheva, L. A., Surova, L. M., and Sukhov, V. S. (2015). Participation of intracellular and extracellular pH changes in photosynthetic response development induced by variation potential in pumpkin seedlings. *Biochem. Mosc.* 80, 776–784. doi: 10.1134/S0006297915060139
- Spalding, E. P. (2000). Ion channels and the transduction of light signals. *Plant Cell Environ.* 23, 665–674. doi: 10.1046/j.1365-3040.2000.00594.x
- Stankovic, B., Zawadzki, T., and Davies, E. (1997). Characterization of the variation potential in sunflower. *Plant Physiol.* 115, 1083–1088. doi: 10.1104/pp.115.3.1083
- Sukhov, V. (2016). Electrical signals as mechanism of photosynthesis regulation in plants. *Photosyn. Res.* 130, 373–387. doi: 10.1007/s11120-016-0270-x
- Sukhov, V., Surova, L., Morozova, E., Sherstnevá, O., and Vodeneev, V. (2016). Changes in H<sup>+</sup>-ATP synthase activity, proton electrochemical gradient, and pH in pea chloroplast can be connected with variation potential. *Front. Plant Sci.* 7:1092. doi: 10.3389/fpls.2016.01092
- Sukhov, V., Surova, L., Sherstnevá, O., Katicheva, L., and Vodeneev, V. (2015). Variation potential influence on photosynthetic cyclic electron flow in pea. *Front. Plant Sci.* 5:766. doi: 10.3389/fpls.2014.00766
- Szarek, I., and Trebacz, K. (1999). The role of light-induced membrane potential changes in guttation in gametophytes of *Asplenium trichomanes*. *Plant Cell Physiol.* 40, 1280–1286. doi: 10.1093/oxfordjournals.pcp.a029516
- Szechyńska-Hebda, M., Czarnocka, W., Hebda, M., and Karpiński, S. (2016a). PAD4, LSD1 and EDS1 regulate drought tolerance, plant biomass production, and cell wall properties. *Plant Cell Rep.* 35, 527–539. doi: 10.1007/s00999-015-1901-y
- Szechyńska-Hebda, M., Hebda, M., Mirek, M., and Miernik, K. (2016b). Cold-induced changes in cell wall stability determine the resistance of winter triticale to fungal pathogen *Microdochium nivale*. *J. Therm. Anal. Calorim.* 126, 77–90. doi: 10.1007/s10973-016-5531-6
- Szechyńska-Hebda, M., and Karpiński, S. (2013). Light intensity-dependent retrograde signalling in higher plants. *J. Plant Physiol.* 170, 1501–1516. doi: 10.1016/j.jplph.2013.06.005
- Szechyńska-Hebda, M., Kruck, J., Górecka, M., Karpińska, B., and Karpiński, S. (2010). Evidence for light wavelength-specific photoelectrophysiological signaling and memory of excess light episodes in *Arabidopsis*. *Plant Cell* 22, 2201–2218. doi: 10.1105/tpc.109.069302
- Szechyńska-Hebda, M., Wąsek, I., Gołębiewska-Pikania, G., Dubas, E., Źur, I., and Wędzony, M. (2015). Photosynthesis-dependent physiological and genetic crosstalk between cold acclimation and cold-induced resistance to fungal pathogens in triticale (*Triticosecale* Wittm.). *J. Plant Physiol.* 177, 30–43. doi: 10.1016/j.jplph.2014.12.017
- Teardo, E., Frare, E., Segalla, A., De Marco, V., Giacometti, G. M., and Szabo, I. (2005). Localization of a putative CLC chloride channel in spinach chloroplasts. *FEBS Lett.* 579, 4991–4996. doi: 10.1016/j.febslet.2005.08.005
- Trebacz, K., Tarnecki, R., and Zawadzki, T. (1989). Characteristics of the light-induced generator potentials in the liverwort *Conocephalum conicum*. *Physiol. Plant.* 75, 20–23.
- Trebacz, K., and Zawadzki, T. (1985). Light-triggered action potentials in *Conocephalum conicum*. *Physiol. Plant.* 64, 482–486.
- van Bel, A. J., Furch, A. C., Will, T., Buxa, S. V., Musetti, R., and Hafke, J. B. (2014). Spread the news: systemic dissemination and local impact of Ca<sup>2+</sup> signals along the phloem pathway. *J. Exp. Bot.* 65, 1761–1787. doi: 10.1093/jxb/ert425
- Veley, K. M., Maksaev, G., Frick, E. M., January, E., Kloepper, S. C., and Haswell, E. S. (2014). *Arabidopsis* MSL10 has a regulated cell death signaling activity that is separable from its mechanosensitive ion channel activity. *Plant Cell* 26, 3115–3131. doi: 10.1105/tpc.114.128082
- Vodeneev, V., Akinchits, E., and Sukhov, V. (2015). Variation potential in higher plants: mechanisms of generation and propagation. *Plant Signal. Behav.* 10, 9:e1057365. doi: 10.1080/15592324.2015.1057365
- Vodeneev, V., Mudrilov, M., Akinchits, E., Balalaeva, I., and Sukhov, V. (2017). Parameters of electrical signals and photosynthetic responses induced by them in pea seedlings depend on the nature of stimulus. *Funct. Plant Biol.* doi: 10.1071/FP16342. [Epub ahead of print].
- Volkov, A. G. (2000). Green plants: electrochemical interfaces. *J. Electroanal. Chem.* 483, 150–156. doi: 10.1016/S0022-0728(99)00497-0
- Volkov, A. G. editor. (2006). *Plant Electrophysiology*. Berlin; Heidelberg; New York, NY: Springer.
- von der Fecht-Bartenbach, J., Bogner, M., Dynowski, M., and Ludewig, U. (2010). CLC-b-mediated NO<sub>3</sub><sup>-</sup>/H<sup>+</sup> exchange across the tonoplast of *Arabidopsis* vacuoles. *Plant Cell Physiol.* 51, 960–968. doi: 10.1093/pcp/pcq062
- Wege, S., De Angeli, A., Droillard, M. J., Kroniewicz, L., Merlot, S., Cornu, D., et al. (2014). Phosphorylation of the vacuolar anion exchanger AtCLCa is required for the stomatal response to abscisic acid. *Sci. Signal.* 8, ra65. doi: 10.1126/scisignal.2005140
- Werhahn, W., Niemeyer, A., Jänsch, L., Kraut, V., Schmitz, U. K., and Braun, H.-P. (2001). Purification and characterization of the preprotein translocase of the outer mitochondrial membrane from *Arabidopsis*. Identification of multiple forms of TOM201. *Plant Physiol.* 125, 943–954. doi: 10.1104/pp.125.2.943
- Wilson, M. E., Jensen, G. S., and Haswell, E. S. (2011). Two mechanosensitive channel homologs influence division ring placement in *Arabidopsis* chloroplasts. *Plant Cell* 23, 2939–2949. doi: 10.1105/tpc.111.088112
- Wituszynska, W., Slesak, I., Vanderauwera, S., Szechyńska-Hebda, M., Kornas, A., Van Der Kelen, K., et al. (2013). Lesion simulating disease1, enhanced disease susceptibility1, and phytoalexin deficient4 conditionally regulate cellular signaling homeostasis, photosynthesis, water use efficiency, and seed yield in *Arabidopsis*. *Plant Physiol.* 161, 1795–1805. doi: 10.1104/pp.112.208116
- Wituszynska, W., Szechyńska-Hebda, M., Sobczak, M., Rusaczonek, A., Kozłowska-Makulska, A., Witon, D., et al. (2015). Lesion simulating disease 1 and enhanced disease susceptibility 1 differentially regulate UV-C induced photooxidative stress signalling and programmed cell death in *Arabidopsis thaliana*. *Plant Cell Envir.* 38, 315–330. doi: 10.1111/pce.12288
- Yan, X., Wang, Z., Huang, L., Wang, C., Hou, R., Xu, Z., et al. (2009). Research progress on electrical signals in higher plants. *Prog. Nat. Sci.* 19, 531–541. doi: 10.1016/j.pnsc.2008.08.009
- Zivanović, B. D., Pang, J., and Shabala, S. (2005). Light-induced transient ion flux responses from maize leaves and their association with leaf growth and photosynthesis. *Plant Cell Environ.* 28, 340–352. doi: 10.1111/j.1365-3040.2005.01270.x
- Zivanović, B. D., Shabala, L., Elzenga, T. J. M., and Shabala, S. (2015). Dissecting blue light signal transduction pathway in leaf epidermis using a pharmacological approach. *Planta* 242, 813–827. doi: 10.1007/s00425-015-2316-2
- Zhang, W., He, S. Y., and Assmann, S. M. (2008). The plant innate immunity response in stomatal guard cells invokes G-protein-dependent ion channel regulation. *Plant J.* 56, 984–996. doi: 10.1111/j.1365-313X.2008.03657.x
- Zimmermann, M. R., Maischak, H., Mithofer, A., Boland, W., and Felle, H. H. (2009). System potentials, a novel electrical long-distance apoplastic signal in plants, induced by wounding. *Plant Physiol.* 149, 1593–1600. doi: 10.1104/pp.108.133884
- Conflict of Interest Statement:** The authors declare that the research was conducted in the absence of any commercial or financial relationships that could be construed as a potential conflict of interest.
- Copyright © 2017 Szechyńska-Hebda, Lewandowska and Karpiński. This is an open-access article distributed under the terms of the Creative Commons Attribution License (CC BY). The use, distribution or reproduction in other forums is permitted, provided the original author(s) or licensor are credited and that the original publication in this journal is cited, in accordance with accepted academic practice. No use, distribution or reproduction is permitted which does not comply with these terms.



# The Integration of Electrical Signals Originating in the Root of Vascular Plants

Javier Canales<sup>1,2</sup>, Carlos Henriquez-Valencia<sup>1</sup> and Sebastian Brauchi<sup>3,4\*</sup>

<sup>1</sup> Facultad de Ciencias, Instituto de Bioquímica y Microbiología, Universidad Austral de Chile, Valdivia, Chile, <sup>2</sup> Millennium Institute for Integrative Systems and Synthetic Biology, Santiago, Chile, <sup>3</sup> Facultad de Medicina, Instituto de Fisiología, Universidad Austral de Chile, Valdivia, Chile, <sup>4</sup> Millennium Nucleus of Ion Channels-Associated Diseases, Valdivia, Chile

## OPEN ACCESS

### Edited by:

Vicenta Salvador Recatala,  
Ronin Institute, United States

### Reviewed by:

Taku Takahashi,  
Okayama University, Japan  
Frantisek Baluska,  
University of Bonn, Germany

### \*Correspondence:

Sebastian Brauchi  
sbrauchi@uach.cl

### Specialty section:

This article was submitted to  
Plant Physiology,  
a section of the journal  
*Frontiers in Plant Science*

Received: 03 October 2017

Accepted: 12 December 2017

Published: 10 January 2018

### Citation:

Canales J, Henriquez-Valencia C and Brauchi S (2018) The Integration of Electrical Signals Originating in the Root of Vascular Plants. *Front. Plant Sci.* 8:2173.  
doi: 10.3389/fpls.2017.02173

Plants have developed different signaling systems allowing for the integration of environmental cues to coordinate molecular processes associated to both early development and the physiology of the adult plant. Research on systemic signaling in plants has traditionally focused on the role of phytohormones as long-distance signaling molecules, and more recently the importance of peptides and miRNAs in building up this communication process has also been described. However, it is well-known that plants have the ability to generate different types of long-range electrical signals in response to different stimuli such as light, temperature variations, wounding, salt stress, or gravitropic stimulation. Presently, it is unclear whether short or long-distance electrical communication in plants is linked to nutrient uptake. This review deals with aspects of sensory input in plant roots and the propagation of discrete signals to the plant body. We discuss the physiological role of electrical signaling in nutrient uptake and how nutrient variations may become an electrical signal propagating along the plant.

**Keywords:** nutrient transport, action potential, ion channels, apoplast, plasmodesma, sensory epithelia

## THE ELECTRICAL NATURE OF LIFE

Pressure-drive swelling is a problem that emerged early in evolution and solved with the emergence of membrane proteins allowing for the synchronous redistribution of ionic gradients across the plasma membrane. A secondary effect of this solution is the generation a voltage drop within the membrane dielectric (Finkelstein, 1976; Armstrong, 2015). The activity of ion channels and transporters selectively regulates the passage of ions, generating transient local variations in the membrane potential while incorporating metabolites or changing membrane permeability in response to an external signal. Allowing for the synchronization of cellular processes and the communication within cellular communities, electrical sensing, and signaling develops as a wide spread mechanism at the different levels of biological organization. From bacterial biofilms (Strahla and Hamoen, 2010; Masi and Ciszak, 2014; Prindle et al., 2015) to higher plants (Sanderson, 1872; Darwin, 1897; Bose, 1907; Pickard, 1973) and animals (Galvani, 1791; Hodgkin, 1937; Cole and Curtis, 1939; Armstrong, 2007) electrical communication adopt different forms varying in its complexity from simple graduated or oscillating changes in membrane voltage to the long-range electrical signaling observed in excitable cells.

## ELECTRICAL SIGNALS IN ANIMALS AND HIGHER PLANTS

It is well-established that both plants and animals utilize long-range electrical signaling to transduce environmental information to the whole body (Armstrong, 2007; Hedrich et al., 2016). In multicellular organisms, information must be conducted from detectors to the effector tissue. For the case of animals, the nervous system plays a central role in homeostasis, serving as the primary integrator for most of the relevant physiological information. The communication between epithelial tissue and excitable cells define the way animals interact with the environment, not only by taking advantage of sensory modalities such as touch, temperature, light, or sound (Frings, 2009; Julius and Nathans, 2012) but also by integrating internal processes such as hormonal discharge, gut physiology, and immune system development (Zhang and Zhang, 2009; Bellono et al., 2017; Clemmensen et al., 2017).

Molecular detectors found in sensory epithelia are activated by environmental cues, triggering (directly or indirectly) the opening of an ion channel conductance that changes the local transmembrane potential (Martinez, 2008). In non-excitable cells, such as epithelial cells in the gut or lung, electrogenic transport orchestrates nutrient uptake, controls pH, and modulates water secretion (Boyd, 2008; Beumer and Clevers, 2017; Clemmensen et al., 2017). For the case of epithelia, the absence of suitable voltage-dependent channels (i.e.,  $\text{Ca}_v$ ,  $\text{Na}_v$ ) impedes the propagation of the initial depolarization over long distances. In excitable cells, depolarization provides the necessary energy to induce the opening of voltage-gated channels (i.e.,  $\text{Ca}_v$ s,  $\text{Na}_v$ s, and  $\text{K}_v$ s) (Bezanilla, 2008; Catterall et al., 2017). Propagation speed, the shape of the propagated potential, and the frequency of the electrical message are determined by the cable properties of the cell, which are defined by both the geometry of each particular cell type and the ion channel set available. In animals, this type of communication extends to the multicellular organism when a released substance from a given cell exert an effect in a post synaptic cell (Gerber and Südhof, 2002; Jackson, 2006; Catterall and Few, 2008). As described originally in *Aplysia* by E. Kandel (Castellucci and Kandel, 1976), excitable cells modify their behavior in response to stimulation. Considering that the control of expression, localization, and activity of cellular receptors and ion channels represent the molecular grounding of non-associative learning in animals (Kandel, 2001), it is tempting to question how plants modulate the different ion fluxes and which are the elements conferring plasticity to plant's learning.

Action potentials have been reported in algae and higher plants (Pickard, 1973; Trebacz and Zawadzki, 1985; Kateriya et al., 2004; Fromm and Lautner, 2007; Hegenauer et al., 2016). As foreseen by Davies (1987), nowadays it is widely accepted that electrical signaling plays a major role in inter- and intra-cellular communication of plants. However, in contrast to detailed knowledge of the molecular and cellular mechanisms that governing electrical signaling in animals, the identity of the cellular sensors and effectors, and their exact distribution

within the plant, is still unclear (Ward et al., 2009; Hedrich, 2012; Hedrich et al., 2016). Moreover, lacking the sophisticated cellular wiring developed by metazoans to transmit their long-range electrical signals, it seems that plants developed an architecture allowing them to shape—or forcing them to adapt—electrical communication differently. Simple questions emerge from this reasoning, how exactly plants wire up? How electrical signals move through the cellular network? How these signals work together connecting environmental sensing, gene expression, nutrient uptake, gas exchange, water balance, energy production, and waste storing? In this review we are not aiming to answer such ambitious questions but rather to put in perspective the different elements that might contribute to the generation and propagation of the electrical message in the root of land plants.

The ability to navigate is an attribute of animals and imposes fundamental problems to solve such as (i) multiplex sensory input at high frequencies, (ii) the rapid integration of these signals, and (iii) to deliver the computed command with exquisite cellular precision, allowing a coherent body response. Unicellular green algae, ancestors of land plants, have navigation capabilities and coincidentally present a different set of ion channels when compared to their descendants, expressing essential elements important in shaping the electrical response of excitable cells in animals (Merchant et al., 2007; Wheeler and Brownlee, 2008). Among these are voltage-activated calcium and sodium channels, TRP channels, and the ryanodine receptor, all absent in modern land plants (Wheeler and Brownlee, 2008; Ward et al., 2009; Fromm and Lautner, 2012; Taylor et al., 2012; Arias-Darraz et al., 2015; Edel et al., 2017). Trapped in the same natural world, animals, and plants share a large set of environmental stress factors. Nevertheless, they have clearly adopted different ways for solving basic problems such as reproduction and self-preservation. Likely the quest for food, mating, and the need for waste disposal cued animals to develop signaling mechanisms that are tuned to navigate. On the other hand, plants not only manufacture their own carbohydrates but also importantly store their waste. Therefore, the sessile nature of land plants demands for robust adaptation mechanisms instead. Accordingly, cellular and molecular sensors are constantly feeding the plant with useful environmental information that has to be distributed through out the body (Karban, 2015). Recent studies suggests that *Arabidopsis* efficiently organize their three dimensional planning to optimize nutrient supply (Conn et al., 2017), strengthening the idea that plant's architecture is controlled by a management mechanism in charge of the trading between total length of the branches and nutrient distribution. Such mechanism must be associated to the nature and propagation properties of electrical signals generated at the root and leafs, tissues where minerals and water are absorbed, carbohydrates produced, and byproducts stored. Further experimental work on intact living plants, using suitable models allowing for simultaneous electrical and imaging recordings are needed to evaluate the impact of electrical signals on food distribution along the plant (Kanchiswamy et al., 2014; Salvador-Recatalà et al., 2014; Gunsé et al., 2016; Candeo et al., 2017).

## The Conducting Plant

Missing not only the cellular architecture but also the ion channel set encoding the electrical message in animals (Ward et al., 2009; Hedrich, 2012), there is no reason to suggest that the sensory input in plants is either integrated or processed in a similar way. It has been proposed that the plant phloem forms a single conducting cable, the equivalent of an axon in a single metazoan neuron (Hedrich et al., 2016). Different cell types including companion cells and sieve elements form the phloem. Unlike other plant cell types, sieve elements cells do not present discontinuities in their permeability due to the presence of sieve plates, enabling a continuous transport of solutes between different organs of the plant and providing a low-resistance, high capacitance conduit that allows for the propagation of relatively slow electrical signals. Decades of theoretical and experimental evidence put forward the concept that the phloem would be the principal conduit, able to electrically couple roots and aerial tissues (Brenner et al., 2006; Fromm et al., 2013; Hedrich et al., 2016). Still, the information detected at epidermal cells of the root must propagate through the cortex's cellular network, integrate, and reach the phloem to be transduced all over the plant's body. Conversely, the signal should exit the phloem to have an impact on cells in the aerial tissue. To accomplish this complex task, vascular plants have an inter-connected extracellular space between the plasma membrane and the cell wall (i.e., the apoplastic space) and direct cellular connectivity via plasmodesmata (Sattelmacher and Horst, 2007; Lee, 2015). These peculiarities serve to different signaling functions in the plant, allowing not only the passage of soluble signals but also defining the electrical coupling between cells and the modulation of specific signals associated to the calcium response that comes together with the detection of diverse environmental cues (Zebelo et al., 2012; Nawrath et al., 2013; Lee, 2015; Choi et al., 2016; Edel et al., 2017).

Two major types of long-distance electrical signals have been described in plants, action potentials (APs), and variation potentials (VPs) (Bose, 1907; Pickard, 1973; Fromm and Lautner, 2007, 2012). The former are induced by voltage depolarization, exhibit a threshold potential, follow an all-or-nothing principle, and travel at constant velocity and amplitude, very much like APs observed in the animal kingdom (Zawadzki et al., 1991; Jackson, 2006; Armstrong, 2007; Yang et al., 2016). In contrast, VPs have shown to be induced by a rapid increase in the internal pressure of the xylem, and appear as slow waves of depolarization of variable sizes (Fromm and Lautner, 2007, 2012). A third mode of electrical signal dubbed system potentials (SPs), consisting of hyperpolarization that propagates over medium range distances has also been described (Zimmermann et al., 2009). While VPs depend on the inactivation of P-type H<sup>+</sup>-ATPase, SPs seems to be caused by the activation of the pump. From the early works of Burdon-Sanderson it is known that rise times for plant APs are in the order of about 0.1 s, with durations of about 1 s and rates of propagation of in the order of few hundreds of mm s<sup>-1</sup> (Sanderson, 1872; Pickard, 1973). These electrical signals not only differ in their shape and magnitude but also in their propagation speed ranging from 1 to 60 mm s<sup>-1</sup> for APs to several minutes per centimeter in VPs. System potentials

are triggered by depolarization, do not have an all-or-nothing character, self-propagate at a constant velocity of about 0.5–2 mm s<sup>-1</sup>, and their magnitude is proportional to the input stimuli (Zimmermann et al., 2009). Interestingly, SPs resemble animal's receptor potentials, self-propagating simultaneously over sensory epithelia. The leaf of arabidopsis, beans, and barley exhibits self-propagating electrical activity, caused by wounding, restricted to leaf-to-leaf communication, and associated to the expression of glutamate receptor-like genes (Zimmermann et al., 2009; Mousavi et al., 2013; Salvador-Recatalà et al., 2014; Salvador-Recatalà, 2016a). In this case, the type of wound seems to be related to distinct types of depolarization. It has been suggested that the anatomy of the tissue will be of importance to define the connectivity between the surface tissue and the phloem (Salvador-Recatalà, 2016a).

Still, it has been difficult to systematize both a theoretical model integrating whole plant electrical signaling and experimental methods to study long-range electrical communication in whole plant configuration (Goldsworthy, 1983; Davies, 1987; Pietruszka et al., 1997; Fromm and Lautner, 2007; Volkov, 2012; Fromm et al., 2013; Hedrich et al., 2016). Nevertheless, it has been established that the different organs of the plant including leaves, stem, flowers, and the root have intrinsic electrical activity (Pickard, 1973; Baldwin et al., 2006; Fromm and Lautner, 2007, 2012; Appel and Croft, 2014; Engineer et al., 2015; Karban, 2015; Zhou et al., 2016). Moreover, long-range electrical communication between roots, shoot, and leaves have been described (extensively reviewed in Pickard, 1973; Fromm and Lautner, 2007; Zimmermann et al., 2009; Hedrich et al., 2016). A detailed description of electrical signal transduction on roots is missing, probably due to the seemingly uncoordinated nature of root's APs (Fromm and Eschrich, 1993; Fromm et al., 1997, 2013; Masi et al., 2015; Salvador-Recatalà, 2016b).

## MAPPING THE ION CHANNEL SET IN ARABIDOPSIS

Electrical properties of cells derive from the expression and control of ion channels, transporters, and pumps. These can be modulated by different stimuli such as: pressure, exogenous and endogenous ligands, temperature, light, membrane voltage, and stretch among others. The molecular machinery outlining the propagation of electrical signals in plants is not known in detail but taking into account experimental data and genetic information available we have learned that plants and animals utilize dissimilar strategies to propagate APs. While animals use voltage-sensitive Na<sup>+</sup> and Ca<sup>2+</sup> channels to drive depolarization (Hodgkin and Huxley, 1952; Armstrong, 2007; Catterall et al., 2017), the toxic nature of sodium makes plant cells to utilize Cl<sup>-</sup> and Ca<sup>2+</sup> instead. While Ca<sup>2+</sup> will cause depolarization by entering the cell, Cl<sup>-</sup> will do by leaving the cell. According to gene expression profiles, depolarization of plant cells is likely driven by ALMT/QUAC-type chloride channels and/or ion channels allowing for calcium influx such as two-pore channels (TPCs), cyclic nucleotide-gated channels (CNGCs), or glutamate

receptor-like channels (GLRs) (Ward et al., 2009; Hedrich, 2012; Hedrich et al., 2016). In the chain of events defining the AP an initial raise in  $\text{Ca}^{2+}$  will trigger a  $\text{Cl}^-$  efflux and the subsequent activation of voltage-dependent potassium channels will likely participate in repolarization (Schroeder et al., 1984; Ward et al., 2009; Hedrich et al., 2016).

As the ability of a tissue to generate electrical signals will be determined by the ion channel set expressed in the different cell types involved in the passage of the electrical message, we mapped functionally-characterized channels and transporters that have been previously associated to electrical signaling in *Arabidopsis thaliana* (Barbier-Brygoo et al., 2011; Hedrich, 2012) (**Table 1**). We performed a hierarchical clustering analysis to group these genes according to the expression profiles obtained from EPlant (Waese et al., 2017). When comparing all relevant tissues at different stages of development, we observed that the different ion channels present a characteristic pattern of expression (**Figure 1A**).

It is known that calcium signaling is important for the control of stomatal opening (Laanemets et al., 2013) and potassium channels are critical in the repolarization phase (Schroeder et al., 1984). As expected, we observed a large expression of GLR and  $K_v$  channels in the leaves (**Figures 1A,B**). Although genes encoding for anionic and potassium channels do not show a clear separation between the aerial part and roots (**Figure 1A**), we found specific genes whose expression is predominant in the roots (VDAC1), stems (GLR3.2), or leaves (GLR3.3) (**Figure 1B**). These tissue-specific expression profiles suggest that there are different pathways for the generation and propagation of electrical signals in plants and that these routes change during development. When observed in more detail, two root-specific anion channels, SLAH3, and VDAC1, showed different expression pattern across cell types (**Figure 2**). The voltage-dependent anion channel VDAC1 is strongly expressed along the root tissue. Comparatively, the expression at the meristematic zone is higher than in root hairs (**Figure 2**). Similarly,  $H^+$ -ATPase is expressed in almost all cell types of the root. In contrast, the slow chloride conductance channel SLAH3 showed greater expression in internal root tissues such as the pericycle and the cortex, important physical barriers on the way to the phloem (Nawrath et al., 2013). While the expression of the electrogenic nitrate transporter NRT1.1 is predominantly observed in root's hairs and at the phloem closer to the stem, the vacuolar channel TPC1 is markedly expressed in root hairs of the maturation zone. Interestingly, none of these membrane proteins showed a marked expression in the phloem along the root (**Figure 2**).

Calcium influx in response to external stimuli seems critical for the generation of the electrical signal. Nearly 50 different ion channels have been associated to  $\text{Ca}^{2+}$  influx in land plants. This large set of calcium channels are segregated in five different families: CNGC, GLR, TPC1, osmotic response-related channels (OSCA), and mechano-sensitive calcium channels (MCA) (Kurusu et al., 2012; Chin et al., 2013; Morgan and Galione, 2014; Edel et al., 2017) (**Table 2**). From these channels CNGC14, CNGC19, GluR2.1, and OSCA1.4 appear to be preferentially expressed in the root tissue (**Figure 3A**). The expression of these channels was also observed to be differential.

CNGC14 is largely expressed at the epithelium close to the meristematic zone and to a lesser extent at the maturation zone. In contrast, the vacuolar channel CNGC19 is concentrated at the endothelium and the phloem. On the other hand, the ligand gated GLR2.1 and osmotic-related OSCA1.4 channels are preferentially expressed in root hairs. While the expression of GLR2.1 at the epithelial tissue somewhat decreases from the meristematic zone toward the maturation zone, OSCA1.4 is preferentially expressed at the maturation zone and the phloem (**Figure 3B**).

Nitrate treatments in nitrogen-starved plants induce a transient depolarization of the plasma membrane (Meharg and Blatt, 1995; Wang and Crawford, 1996; Wang et al., 1998). Likewise, it has been recently reported that nitrate treatments trigger an intracellular calcium increase, which initiates the nitrate-signaling pathway (Liu et al., 2017). Moreover, genetic evidence indicates that elevations in intracellular calcium are associated to NRT1.1. (Riveras et al., 2015). Given the observed expression profile, we may hypothesize that a nitrate uptake-induced depolarization of the epithelial cell, caused by an increase in the activity of the nitrate transporter NRT1.1, will trigger calcium influx through OSCA1.4 and/or GLR2.1, further activating a calcium or voltage-dependent chloride conductance (e.g., SLAH3 or VDAC1), allowing for the propagation of the electrical signal along the cortex toward the phloem (**Figure 4**).

## CELLULAR CONNECTIVITY AS PART OF PLANT'S ELECTRICAL SIGNALING

A united model connecting plant sensing and controlled behavior is needed to explain whether the stimuli detected at the boundaries of the plant body (e.g., root hairs, leaf's epithelial cells), transduce the electrical information to the phloem cable, how the signal is further integrated, and lastly how the electrical signal exits the phloem, reaching the effector tissue located in a distant epithelia (e.g., guard cells at leaf stoma). While the differential expression of the ion channel set is important to determine excitability, the plant's interconnected cellular architecture will be critical in governing the amplitude and propagation properties in three-dimensional space. Modulation of these elements in response to repetitive, acute, or chronic sensory input may confer plasticity to the plant's response and will allow for both learning and adaptation, without the need for a "brain-like" integrator or cognitive behavior as suggested in literature (Baluska et al., 2004).

One of the main structural differences between animal and plant cells is the presence of a cell wall. The plant cell wall creates an unusual extracellular environment known as the apoplast which constitutes a physical/chemical barrier that participates in cell-to-cell communication pathways including long-range electrical signaling (Sattelmacher, 2001; Fromm and Lautner, 2007; Choi et al., 2017). In plants, the extracellular concentration of ions corresponds to the apoplastic ionic concentrations, which are highly regulated. The ionic composition of the apoplast is variable and depends on both internal factors such as tissue or development stage and external factors such as nutritional stress (López-Millán et al., 2001). Ions in the apoplastic

**TABLE 1 |** Functional ion channels in Arabidopsis.

	<b>Name</b>	<b>Locus</b>	<b>Fuction</b>	<b>References</b>
Voltage-gated K <sup>+</sup> channel	KAT1	At5g46240	Stomatal opening	Ronzier et al., 2014
	KAT2	At4g18290	Stomatal opening	Ronzier et al., 2014
	AKT1	At2g26650	K <sup>+</sup> uptake from soil	Xu et al., 2006; Geiger et al., 2009
	SIPK (AKT6)	At2g25600	Pollen tube development	Mouline et al., 2002
	AtKC1	At4g32650	Regulation AKT1	Geiger et al., 2009
	AKT2	At4g22200	K <sup>+</sup> battery, stomatal movement	Szyroki et al., 2001; Gajdanowicz et al., 2011
	SKOR	At3g02850	K <sup>+</sup> loading to xilem	Liu et al., 2006
	GORK	At5g32500	Involved in stomatal closure, stomatal movement	Hosy et al., 2003
Voltage-independent K <sup>+</sup> channel	TPK1	At5g55630	K <sup>+</sup> homeostasis, germination, stomatal movement	Gobert et al., 2007
	TPK2	At5g46370	Unknown	Voelker et al., 2006
	TPK3	At4g18160	Unknown	Voelker et al., 2006
	TPK4	At1g02510	K <sup>+</sup> homeostasis, growing tube pollen	Becker et al., 2004
	KCO3	At5g46360	Unknown	Voelker et al., 2006; Rocchetti et al., 2012
Ca <sup>2+</sup> channels	CNGC1	At5g53130	Response to pathogen, senescence	Leng et al., 1999; Ma et al., 2010; Chin et al., 2013
	CNGC2	At5g15410	Response to pathogen	Leng et al., 2002; Chin et al., 2013
	CNGC4	At5g54250	Pathogen infection	Balagué et al., 2003
	GLR 3.2	At4g35290	Ca <sup>2+</sup> homeostasis, ionic stress	Kim et al., 2001
	GLR 3.3	At1g42540	Ca <sup>2+</sup> homeostasis, wound response	Mousavi et al., 2013; Salvador-Recatalà, 2016a
	GLR 3.5	At2g32390	Ca <sup>2+</sup> homeostasis, wound response	Salvador-Recatalà, 2016a
	GLR 3.6	At3g51480	Ca <sup>2+</sup> homeostasis, wound response	Mousavi et al., 2013; Salvador-Recatalà, 2016a
	TPC1	At4g03560	Stomatal opening, germination	Peiter et al., 2005; Guo et al., 2016
	VDAC1	At3g01280	Regulate cold stress response, growth pollen	Tateda et al., 2011; Li et al., 2013
	VDAC2	At5g67500	Seedling development, energy production	Yan et al., 2009; Tateda et al., 2011
Voltage-dependent anion channel (VDAC)	VDCA3	At5g15090	Germination, energy production	Tateda et al., 2011; Yang et al., 2011; Berrier et al., 2015
	VDCA4	At5g57490	Energy production, plant growth	Tateda et al., 2011
	QUAC1 (ALMT12)	At4g17970	Involved in stomatal closure, stomatal movement, sulfate transporter	Meyer et al., 2010; Malcheska et al., 2017
	AtALMT9	At3g18440	Stomatal opening	De Angeli et al., 2013; Zhang et al., 2014
S-type anion channel	SLAC1	At1g12480	Stomatal opening	Zhang et al., 2016
	SLAH3 (SLAC1 homolog 3)	At5g24030	Stomatal opening, nitrate efflux channel	Zheng et al., 2015; Zhang et al., 2016
Voltage dependent Cl-	AtCLCa	At5g40890	NO <sub>3</sub> <sup>-</sup> transporter, nitrate homeostasis	De Angeli et al., 2006

compartment are usually found in low concentrations consisting predominantly of inorganic cations and anions such as K<sup>+</sup>, Ca<sup>2+</sup>, Mg<sup>2+</sup>, Cl<sup>-</sup>, NO<sub>3</sub><sup>-</sup>, and PO<sub>4</sub><sup>3-</sup> (Gabriel and Kesselmeier, 1999). The apoplastic and intracellular ion concentrations together with ion permeability will define the resting potential of the root epidermal cell and has been reported to be about -120 mV, negative inside (Fromm and Eschrich, 1993). Biochemical properties of the cell wall will define the apoplastic space and nutrient permeability in the first place. In the adult plant, a high

content of lignin or suberin in cell walls considerably decreases their permeability (Nawrath et al., 2013) and therefore constitutes a tight barrier to free diffusion of nutrients in and out of the plant tissue. In contrast, the structure and composition of cell walls change during root development (Somssich et al., 2016). The meristematic zone contains young cells localized close to the root tip, while the older cells are localized at the root base close to the stem. Cell walls of the meristematic zone are thin and more permeable because of a higher mitotic activity (Baluska et al.,

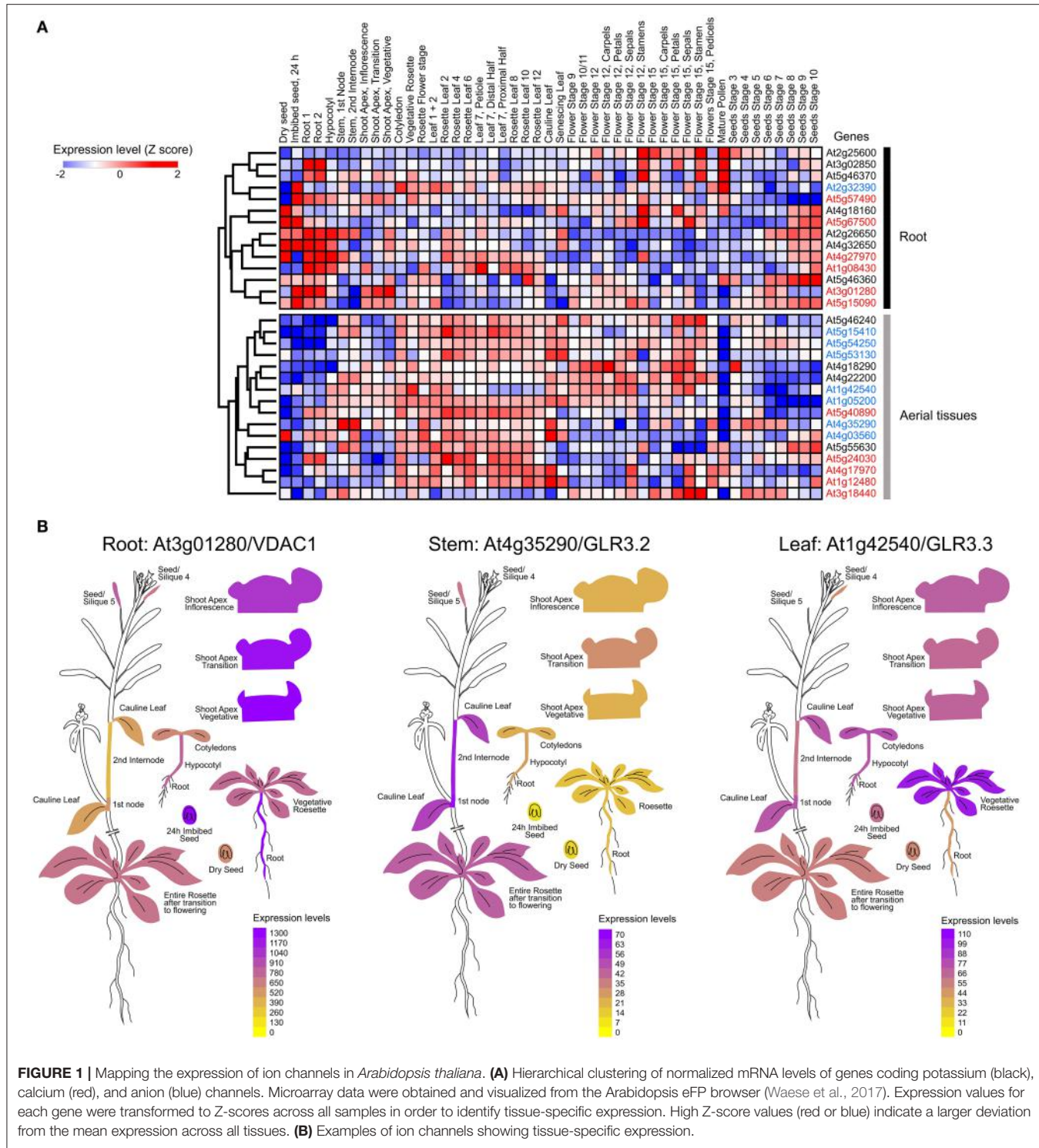
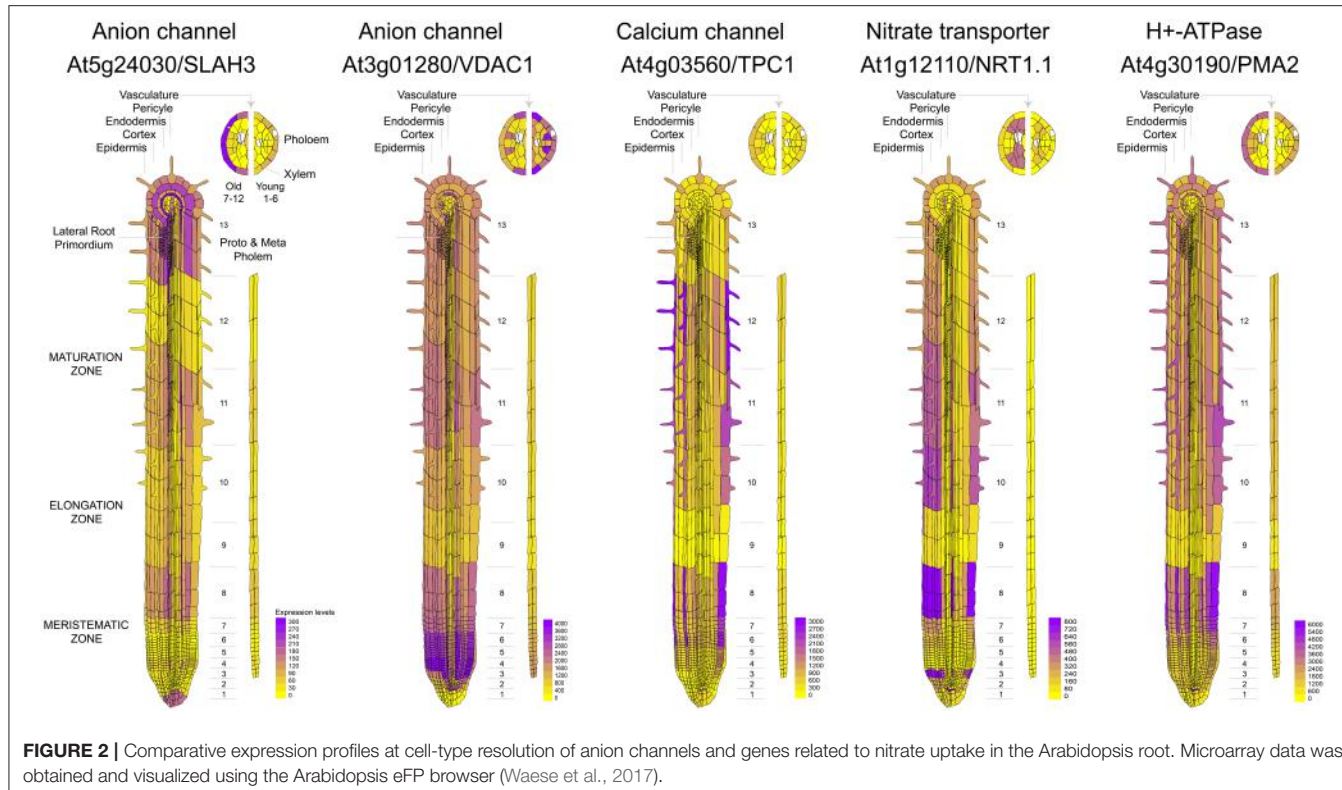


**FIGURE 1 |** Mapping the expression of ion channels in *Arabidopsis thaliana*. **(A)** Hierarchical clustering of normalized mRNA levels of genes coding potassium (black), calcium (red), and anion (blue) channels. Microarray data were obtained and visualized from the *Arabidopsis* eFP browser (Waese et al., 2017). Expression values for each gene were transformed to Z-scores across all samples in order to identify tissue-specific expression. High Z-score values (red or blue) indicate a larger deviation from the mean expression across all tissues. **(B)** Examples of ion channels showing tissue-specific expression.

1996). Cells from the differentiation zone are more rigid due to the accumulation of lignin associated with the development of secondary cell walls, which provides extra strength to the walls and makes them waterproof Somssich et al. (2016). Therefore, there is a longitudinal permeability gradient in primary roots determined by the differentiation degree of epidermal cells.

The equilibrium concentration of ions can be calculated from the Nernst equation of the form  $[X]_{\text{out}}/[X]_{\text{in}} = \exp(V_m ZF/RT)$ , where  $[X]_{\text{out}}$  and  $[X]_{\text{in}}$  are the external and internal concentrations of an ion X,  $V_m$  is the membrane voltage, Z is the valence of the permeable ion, F the Faraday constant, R the gas constant, and T the absolute temperature. From this equation, it is clear



that variations in the extracellular concentration of a permeable charged solute will affect the membrane potential at rest. In fact, early studies have shown that both the peak of the action potential and magnitude of the inward current are dependent on the apoplastic calcium concentration (Hope, 1961a,b; Hope and Findlay, 1964). On the other hand, the activity of the  $H^+$ -ATPase maintains apoplastic pH usually acidic (4.7–5) (Sattelmacher and Horst, 2007). As the resting membrane potential in plant cells is likely to be set by proton transport, therefore, one should expect a high sensitivity to variations in the activity of the proton pump (Brault et al., 2004). Considering that the apoplast occupies a relatively small volume of the plant tissues, representing less than 5% for the case of leaves (López-Millán et al., 2001) it is reasonable to expect that environmental changes might cause rapid alkalinization of the apoplast that in turn will produce a local depolarization (Grams et al., 2009). Anionic nutrients such as nitrate, sulfate and phosphate are acquired passively by means of electrogenic co-transport helped by the proton gradient (Ullrich-Eberius et al., 1981; Muchhal and Raghothama, 1999). Likewise, apoplastic pH will be sensitive to the activity of phosphate and nitrate transporters (Amtmann et al., 1999). Accordingly, acute treatments with nitrate in nitrogen-starved plants induce a transient depolarization of the plasma membrane (Meharg and Blatt, 1995; Wang and Crawford, 1996). Experimental evidence suggests that 2–4 protons are co-transported during phosphate uptake (Sakano, 1990). For the case of nitrate, the stoichiometry of co-transport with protons has been calculated to be 2:1 (McClure et al., 1990; Glass et al., 1992; Wang and

Crawford, 1996). Considering experimental evidence from *in vitro* studies with membrane vesicles and also genetic analyses such as yeast complementation, the most probable stoichiometry for proton/sulfate co-transport would be 3:1 (Buchner et al., 2004).

The root is the first organ that comes in contact with water and nutrients. Therefore, when plants are deprived of nutrients, the root constitutes a primary site for detection. Comparative transcriptomic analyses between root and shoot samples showed that the plant's response to nitrate initiates at the root (Wang et al., 2003). Plants must integrate the information from the external environment and contrast it with their nutritional status. In fact, it has been reported that the balance between nitrogen and carbon is important for the control of nitrogen assimilation (Zheng, 2009). Therefore, plants require an efficient communication system between the site of nutrient perception and uptake (i.e., roots) and the metabolic center where carbon is produced (i.e., leaves) to respond adequately to changes in nutrient availability. Epidermal cells of the plant root elicit a higher permeability through a cell wall, making electrogenic transporters at the plasma membrane to face high concentrations of nutrients when they happen to get dissolved in the soil surrounding the root. The uptake of any these nutrients will produce a rapid and transient membrane depolarization of the epithelial cell in the root (Dunlop and Grdinier, 1993; Meharg and Blatt, 1995). Moreover, the diffusion of substances within the root's apoplast is internally restricted by the Caspary strip, a lignin-made hydrophobic impregnation of the primary

**TABLE 2 |** Calcium channels in Arabidopsis.

Channel family	Name	Locus
CGNCs	CNGC10	AT1G01340
	CNGC7	AT1G15990
	CNGC8	AT1G19780
	CNGC6	AT2G23980
	CNGC14	AT2G24610
	CNGC15	AT2G28260
	CNGC3	AT2G46430
	CNGC12	AT2G46450
	CNGC19	AT3G17690
	CNGC16	AT3G48010
	CNGC13	AT4G01010
	CNGC17	AT4G30360
	CNGC9	AT4G30560
	CNGC18	AT5G14870
	CNGC2	AT5G15410
	CNGC1	AT5G53130
	CNGC4	AT5G54250
	CNGC5	AT5G57940
GLRs	GLR3.4	AT1G05200
	GLR3.3	AT1G42540
	GLR3.1	AT2G17260
	GLR2.3	AT2G24710
	GLR2.2	AT2G24720
	GLR2.9	AT2G29100
	GLR2.8	AT2G29110
	GLR2.7	AT2G29120
	GLR3.5	AT2G32390
	GLR3.7	AT2G32400
	GLR1.1	AT3G04110
	GLR1.4	AT3G07520
	GLR3.6	AT3G51480
	GLR2.4	AT4G31710
	GLR2	AT4G35290
	GLR2.6	AT5G11180
	GLR2.5	AT5G11210
TPC	GLR2.1	AT5G27100
	GLR1.2	AT5G48400
MCAs	GLR3.1	AT5G48410
	TPC1	AT4G03560
OSCA	MCA2	AT2G17780
	MCA1	AT4G35920
OSCA	OSCA2.2	At1g10090
	OSCA1.3	At1g11960
	OSCA3.1	At1g30360
	OSCA1.8	At1g32090
	OSCA2.1	At1g58520
	OSCA1.4	At1g62320
	OSCA2.4	At1g69450
	OSCA2.3	At3g01100
	OSCA1.5	At3g21620
	OSCA2.4	At3g54510

(Continued)

**TABLE 2 |** Continued

Channel family	Name	Locus
	OSCA1.7	At4g02900
	OSCA1.1	AT4G04340
	OSCA1.6	At4g15430
	OSCA1.2	At4g22120
	OSCA4.1	At4g35870

cell wall that seal the extracellular space of endodermal cells, forcing the passage of ions, nutrients, and water through the plasma membrane of endothelial cells (Nawrath et al., 2013; von Wangenheim et al., 2017) (**Figure 4**).

In addition to the apoplastic communication pathway in the extracellular space, the cytoplasm of plant cells can be internally connected by cell-to-cell junctions known as plasmodesma (Lee, 2015; Kitagawa and Jackson, 2017). Intercellular communication of root tissues has been demonstrated by the rapid diffusion of fluorescent tracer molecules (e.g., propidium iodide) through plasmodesmata into inner layers of the root tissue (Nawrath et al., 2013). It has been demonstrated that the undifferentiated cells from the apical root meristem and elongation zone are dye-coupled and, therefore, are symplastically connected through plasmodesmata (Duckett et al., 1994). Ions and larger molecules can freely diffuse though the pore from one cell to the other making these cellular structures a focal point of signaling through the cortex tissue (Burch-Smith and Zambryski, 2012; Lee, 2015). Moreover, the complexity of plasmodesmata is underscored by the presence of endoplasmic reticulum (ER) passing through the pore, providing a secondary and likely more selective pathway of communication between neighbor cells. It is known that different lipids and *callose*, a soluble protein able to occlude the cytoplasmic pathway, tune permeation through plasmodesmata (Tilsner et al., 2016). Moreover, it has been reported that cytoplasmic calcium elevations promote the closure of the cytoplasmic pathway of the pore (Lee, 2015). Additional data is needed to determine the contribution of these ER tubes in the propagation of both calcium and electrical signals through root cortex.

In plants, direct coupling between the ER and the electrical activity at the plasma membrane is not associated to the stromal interaction molecule 1 (STIM1) or to Orai1 calcium channels, as in animal cells. STIM-related proteins were lost at the level of single-celled algae and Orai relatives are present only up to gymnosperms (Edel et al., 2017). Nevertheless, it has been suggested that anchoring proteins, cytoskeleton elements, and lipids might modulate localization and activity of membrane proteins at the contact site between ER and plasma membrane (Lee, 2015). Thus, the differential expression and modulation of a specific set of calcium-sensitive ion channels, plasmodesmata occlusion, or the remodeling of the pore's shape at the contact site might provide amplification or suppression of the propagating electrical signal through the cortex (**Figure 4**).

The differentiation of root epidermal cells in Arabidopsis progressively reduces these cytoplasmic connections in such a way that become symplastically uncoupled in the last stage

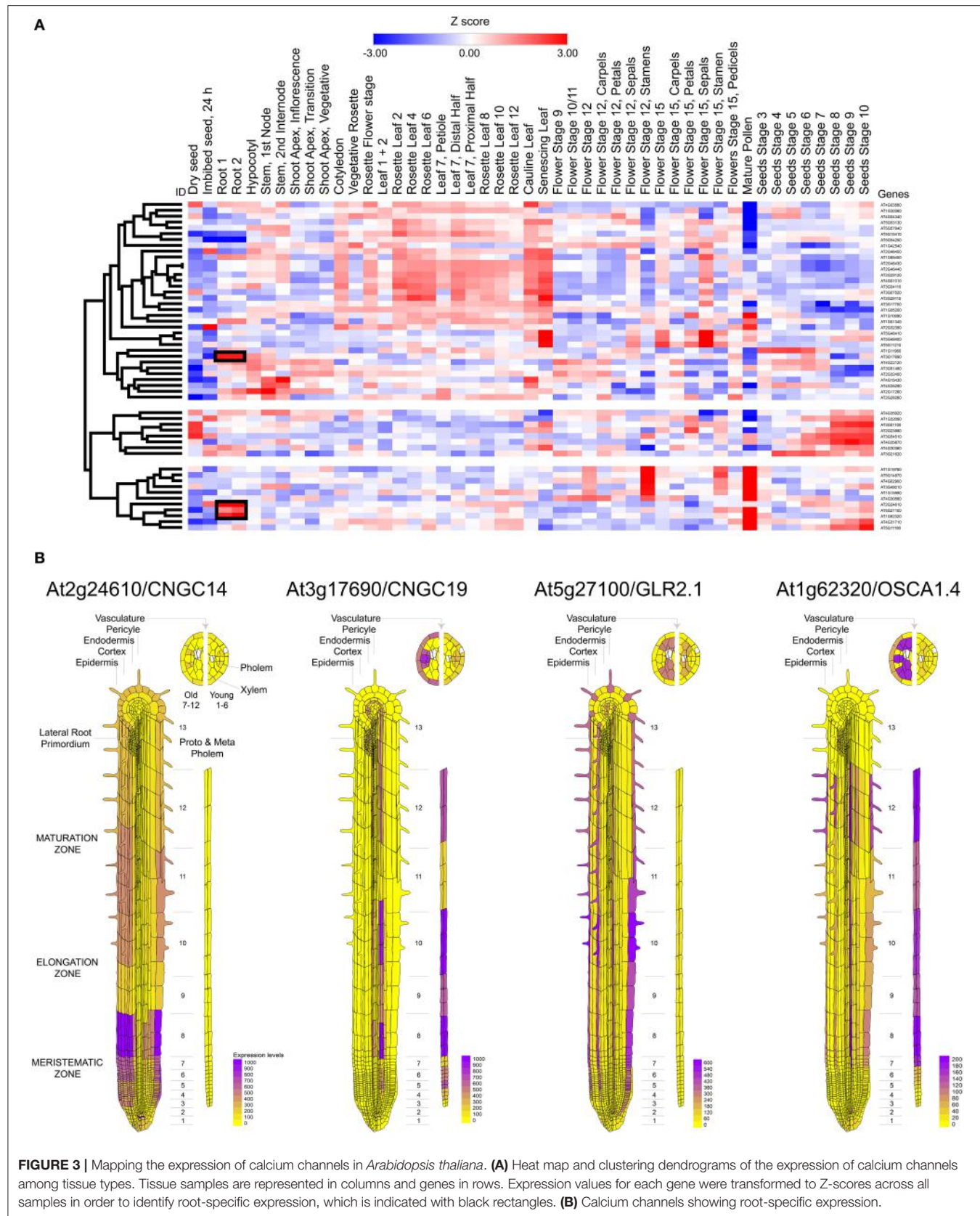


**FIGURE 3 |** Mapping the expression of calcium channels in *Arabidopsis thaliana*. **(A)** Heat map and clustering dendograms of the expression of calcium channels among tissue types. Tissue samples are represented in columns and genes in rows. Expression values for each gene were transformed to Z-scores across all samples in order to identify root-specific expression, which is indicated with black rectangles. **(B)** Calcium channels showing root-specific expression.

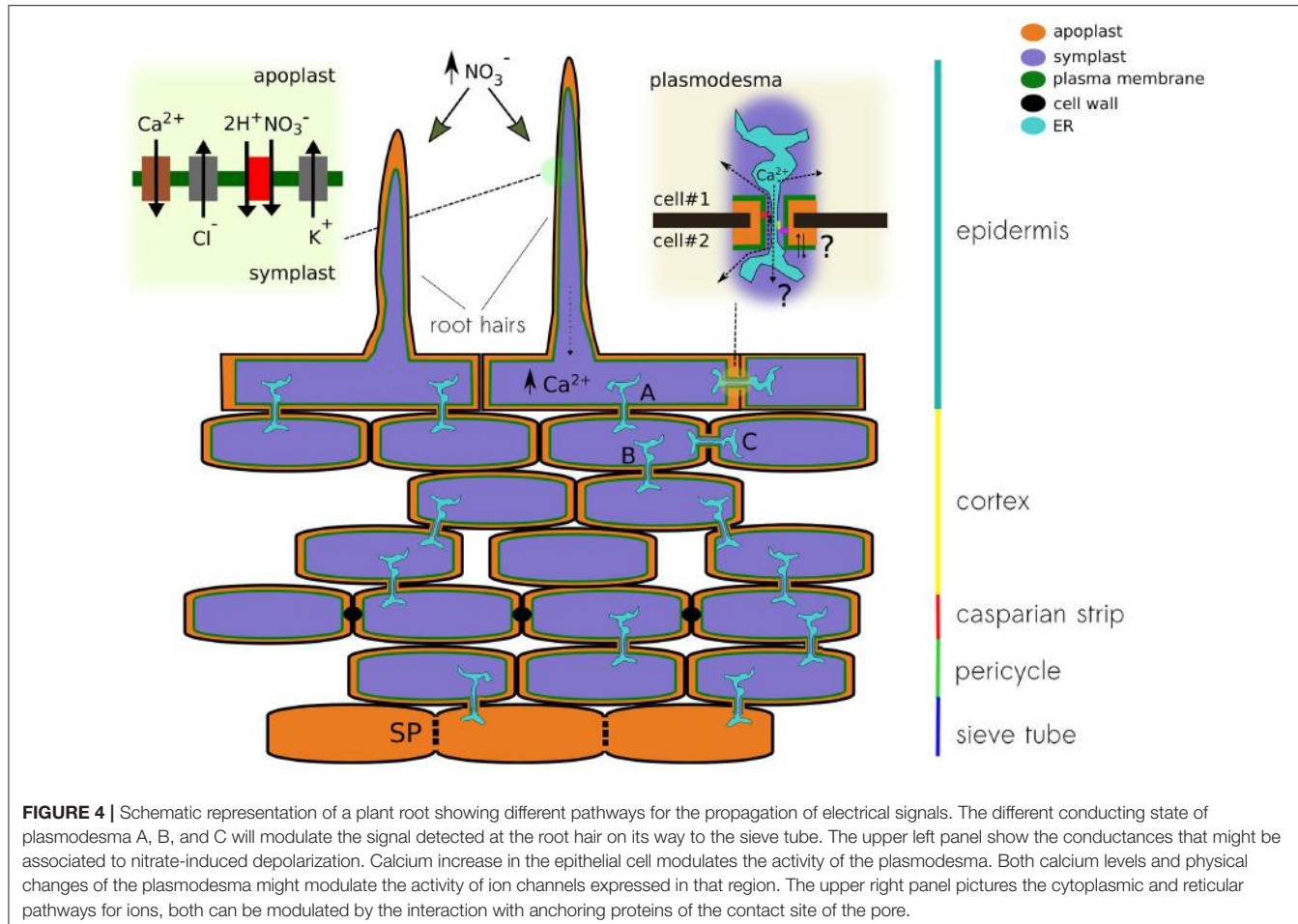


**FIGURE 4 |** Schematic representation of a plant root showing different pathways for the propagation of electrical signals. The different conducting state of plasmodesma A, B, and C will modulate the signal detected at the root hair on its way to the sieve tube. The upper left panel show the conductances that might be associated to nitrate-induced depolarization. Calcium increase in the epithelial cell modulates the activity of the plasmodesma. Both calcium levels and physical changes of the plasmodesma might modulate the activity of ion channels expressed in that region. The upper right panel pictures the cytoplasmic and reticular pathways for ions, both can be modulated by the interaction with anchoring proteins of the contact site of the pore.

of their development (Duckett et al., 1994). Conversely, the cells of the hypocotyl epidermis are symplastically connected to one another regardless of their state of development (Duckett et al., 1994). Earlier evidence of electrical coupling was given by Spanswick and Costerton, who showed that when injecting current in a cell of the multicellular alga Nitella, the signal could be traced several cells away from the site of injection (Spanswick and Costerton, 1967).

Recent calcium imaging experiments using a genetically encoded ratiometric calcium indicator (i.e., Y-Cameleon 3.6), expressed in living Arabidopsis, showed how the spontaneous response originating in a root hair propagates through the root tissue in well-defined “patches” (Candeo et al., 2017). Although the authors did not comment about this patterned response, by analogy to sensory receptors in animals, it is tempting to interpret such readout as the physical dimension of the “*sensory field*” that correspond to a particular epithelial cell or a group of them. After the stimulation of a cell from root epidermis, an electrical signal is generated; in the example above, the influx of calcium can be directly related to cell depolarization. The generated electrical signal can be transmitted via plasmodesmata to neighbor connected cells in the root cortex. Once the signal reaches the low-resistance sieve tube in the phloem, it propagates throughout the entire plant (Figure 4). The question then is

whether the phloem integrates multiple signals coming from individual receptor fields dispersed along the root’s epithelia and how the network of cell-to-cell connectivity might provide plasticity, modulating the propagation of the electrical message by controlling the localization and activity of plasmodesmata (Figure 4). Moreover, diffusion experiments with fluorescent dyes showed that the communication of the hypocotyl epidermal cells ends at the base of the stem (Duckett et al., 1994). Therefore, it is likely that epidermal cells of the hypocotyl and root are electrically uncoupled, making sieve tubes the only pathway possible to propagate APs from the root to the shoot. All these physical barriers create nodes of resistive elements, useful for signal filtering not only at the exit of root tissue but also in and out of branches coming out of the stem.

It has been proposed that plants might integrate information through a “*brain-like*” structure, located in the root apex (Baluska et al., 2004; Brenner et al., 2006). However, the striking features of animal’s brain not only come from the fact that neurons establish synapses, but rather from the ability to create complex cell-based logic circuits. A single neuron can host hundreds of cell-specific synapses, each one capable of plastic adaptation. In the absence of this kind of cellular interaction, it sounds unlikely that the integration of electrical information in the whole plant led to cognitive processing of sensory information. Moreover, recent

works on unicellular organisms such as slime mold and bacteria demonstrate that there is no need for a central nervous system to spawn intelligent solutions (Nakagaki, 2001; Kotula et al., 2014).

Making a very simplistic picture of plant electrical connectivity, we observe it composed by a very inefficient cable surrounded by epithelial tissue formed by absorptive and excitable cells. In such a model epithelial hair cells of the root might function as spines in a neuron, providing signals generated by external stimuli to the cortex circuit where they are processed before reaching the phloem. At the same time, the transition from root to the stem might provide an additional filter, acting as a macroscopic version of the spine neck modulating the transit of long-range electrical signals. The number of cells in the cortex that are electrically connected define the size of the circuit's capacitor and outlines the electrical properties of the paths reaching the phloem. The presence of hypothetical "synapse-like" structures based on actin might contribute in shaping the network of cell-to-cell connectivity (Baluška et al., 2005). In this context, systemic soluble signals such as auxins might also play an important role in regulating cell-to-cell connectivity, for example by interacting with plasmodesmata (Baluška et al., 2004; Brenner et al., 2006). Furthermore, sensory input might also affect fundamental cable properties along the phloem conduit, shaping and filtering the propagated action potentials. The nature of the physical/molecular barriers (e.g., root cortex-to-phloem and phloem-to-leaf epithelia transitions) will be of mayor importance to understand the integration of sensory information in plants.

## NUTRIENT SENSING AND LONG-RANGE ELECTRICAL SIGNALING

Plants acquire the essential chemical components for the synthesis of biomolecules from the minerals present in the soil (Maathuis, 2009). Phosphorus, nitrogen, sulfur, potassium, magnesium, and calcium are nutrients required in greater quantities by higher plants (Kirkby, 2011). Therefore, plants must acquire these nutrients continuously to ensure suitable growth and development (Maathuis, 2009). Unlike heterotrophic organisms, plants mainly acquired nutrients in inorganic form by specific transporters localized in the roots. The expression of these nutrient transporters, as well as their activity, is regulated by nutrient availability, metabolism and environmental factors (Giehl and von Wirén, 2014). Lacking one of these essential nutrients has a direct impact on plant growth and development, especially in the case of root tissue (Gruber et al., 2013). Consequently, plants have developed sophisticated regulatory systems to ensure the uptake of these inorganic nutrients (Schachtman and Shin, 2007). In fact, the response to nutrient starvation involves complex signaling networks including sensor proteins (Ho et al., 2009), transcription factors (Rubio et al., 2001), miRNAs (Vidal et al., 2010), peptides (Ohkubo et al., 2017), and phytohormones (Kiba et al., 2011). Interestingly, these signaling pathways not only trigger short-term responses involving metabolic adjustments and/or regulation of nutrient transporters, but also induce modifications of the root system architecture.

Among macronutrients, phosphorus and nitrogen have a greater impact on the root architecture when compared to others (Gruber et al., 2013). Phosphate starvation strongly induces the development of root hairs (Péret et al., 2011), whereas the addition of nitrate causes an increase in root hair density (Canales et al., 2017). In addition, phosphate deficiency causes an important decrease of primary root growth and stimulates the development of lateral roots (Shahzad and Amtmann, 2017). In contrast, lower availability of nitrate increases the primary root growth and decreases the development of lateral roots. These opposite effects on the cellular architecture of the root suggest the presence of different signaling pathways for nitrate and phosphate, probably associated to electrical signals of different nature that do not necessarily propagate in the same way or generate in the same epithelial cell type.

## CONCLUSION

Intracellular calcium variations in root hair cells of plant epidermis are generated by a mechanism involving a local variation in membrane potential, caused by electrogenic transport or by the direct activation of plant receptors by extracellular ligands. These local variations in membrane voltage will provide amplification of the input signal by increasing calcium permeability of the epithelial cell and further trigger action potentials by increasing the permeability of chloride conductances, followed by potassium/proton-driven repolarization. These electrical signals are initially propagated through cells in the cortex by highly regulated networks of plasmodesmata, and by taking advantage of the continuum of the apoplastic space until reaching the sieve tube of the phloem, where it gets access to be transmitted throughout the plant body. Physical barriers, ion channel distribution, and cell-to-cell communication in the root are critical aspects that shape the electrical signals generated at the sensory tissue. All subject of cellular control, these elements might provide plasticity to plant response. The role of plasmodesmata in the propagation and fine-tuning of electrical signals in plant's sensory epithelia is a fundamental topic somewhat neglected and evidently requires more attention.

## AUTHOR CONTRIBUTIONS

SB, JC, and CH-V wrote the paper. SB and JC prepared figures.

## ACKNOWLEDGMENTS

MiNICAD is a Millennium Nucleus supported by Iniciativa Científica Milenio, Ministry of Economy, Development and Tourism, Chile. Anillo Científico ACT-1401 supports SB. SB is part of CISNe-UACH and UACH Program for Cell Biology. JC is supported by FONDECYT grant 11150070. Millennium Institute for Integrative Systems and Synthetic Biology is supported by "Iniciativa Científica Milenio," Ministry of Economy, Development and Tourism, Chile. We thank Charlotte K. Colenso for her comments on this manuscript.

## REFERENCES

- Amtmann, A., Jelitto, T. C., and Sanders, D. (1999). K+-Selective inward-rectifying channels and apoplastic pH in barley roots. *Plant Physiol.* 120, 331–338. doi: 10.1104/pp.120.1.331
- Appel, H. M., and Crocroft, R. B. (2014). Plants respond to leaf vibrations caused by insect herbivore chewing. *Oecologia* 175, 1257–1266. doi: 10.1007/s00442-014-2995-6
- Arias-Darraz, L., Cabezas, D., Colenso, C. K., Alegría-Arcos, M., Bravo-Moraga, F., Varas-Concha, I., et al. (2015). A transient receptor potential ion channel in chlamydomonas shares key features with sensory transduction-associated TRP Channels in mammals. *Plant Cell* 27, 177–188. doi: 10.1105/tpc.114.31862
- Armstrong, C. M. (2007). Life among the axons. *Annu. Rev. Physiol.* 69, 1–18. doi: 10.1146/annurev.physiol.69.120205.124448
- Armstrong, C. M. (2015). Packaging life: the origin of ion-selective channels. *Biophys. J.* 109, 173–177. doi: 10.1016/j.bpj.2015.06.012
- Balagúe, C., Lin, B., Alcon, C., Flottes, G., Malmström, S., Köhler, C., et al. (2003). HLM1, an essential signaling component in the hypersensitive response, is a member of the cyclic nucleotide-gated channel ion channel family. *Plant Cell* 15, 365–379. doi: 10.1105/tpc.006999
- Baldwin, I. T., Halitschke, R., Paschold, A., von Dahl, C. C., and Preston, C. A. (2006). Volatile signaling in plant-plant interactions: “talking trees” in the genomics era. *Science* 311, 812–815. doi: 10.1126/science.1118446
- Baluška, F., Mancuso, S., Volkmann, D., and Barlow, P. (2004). Root apices as plant command centres: the unique “brain-like” status of the root apex transition zone. *Biology* 59, 7–19.
- Baluška, F., Volkmann, D., and Barlow, P. W. (1996). Specialized zones of development in roots: view from the cellular level. *Plant Physiol.* 112, 3–4.
- Baluška, F., Volkmann, D., and Menzel, D. (2005). Plant synapses: actin-based domains for cell-to-cell communication. *Trends Plant Sci.* 10, 106–111. doi: 10.1016/j.tplants.2005.01.002
- Barbier-Brygoo, H., De Angeli, A., Filleur, S., Frachisse, J.-M., Gambale, F., Thomine, S., et al. (2011). Anion channels/transports in plants: from molecular bases to regulatory networks. *Annu. Rev. Plant Biol.* 62, 25–51. doi: 10.1146/annurev-arplant-042110-103741
- Becker, D., Geiger, D., Dunkel, M., Roller, A., Bertl, A., Latz, A., et al. (2004). AtTPK4, an *Arabidopsis* tandem-pore K<sup>+</sup> channel, poised to control the pollen membrane voltage in a pH- and Ca<sup>2+</sup>-dependent manner. *Proc. Natl. Acad. Sci. U.S.A.* 101, 15621–15626. doi: 10.1073/pnas.0401502101
- Bellono, N. W., Bayerer, J. R., Leitch, D. B., Brierley, S. M., Ingraham, H. A., Julius, D., et al. (2017). Enterochromaffin cells are gut chemosensors that couple to sensory neural pathways article enterochromaffin cells are gut chemosensors that couple to sensory neural pathways. *Cell* 170, 1–14. doi: 10.1016/j.cell.2017.05.034
- Berrier, C., Peyronnet, R., Betton, J. M., Ephrithikhine, G., Barbier-Brygoo, H., Frachisse, J. M., et al. (2015). Channel characteristics of VDAC-3 from *Arabidopsis thaliana*. *Biochem. Biophys. Res. Commun.* 459, 24–28. doi: 10.1016/j.bbrc.2015.02.034
- Beumer, J., and Clevers, H. (2017). How the gut feels, smells, and talks. *Cell* 170, 10–11. doi: 10.1016/j.cell.2017.06.023
- Bezanilla, F. (2008). How membrane proteins sense voltage. *Nat. Rev. Mol. Cell Biol.* 9, 323–332. doi: 10.1038/nrm2376
- Bose, J. C. (1907). *Comparative Electro-Physiology, a Physico-Physiological Study*. London: Longmans.
- Boyd, C. A. (2008). Facts, fantasies and fun in epithelial physiology. *Exp. Physiol.* 93, 303–314. doi: 10.1113/expphysiol.2007.037523
- Brault, M., Amiar, Z., Pennarun, A.-M., Monestiez, M., Zhang, Z., Cornel, D., et al. (2004). Plasma membrane depolarization induced by abscisic acid in *Arabidopsis* suspension cells involves reduction of proton pumping in addition to anion channel activation, which are both Ca<sup>2+</sup> dependent. *Plant Physiol.* 135, 231–243. doi: 10.1104/pp.103.039255
- Brenner, E. D., Stahlberg, R., Mancuso, S., Vivanco, J., Baluška, F., and Van Volkenburgh, E. (2006). Plant neurobiology: an integrated view of plant signaling. *Trends Plant Sci.* 11, 413–419. doi: 10.1016/j.tplants.2006.06.009
- Buchner, P., Takahashi, H., and Hawkesford, M. J. (2004). Plant sulphate transporters: co-ordination of uptake, intracellular and long-distance transport. *J. Exp. Bot.* 55, 1765–1773. doi: 10.1093/jxb/erh206
- Burch-Smith, T. M., and Zambryski, P. C. (2012). Plasmodesmata paradigm shift: regulation from without versus within. *Annu. Rev. Plant Biol.* 63, 239–260. doi: 10.1146/annurev-arplant-042811-105453
- Canales, J., Contreras-López, O., Álvarez, J. M., and Gutiérrez, R. A. (2017). Nitrate induction of root hair density is mediated by TGA1/TGA4 and CPC transcription factors in *Arabidopsis thaliana*. *Plant J.* 92, 305–316. doi: 10.1111/tpj.13656
- Candeo, A., Docula, F. G., Valentini, G., Bassi, A., and Costa, A. (2017). Light sheet fluorescence microscopy quantifies calcium oscillations in root hairs of *Arabidopsis thaliana*. *Plant Cell Physiol.* 58, 1–12. doi: 10.1093/pcp/pcx045
- Castellucci, V., and Kandel, E. (1976). Presynaptic facilitation as a mechanism for behavioral sensitization in *Aplysia*. *Science* 194, 1176–1178. doi: 10.1126/science.11560
- Catterall, W. A., and Few, A. P. (2008). Calcium channel regulation and presynaptic plasticity. *Neuron* 59, 882–901. doi: 10.1016/j.neuron.2008.09.005
- Catterall, W. A., Wisedchaisri, G., Zheng, N. (2017). The chemical basis for electrical signaling. *Nat. Chem. Biol.* 13, 455–463. doi: 10.1038/ncheimbio.2353
- Chin, K., Defalco, T. A., Moeder, W., and Yoshioka, K. (2013). The *Arabidopsis* cyclic nucleotide-gated ion channels AtCNGC2 and AtCNGC4 work in the same signaling pathway to regulate pathogen defense and floral transition. *Plant Physiol.* 163, 611–624. doi: 10.1104/pp.113.225680
- Choi, W.-G., Hilleary, R., Swanson, S. J., Kim, S.-H., and Gilroy, S. (2016). Rapid, long-distance electrical and calcium signaling in plants. *Annu. Rev. Plant Biol.* 67, 287–307. doi: 10.1146/annurev-arplant-043015-112130
- Choi, W.-G., Miller, G., Wallace, I., Harper, J., Mittler, R., and Gilroy, S. (2017). Orchestrating rapid long-distance signaling in plants with Ca<sup>2+</sup>, ROS and electrical signals. *Plant J.* 90, 698–707. doi: 10.1111/tpj.13492
- Clemmensen, C., Müller, T. D., Woods, S. C., Berthoud, H., Seeley, R. J., and Tschöp, M. H. (2017). Gut-brain cross-talk in metabolic control. *Cell* 168, 758–774. doi: 10.1016/j.cell.2017.01.025
- Cole, K. S., and Curtis, H. J. (1939). Electric impedance of the squid giant axon during activity. *J. Gen. Physiol.* 22, 649–670. doi: 10.1085/jgp.22.5.649
- Conn, A., Pedmale, U. V., Chory, J., Stevens, C. F., and Navlakha, S. (2017). A statistical description of plant shoot architecture. *Curr. Biol.* 27, 2078.e3–2088.e3. doi: 10.1016/j.cub.2017.06.009
- Darwin, C. (1897). *Insectivorous Plants*. ed D. Appleton. New York, NY; J. Murray.
- Davies, E. (1987). Action potentials as multifunctional signals in plants: a unifying hypothesis to explain apparently disparate wound responses. *Plant Cell Environ.* 10, 623–631.
- De Angeli, A., Monachello, D., Ephritikhine, G., Frachisse, J. M., Thomine, S., Gambale, F., et al. (2006). The nitrate/proton antiporter AtCLCa mediates nitrate accumulation in plant vacuoles. *Nature* 442, 939–942. doi: 10.1038/nature05013
- De Angeli, A., Zhang, J., Meyer, S., and Martinoia, E. (2013). AtALMT9 is a malate-activated vacuolar chloride channel required for stomatal opening in *Arabidopsis*. *Nat Commun.* 4, 1804. doi: 10.1038/ncomms2815
- Duckett, C. M., Oparka, K. J., Prior, D. A. M., Dolan, L., and Roberts, K. (1994). Dye-coupling in the root epidermis of *Arabidopsis* is progressively reduced during development. *Development* 3255, 3247–3255.
- Dunlop, J., and Grdinier, S. (1993). Phosphate uptake, proton extrusion and membrane electropotentials of phosphorus-deficient *Trifolium repens* L. *J. Exp. Bot.* 44, 1801–1808. doi: 10.1093/jxb/44.12.1801
- Edel, K. H., Marchadier, E., Brownlee, C., Kudla, J., and Hetherington, A. M. (2017). The evolution of calcium-based signalling in Plants. *Curr. Biol.* 27, R667–R679. doi: 10.1016/j.cub.2017.05.020
- Engineer, C. B., Hashimoto-Sugimoto, M., Negi, J., Israelsson-Nordström, M., Azoulay-Shemer, T., Rappel, W. J., et al. (2015). CO<sub>2</sub> sensing and CO<sub>2</sub> regulation of stomatal conductance: advances and open questions. *Trends Plant Sci.* 21, 16–30. doi: 10.1016/j.tplants.2015.08.014
- Finkelstein, A. (1976). Water and nonelectrolyte permeability of lipid bilayer membranes. *J. Gen. Physiol.* 68, 127–135. doi: 10.1085/jgp.68.2.127
- Frings, S. (2009). Primary processes in sensory cells: current advances. *J. Comp. Physiol. A Neuroethol. Sens. Neural. Behav. Physiol.* 195, 1–19. doi: 10.1007/s00359-008-0389-0
- Fromm, J., and Eschrich, W. (1993). Electric signals released from roots of willow (*Salix viminalis* L.) change transpiration and photosynthesis. *J. Plant Physiol.* 141, 673–680. doi: 10.1016/S0176-1617(11)81573-7

- Fromm, J., Hajirezaei, M.-R., Becker, V. K., and Lautner, S. (2013). Electrical signaling along the phloem and its physiological responses in the maize leaf. *Front. Plant Sci.* 4:239. doi: 10.3389/fpls.2013.00239
- Fromm, J., and Lautner, S. (2007). Electrical signals and their physiological significance in plants. *Plant Cell Environ.* 30, 249–257. doi: 10.1111/j.1365-3040.2006.01614.x
- Fromm, J., and Lautner, S. (2012). "Plant electrophysiology: signaling and responses," in *Plant Electrophysiology*, ed A. G. Volkov (Berlin; Heidelberg: Springer-Verlag), 1–377.
- Fromm, J., Meyer, A. J., and Weisenseel, M. H. (1997). Growth, membrane potential and endogenous ion currents of willow (*Salix viminalis*) roots are all affected by abscisic acid and spermine. *Physiol. Plant.* 99, 529–537. doi: 10.1034/j.1399-3054.1997.990403.x
- Gabriel, R., and Kesselmeier, J. (1999). Apoplastic solute concentrations of organic acids and mineral nutrients in the leaves of several fagaceae. *Plant Cell Physiol.* 40, 604–612. doi: 10.1093/oxfordjournals.pcp.a029583
- Gajdanowicz, P., Michard, E., Sandmann, M., Rocha, M., Corrêa, L. G., Ramírez-Aguilar, S. J., et al. (2011). Potassium (K<sup>+</sup>) gradients serve as a mobile energy source in plant vascular tissues. *Proc. Natl. Acad. Sci. U.S.A.* 108, 864–869. doi: 10.1073/pnas.1009777108
- Galvani, L. (1791). De viribus electricitatis in motu muscularis commentarius. *Bononiensi Sci. Artium Inst. atque Acad. Comment.* 7, 363–418. doi: 10.1097/00000441-195402000-00023
- Geiger, D., Becker, D., Vosloh, D., Gambale, F., Palme, K., Rehers, M., et al. (2009). Heteromeric AtKC1{middle dot}AKT1 channels in Arabidopsis roots facilitate growth under K<sup>+</sup>-limiting conditions. *J. Biol. Chem.* 284, 21288–21295. doi: 10.1074/jbc.M109.017574
- Gerber, S. H., and Südhof, T. C. (2002). Molecular determinants of regulated exocytosis. *Diabetes* 51, 3–11. doi: 10.2337/diabetes.51.2007.S3
- Giehl, R. F., and von Wirén, N. (2014). Root nutrient foraging. *Plant Physiol.* 166, 509–517. doi: 10.1104/pp.114.245225
- Glass, A. D., Shaff, J. E., and Kochian, L. V. (1992). Studies of the uptake of nitrate in barley: IV. Electrophysiology. *Plant Physiol.* 99, 456–463.
- Gobert, A., Isayenkov, S., Voelker, C., Czempinski, K., and Maathuis, F. J. M. (2007). The two-pore channel *TPK1* gene encodes the vacuolar K<sup>+</sup> conductance and plays a role in K<sup>+</sup> homeostasis. *Proc. Natl. Acad. Sci. U.S.A.* 104, 10726–10731. doi: 10.1073/pnas.0702595104
- Goldsworthy, A. (1983). The evolution of plant action potentials. *J. Theor. Biol.* 103, 645–648.
- Grams, T. E., Lautner, S., Felle, H. H., Matyssek, R., and Fromm, J. (2009). Heat-induced electrical signals affect cytoplasmic and apoplastic pH as well as photosynthesis during propagation through the maize leaf. *Plant Cell Environ.* 32, 319–326. doi: 10.1111/j.1365-3040.2008.01922.x
- Gruber, B. D., Giehl, R. F. H., Friedel, S., and von Wirén, N. (2013). Plasticity of the Arabidopsis root system under nutrient deficiencies. *Plant Physiol.* 163, 161–179. doi: 10.1104/pp.113.218453
- Gunsé, B., Poschenrieder, C., Rankl, S., Schröeder, P., Rodrigo-Moreno, A., and Barceló, J. (2016). A highly versatile and easily configurable system for plant electrophysiology. *Methods* 3, 436–451. doi: 10.1016/j.mex.2016.05.007
- Guo, J., Zeng, W., Chen, Q., Lee, C., Chen, L., Yang, Y., et al. (2016). Structure of the voltage-gated two-pore channel TPC1 from *Arabidopsis thaliana*. *Nature* 531, 196–201. doi: 10.1038/nature16446
- Hedrich, R. (2012). Ion channels in plants. *Physiol. Rev.* 92, 1777–1811. doi: 10.1152/physrev.00038.2011
- Hedrich, R., Salvador-Recalà, V., and Dreyer, I. (2016). Electrical wiring and long-distance plant communication. *Trends Plant Sci.* 21, 376–387. doi: 10.1016/j.tplants.2016.01.016
- Hegenauer, V., Fürst, U., Kaiser, B., Smoker, M., Zipfel, C., Felix, G., et al. (2016). Detection of the plant parasite *Cuscuta reflexa* by a tomato cell surface receptor. *Science* 353, 478–481. doi: 10.1126/science.aaf3919
- Ho, C.-H., Lin, S.-H., Hu, H.-C., and Tsay, Y.-F. (2009). CHL1 functions as a nitrate sensor in plants. *Cell* 138, 1184–1194. doi: 10.1016/j.cell.2009.07.004
- Hodgkin, A. L. (1937). Evidence for electrical transmission in nerve. *J. Physiol.* 90, 183–210.
- Hodgkin, A. L., and Huxley, A. F. (1952). A quantitative description of membrane current and its application to conduction and excitation in nerve. *J. Physiol.* 117, 500–544.
- Hope, A. B. (1961a). Ionic relations of cells of *chara australis*. *Aust. J. Biol. Sci.* 14, 312–322. doi: 10.1071/B19610312
- Hope, A. B. (1961b). The action potential in cells of *chara*. *Nature* 191, 811–812. doi: 10.1038/191811a0
- Hope, A. B., and Findlay, G. P. (1964). The action potential in *Chara*. *Plant Cell Physiol.* 5, 377–380. doi: 10.1093/oxfordjournals.pcp.a079056
- Hosy, E., Vavasseur, A., Mouline, K., Dreyer, I., Gaymard, F., Porée, F., et al. (2003). The *Arabidopsis* outward K<sup>+</sup> channel GORK is involved in regulation of stomatal movements and plant transpiration. *Proc. Natl. Acad. Sci. U.S.A.* 100, 5549–5554. doi: 10.1073/pnas.0733970100
- Jackson, M. B. (2006). *Molecular and Cellular Biophysics*. Cambridge: Cambridge University Press.
- Julius, D., and Nathans, J. (2012). Signaling by sensory receptors. *Cold Spring Harb. Perspect. Biol.* 4:a005991. doi: 10.1101/cshperspect.a005991
- Kanchiswamy, C. N., Malnoy, M., Occhipinti, A., and Maffei, M. E. (2014). Calcium imaging perspectives in plants. *Int. J. Mol. Sci.* 15, 3842–3859. doi: 10.3390/ijms15033842
- Kandel, E. R. (2001). The molecular biology of memory storage: a dialogue between gene and synapses. *Science* 294, 1030–1038. doi: 10.1126/science.1067020
- Karban, R. (2015). *Plant Sensing and Communication*. Chicago, IL: University of Chicago Press.
- Kateriya, S., Nagel, G., Bamberg, E., and Hegemann, P. (2004). "Vision" in single-celled algae. *News Physiol. Sci.* 19, 133–137. doi: 10.1152/nips.01517.2004
- Kiba, T., Kudo, T., Kojima, M., and Sakakibara, H. (2011). Hormonal control of nitrogen acquisition: roles of auxin, abscisic acid, and cytokinin. *J. Exp. Bot.* 62, 1399–1409. doi: 10.1093/jxb/erq410
- Kim, S. A., Kwak, J. M., Jae, S. K., Wang, M. H., and Nam, H. G. (2001). Overexpression of the *AtGluR2* gene encoding an Arabidopsis homolog of mammalian glutamate receptors impairs calcium utilization and sensitivity to ionic stress in transgenic plants. *Plant Cell Physiol.* 42, 74–84. doi: 10.1093/pcp/pce008
- Kirkby, E. (2011). "Introduction, definition and classification of nutrients," in *Marschner's Mineral Nutrition of Higher Plants*, 3rd Edn., ed P. Marschner (London: Elsevier), 3–5. doi: 10.1016/B978-0-12-384905-2.00001-7
- Kitagawa, M., and Jackson, D. (2017). Plasmodesmata-mediated cell-to-cell communication in the shoot apical meristem: how stem cells talk. *Plants* 6:12. doi: 10.3390/plants6010012
- Kotula, J. W., Kerns, S. J., Shaket, L. A., Siraj, L., Collins, J. J., Way, J. C., et al. (2014). Programmable bacteria detect and record an environmental signal in the mammalian gut. *Proc. Natl. Acad. Sci. U.S.A.* 111, 4838–4843. doi: 10.1073/pnas.1321321111
- Kurusu, T., Hamada, H., Koyano, T., and Kuchitsu, K. (2012). Intracellular localization and physiological function of a rice Ca<sup>2+</sup>-permeable channel OsTPC1. *Plant Signal. Behav.* 7, 1428–1430. doi: 10.4161/psb.22086
- Laanemets, K., Brandt, B., Li, J., Merilo, E., Wang, Y.-F., Keshwani, M. M., et al. (2013). Calcium-dependent and -independent stomatal signaling network and compensatory feedback control of stomatal opening via Ca<sup>2+</sup> sensitivity priming. *Plant Physiol.* 163, 504–513. doi: 10.1104/pp.113.220343
- Lee, J. Y. (2015). Plasmodesmata: a signaling hub at the cellular boundary. *Curr. Opin. Plant Biol.* 27, 133–140. doi: 10.1016/j.pbi.2015.06.019
- Leng, Q., Mercier, R. W., Hua, B.-G., Fromm, H., and Berkowitz, G. A. (2002). Electrophysiological analysis of cloned cyclic nucleotide-gated ion channels. *Plant Physiol.* 128, 400–410. doi: 10.1104/pp.010832
- Leng, Q., Mercier, R. W., Yao, W., and Berkowitz, G. A. (1999). Cloning and first functional characterization of a plant cyclic nucleotide-gated cation channel. *Plant Physiol.* 121, 753–761.
- Li, Z. Y., Xu, Z. S., He, G. Y., Yang, G. X., Chen, M., Li, L. C., et al. (2013). The voltage-dependent anion channel 1 (AtVDAC1) negatively regulates plant cold responses during germination and seedling development in *Arabidopsis* and interacts with calcium sensor CBL1. *Int. J. Mol. Sci.* 14, 701–713. doi: 10.3390/ijms14010701
- Liu, K., Li, L., and Luan, S. (2006). Intracellular K<sup>+</sup> sensing of SKOR, a Shaker-type K<sup>+</sup> channel from *Arabidopsis*. *Plant J.* 46, 260–268. doi: 10.1111/j.1365-313X.2006.02689.x
- Liu, K. H., Niu, Y., Konishi, M., Wu, Y., Du, H., Sun Chung, H., et al. (2017). Discovery of nitrate-CPK-NLP signalling in central nutrient-growth networks. *Nature* 545, 311–316. doi: 10.1038/nature22077

- López-Millán, A. F., Morales, F., Abadía, A., and Abadía, J. (2001). Iron deficiency-associated changes in the composition of the leaf apoplastic fluid from field-grown pear (*Pyrus communis* L.) trees. *J. Exp. Bot.* 52, 1489–1498. doi: 10.1093/jexbot/52.360.1489
- Ma, W., Smigel, A., Walker, R. K., Moeder, W., Yoshioka, K., and Berkowitz, G. A. (2010). Leaf senescence signaling: the Ca<sup>2+</sup>-conducting Arabidopsis cyclic nucleotide gated channel2 acts through nitric oxide to repress senescence programming. *Plant Physiol.* 154, 733–743. doi: 10.1104/pp.110.161356
- Maathuis, F. J. (2009). Physiological functions of mineral macronutrients. *Curr. Opin. Plant Biol.* 12, 250–258. doi: 10.1016/j.pbi.2009.04.003
- Malcheska, F., Ahmad, A., Batool, S., Müller, H. M., Ludwig-Müller, J., Kreuzwieser, J., et al. (2017). Drought enhanced xylem sap sulfate closes stomata by affecting ALMT12 and guard cell ABA synthesis. *Plant Physiol.* 174, 798–814. doi: 10.1104/pp.16.01724
- Martinac, B. (2008). *Sensing with Ion Channels*. ed B. Martinac. Berlin; Heidelberg: Springer.
- Masi, E., and Ciszak, M. (2014). Electrical spiking in bacterial biofilms. *J. R. Soc. Interface* 12:20141036. doi: 10.1098/rsif.2014.1036
- Masi, E., Ciszak, M., Comparini, D., Monetti, E., Pandolfi, C., Azzarello, E., et al. (2015). The Electrical network of maize root apex is gravity dependent. *Sci. Rep.* 5:7730. doi: 10.1038/srep07730
- McClure, P. R., Kochian, L. V., Spanswick, R. M., and Shaff, J. E. (1990). Evidence for cotransport of nitrate and protons in maize roots: I. Effects of nitrate on the membrane potential. *Plant Physiol.* 93, 281–289.
- Meharg, A. A., and Blatt, M. R. (1995). NO<sub>3</sub><sup>-</sup> transport across the plasma membrane of *Arabidopsis thaliana* root hairs: kinetic control by pH and membrane voltage. *J. Membr. Biol.* 145, 49–66. doi: 10.1007/BF00233306
- Merchant, S. S., Prochnik, S. E., Vallon, O., Harris, E. H., Karpowicz, S. J., Witman, G. B., et al. (2007). The Chlamydomonas genome reveals the evolution of key animal and plant functions. *Science* 318, 245–250. doi: 10.1126/science.1143609
- Meyer, S., Mumm, P., Imes, D., Endler, A., Weder, B., Al-Rasheid, K. A., et al. (2010). AtALMT12 represents an R-type anion channel required for stomatal movement in Arabidopsis guard cells. *Plant J.* 63, 1054–1062. doi: 10.1111/j.1365-313X.2010.04302.x
- Morgan, A. J., and Galione, A. (2014). Two-pore channels (TPCs): current controversies. *Bioessays* 36, 173–183. doi: 10.1002/bies.201300118
- Mouline, K., Véry, A.-A., Gaymard, F., Boucherez, J., Pilot, G., Devic, M., et al. (2002). Pollen tube development and competitive ability are impaired by disruption of a Shaker K<sup>+</sup> channel in *Arabidopsis*. *Genes Dev.* 16, 339–350. doi: 10.1101/gad.213902
- Mousavi, S. A., Chauvin, A., Pascaud, F., Kellenberger, S., and Farmer, E. E. (2013). GLUTAMATE RECEPTOR-LIKE genes mediate leaf-to-leaf wound signalling. *Nature* 500, 422–426. doi: 10.1038/nature12478
- Muchhal, U. S., and Raghothama, K. G. (1999). Transcriptional regulation of plant phosphate transporters. *Proc. Natl. Acad. Sci. U.S.A.* 96, 5868–5872.
- Nakagaki, T. (2001). Smart behavior of true slime mold in a labyrinth. *Res. Microbiol.* 152, 767–770. doi: 10.1016/S0923-2508(01)01259-1
- Nawrath, C., Schreiber, L., Franke, R. B., Geldner, N., Reina-Pinto, J. J., and Kunst, L. (2013). Apoplastic diffusion barriers in arabidopsis. *Arab. B.* 11:e0167. doi: 10.1199/tab.0167
- Ohkubo, Y., Tanaka, M., Tabata, R., Ogawa-Ohnishi, M., and Matsubayashi, Y. (2017). Shoot-to-root mobile polypeptides involved in systemic regulation of nitrogen acquisition. *Nat. Plants* 3, 17029. doi: 10.1038/nplants.2017.29
- Peiter, E., Maathuis, F. J. M., Mills, L. N., Knight, H., Pelloux, J., Hetherington, A. M., et al. (2005). The vacuolar Ca<sup>2+</sup>-activated channel TPC1 regulates germination and stomatal movement. *Nature* 434, 404–408. doi: 10.1038/nature03381
- Péret, B., Clément, M., Nussaume, L., and Desnos, T. (2011). Root developmental adaptation to phosphate starvation: better safe than sorry. *Trends Plant Sci.* 16, 442–450. doi: 10.1016/j.tplants.2011.05.006
- Pickard, B. G. (1973). Action potentials in higher plants. *Bot. Rev.* 39, 172–201. doi: 10.1007/BF02859299
- Pietruszka, M., Stolarek, J. A. N., and Pazurkiewicz-kocot, K. (1997). Time evolution of the action potential in plant cells. *J. Biol. Phys.* 23, 219–232.
- Prindle, A., Liu, J., Asally, M., Ly, S., Garcia-Ojalvo, J., Siel, G. M., et al. (2015). Ion channels enable electrical communication in bacterial communities. *Nature* 527, 59–63. doi: 10.1038/nature15709
- Riveras, E., Alvarez, J. M., Vidal, E. A., Oses, C., Vega, A., and Gutiérrez, R. A. (2015). The calcium ion is a second messenger in the nitrate signaling pathway of Arabidopsis. *Plant Physiol.* 169, 1397–1404. doi: 10.1104/pp.15.00961
- Rocchetti, A., Sharma, T., Wulfetange, C., Scholz-Starke, J., Grippa, A., Carpaneto, A., et al. (2012). The putative K(+) channel subunit AtKCO3 forms stable dimers in Arabidopsis. *Front Plant Sci.* 3:251. doi: 10.3389/fpls.2012.00251
- Ronzier, E., Corratgé-Faillie, C., Sanchez, F., Prado, K., Brière, C., Leonhardt, N., et al. (2014). CPK13, a noncanonical Ca<sup>2+</sup>-dependent protein kinase, specifically inhibits KAT2 and KAT1shaker K<sup>+</sup> channels and reduces stomatal opening. *Plant Physiol.* 166, 314–326. doi: 10.1104/pp.114.240226
- Rubio, V., Linhares, F., Solano, R., Martín, A. C., Iglesias, J., Leyva, A., et al. (2001). A conserved MYB transcription factor involved in phosphate starvation signaling both in vascular plants and in unicellular algae. *Genes Dev.* 15, 2122–2133. doi: 10.1101/gad.204401
- Sakano, K. (1990). Proton/phosphate stoichiometry in uptake of inorganic phosphate by cultured cells of *Catharanthus roseus* (L.) G. Don. *Plant Physiol.* 93, 479–83.
- Salvador-Recatalà, V. (2016a). New roles for the Glutamate Receptor-Like 3.3, 3.5, and 3.6 genes as on/off switches of wound-induced systemic electrical signals. *Plant Signal. Behav.* 11:e1161879. doi: 10.1080/15592324.2016.1161879
- Salvador-Recatalà, V. (2016b). The AKT2 potassium channel mediates NaCl induced depolarization in the root of *Arabidopsis thaliana*. *Plant Signal. Behav.* 11:e1165381. doi: 10.1080/15592324.2016.1165381
- Salvador-Recatalà, V., Tjallingii, W. F., and Farmer, E. E. (2014). Real-time, *in vivo* intracellular recordings of caterpillar-induced depolarization waves in sieve elements using aphid electrodes. *New Phytol.* 203, 674–684. doi: 10.1111/nph.12807
- Sanderson, J. B. (1872). Note on the electrical phenomena which accompany irritation of the leaf of *Dionaea muscipula*. *Proc. R. Soc. Lond.* 21, 495–496. doi: 10.1098/rspa.1872.0092
- Sattelmacher, B. (2001). The apoplast and its significance for plant mineral nutrition. *New Phytol.* 149, 167–192. doi: 10.1046/j.1469-8137.2001.00034.x
- Sattelmacher, B., and Horst, W. J. (2007). *The Apoplast of Higher Plants: Compartment of Storage, Transport and Reactions: The Significance of the Apoplast for the Mineral Nutrition of Higher Plants*. Dordrecht: Springer.
- Schachtman, D. P., and Shin, R. (2007). Nutrient Sensing and Signaling: NPKS. *Annu. Rev. Plant Biol.* 58, 47–69. doi: 10.1146/annurev.arplant.58.032806.103750
- Schroeder, J. I., Hedrich, R., and Fernandez, J. M. (1984). Potassium-selective single channels in guard cell protoplasts of *Vicia faba*. *Nature* 312, 361–362. doi: 10.1038/312361a0
- Shahzad, Z., and Amtmann, A. (2017). Food for thought: how nutrients regulate root system architecture. *Curr. Opin. Plant Biol.* 39, 80–87. doi: 10.1016/j.pbi.2017.06.008
- Somssich, M., Khan, G. A., and Persson, S. (2016). Cell Wall heterogeneity in root development of Arabidopsis. *Front. Plant Sci.* 7:1242. doi: 10.3389/fpls.2016.01242
- Spanswick, R. M., and Costerton, J. W. F. (1967). Plasmodesmata in *Nitella translucens*: structure and electrical resistance. *J. Cell Sci.* 2, 451–464.
- Strahl, H., and Hamoen, L. W. (2010). Membrane potential is important for bacterial cell division. *Proc. Natl. Acad. Sci. U.S.A.* 107, 12281–12286. doi: 10.1073/pnas.1005485107
- Szyroki, A., Ivashikina, N., Dietrich, P., Roelfsema, M. R. G., Ache, P., Reintanz, B., et al. (2001). KAT1 is not essential for stomatal opening. *Proc. Natl. Acad. Sci. U.S.A.* 98, 2917–2921. doi: 10.1073/pnas.051616698
- Tateda, C., Watanabe, K., Kusano, T., and Takahashi, Y. (2011). Molecular and genetic characterization of the gene family encoding the voltage-dependent anion channel in Arabidopsis. *J. Exp. Bot.* 62, 4773–4785. doi: 10.1093/jxb/err113
- Taylor, A. R., Brownlee, C., and Wheeler, G. L. (2012). Proton channels in algae: reasons to be excited. *Trends Plant Sci.* 17, 675–684. doi: 10.1016/j.tplants.2012.06.009
- Tilsner, J., Nicolas, W., Rosado, A., and Bayer, E. M. (2016). Staying tight: plasmodesmal membrane contact sites and the control of cell-to-cell connectivity in plants. *Annu. Rev. Plant Biol.* 67, 1–28. doi: 10.1146/annurev-arplant-043015-111840

- Trebacz, K., and Zawadzki, T. (1985). Light-triggered action potentials in the liverwort *Conocephalum conicum*. *Physiol. Plant.* 64, 482–486. doi: 10.1111/j.1399-3054.1985.tb08526.x
- Ullrich-Eberius, C. I., Novacky, A., Fischer, E., and Lüttege, U. (1981). Relationship between energy-dependent phosphate uptake and the electrical membrane potential in *lemon gibba* G1. *Plant Physiol.* 67, 797–801.
- Vidal, E. A., Araus, V., Lu, C., Parry, G., Green, P. J., Coruzzi, G. M., et al. (2010). Nitrate-responsive miR393/AFB3 regulatory module controls root system architecture in *Arabidopsis thaliana*. *Proc. Natl. Acad. Sci. U.S.A.* 107, 4477–4482. doi: 10.1073/pnas.0909571107
- Voelker, C., Schmidt, D., Mueller-Roeber, B., and Czempinski, K. (2006). Members of the Arabidopsis AtTPK/KCO family form homomeric vacuolar channels in *planta*. *Plant J.* 48, 296–306. doi: 10.1111/j.1365-313X.2006.02868.x
- Volkov, A. G. (2012). *Plant Electrophysiology*. ed A. G. Volkov. Berlin; Heidelberg: Springer.
- von Wangenheim, D., Goh, T., Dietrich, D., and Bennett, M. J. (2017). Plant biology: building barriers... in roots. *Curr. Biol.* 27, R172–R174. doi: 10.1016/j.cub.2017.01.060
- Waese, J., Fan, J., Pasha, A., Yu, H., Fucile, G., Shi, R., et al. (2017). ePlant: visualizing and exploring multiple levels of data for hypothesis generation in plant biology. *Plant Cell* 29, 1806–1821. doi: 10.1105/tpc.17.00073
- Wang, R., and Crawford, N. M. (1996). Genetic identification of a gene involved in constitutive, high-affinity nitrate transport in higher plants. *Proc. Natl. Acad. Sci. U.S.A.* 93, 9297–9301.
- Wang, R., Liu, D., and Crawford, N. M. (1998). The Arabidopsis CHL1 protein plays a major role in high-affinity nitrate uptake. *Proc. Natl. Acad. Sci. U.S.A.* 95, 15134–15139.
- Wang, R., Okamoto, M., Xing, X., and Crawford, N. M. (2003). Microarray analysis of the nitrate response in Arabidopsis Roots and shoots reveals over 1,000 rapidly responding genes and new linkages to glucose, trehalose-6-phosphate, iron, and sulfate metabolism. *Plant Physiol.* 132, 556–567. doi: 10.1104/pp.103.021253
- Ward, J. M., Mäser, P., and Schroeder, J. I. (2009). Plant ion channels: gene families, physiology, and functional genomics analyses. *Annu. Rev. Physiol.* 71, 59–82. doi: 10.1146/annurev.physiol.010908.163204
- Wheeler, G. L., and Brownlee, C. (2008). Ca<sup>2+</sup> signalling in plants and green algae - changing channels. *Trends Plant Sci.* 13, 506–514. doi: 10.1016/j.tplants.2008.06.004
- Xu, J., Li, H.-D., Chen, L.-Q., Wang, Y., Liu, L.-L., He, L., et al. (2006). A protein kinase, interacting with two calcineurin B-like proteins, regulates K<sup>+</sup> transporter AKT1 in *Arabidopsis*. *Cell* 125, 1347–1360. doi: 10.1016/j.cell.2006.06.011
- Yan, J., He, H., Tong, S., Zhang, W., Wang, J., Li, X., et al. (2009). Voltage-dependent anion channel 2 of *Arabidopsis thaliana* (AtVDAC2) is involved in ABA-mediated early seedling development. *Int. J. Mol. Sci.* 10, 2476–2486. doi: 10.3390/ijms10062476
- Yang, W., Nagasawa, K., Münch, C., Xu, Y., Satterstrom, K., Jeong, S., et al. (2016). Mitochondrial sirtuin network reveals dynamic SIRT3-dependent deacetylation in response to membrane depolarization. *Cell* 0, 14447–14452. doi: 10.1016/j.cell.2016.10.016
- Yang, X. Y., Chen, Z. W., Xu, T., Qu, Z., Pan, X. D., Qin, X. H., et al. (2011). Arabidopsis kinesin KP1 specifically interacts with VDAC3, a mitochondrial protein, and regulates respiration during seed germination at low temperature. *Plant Cell* 23, 1093–1106. doi: 10.1105/tpc.110.082420
- Zawadzki, T., Davies, E., Bziubinska, H., Htkbacz, K., and Characteristics, K. (1991). Characteristics of action potentials in *Helianthus annuus*. *Physiol. Plant.* 83, 601–604.
- Zebelo, S. A., Matsui, K., Ozawa, R., and Maffei, M. E. (2012). Plasma membrane potential depolarization and cytosolic calcium flux are early events involved in tomato (*Solanum lycopersicum*) plant-to-plant communication. *Plant Sci.* 196, 93–100. doi: 10.1016/j.plantsci.2012.08.006
- Zhang, A., Ren, H.-M., Tan, Y.-Q., Qi, G.-N., Yao, F.-Y., Wu, G.-L., et al. (2016). S-type anion channels SLAC1 and SLAH3 function as essential negative regulators of inward K<sup>+</sup> channels and stomatal opening in *Arabidopsis*. *Plant Cell* 28, 949–965. doi: 10.1105/tpc.16.01050
- Zhang, J., Martinoia, E., and De Angeli, A. (2014). Cytosolic nucleotides block and regulate the Arabidopsis vacuolar anion channel AtALMT9. *J. Biol. Chem.* 289, 25581–25589. doi: 10.1074/jbc.M114.576108
- Zhang, X., and Zhang, Y. (2009). Neural-Immune Communication in *Caenorhabditis elegans*. *Cell Host Microbe* 5, 425–429. doi: 10.1016/j.chom.2009.05.003
- Zheng, X., He, K., Kleist, T., Chen, F., and Luan, S. (2015). Anion channel SLAH3 functions in nitrate-dependent alleviation of ammonium toxicity in *Arabidopsis*. *Plant Cell Environ.* 38, 474–486. doi: 10.1111/pce.12389
- Zheng, Z.-L. (2009). Carbon and nitrogen nutrient balance signaling in plants. *Plant Signal. Behav.* 4, 584–591. doi: 10.4161/psb.4.7.8540
- Zhou, W., Brockmöller, T., Ling, Z., Omdahl, A., Baldwin, I. T., and Xu, S. (2016). Evolution of herbivore-induced early defense signaling was shaped by genome-wide duplications in *Nicotiana*. *eLife* 5:e19531. doi: 10.7554/eLife.19531
- Zimmermann, M. R., Maischak, H., Mithöfer, A., Boland, W., and Felle, H. H. (2009). System potentials, a novel electrical long-distance apoplastic signal in plants, induced by wounding. *Plant Physiol.* 149, 1593–1600. doi: 10.1104/pp.108.133884
- Conflict of Interest Statement:** The authors declare that the research was conducted in the absence of any commercial or financial relationships that could be construed as a potential conflict of interest.
- Copyright © 2018 Canales, Henriquez-Valencia and Brauchi. This is an open-access article distributed under the terms of the Creative Commons Attribution License (CC BY). The use, distribution or reproduction in other forums is permitted, provided the original author(s) or licensor are credited and that the original publication in this journal is cited, in accordance with accepted academic practice. No use, distribution or reproduction is permitted which does not comply with these terms.



# Osmotic and Salt Stresses Modulate Spontaneous and Glutamate-Induced Action Potentials and Distinguish between Growth and Circumnutation in *Helianthus annuus* Seedlings

Maria Stolarz\* and Halina Dziubinska

Department of Biophysics, Institute of Biology and Biochemistry, Maria Curie-Skłodowska University, Lublin, Poland

## OPEN ACCESS

### Edited by:

Vicenta Salvador Recatala,  
Ronin Institute, United States

### Reviewed by:

Alexandra C. U. Furch,  
Friedrich-Schiller-Universität Jena,  
Germany  
Yutaka Miyazawa,  
Yamagata University, Japan

### \*Correspondence:

Maria Stolarz  
maria.stolarz@poczta.umcs.lublin.pl

### Specialty section:

This article was submitted to  
Plant Physiology,  
a section of the journal  
*Frontiers in Plant Science*

Received: 21 June 2017

Accepted: 27 September 2017

Published: 18 October 2017

### Citation:

Stolarz M and Dziubinska H (2017)  
Osmotic and Salt Stresses Modulate  
Spontaneous and Glutamate-Induced  
Action Potentials and Distinguish  
between Growth and Circumnutation  
in *Helianthus annuus* Seedlings.  
*Front. Plant Sci.* 8:1766.  
doi: 10.3389/fpls.2017.01766

Action potentials (APs), i.e., long-distance electrical signals, and circumnutations (CN), i.e., endogenous plant organ movements, are shaped by ion fluxes and content in excitable and motor tissues. The appearance of APs and CN as well as growth parameters in seedlings and 3-week old plants of *Helianthus annuus* treated with osmotic and salt stress (0–500 mOsm) were studied. Time-lapse photography and extracellular measurements of electrical potential changes were performed. The hypocotyl length was strongly reduced by the osmotic and salt stress. CN intensity declined due to the osmotic but not salt stress. The period of CN in mild salt stress was similar to the control (~164 min) and increased to more than 200 min in osmotic stress. In sunflower seedlings growing in a hydroponic medium, spontaneous APs (SAPs) propagating basipetally and acropetally with a velocity of 12–20 cm min<sup>-1</sup> were observed. The number of SAPs increased 2–3 times (7–10 SAPs 24 h<sup>-1</sup> plant<sup>-1</sup>) in the mild salt stress (160 mOsm NaCl and KCl), compared to the control and strong salt stress (3–4 SAPs 24 h<sup>-1</sup> plant<sup>-1</sup> in the control and 300 mOsm KCl and NaCl). Glutamate-induced series of APs were inhibited in the strong salt stress-treated seedlings but not at the mild salt stress and osmotic stress. Additionally, in 3-week old plants, the injection of the hypo- or hyperosmotic solution at the base of the sunflower stem evoked series of APs (3–24 APs) transmitted along the stem. It has been shown that osmotic and salt stresses modulate differently hypocotyl growth and CN and have an effect on spontaneous and evoked APs in sunflower seedlings. We suggested that potassium, sodium, and chloride ions at stress concentrations in the nutrient medium modulate sunflower excitability and CN.

**Keywords:** osmotic potential, salt stress, circumnutiation, plant movement, electrophysiology, action potential, electrical transmission, signaling

## INTRODUCTION

Responses to stress and stimuli are essential for adaptation of organisms to environmental conditions. The role of signals propagated along plants organ and organ movements in these responses is an intriguing question. Universal electrical signals, i.e., action potentials (APs) propagating acropetally and basipetally many centimeters along plant organs from cell to cell

are well-documented. Complete electrophysiological characterization of APs (threshold, refractory periods, “all-or-none” law, velocity of propagation, chronaxie, rebase) has been carried out for *Helianthus annuus*, *Lupinus angustifolius*, and *Conocephalum conicum* (Paszewski and Zawadzki, 1973, 1974, 1976a,b; Zawadzki, 1979, 1980; Zawadzki et al., 1991, 1995; Favre et al., 1999). It is known that APs are involved in rapid plant movement and regulate many physiological processes and the circumstances of their appearance are still studied (Sibaoka, 1991; Stankovic et al., 1998; Dziubinska, 2003; Stahlberg et al., 2006; Zimmermann et al., 2009, 2016; Król et al., 2010; Stolarz et al., 2010; Salvador-Recatala et al., 2014; van Bel et al., 2014; Kiep et al., 2015; Macedo et al., 2015; Salvador-Recatala and Tjallingii, 2015; Hedrich et al., 2016; Salvador-Recatala, 2016). A spontaneous action potential (SAP) is an action potential in which exogenous or endogenous stimuli evoking them are not known. Usually, in plants, APs result from an external stimulus (Paszewski and Zawadzki, 1973; Trebacz and Zawadzki, 1985; Favre et al., 1999; Krol et al., 2006; Król et al., 2010). However, some excitable cells do not require stimuli for generation of APs (Zawadzki et al., 1995). They spontaneously depolarize and generate an AP usually at a regular rate/rhythm. This SAP rate/rhythm can be adjusted by environmental condition as was shown recently in *H. annuus* (Stolarz and Dziubinska, 2017). The external stimuli or environmental conditions do not cause SAPs, but merely alter their rate/rhythm. In plants, SAPs were described over 20 years ago by Zawadzki et al. (1995) in *H. annuus* and lately they have been observed in *Solanum lycopersicum* plants (Macedo et al., 2015). The AP ion mechanism in plants has been elaborated in many species, for example *C. conicum*, *Arabidopsis thaliana*, and *Physcomytrella patens* (Trebacz and Zawadzki, 1985; Trebacz et al., 1989, 1994, 2007; Trebacz, 1992; Krol et al., 2006, 2007; Koselski et al., 2015, 2017). Fundamental players in the AP ion mechanism in plants are  $\text{H}^+$ ,  $\text{Ca}^{2+}$ ,  $\text{K}^+$ , and  $\text{Cl}^-$ . The latter ones ( $\text{K}^+$  and  $\text{Cl}^-$ ) are also the major osmotically active elements in the cytoplasm and vacuole and are involved in both osmoregulation and turgor maintenance and thus water fluxes and cell volume changes (White, 2001; Zhu, 2003; Ashley et al., 2006; Shabala and Cuin, 2008; Szczerba et al., 2009; Aleman et al., 2011; Shabala and Pottosin, 2014; Shabala et al., 2015; Coskun et al., 2016). Osmotically driven water fluxes resulting in cell volume changes are fundamental for cell elongation and essential for endogenous movement named circumnutiation (CN) (Johnsson, 1979; Millet and Badot, 1996; Shabala and Newman, 1997; Shabala and Knowles, 2002; Shabala, 2003; Stolarz, 2009; Grefen et al., 2011; Kurenda et al., 2015). An endogenous CN can be modulated by multiple external stimuli e.g., light, wounding, touch, temperature, chemicals, and gravity as well as by organ morphology and biological clock (Buda et al., 2003; Hayashi et al., 2004; Charzewska and Zawadzki, 2006; Stolarz, 2009; Stolarz et al., 2010). CNs are an effect of highly coordinated and phase synchronized cell elongation and intercellular communication inside the motor/elongation zone of a growing organ. The membrane potential changes and ion fluxes are important elements of the CN mechanism (Millet and Badot, 1996; Stolarz, 2009; Kurenda et al., 2015). The ion content in the soil (nutrient solution), ion uptake, and

ion content in the apoplast and symplast is therefore essential for transmembrane potential maintenance; it could change plant excitability and cell volume and growth and thus CN. Growth inhibition in plants is a most frequently defined effect of environmental stress, including salt stress (Zhu, 2003; Foster and Miklavcic, 2015; Wu et al., 2015a). CNs are closely related to growth, and CN changes after many environmental stimuli have been described (Buda et al., 2003; Stolarz et al., 2008, 2015; Stolarz, 2009; Kurenda et al., 2015). An endogenous motor activity and electrical long-distance signaling in the form of CNs and APs have been well-characterized in *H. annuus*. *H. annuus* is an important agricultural crop grown for oil, fresh green mass, and as ornamental plants whose yield can be reduced by drought and the accompanying osmotic and salt stress. The sunflower is studied simultaneously as a crop with relatively high tolerance to drought and therefore osmotic and saline stress (Mukherjee et al., 2014; Ceccoli et al., 2015; Wu et al., 2015b; Singh and Bhatla, 2016). Investigations of the effect of the osmotic potential of the nutrient medium on the transmission of electrical signals and changes in endogenous motor activity of the sunflower may provide new information on the role of intercellular communication in plant adaptation to changing environmental conditions.

The aim of our study was to characterize the effect of osmotic and salt stress on growth, CN parameters, and appearance of APs. A different effect of salt stress than osmotic stress on CN and, hence, on the growth and appearance of APs was revealed. For the first time, spontaneous APs in seedlings growing in a hydroponic medium and enhancement of spontaneous excitation in sunflower seedlings by salinity were shown.

## MATERIALS AND METHODS

### Experimental Plants

#### Sunflower Seedlings

Seeds of *H. annuus* L. (PNOS, Ozarów Maz., Poland) were germinated on wet filter paper in a thermostatted ( $24 \pm 1^\circ\text{C}$ ) darkened chamber. After 4 days, seedlings with  $4.5 \pm 0.5$ -cm-long hypocotyls were cultivated hydroponically (10 plants per pot) in an aerated nutrient solution. The hydroponic culture was maintained for 3 days under constant illumination,  $40 \mu\text{mol m}^{-2}\text{s}^{-1}$  white light (Power Star HQT-T400 W/D OSRAM GmbH, Munich, Germany), at a temperature of  $24 \pm 1^\circ\text{C}$  and relative humidity 50–70%. The seedlings were grown for 3 days in a control medium or were treated with different  $\text{KCl}$ ,  $\text{NaCl}$ , and D-sorbitol concentrations and simultaneously filmed for CN measurements. In 7-day-old seedlings, the length of the seedling hypocotyl was measured and electrophysiological measurements of the seedlings were performed.

#### Three Week-Old Sunflowers

The studies were carried out on 3 week-old *H. annuus* L. plants (PNOS, Ożarów Maz. Poland) grown in a vegetation room in pots filled with garden soil. They were watered with tap water and no other treatment was applied. A 16:8 h light:dark (4:00 a.m.–8:00 p.m.) photoperiod was maintained. The intensity of white light in the PAR (Photosynthetic Active Radiation) range (Power Star

HQT-T400 W/DOSRAM GmbH, Munich, Germany) at the level of plant leaves was  $\sim 70 \mu\text{mol m}^{-2}\text{s}^{-1}$ . The vegetation room was air-conditioned; the temperature was  $24 \pm 1^\circ\text{C}$  and humidity 50–70%. Approximately 20–30 cm high plants with one or two pairs of developed leaves were taken for the experiments. The 3-week old plants were transferred to a Faraday cage at  $\sim 12:00$  and electrodes were inserted. Distilled water, D-sorbitol, KCl, or NaCl were injected between 6:00 p.m.–7:00 p.m.

## Time-Lapse Method and CN Measurements

For CN measurements, time-lapse photography recordings were made from 09:00 a.m. on the fourth day to 09:00 a.m. on the seventh day of seedling growth. A monochromatic camera (Mintron MTV-1368CD, Mintron Enterprise Co. Ltd, Taipei, Taiwan) was used to record the circumnutiation trajectory of the hypocotyls apex. The plants were filmed from the top. Time-lapse images were recorded one frame per 5 min by Gotcha! Multicam software (Prescient System Inc., West Chester, PA, USA). The system was calibrated in a millimeter scale. The time-lapse images were digitized using *Circumnutiation Tracker* (Stolarz et al., 2014) and Microsoft Excel programs. Experimental points (coordinates  $x, y$  of the stem apex on the horizontal plane) were determined at 5-min intervals. In the geographic direction plane, the single circumnutiation cycle is determined by two subsequent maximum northward bends of the organ (Stolarz et al., 2014). Supplementary Video S1 shows subsequent CN cycles of sunflower seedlings. The distance covered by the hypocotyls apex during one CN cycle was used to calculate the CN rate. CN intensity was the rate of CN divided by the length of the hypocotyls. The CN period was the time required for the hypocotyls apex to trace a single CN cycle (time between two subsequent maximum northward bends of the organ) (Stolarz et al., 2014).

## Electrophysiological Measurements—Extracellular Method

The electrical measurements were carried out in a Faraday cage on 7- to 8-day-old seedlings or 3-week-old sunflowers. The changes in the electrical potential were measured with two or four extracellular Ag/AgCl electrodes (a silver wire, 0.2 mm diameter, World Precision Instruments, Sarasota, FL, USA) inserted across the sunflower hypocotyl or stem and then interfaced with a multi-channel data acquisition system composed of a differential amplifier (ME-4600 Meilhaus, Germany) and RealView software (Abacom, Germany) (Supplementary Figure S1). During the preparation of the Ag/AgCl electrodes, the silver wire was electrolytically coated with silver chloride. The electrical potential was recorded from tissues adjacent to the electrode, i.e., vascular bundles, parenchyma, and epidermis (Dziubinska et al., 2001). The reference electrode (Ag/AgCl) was placed in the hydroponic medium or soil. The frequency of sample recording was 1 Hz. For registration of SAPs (spontaneous action potentials), seedlings grew in the Faraday cage in a hydroponic solution for 3 days. Glutamate (Glu) injection was applied between 8:00 a.m.–2:00

p.m. in 7–8-day-old seedlings growing in different nutrient solutions for 3 days.

## Chemicals

### Hydroponic Culture

The nutrient solution contained  $4 \text{ mM } \text{Ca}(\text{NO}_3)_2 \times 4\text{H}_2\text{O}$ ,  $5 \text{ mM } \text{KNO}_3$ ,  $1 \text{ mM } \text{NH}_4\text{H}_2\text{PO}_4$ ,  $2 \text{ mM } \text{MgSO}_4 \times 7\text{H}_2\text{O}$ ; microelements:  $0.085 \text{ mM } \text{Fe(III)citrate}$ ,  $0.046 \text{ mM } \text{H}_3\text{BO}_3$ ,  $0.0009 \text{ mM } \text{MnCl}_2 \times 4\text{H}_2\text{O}$ ,  $0.0003 \text{ mM } \text{CuSO}_4 \times 5\text{H}_2\text{O}$ ,  $0.0008 \text{ mM } \text{ZnSO}_4 \times 7\text{H}_2\text{O}$ ,  $0.0001 \text{ mM } \text{H}_2\text{MoO}_4 \times 2\text{H}_2\text{O}$ ; (pH 6.0); the osmotic potential was 23 mOsm. Additionally,  $80 \text{ mM}$  (160 mOsm),  $120 \text{ mM}$  (240 mOsm), and  $160 \text{ mM}$  (300 mOsm) potassium chloride (POCH, Poland) and sodium chloride (POCH, Poland) in the nutrient solution was used as a hyperosmotic salt stress. Hyperosmotic stress was adjusted by  $160 \text{ mM}$  (160 mOsm) D-sorbitol (POCH, Poland). The osmotic potential was measured with a cryoscopic osmometer (Osmomat 030, Gonotec GmbH, Berlin, Germany).

## Injection

Twenty microliters of a  $50 \text{ mM}$  Glu solution (L-glutamic acid, ICN Biomedicals, Germany, pH adjusted to 7 by Tris/Mes buffer), distilled water,  $250 \text{ mM}$  KCl (500 mOsm) (POCH, Poland),  $250 \text{ mM}$  NaCl (500 mOsm) (POCH, Poland), and  $500 \text{ mM}$  D-sorbitol (500 mOsm) (POCH, Poland) were injected with a syringe into the seedlings at the base of the hypocotyls (Glu), 1 cm above the root collar, or at the base of the stem in the 3-week old plants. The injection of the solution lasted a few seconds. The injury of the sunflower hypocotyls or stem with a syringe needle induced either only one AP or none (Stolarz et al., 2010).

## Statistical Analysis

The data were analyzed using Statistica ver. 12 software (StatSoft, Inc., 2014). The data set was first tested for normality using Shapiro-Wilk test and homogeneity of variance by Levene's test. The non-parametric Kruskal-Wallis ANOVA and non-parametric Mann-Whitney *U*-test for pairwise analysis were used when the data had non-normal distribution or unequal variance. The one-way ANOVA and *post-hoc* Tukey test for pairwise analysis were used when the data had normal distribution and equal variance. The level of statistical significance for all tests was set at  $p < 0.05$ .

## RESULTS

The sunflower seedlings treated with hypoosmotic (distilled water) and hyperosmotic (D-sorbitol, KCl and NaCl) nutrient solutions in the hydroponic culture were characterized by decreased growth and changes in the CN parameters. Spontaneous excitation was also modified by the osmotic potential of the nutrient solution. Additionally, localized stimuli—the injection of the glutamate solution at the base of hypocotyls or the hypo- or hyperosmotic solution at the base of the stem induced different numbers of APs dependent on the kind of the injected solution and the osmotic potential of the nutrient.

## Effect of Osmotic and Salt Stress on the Growth and CN Intensity in Sunflower Seedlings

The sunflower seedlings growing in the control nutrient solution (23 mOsm) had  $10 \pm 0.6$  cm ( $n = 20$ ) long hypocotyls. Both the hypoosmotic and hyperosmotic nutrient solutions reduced the hypocotyl length in a statistically significant way by  $\sim 10\text{--}30\%$  (Figure 1A, Supplementary Figure S2). Simultaneously, the CN parameters changed differently in the osmotic and salt stress conditions. Sunflower seedlings growing in distilled water (0 mOsm) had significantly shortened hypocotyls and drastically reduced CN intensity in relation to those growing in the control nutrient solution (Figures 1A,B). Similarly, the high osmotic potential (160 mOsm) evoked by D-sorbitol significantly shortened the hypocotyl length and drastically reduced CN intensity (Figures 1A,B). In turn, the increase in the osmotic potential to 160–300 mOsm induced by salt (KCl or NaCl) did not influence the CN intensity although the hypocotyl length was significantly reduced (Figures 1A,B). Sunflower seedlings with similar hypocotyl length exhibited completely different CN intensity in osmotic and salt stress. The CNs were strongly inhibited in distilled water and 160 mM D-sorbitol (160 mOsm) but were vigorous (as in the control seedlings) in the salt stress inducing solutions (160–300 mOsm KCl and NaCl). The osmotically induced growth inhibition was accompanied by a decrease in the CN intensity but the salt-induced growth inhibition had little effect on the CN intensity.

## Effect of Osmotic and Salt Stress on the CN Period in Sunflower Seedlings

In the sunflower seedlings, the mean CN period in the control solution was  $174 \pm 6$  min ( $n = 20$ , Figure 1C). The CN period was lengthened in a statistically significant way in seedlings growing in distilled water (0 mOsm) to  $245 \pm 19$  min ( $n = 10$ ). The CN period was longer by 70 min. Simultaneously, the CN period in seedlings growing in the D-sorbitol, KCl, and NaCl solutions (160–300 mOsm) was the same as in the control conditions. In 120 mM NaCl and 160 mM KCl, it was significantly longer but only by  $\sim 15$  min. The CN period was the same as in the control in the mild salt stress and even in the strong stress (160 mM NaCl). The hypocotyls of the same length had a completely different CN period in the osmotic and salt solution, which proves the absence of a strict connection between the CN and hypocotyl growth.

Given the above results, it can be assumed that only the osmotic stress disturbs growth and CN (intensity and period); in turn, the salt stress disturbs the growth mechanism only and does not influence the CN mechanism. This shows that there is a salt stress-resistant ultradian pacemaker in the sunflower and confirms that the presence of ions in the nutrient solution is basic for the CN mechanism.

$K^+$ ,  $Cl^-$ , and  $Na^+$  are also essential for membrane potential maintenance and excitability of organisms; therefore, we expect that the sunflower seedlings growing under different  $K^+$ ,  $Cl^-$ , and  $Na^+$  contents in the nutrient solution could have a different excitability.

## Spontaneous Action Potentials in Sunflower Seedlings

The number, velocity, and direction of propagation of SAPs were determined in salt and osmotically stressed sunflower seedlings (Figure 2, Table 1). An example of SAPs in sunflower seedlings is shown in Figure 2 and Supplementary Video S2. In the control conditions,  $3 \pm 1$  SAPs  $24\text{ h}^{-1}$  plant $^{-1}$  ( $n = 12$ ) were registered, which propagated mainly basipetally (75%) with a mean velocity  $14 \pm 1\text{ cm min}^{-1}$ . This was similar in the strong salt stress conditions (300 mOsm KCl and NaCl) (Table 1). In the seedlings growing in distilled water and in D-sorbitol (160 mOsm), SAPs were completely silenced. The number of SAPs significantly increased in mild KCl stress where the number of SAPs increased two and three times to 10 SAPs  $24\text{ h}^{-1}$  plant $^{-1}$ , compared to the control and 300 mOsm salt solution. Similarly, in mild NaCl stress, the SAP number slightly increased to 7 SAPs  $24\text{ h}^{-1}$  plant $^{-1}$  and SAP propagation velocity significantly increased to  $20 \pm 1\text{ cm min}^{-1}$  in those seedlings. The percentage of basipetally and acropetally propagating SAPs remained similar in all conditions (Table 1). The complete lack of SAPs in distilled water and the 160 mOsm D-sorbitol solution as well as the significantly increased number of SAPs and their propagation velocity in mild salt stress showed that the  $K^+$ ,  $Cl^-$ , and  $Na^+$  concentration in the nutrient solution modulated spontaneous excitability. The silencing of SAPs and the reduced vigor of CNs indicates that SAPs and CNs were repressed by the lack of ions or ion uptake disturbance in distilled water and the hyperosmotic D-sorbitol solution. Mild and strong salt stress nutrient conditions maintain CNs and maintain or even enhance SAPs; thus, these results show an essential role of  $K^+$ ,  $Cl^-$ , and  $Na^+$  ions in both phenomena.

## Glu-Induced Series of APs in the Hypocotyls of Sunflower Seedlings

Besides SAPs, Glu-induced series of APs in osmotically and salt-stressed seedlings were studied. The series of APs evoked by injection of the 50 mM Glu solution in the control plants consisted of  $10 \pm 1$  APs ( $n = 10$ ) (Figure 2D, Table 2). Similar series were obtained in mild stress in the D-sorbitol, KCl and NaCl (160 mOsm) treated seedlings; however, in strong KCl and NaCl (320 mOsm) stress, the series were significantly inhibited to 2–3 APs in a series (Figure 2D, Table 2). Seedlings growing in distilled water exhibited reduced growth, CNs (Figures 1A,B), and Glu-induced series of APs (only 30% of the seedlings were excitable, Table 2), compared to the control plants. Seedlings growing in D-sorbitol (160 mOsm) had shorter hypocotyls and reduced CN but generated Glu-induced series, likewise the control and mild stress-treated plants, which had shorter hypocotyls and unchanged vigor of CN. Additionally, sunflower seedlings treated with strong salt stress (300 mOsm) had a reduced hypocotyl length and unchanged CN, but the Glu-induced series of APs were strongly inhibited.

The spontaneous and glutamate-induced excitability changes in seedlings growing in the osmotic and salt stress conditions

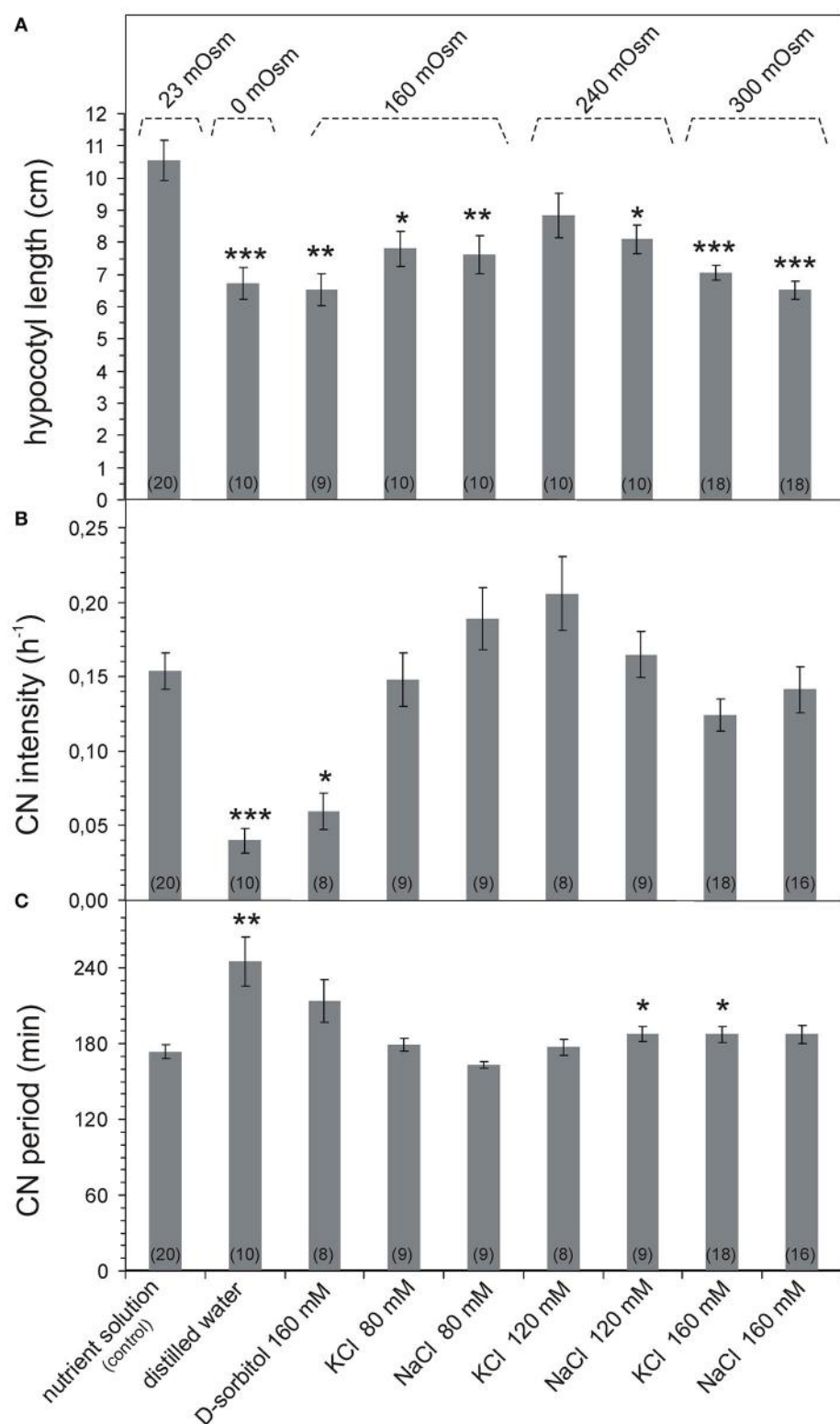


**FIGURE 1 |** Parameters of growth and CN of *Helianthus annuus* seedlings under osmotic and salt stresses. Bars represent mean  $\pm$  SE. The number of plants is indicated in parentheses. The data were tested for normality distribution using the Shapiro-Wilk test. The non-parametric Mann-Whitney *U*-test for pairwise analysis (A,C) and Tukey test (B) were used to assess the statistical difference between the control plants and each sunflower group growing in different nutrients; *p*-value ranges are marked by asterisks: \*\*\**p* < 0.001, \*\**p* < 0.01, \**p* < 0.05. (A) Changes in hypocotyl length, data normally distributed, unequal variance

(Continued)

**FIGURE 1 |** continued

(Levene's test  $p = 0.000109$ ), Kruskal-Wallis ANOVA (Chi square = 27.39 df = 8  $p = 0.0006$ ). **(B)** Changes in hypocotyl CN intensity. The distance covered by the hypocotyl apex during one cycle was used to calculate the CN rate. CN intensity was the rate of CN divided by hypocotyl length. Data normally distributed, equal variance Levene's test ( $p = 0.30$ ), one-way ANOVA (SS = 0.2149 df = 8 F = 10.015  $p = 0.0000$ ). **(C)** Changes in hypocotyl CN period. The CN period was the time required by the hypocotyl apex to trace a single CN cycle (time between two subsequent maximum northward bends of the hypocotyl). Data normally distributed, unequal variance (Levene's test  $p = 0.000053$ ), Kruskal-Wallis ANOVA (Chi square = 24.55 df = 8  $p = 0.0018$ ).

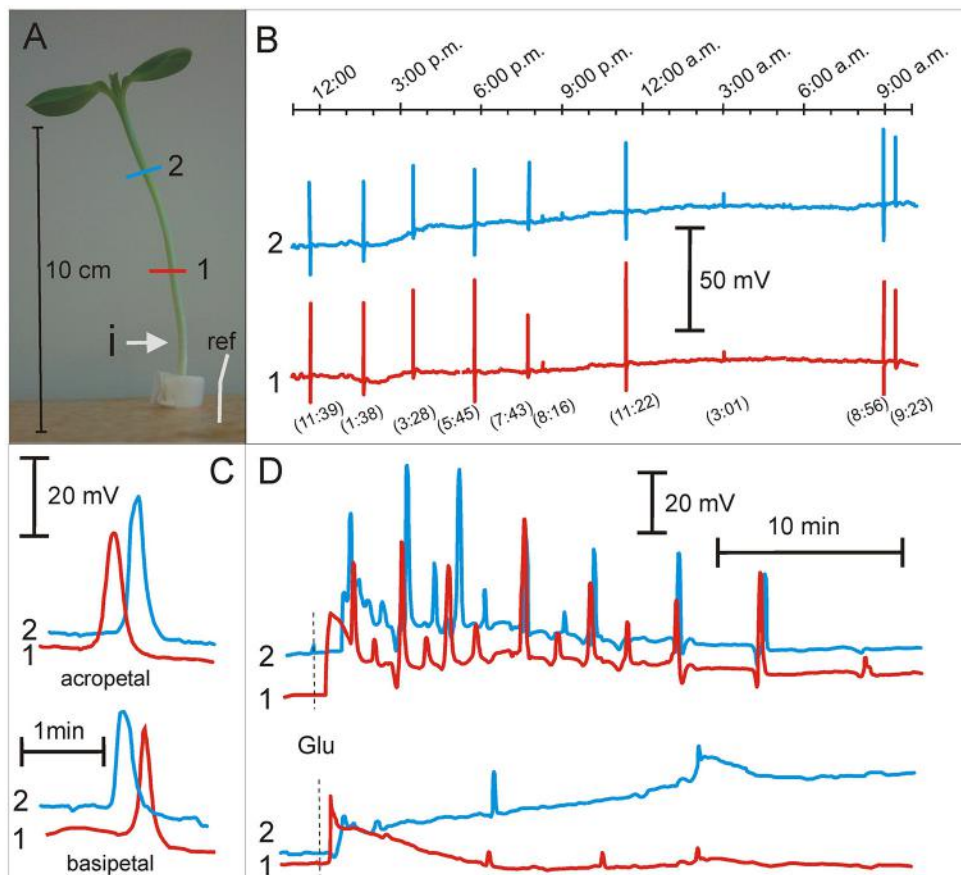


**FIGURE 2 |** Spontaneous action potentials and glutamate induced series of action potentials in *Helianthus annuus* seedlings under osmotic and salt stresses. **(A)** *Helianthus annuus* seedlings, electrode arrangement (1, 2, ref—reference electrode) and site of glutamate injection (i). **(B)** Example of recordings of spontaneous action potentials during 1 day (also shown in Supplementary Video S2). In the parentheses, the time of SAP appearing. **(C)** Example of recordings of acropetally and basipetally propagating spontaneous action potentials. **(D)** Example of recordings of action potential series after glutamate (Glu) injection into the hypocotyl base of seedlings growing under 80 mM KCl (upper) as well as 160 mM NaCl nutrient solutions (lower). Data details are presented in **Tables 1, 2**.

encouraged us to check the APs appearing after injection of the hypoosmotic and hyperosmotic solution in 3-week old sunflower plants.

### Osmotically and Salt-Induced Series of APs in the Stem of 3-Week Old Sunflowers

Injection of distilled water or 500 mOsm solutions (D-sorbitol, KCl) into the sunflower stem evoked series of APs presented in **Figure 3**. The parameters of sunflower excitation after injection of the osmotic and salt solutions are presented in **Table 3**. Distilled water, D-sorbitol, and KCl solutions evoked series of 3 to 24 APs in 70–100% of treated plants. APs propagated mainly

acropetally from the site of injection toward the stem apex, at an ~15 cm long distance. The injection of the NaCl 250 mM solution did not evoke APs (Supplementary Figure S3). These results show that a series of long-distance propagating (~15 cm) APs in the sunflower stem can be induced by distilled water, D-sorbitol and KCl but not by NaCl.

### DISCUSSION

Closure of the trap leaf in *Dionaea* and leaf folding in *Mimosa* after touching are commonly known, easily observable examples of plant responses to environmental stimuli, in which

**TABLE 1 |** Parameters of spontaneous excitation in *Helianthus annuus* seedlings under osmotic and salt stresses.

Hydroponic medium (mM)	Number of studied plants	% of excitable plants	n	SAPs 24 h <sup>-1</sup> plant <sup>-1</sup>	SAPs velocity (cm min <sup>-1</sup> )	SAPs direction of propagation %
						basipetal      acropetal
Distilled water	8	0	0		lack of SAPs	
Nutrient solution (control)	12	75	9	3 ± 1	14 ± 1	75      25
160 mM D-sorbitol	6	0	0		lack of SAPs	
80 mM KCl	12	100	12	10 ± 2***	14 ± 1	77      23
80 mM NaCl	8	62	5	7 ± 2	20 ± 1***	71      29
160 mM KCl	8	100	8	4 ± 1	15 ± 1*	75      25
160 mM NaCl	8	75	6	4 ± 1	12 ± 1	80      20

Propagation velocity of APs was calculated by taking the distance between the electrodes and dividing it by the time necessary for AP to move between the electrodes. Basipetal SAPs are SAPs propagating downwards the stem; acropetal SAPs are SAPs propagating upwards the stem; n—number of seedlings with SAPs.

SAPs 24 h<sup>-1</sup> plant<sup>-1</sup>: data non-normally distributed, unequal variance (Levene's test p = 0.000022), Kruskal-Wallis ANOVA (Chi square = 10.31 df = 4 p = 0.0354). SAP velocity: data non-normally distributed, unequal variance (Levene's test p = 0.000022), Kruskal-Wallis ANOVA (Chi square = 33.66 df = 4 p = 0.0000). Mann-Whitney U-test was used to assess the statistical difference between the control plants and each sunflower group growing in different nutrients. p-value ranges are marked by asterisks: \*\*\*p < 0.001, \*p < 0.05.

**TABLE 2 |** Parameters of glutamate induced series of action potentials in *Helianthus annuus* seedlings growing under osmotic and salt stresses.

Hydroponic medium (mM)	Number of studied plants	% of excitable plants	n	APs series	
				APs number	Series duration (min)
Distilled water	7	29	2	5 ± 2	13 ± 2
Nutrient solution (control)	10	100	10	10 ± 1	20 ± 5
160 mM D-sorbitol	14	100	14	10 ± 1	22 ± 5
80 mM KCl	16	100	16	11 ± 1	35 ± 3*
80 mM NaCl	8	50	4	7 ± 1	16 ± 5
160 mM KCl	12	58	7	2.4 ± 0.2***	9 ± 2
160 mM NaCl	13	69	9	2.8 ± 0.3***	33 ± 15

The duration of the series is the time between the first and the last AP in the series. n—number of excitable plants. AP number: data non-normally distributed, unequal variance (Levene's test p = 0.0020), Kruskal-Wallis ANOVA (Chi square = 27.22 df = 6 p = 0.0001). Series duration: data non-normally distributed, unequal variance (Levene's test p = 0.0421), Kruskal-Wallis ANOVA (Chi square = 13.57 df = 6 p = 0.0421). Mann-Whitney U-test was used to assess the statistical difference between the control plants and each sunflower group growing in different nutrients. p-value ranges are marked by asterisks: \*\*\*p < 0.001, \*p < 0.05.

the universal biological signal AP is involved. Thanks to the recent well-developed time-lapse photography method, slow endogenous organ motion can be visualized and investigated under stimuli and environmental changes (Buda et al., 2003; Stolarz et al., 2003, 2014; Kurenda et al., 2015). Long lasting extracellular electrical measurements can show also plant excitability in a wide time span of even a few days (Zawadzki et al., 1995; Favre et al., 1999; Macedo et al., 2015). For better understanding of the role of APs as physiological signals in plants, SAPs and Glu-induced excitation was studied in osmotically and salt-stressed sunflower seedlings in relation to hypocotyl growth and CN.

## Hypocotyl Elongation, But Not CN Intensity, was Decreased by Salinity Stress

The problem of CN dependence on growth has been considered many times (Spurny, 1975; Johnsson, 1979, 1997; Millet and Badot, 1996; Stolarz et al., 2008). In general, CNs are dependent on growth, but in some environmental conditions, for example under lithium, red light, or ethylene treatment, growth and CN uncoupling was observed (Spurny, 1968; Zachariassen and Johnsson, 1988; Millet and Badot, 1996; Yoshihara and Iino, 2005; Binder et al., 2006; Stolarz et al., 2008, 2015). This study has shown that the osmotic and salt stress treatments distinguish between growth and CN behavior (**Figures 1A,B**). Significant inhibition of elongation of hypocotyls was observed when distilled water, D-sorbitol, KCl, and NaCl were applied (**Figure 1A**). The CN intensity decreased significantly only in seedlings growing in distilled water and D-sorbitol (**Figure 1B**). Seedlings with a similar hypocotyl length had different CN intensity in osmotic and salt stress. These results showed that the mechanism of elongation is influenced differently than the mechanism of CN. The concentration of 80–160 mM K<sup>+</sup>, Na<sup>+</sup>, and Cl<sup>-</sup> decreased growth but did not affect the CN intensity. The absence of ions or ion uptake disturbance in distilled water or D-sorbitol inhibited growth and CN.

Some other studies showed the different physiological effect of the “osmotic” and “ionic” component of salt stress. The “osmotic” and “ionic” component of salt stress differently modulated net ion fluxes in leaf mesophyll of *Vicia faba* (Shabala, 2000). Osmotic stress in barley regulated expression of a different set of genes than salt stress (Ueda et al., 2004). The effect of osmotic stress was also shown in *Beta vulgaris* when D-sorbitol-induced osmotic stress strongly reduced its growth and led to a significant decrease in shoot osmotic potential, water content, and K<sup>+</sup> concentrations (Wu et al., 2015a).

## Stable CN Period in Salt Stress

Circumnutation, a rhythmic phenomenon can be considered as a “cue” internal ultradian oscillator (Millet and Badot, 1996;

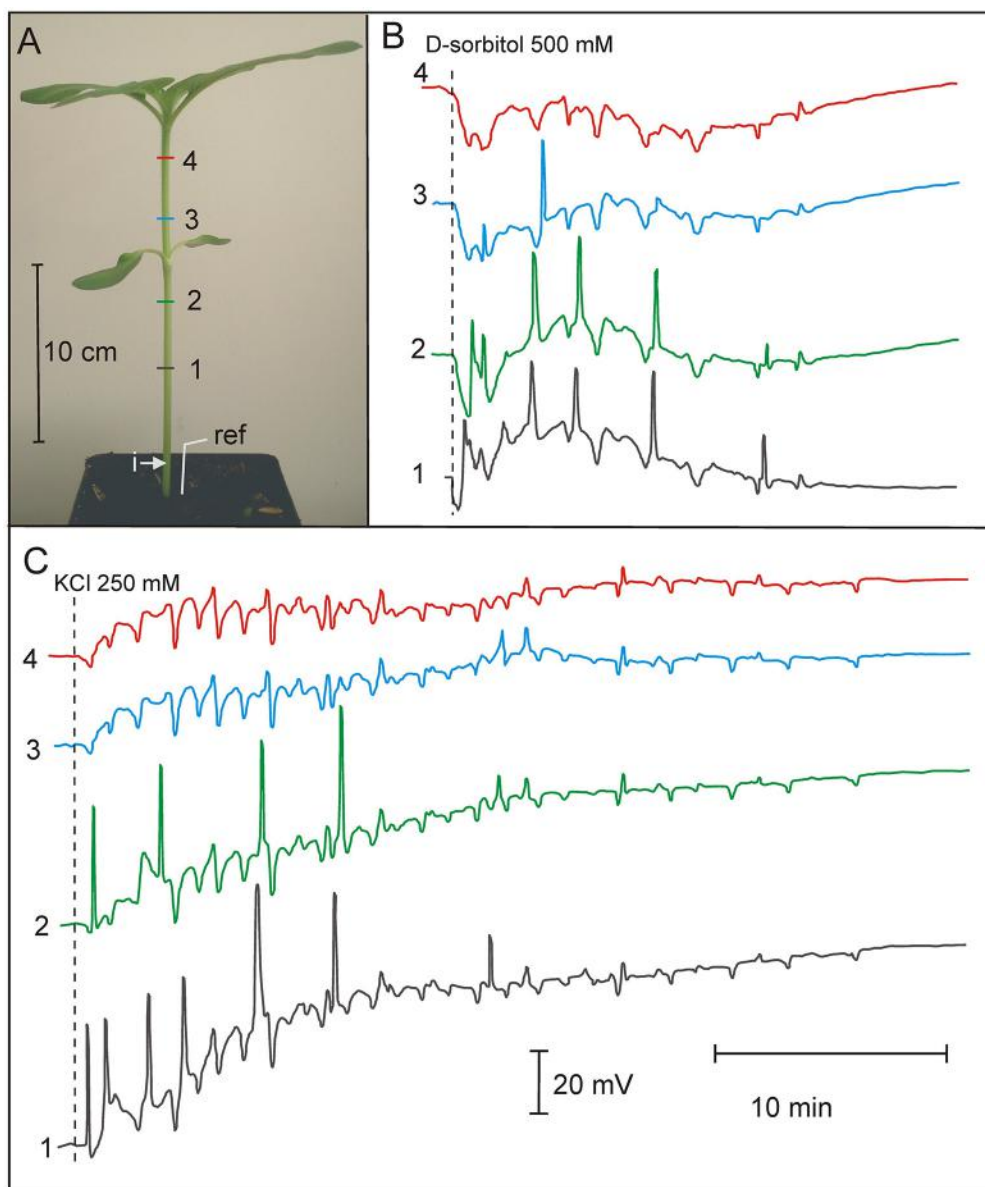


**FIGURE 3 |** Osmotically and potassium chloride-induced series of action potentials in 3-week old *Helianthus annuus*. **(A)** *Helianthus annuus* plants, electrode arrangement (1, 2, 3, 4, ref—reference electrode) and site of solution injection (i). **(B)** Example of recordings of action potential series after D-sorbitol 500 mOsm (500 mM) injection into the stem base. **(C)** Example of recordings of action potential series after KCl 500 mOsm (250 mM) injection into the stem base. Data details are presented in Table 3.

Shabala, 2003; Lloyd, 2006). The CN period and its shortening or lengthening in various environmental conditions is important in a study of the ultradian pacemaker mechanism (Johnsson, 1979, 1997; Zachariassen and Johnsson, 1988; Stolarz, 2009; Hinrichsen et al., 2012). In this study, a stable period, despite the growth reduction, was shown (Figures 1A,C). The period of CNs in the mild and strong salt stress (163–188 min) was close to the CN period of the control plants (174 min). The CN period was lengthened significantly only in distilled water (245 min). This confirms a strong resistance of the CN

period to osmotic and salt stress (Erdei et al., 1998). The independence of the CN period of the growth of hypocotyls confirmed some degree of independence between growth and CN behavior, as in the case of lithium treatment (Stolarz et al., 2015).

The results presented above confirmed again the autonomy of CN behavior in relation to elongation and special physiological and ecological functions of CN being not merely a strict result of growth (Darwin and Darwin, 1880; Inoue et al., 1999; Larson, 2000; Kosuge et al., 2013; Migliaccio et al., 2013).

**TABLE 3 |** Parameters of osmotic and salt-induced series of action potentials in 3-week old *Helianthus annuus*.

Solution injected	Number of treated plants	% of excitable plants	n	Series of AP	
				APs number	Series duration (min)
Distilled water 0 mM Osm	9	70	6	6 ± 1 <sup>a</sup>	11 ± 2 <sup>a</sup>
D-sorbitol 500 mM 500 mM Osm	8	100	8	8 ± 1 <sup>a</sup>	13 ± 1 <sup>a</sup>
KCl 250 mM 500 mM Osm	7	100	7	17 ± 1 <sup>b</sup>	27 ± 2 <sup>b</sup>
NaCl 250 mM 500 mM Osm	10	0	0	lack of series of APs	

The duration of the series is the time between the first and the last AP in the series. n—number of excitable plants. AP number: data normally distributed, unequal variance (Levene's test  $p = 0.0025$ ), Kruskal-Wallis ANOVA (Chi square = 13.48 df = 2  $p = 0.0012$ ). Series duration: data normally distributed, unequal variance (Levene's test  $p = 0.0017$ ), Kruskal-Wallis ANOVA (Chi square = 17.29 df = 2  $p = 0.0002$ ). Mann-Whitney U-test was used to assess the statistical differences in one parameter between the groups; different letters denote statistical difference.

## Mild Salt Stress Enhances Spontaneous Action Potentials in Sunflower Seedlings

In plants, beside the stimulus-induced APs (electrical and mechanical stimuli, light, temperature, chemicals), there are SAPs. The SAPs appear in the absence of external stimuli and their endogenous source is unknown. SAPs were previously observed in 3-week old *Helianthus* and *Lycopersicum* plants growing in pots with standard soil (Zawadzki et al., 1995; Macedo et al., 2015). In this study, we have shown for the first time SAPs in sunflower seedlings growing in a hydroponic medium (**Figure 2**, Supplementary Video S2). This offered a new opportunity to modify the nutrient composition and investigate SAPs in plants in a specified nutrient environment.

In this work, we have described the number of SAPs per  $24\text{ h}^{-1}\text{ plant}^{-1}$  as a parameter of endogenous “firing,” which we have shown to be able to appear in control conditions (no external stimuli) but were modulated by osmotic and ionic stress. In the controlled nutrient conditions, the sunflower seedlings generated  $3 \pm 1$  SAPs  $24\text{ h}^{-1}\text{ plant}^{-1}$  ( $n = 12$ ). This number of SAPs persisted even under strong salt stress but completely disappeared in the distilled water and D-sorbitol (160 mM, 160 mM Osm) treatment (**Table 1**). The number of SAPs increased significantly to  $10 \pm 2$  SAPs  $24\text{ h}^{-1}\text{ plant}^{-1}$  ( $n = 12$ ) in 80 mM KCl (160 mM Osm). This showed that the “ionic” but not “osmotic” component of salt stress increased the number of SAPs. The number of SAPs  $24\text{ h}^{-1}\text{ plant}^{-1}$  differed in the different nutrient conditions. These results demonstrate that sunflower seedlings are capable of generating many APs, and in a sufficiently long time, we can consider this as a specific frequency code of APs. In slowly moving hypocotyls of sunflower seedlings, this approach

is justified. Slow motion of hypocotyls is accompanied by low frequency electrical signals (from 1 to 45 of APs during 24 h per seedling). In such a long time span, there are various numbers of SAPs and this amount can be modulated by the nutrient environment; therefore, there is endogenous electrical activity with very low frequency coding in sunflower seedlings. SAPs are known to propagate acropetally and basipetally. Basipetally propagating SAPs dominated in all nutrient solutions. They appeared in the upper part of the seedlings and propagated downwardly. This showed that the upper part of the seedlings generated more SAPs than the lower part. The amplitudes were in the range of 5–60 mV and the rate of propagation was  $12\text{--}20\text{ cm min}^{-1}$ . In evoked APs, the amplitude is relatively constant (50–60 mV). Significantly lower amplitudes of some SAPs indicate that the excitation is transmitted along individual phloem vessels but not along the transmitting system as in the case of evoked APs. Seedlings growing in the mild NaCl stress exhibited significantly higher SAP propagation velocity than the control plants. The amplitude and velocity of propagation was similar to that in 3-week old *Helianthus* and *Lycopersicum* plants growing in pots with standard soil (Zawadzki et al., 1995; Macedo et al., 2015).

In the research of changes in excitability in sunflowers, we used KCl and NaCl. A treatment with the KCl solution was applied because  $\text{K}^+$  is an important component of the AP mechanism and transmembrane potential maintenance (Trebacz et al., 1989, 1994; Shabala, 2003; Johansson et al., 2006; Shabala and Cuin, 2008; Aleman et al., 2011; Dreyer and Uozumi, 2011; Shabala and Pottosin, 2014; Salvador-Recatala, 2016). In turn, NaCl was used because it is the most commonly occurring salt in the environmental salt stress (Munns and Tester, 2008; Maathuis, 2014; Foster and Miklavcic, 2015). The mechanism of the action of environmental salt (NaCl) stress on plants also includes  $\text{K}^+$  homeostasis disturbance (Shabala and Cuin, 2008; Foster and Miklavcic, 2015). The effect of KCl and NaCl on SAP appearance was different (**Table 1**). The mild stress induced by KCl raises the number of SAPs  $24\text{ h}^{-1}\text{ plant}^{-1}$  in a statistically significant way, while NaCl slightly increases this value. The strong stress caused by NaCl and KCl keeps SAPs at a control level. This shows that only the mild stress induced by KCl increases the appearance of SAPs in sunflower seedlings. Potassium ions are an important part of the mechanism of maintaining the excitability of the cell membrane and we can assume that its slight increase in the environment affects the membrane transport (Trebacz et al., 1989, 1994; Shabala, 2003; Johansson et al., 2006; Shabala and Cuin, 2008; Shabala and Pottosin, 2014; Salvador-Recatala, 2016). The mild stress induced by NaCl slightly increases the number of SAPs and increases SAP velocity in a statistically significant way. An increase in SAP velocity occurs also in strong stress induced by KCl. It is presumed that both these effects are due to the involvement of  $\text{K}^+$  and  $\text{Na}^+$  ions in membrane transport and the function of cation channels. The increased velocity of SAP propagation is in accordance with the cable theory, which postulates such an effect after lowering of the external (apoplast) electrical resistance caused by the applied ions.

Additionally, we have shown changes in the growth and intensity of the endogenous movement of the hypocotyl in

spontaneously excited seedlings. The complete lack of SAPs in distilled water and D-sorbitol (with an ability to generate Glu-induced APs) growing seedlings with strongly inhibited CN may be associated with CN inhibition. In our recent work, the relationship between SAPs and CN was shown, i.e., the number of SAPs decreased with the restricted CN (Stolarz and Dziubinska, 2017). On the other hand, the similarly circumnavigating seedlings had a significantly lower number of SAPs in the strong salt stress [ $4 \pm 1$  SAPs  $24\text{ h}^{-1}$  plant $^{-1}$  ( $n = 8$ )] than in the mild salt stress [ $10 \pm 2$  SAPs  $24\text{ h}^{-1}$  plant $^{-1}$  ( $n = 12$ )]. This confirms a possible complex relation between endogenous APs and endogenous hypocotyl movements in sunflower seedlings.

## Osmotically and Salt-Induced Series of Action Potential in 3-Week Old Sunflower

A treatment with KCl combined with prior pricking induced series of APs in *C. conicum* (Favre et al., 1999) and *A. thaliana* (Favre et al., 2011). Recently, Salvador-Recatala (2016) used NaCl and KCl solutions to evoke depolarization of root cells of *A. thaliana*. The salts were also administered in *Vicia faba* and *Hordeum vulgare* to evoke system potentials (SPs) (Zimmermann et al., 2009). An electrical response after the hypo- or hyperosmotic solution injection (Figure 3, Table 3, Supplementary Figure S3) was dependent on the kind of treatment. Usually, a series of APs appeared, but we assume that some of the recorded spikes (Figure 3, electrode 3 and 4) are SPs. A similar recording was shown in *Vicia faba*, *Hordeum vulgare*, and *Nicotiana tabacum* after wounding as well as abiotic and biotic stress (Zimmermann et al., 2009, 2016). The injection of NaCl did not evoke series of APs (Supplementary Figure S3). It is probable that the presence of K $^{+}$  (but not Na $^{+}$ ) decreases the membrane potential difference and the excitation threshold, which facilitates the generation of APs.

In this study, osmotically driven APs propagating for many centimeters along the sunflower stem have been shown for the first time. Moreover, we have shown that not only salt stimuli but also distilled water and osmotically active solutions (D-sorbitol) induce electrical signals propagating along stem.

Our working hypothesis is that osmotically active solutions and salt solutions affect membrane transport and thus evoke propagated electrical signals and changes in CN. APs could result from adjustment of membrane polarization of some cells over the threshold by ions (K $^{+}$ , Na $^{+}$ , and Cl $^{-}$ ) contained in the solutions (in the nutrient or injected). At first, the salt stress affected the membrane transport (Foster and Miklavcic, 2015) via primary active proton pumps, secondary active antiporters and symporters, as well as passive ion channels. High salinity inhibits also plant growth via increasing osmotic pressure disrupting the plant ability to take up water and hence nutrients. Next, accumulation of salt ions (usually Na $^{+}$ ) leads to concentrations that are toxic (Munns and Tester, 2008). The maintenance of a high cytosolic K $^{+}$ /Na $^{+}$  ratio appears to be critical to plant salt tolerance (Shabala and Cuin, 2008). Exposure to high

concentrations of Na $^{+}$  can also disrupt the homeostasis of K $^{+}$ , which is essential for many physiological processes including excitability and organ movement.

## Strong but Not Mild Salt Stress Decreases Glu-Induced Series of APs

Besides ions, nitrogen is a major factor of plant growth (Debouba et al., 2006). The sensitivity to nitrogen sources in soil and capability of nitrogen uptake are basic features of growing plants. Glutamate is a major amino acid involved both in nitrogen metabolism and in nitrogen signaling (Forde and Lea, 2007; Mousavi et al., 2013). Previously, we showed that lithium modulated Glu-induced excitability and CN in sunflower seedlings (Stolarz et al., 2015). Thus, we expected that also the external concentration of K, Na, and Cl could modulate the Glu-induced series of APs. Here, we have shown for the first time the modulation of Glu-induced excitation by salinity. Seedlings growing in distilled water did not generate SAPs under 3-day observations (Table 1), but these plants were able to generate Glu-induced series of APs (Figure 2D, Table 2). Strong salt stress disturbed significantly the Glu-induced series of APs (Figure 2D, Table 2). Thus, it has been shown that only strong salt stress, but not osmotic stress, decreased Glu-induced series of APs. These results suggested that Glu-induced APs could be a part of the signaling pathway in nitrogen metabolism.

## CONCLUSIONS

Ions are important components of the cytoplasm and vacuole of living cells; therefore, their content in the environment as well as sensing and acquisition by plants is essential for survival. Potassium, chlorine, and sodium are crucial for plasma membrane potential maintenance and thus excitability of organisms, cell volume, growth, and movements. We have demonstrated the physiological impact of osmotic and salt stress on electrical signal induction and propagation as well as on CN and elongation of hypocotyls in whole *H. annuus* plants. Identification of SAPs accompanying varied CN vigor in seedlings growing in the hydroponic medium opens a new avenue for studying the relation between plant excitability and movements under different environment nutrient condition.

## AUTHOR CONTRIBUTIONS

MS designed and carried out the experiments, collected, and analyzed the results, and wrote the manuscript. HD helped in the analysis of the results and editing the manuscript.

## SUPPLEMENTARY MATERIAL

The Supplementary Material for this article can be found online at: <https://www.frontiersin.org/articles/10.3389/fpls.2017.01766/full#supplementary-material>

## REFERENCES

- Aleman, F., Nieves-Cordones, M., Martinez, V., and Rubio, F. (2011). Root K<sup>+</sup> acquisition in plants: the *Arabidopsis thaliana* model. *Plant Cell Physiol.* 52, 1603–1612. doi: 10.1093/pcp/pcr096
- Ashley, M. K., Grant, M., and Gravob, A. (2006). Plant responses to potassium deficiencies: a role for potassium transport proteins. *J. Exp. Bot.* 57, 425–436. doi: 10.1093/jxb/erj034
- Binder, B. M., O’Malley, R. C., Wang, W., Zutz, T. C., and Bleecker, A. B. (2006). Ethylene stimulates nutations that are dependent on the ETR1 receptor. *Plant Physiol.* 142, 1690–1700. doi: 10.1104/pp.106.087858
- Buda, A., Zawadzki, T., Krupa, M., Stolarz, M., and Okulski, W. (2003). Daily and infradian rhythms of circumnutational intensity in *Helianthus annuus*. *Physiol. Plant.* 119, 582–589. doi: 10.1046/j.1399-3054.2003.00198.x
- Cecconi, G., Bustos, D., Ortega, L. I., Senn, M. E., Vegetti, A., and Taleisnik, E. (2015). Plasticity in sunflower leaf and cell growth under high salinity. *Plant Biol.* 17, 41–51. doi: 10.1111/plb.12205
- Charzewska, A., and Zawadzki, T. (2006). Circadian modulation of circumnutational length, period, and shape in *Helianthus annuus*. *J. of Plant Growth Regul.* 25, 324–331. doi: 10.1007/s00344-006-0042-5
- Coskun, D., Britto, D. T., Kochian, L. V., and Kronzucker, H. J. (2016). How high do ion fluxes go? A re-evaluation of the two-mechanism model of K<sup>+</sup> transport in plant roots. *Plant Sci.* 243, 96–104. doi: 10.1016/j.plantsci.2015.12.003
- Darwin, C., and Darwin, F. (1880). *The Power of Movement in Plants*. London: John Murray
- Debouba, M., Gouia, H., Valadier, M. H., Ghorbel, M. H., and Suzuki, A. (2006). Salinity-induced tissue-specific diurnal changes in nitrogen assimilatory enzymes in tomato seedlings grown under high or low nitrate medium. *Plant Physiol. Bioch.* 44, 409–419. doi: 10.1016/j.jplphys.2006.06.017
- Dreyer, I., and Uozumi, N. (2011). Potassium channels in plant cells. *FEBS J.* 278, 4293–4303. doi: 10.1111/j.1742-4658.2011.08371.x
- Dziubinska, H. (2003). Ways of signal transmission and physiological role of electrical potentials in plants. *Acta Soc. Bot. Pol.* 72, 309–318. doi: 10.5586/asbp.2003.040
- Dziubinska, H., Trebacz, K., and Zawadzki, T. (2001). Transmission route for action potentials and variation potentials in *Helianthus annuus* L. *J. Plant Physiol.* 158, 1167–1172. doi: 10.1078/S0176-1617(04)70143-1
- Erdei, L., Szegletes, Z., Barabas, K. N., Pestenacz, A., Fulop, K., Kalmar, L., et al. (1998). Environmental stress and the biological clock in plants: changes of rhythmic behavior of carbohydrates, antioxidant enzymes and stomatal resistance by salinity. *J. Plant. Physiol.* 152, 265–271. doi: 10.1016/S0176-1617(98)80141-7
- Favre, P., Greppin, H., and Degli Agosti, R. (2011). Accession-dependent action potentials in *Arabidopsis*. *J. Plant Physiol.* 168, 653–660. doi: 10.1016/j.jplph.2010.09.014
- Favre, P., Zawadzki, T., Dziubinska, H., Trebacz, K., Greppin, H., and Degli Agosti, R. (1999). Repetitive action potentials induced in the liverwort *Conocephalum conicum* (L.). *Arch. Sci.* 52, 187–198.
- Forde, B. G., and Lea, P. J. (2007). Glutamate in plants: metabolism, regulation, and signalling. *J. Exp. Bot.* 58, 2339–2358. doi: 10.1093/jxb/erm121
- Foster, K. J., and Miklavcic, S. J. (2015). Toward a biophysical understanding of the salt stress response of individual plant cells. *J. Theor. Biol.* 385, 130–142. doi: 10.1016/j.jtbi.2015.08.024
- Grefen, C., Honsbein, A., and Blatt, M. R. (2011). Ion transport, membrane traffic and cellular volume control. *Curr. Opin. Plant Biol.* 14, 332–339. doi: 10.1016/j.pbi.2011.03.017
- Hayashi, Y., Nishiyama, H., Tanoi, K., Ohya, T., Nihei, N., Tanioka, K., et al. (2004). An aluminum influence on root circumnutiation in dark revealed by a new super-HARP (high-gain avalanche rushing amorphous photoconductor) camera. *Plant Cell Physiol.* 45, 351–356. doi: 10.1093/pcp/pch042
- Hedrich, R., Salvador-Recatala, V., and Dreyer, I. (2016). Electrical wiring and long-distance plant communication. *Trends Plant Sci.* 21, 376–387. doi: 10.1016/j.tplants.2016.01.016
- Hinrichsen, R. D., Belsky, D., Jones, L. A., and Mialki, R. (2012). The frequency of the spontaneous behavioral response in *Paramecium tetraurelia* is simultaneously modulated by both ultradian and circadian rhythms. *Biol. Rhythms Res.* 41, 1–14. doi: 10.1080/09291016.2012.692254
- Inoue, N., Arase, T., Hagiwara, M., Amano, T., Hayashi, T., and Ikeda, R. (1999). Ecological significance of root tip rotation for seedling establishment of *Oryza sativa* L. *Ecol. Res.* 14, 31–38. doi: 10.1046/j.1440-1703.1999.141282.x
- Johansson, I., Wulfetange, K., Porée, F., Michard, E., Gajdanowicz, P., Lacombe, B., et al. (2006). External K<sup>+</sup> modulates the activity of the *Arabidopsis* potassium channel SKOR via an unusual mechanism. *Plant J.* 46, 269–281. doi: 10.1111/j.1365-313X.2006.02690.x
- Johansson, A. (1979). “Circumnutation,” in *Encyclopedia of Plant Physiology. Physiology of Movements*, eds W. Haupt and E. Feinleib (Berlin: Springer), 627–646.
- Johansson, A. (1997). Circumnutations: results from recent experiments on Earth and in space. *Planta* 203, 147–158. doi: 10.1007/PL00008103
- Kiep, V., Vadassery, J., Lattke, J., Maaf, J.-P., Boland, W., Peiter, E., et al. (2015). Systemic cytosolic Ca<sup>2+</sup> elevation is activated upon wounding and herbivory in *Arabidopsis*. *New Phytol.* 207, 996–1004. doi: 10.1111/nph.13493
- Koselski, M., Dziubinska, H., Seta-Koselska, A., and Trebacz, K. (2015). A nitrate-permeable ion channel in the tonoplast of the moss *Physcomitrella patens*. *Planta* 241, 1207–1219. doi: 10.1007/s00425-015-250-3
- Koselski, M., Trebacz, K., and Dziubinska, H. (2017). Vacuolar ion channels in the liverwort *Marchantia polymorpha*: influence of ion channel inhibitors. *Planta* 245, 1049–1060. doi: 10.1007/s00425-017-2661-4
- Kosuge, K., Iida, S., Katou, K., and Mimura, T. (2013). Circumnutation on the water surface: female flowers of *Vallisneria*. *Sci. Rep.* 3:1133. doi: 10.1038/srep01133
- Krol, E., Dziubinska, H., Stolarz, M., and Trebacz, K. (2006). Effects of ion channel inhibitors on cold- and electrically-induced action potentials in *Dionaea muscipula*. *Biol. Plant.* 50, 411–416. doi: 10.1007/s10535-006-0058-5
- Król, E., Dziubinska, H., and Trebacz, K. (2010). “What do plants need action potentials for?”, in *Action Potential*, ed M. L. DuBois (New York, NY: Nova Science Publisher), 1–28.
- Król, E., Dziubinska, H., Trebacz, K., Koselski, M., and Stolarz, M. (2007). The influence of glutamic and aminoacetic acids on the excitability of the liverwort *Conocephalum conicum*. *J. Plant Physiol.* 164, 773–784. doi: 10.1016/j.jplph.2006.04.015
- Kurenda, A., Stolarz, M., and Zdunek, A. (2015). Electrical potential oscillations - movement relations in circumnating sunflower stem and effect of ion channel and proton pump inhibitors on circumnutiation. *Physiol. Plant.* 153, 307–317. doi: 10.1111/ppl.12277
- Larson, K. C. (2000). Circumnutation behavior of an exotic honeysuckle vine and its native congener: influence on clonal mobility. *Am. J. Bot.* 87, 533–538. doi: 10.2307/2656597
- Lloyd, D. (2006). Ultradian rhythms and clocks in plants and yeast. *Biol. Rhythm Res.* 37, 281–296. doi: 10.1080/09291010600804379
- Maathuis, F. J. (2014). Sodium in plants: perception, signalling, and regulation of sodium fluxes. *J. Exp. Bot.* 65, 849–858. doi: 10.1093/jxb/ert326
- Macedo, F. C. O., Dziubinska, H., Trebacz, K., Oliveira, R. F., and Moral, R. A. (2015). Action potentials in abscisic acid-deficient tomato mutant generated spontaneously and evoked by electrical stimulation. *Acta Physiol. Plant.* 37, 207. doi: 10.1007/s11738-015-1950-4
- Migliaccio, F., Tassone, P., and Fortunati, A. (2013). Circumnutation as an autonomous root movement in plants. *Am. J. Bot.* 100, 4–13. doi: 10.3732/ajb.1200314
- Millet, B., and Badot, P. (1996). “The revolving movement mechanism in Phaseolus; New approaches to old questions,” in *Vistas on Biorhythmicity*, eds H. Greppin, R. Degli Agosti, and M. Bonzon (Geneva: University of Geneva), 77–98.
- Mousavi, S. A., Chauvin, A., Pascaud, F., Kellenberger, S., and Farmer, E. E. (2013). Glutamate receptor-like genes mediate leaf-to-leaf wound signalling. *Nature* 500, 422–426. doi: 10.1038/nature12478
- Mukherjee, S., David, A., Yadav, S., Baluska, F., and Bhatla, S. C. (2014). Salt stress-induced seedling growth inhibition coincides with differential distribution of serotonin and melatonin in sunflower seedling roots and cotyledons. *Physiol. Plant.* 152, 714–728. doi: 10.1111/ppl.12218
- Munns, R., and Tester, M. (2008). Mechanisms of salinity tolerance. *Annu. Rev. Plant Biol.* 59, 651–681. doi: 10.1146/annurev.arplant.59.032607.092911
- Paszewski, A., and Zawadzki, T. (1973). Action potentials in *Lupinus angustifolius* shoots. *J. Exp. Bot.* 24, 804–809. doi: 10.1093/jxb/24.5.804

- Paszewski, A., and Zawadzki, T. (1974). Action potentials in *Lupinus angustifolius* shoots. 2. Determination of strength-duration relation and all-or-nothing law. *J. Exp. Bot.* 25, 1097–1103. doi: 10.1093/jxb/25.6.1097
- Paszewski, A., and Zawadzki, T. (1976a). Action potentials in *Lupinus angustifolius* shoots. 3. Determination of refractory periods. *J. Exp. Bot.* 27, 369–374.
- Paszewski, A., and Zawadzki, T. (1976b). Action potentials in *Lupinus angustifolius* shoots. 4. Application of thermal stimuli and investigations on conduction pathways of. *J. Exp. Bot.* 27, 859–863.
- Salvador-Recatala, V. (2016). The AKT2 potassium channel mediates NaCl induced depolarization in the root of *Arabidopsis thaliana*. *Plant Signal. Behav.* 11:e1165381. doi: 10.1080/15592324.2016.1165381
- Salvador-Recatala, V., and Tjallingii, W. F. (2015). A new application of the electrical penetration graph (EPG) for acquiring and measuring electrical signals in phloem sieve elements. *J. Vis. Exp.* e52826. doi: 10.3791/52826
- Salvador-Recatala, V., Tjallingii, W. F., and Farmer, E. E. (2014). Real-time, *in vivo* intracellular recordings of caterpillar-induced depolarization waves in sieve elements using aphid electrodes. *New Phytol.* 203, 674–684. doi: 10.1111/nph.12807
- Shabala, S. (2000). Ionic and osmotic components of salt stress specifically modulate net ion fluxes from bean leaf mesophyll. *Plant Cell. Environ.* 23, 825–837. doi: 10.1046/j.1365-3040.2000.00606.x
- Shabala, S. (2003). Physiological implications of ultradian oscillations in plant roots. *Plant Soil* 255, 217–226. doi: 10.1023/A:1026198927712
- Shabala, S., and Cuin, T. A. (2008). Potassium transport and plant salt tolerance. *Physiol. Plant.* 133, 651–669. doi: 10.1111/j.1399-3054.2007.01008.x
- Shabala, S., and Knowles, A. (2002). Rhythmic patterns of nutrient acquisition by wheat roots. *Funct Plant Biol.* 29, 595–605. doi: 10.1071/PP01130
- Shabala, S. N., and Newman, I. A. (1997). Proton and calcium flux oscillations in the elongation region correlate with root nutation. *Physiol. Plant.* 100, 917–926. doi: 10.1111/j.1399-3054.1997.tb00018.x
- Shabala, S., and Pottosin, I. (2014). Regulation of potassium transport in plants under hostile conditions: implications for abiotic and biotic stress tolerance. *Physiol. Plant.* 151, 257–279. doi: 10.1111/ppl.12165
- Shabala, S., Wu, H. H., and Bose, J. (2015). Salt stress sensing and early signalling events in plant roots: current knowledge and hypothesis. *Plant Sci.* 241, 109–119. doi: 10.1016/j.plantsci.2015.10.003
- Sibaoka, T. (1991). Rapid plant movements triggered by action potentials. *Bot. Mag. Tokyo* 104, 73–95. doi: 10.1007/BF02493405
- Singh, N., and Bhatla, S. C. (2016). Nitric oxide and iron modulate heme oxygenase activity as a long distance signaling response to salt stress in sunflower seedling cotyledons. *Nitric Oxide* 53, 54–64. doi: 10.1016/j.niox.2016.01.003
- Spurny, M. (1968). Effect of root tip amputation on spiral oscillations of growing hypocotyl with radicle of pea (*Pisum sativum* L.). *Biol. Plant.* 10, 98–111. doi: 10.1007/BF02921024
- Spurny, M. (1975). Elongation and circumnutiation oscillations of hypocotyl of pine seedlings (*Pinus sylvestris* L.). *Biol. Plant.* 17, 43–49. doi: 10.1007/BF02921073
- Stahlberg, R., Stephens, N. R., Cleland, R. E., and Van Volkenburgh, E. (2006). Shade-induced action potentials in *Helianthus annuus* L. Originate Primarily from the Epicotyl. *Plant Signal. Behav.* 1, 15–22. doi: 10.4161/psb.1.1.2275
- Stankovic, B., Witters, D. L., Zawadzki, T., and Davies, E. (1998). Action potentials and variation potentials in sunflower: an analysis of their relationships and distinguishing characteristics. *Physiol. Plant.* 103, 51–58. doi: 10.1034/j.1399-3054.1998.1030107.x
- Stolarz, M. (2009). Circumnutiation as a visible plant action and reaction: physiological, cellular and molecular basis for circumnutiations. *Plant. Signal. Behav.* 4, 380–387. doi: 10.4161/psb.4.5.8293
- Stolarz, M., and Dziubinska, H. (2017). Spontaneous action potentials and circumnutiation in *Helianthus annuus*. *Acta Physiol. Plant.* 39, 234 doi: 10.1007/s11738-017-2528-0
- Stolarz, M., Dziubinska, H., Krupa, M., Buda, A., Trebacz, K., and Zawadzki, T. (2003). Disturbances of stem circumnutiations evoked by wound-induced variation potentials in *Helianthus annuus* L. *Cell. Mol. Biol. Lett.* 8, 31–40.
- Stolarz, M., Król, E., and Dziubinska, H. (2015). Lithium distinguishes between growth and circumnutiation and augments glutamate-induced excitation of *Helianthus annuus* seedlings. *Acta Physiol. Plant.* 37, 1–9. doi: 10.1007/s11738-015-1814-y
- Stolarz, M., Krol, E., Dziubinska, H., and Kurenda, A. (2010). Glutamate induces series of action potentials and a decrease in circumnutiation rate in *Helianthus annuus*. *Physiol. Plant.* 138, 329–338. doi: 10.1111/j.1399-3054.2009.01330.x
- Stolarz, M., Krol, E., Dziubinska, H., and Zawadzki, T. (2008). Complex relationship between growth and circumnutiations in *Helianthus annuus* stem. *Plant Signal. Behav.* 3, 376–380. doi: 10.4161/psb.3.6.5714
- Stolarz, M., Zuk, M., Krol, E., and Dziubinska, H. (2014). Circumnutiation Tracker: novel software for investigation of circumnutiation. *Plant Methods* 10:24. doi: 10.1186/1746-4811-10-24
- Szczerba, M. W., Britto, D. T., and Kronzucker, H. J. (2009). K<sup>+</sup> transport in plants: physiology and molecular biology. *J. Plant Physiol.* 166, 447–466. doi: 10.1016/j.jplph.2008.12.009
- Trebacz, K. (1992). Measurements of intracellular and extracellular pH in the liverwort *Conocephalum conicum* during action potentials. *Physiol. Plant.* 84, 448–452. doi: 10.1111/j.1399-3054.1992.tb04689.x
- Trebacz, K., Schonknecht, G., Dziubinska, H., and Hanaka, A. (2007). Characteristics of anion channels in the tonoplast of the liverwort *Conocephalum conicum*. *Plant Cell. Physiol.* 48, 1747–1757. doi: 10.1093/pcp/pcm147
- Trebacz, K., Simonis, W., and Schonknecht, G. (1994). Cytoplasmic Ca<sup>2+</sup>, K<sup>+</sup>, Cl<sup>-</sup>, and NO<sup>3-</sup> activities in the liverwort *Conocephalum conicum* at rest and during action potentials. *Plant Physiol.* 106, 1073–1084. doi: 10.1104/pp.106.3.1073
- Trebacz, K., Tarnecki, R., and Zawadzki, T. (1989). The effects of ionic channel inhibitors and factors modifying metabolism on the excitability of the liverwort *Conocephalum conicum*. *Physiol. Plant.* 75, 24–30. doi: 10.1111/j.1399-3054.1989.tb02058.x
- Trebacz, K., and Zawadzki, T. (1985). Light triggered action potentials in the liverwort *Conocephalum conicum*. *Physiol. Plant.* 64, 482–486. doi: 10.1111/j.1399-3054.1985.tb08526.x
- Ueda, A., Kathiresan, A., Inada, M., Narita, Y., Nakamura, T., Shi, W. M., et al. (2004). Osmotic stress in barley regulates expression of a different set of genes than salt stress does. *J. Exp. Bot.* 55, 2213–2218. doi: 10.1093/jxb/erh242
- van Bel, A. J. E., Furch, A. C. U., Will, T., Buxa, S. V., Musetti, R., and Hafke, J. B. (2014). Spread the news: systemic dissemination and local impact of Ca<sup>2+</sup> signals along the phloem pathway. *J. Exp. Bot.* 65, 1761–1787. doi: 10.1093/jxb/ert425
- White, P. (2001). Chloride in soils and its uptake and movement within the plant: a review. *Ann. Bot.* 88, 967–988. doi: 10.1006/anbo.2001.1540
- Wu, G. Q., Feng, R. J., Liang, N., Yuan, H. J., and Sun, W. B. (2015a). Sodium chloride stimulates growth and alleviates sorbitol-induced osmotic stress in sugar beet seedlings. *Plant Growth Regul.* 75, 307–316. doi: 10.1007/s10725-014-9954-4
- Wu, G. Q., Jiao, Q., and Shui, Q. Z. (2015b). Effect of salinity on seed germination, seedling growth, and inorganic and organic solutes accumulation in sunflower (*Helianthus annuus* L.). *Plant Soil Environ.* 61, 220–226. doi: 10.17221/22/2015-PSE
- Yoshihara, T., and Iino, M. (2005). Circumnutiation of rice coleoptiles: its occurrence, regulation by phytochrome, and relationship with gravitropism. *Plant Cell Environ.* 28, 134–146. doi: 10.1111/j.1365-3040.2004.01249.x
- Zachariassen, E., and Johnsson, A. (1988). Effects of lithium ions on the circumnutiations of *Helianthus* hypocotyls. *Physiol. Plant.* 72, 147–152. doi: 10.1111/j.1399-3054.1988.tb06636.x
- Zawadzki, T. (1979). Electrical properties of *Lupinus angustifolius* L. stem.1. Sub-threshold potentials. *Acta Soc. Bot. Pol.* 48, 99–107. doi: 10.5586/asbp.1979.009
- Zawadzki, T. (1980). Action potentials in *Lupinus angustifolius* shoots. 5. Spread of excitation in the stem, leaves, and root. *J. Exp. Bot.* 31, 1371–1377. doi: 10.1093/jxb/31.5.1371
- Zawadzki, T., Davies, E., Dziubinska, H., and Trebacz, K. (1991). Characteristics of action potentials in *Helianthus annuus*. *Physiol. Plant.* 83, 601–604. doi: 10.1111/j.1399-3054.1991.tb02475.x
- Zawadzki, T., Dziubinska, H., and Davies, E. (1995). Characteristics of action potentials generated spontaneously in *Helianthus annuus*. *Physiol. Plant.* 93, 291–297. doi: 10.1111/j.1399-3054.1995.tb02231.x

- Zhu, J. K. (2003). Regulation of ion homeostasis under salt stress. *Curr. Opin. Plant Biol.* 6, 441–445. doi: 10.1016/S1369-5266(03)00085-2
- Zimmermann, M. R., Maischak, H., Mithöfer, A., Boland, W., and Felle, H. H. (2009). System potentials, a novel electrical long-distance apoplastic signal in plants, induced by wounding. *Plant Physiol.* 149, 1593–1600. doi: 10.1104/pp.108.133884
- Zimmermann, M. R., Mithöfer, A., Will, T., Felle, H. H., and Furch, A. C. U. (2016). Herbivore triggered electrophysiological reactions: candidates for systemic signals in higher plants and the challenge of their identification. *Plant Physiol.* 170, 2407–2419. doi: 10.1104/pp.15.01736

**Conflict of Interest Statement:** The authors declare that the research was conducted in the absence of any commercial or financial relationships that could be construed as a potential conflict of interest.

Copyright © 2017 Stolarz and Dziubinska. This is an open-access article distributed under the terms of the Creative Commons Attribution License (CC BY). The use, distribution or reproduction in other forums is permitted, provided the original author(s) or licensor are credited and that the original publication in this journal is cited, in accordance with accepted academic practice. No use, distribution or reproduction is permitted which does not comply with these terms.



# Barley yellow dwarf virus Infection Leads to Higher Chemical Defense Signals and Lower Electrophysiological Reactions in Susceptible Compared to Tolerant Barley Genotypes

Maria K. Paulmann<sup>1,2</sup>, Grit Kunert<sup>2</sup>, Matthias R. Zimmermann<sup>1</sup>, Nina Theis<sup>2,3</sup>, Anatoli Ludwig<sup>1</sup>, Doreen Meichsner<sup>1</sup>, Ralf Oelmüller<sup>1</sup>, Jonathan Gershenson<sup>2</sup>, Antje Habekuss<sup>4</sup>, Frank Ordon<sup>4</sup>, Alexandra C. U. Furch<sup>1\*</sup> and Torsten Will<sup>4</sup>

## OPEN ACCESS

### Edited by:

Vicenta Salvador Recatala,  
Ronin Institute, United States

### Reviewed by:

Michael Robert Thorpe,  
Australian National University,  
Australia

Stefanie Wienkoop,  
University of Vienna, Austria

### \*Correspondence:

Alexandra C. U. Furch  
alexandra.furch@uni-jena.de

### Specialty section:

This article was submitted to  
Plant Physiology,  
a section of the journal  
*Frontiers in Plant Science*

Received: 06 October 2017

Accepted: 25 January 2018

Published: 06 March 2018

### Citation:

Paulmann MK, Kunert G, Zimmermann MR, Theis N, Ludwig A, Meichsner D, Oelmüller R, Gershenson J, Habekuss A, Ordon F, Furch ACU and Will T (2018) Barley yellow dwarf virus Infection Leads to Higher Chemical Defense Signals and Lower Electrophysiological Reactions in Susceptible Compared to Tolerant Barley Genotypes. *Front. Plant Sci.* 9:145. doi: 10.3389/fpls.2018.00145

<sup>1</sup> Department of Plant Physiology, Matthias-Schleiden-Institute for Genetics, Bioinformatics and Molecular Botany, Faculty of Biological Sciences, Friedrich Schiller University Jena, Jena, Germany, <sup>2</sup> Department of Biochemistry, Max Planck Institute for Chemical Ecology, Jena, Germany, <sup>3</sup> Department of Biology, Elms College, Chicopee, MA, United States, <sup>4</sup> Institute for Resistance Research and Stress Tolerance, Federal Research Centre for Cultivated Plants, Julius Kuehn-Institute, Quedlinburg, Germany

Barley yellow dwarf virus (BYDV) is a phloem limited virus that is persistently transmitted by aphids. Due to huge yield losses in agriculture, the virus is of high economic relevance. Since the control of the virus itself is not possible, tolerant barley genotypes are considered as the most effective approach to avoid yield losses. Although several genes and quantitative trait loci are known and used in barley breeding for virus tolerance, little is known about molecular and physiological backgrounds of this trait. Therefore, we compared the anatomy and early defense responses of a virus susceptible to those of a virus-tolerant cultivar. One of the very early defense responses is the transmission of electrophysiological reactions. Electrophysiological reactions to BYDV infection might differ between susceptible and tolerant cultivars, since BYDV causes disintegration of sieve elements in susceptible cultivars. The structure of vascular bundles, xylem vessels and sieve elements was examined using microscopy. All three were significantly decreased in size in infected susceptible plants where the virus causes disintegration of sieve elements. This could be associated with an uncontrolled ion exchange between the sieve-element lumen and apoplast. Further, a reduced electrophysiological isolation would negatively affect the propagation of electrophysiological reactions. To test the influence of BYDV infection on electrophysiological reactions, electropotential waves (EPWs) induced by leaf-tip burning were recorded using aphids as bioelectrodes. EPWs in infected susceptible plants disappeared already after 10 cm in contrast to those in healthy susceptible or infected tolerant or healthy tolerant plants. Another early plant defense reaction is an increase in reactive oxygen species (ROS). Using a fluorescent dye, we found a significant increase in ROS content in infected susceptible plants but not in infected

tolerant plants. Similar results were found for the phytohormones abscisic acid and three jasmonates. Salicylic acid levels were generally higher after BYDV infection compared to uninfected plants. Heat stimulation caused an increase in jasmonates. By shedding light on the plant defense mechanisms against BYDV, this study, provides further knowledge for breeding virus tolerant plants.

**Keywords:** *Barley yellow dwarf virus, electrical penetration graph, electropotential waves, phloem, phytohormones, reactive oxygen species, sieve element, xylem*

## INTRODUCTION

The barley yellow dwarf disease caused by different viruses of the genus *Luteovirus* [e.g., *Barley yellow dwarf virus* (BYDV) -PAV] and the genus *Poherovirus* (e.g., *Cereal yellow dwarf virus-RPV*) of the family *Luteoviridae*, infects a wide range of plants including, e.g., maize, wheat, rye, oat and barley and causes one of the most serious viral diseases in cereal crops and grasses worldwide (D'Arcy, 1995). The primary symptoms of infected barley are stunted growth and yellow discoloration of leaves. The virus is phloem restricted and is transmitted in a persistent manner by many aphid species, e.g., *Rhopalosiphum padi* and *Sitobion avenae* (Slykhuis, 1967; Jensen, 1969). BYDV infection leads to a collapse of sieve elements accompanied by an accumulation of "wound gum" resulting in necrosis (Esau, 1957). Esau (1957) also showed that companion cells (CCs) and parenchyma cells are affected by necrosis as well. How this affects phloem physiology has not yet been studied.

The control of the aphid vector with insecticides is one approach to prevent BYDV infection. However, for environmental reasons and the risk of resistance development, the use of insecticides is being actively discouraged. Thus, growing virus tolerant cultivars may be one of the most suitable ways to reduce the negative impact of virus infection on agriculture. Susceptibility to a virus means that it can multiply and spread (move from cell to cell) inside its host plant and causes strong disease symptoms. A tolerant genotype is characterized by weak or no disease symptoms even though infection, multiplication and spread are the same as in susceptible genotypes (Cooper and Jones, 1983). One form of tolerance/resistance of BYDV in barley is mediated by the gene *Ryd2* (Schaller et al., 1964). The *Ryd2* based tolerance is used in, e.g., the winter barley cultivar 'Vixen' since 1986 (Parry and Habgood, 1986) but until now no information was available about the functional background of this tolerance. Other genes, such as *Ryd3* (Niks et al., 2004) and *Ryd4<sup>Hb</sup>* (Scholz et al., 2009) and additional quantitative trait loci (Scheurer et al., 2001) are known as well. Although the modes of action of these genes are not known, it is assumed that these prevent the negative effects of the virus on the phloem.

The phloem is composed of sieve elements (SEs), CCs and phloem parenchyma cells (PPCs), which are mainly involved in long distance transport of nutrients (van Bel, 2003). SEs are elongated cells that contain only a plasma membrane, a few mitochondria, a parietally located smooth endoplasmic reticulum, SE plastids and an extensive set of phloem-specific proteins (Giavalisco et al., 2006). The perforated sieve plates,

located at the terminal ends of SEs, are modified cell walls that allow the flow of sap from one SE to the next one. Mass flow inside sieve tubes is driven by an osmotic pressure gradient between source and sink tissues (Münch, 1930; Knoblauch et al., 2016) that distributes carbohydrates, amino acids, proteins, vitamins, phytohormones, and other signaling molecules throughout the whole plant.

Besides the transport of nutrients, the phloem is also involved in long-distance communication through electropotential waves (EPWs) (Furch et al., 2007, 2009). EPWs have been recorded in response to mechanical and physical stimuli, such as wounding, cold, heat, and electrical shocks (Fromm and Spanswick, 1993; Rhodes et al., 1996; Mancuso, 1999; Furch et al., 2007) but also in response to biotic stimuli such as feeding by caterpillars (Salvador-Recatalà et al., 2014; Zimmermann et al., 2016). EPWs include features of action potentials and variation potentials (Hafke et al., 2009) and are involved in signaling regarding growth regulation, adjustment of photosynthesis and respiration, and defense (Trébacz et al., 2006). Burning induced EPWs are associated with distant occlusion of sieve tubes by proteins and callose deposition (Furch et al., 2007, 2009, 2010; Will et al., 2009).

Defense signaling against plant pathogens also has chemical components. During biotrophic pathogen attack salicylic acid (SA) and its derivative, methyl salicylate, are known to be key signals in systemic acquired resistance (SAR) and the hypersensitive response (HR) (Métraux et al., 1990; Vlot et al., 2009; Dempsey et al., 2011). The (+)-7-*iso*-jasmonoyl-L-isoleucine (JA-Ile) but also other jasmonic acids (JA) – amino acid conjugates like JA-valine (JA-Val), have been discussed as general inter- and intracellular signaling compounds typically involved in multiple defense reactions to both, necrotrophic microbial pathogens and herbivore attack (Wang et al., 2007; Verhage et al., 2011; Koo and Howe, 2012; Pel and Pieterse, 2013; Wasternack and Hause, 2013). Various abiotic stimuli lead to the overproduction of reactive oxygen species (ROS) in plants. ROS also control many processes like programmed cell death, abiotic stress responses, pathogen defense and systemic signaling (Gill and Tuteja, 2010).

To learn more about the defense responses of barley plants to BYDV infection, we investigated viral-induced changes in the structure of vascular bundles, which could alter mass flow and therefore the propagation of EPWs and chemical signals. In addition, we measured the propagation of EPWs in the sieve tubes and measured defense responses, including the accumulation of ROS and phytohormones.

## MATERIALS AND METHODS

### Aphid Cultivation

*Sitobion avenae* and *R. padi* were reared on 14–28 day old plants of *Hordeum vulgare* cv. Rubina in a greenhouse under controlled-environment conditions at 20°C and a 16 h:8 h L:D regime. Aphids were maintained in perspex cages with large gauze-covered windows.

### Plant Material and General Experimental Set-ups

*Hordeum vulgare* cv. Rubina (BYDV-susceptible) and *H. vulgare* cv. Vixen (BYDV tolerant) plants were grown in a greenhouse at 20°C with natural lighting supported by artificial light to maintain a 14 h:10 h L:D period. Two to three week old plants of both cultivars were infested with (i) virus free or (ii) viruliferous (BYDV-PAV; Sip et al., 2006) aphids of the species *R. padi*. For both treatments five adult apterous aphids were placed in a clip cage on the first leaf of a single plant for a period of 48 h. Subsequently, aphids were removed mechanically and all plants were additionally sprayed with an insecticide (Confidor® 0.035%; Bayer, Germany). Treated plants were cultivated in a climate chamber under the same conditions as in the greenhouse.

All experiments were conducted on healthy and BYDV infected plants (below only called infected plants) of the cv. Rubina and the cv. Vixen (Schaller et al., 1964; Figure 1A). After four weeks the plants were well infected by BYDV-PAV and used to study the propagation of electrophysiological reactions with the electrical penetration graph (EPG) technique. All other analyses (morphological and chemical parameters) were conducted six weeks after virus infection.

The morphological effects of the infection were solely studied at the middle of the youngest mature leaf (number (no.) [2]) to guarantee the comparability among all considered plants (Figure 1B). One leaf per plant was analyzed and considered as a biological replicate. Using a fresh razor blade, one cross section per leaf was made by hand, covered with H<sub>2</sub>O<sub>dest</sub> and a cover glass and immediately observed with the light microscope. Per cross section two xylem vessels were measured and the mean of both was used for the statistical analyses and creation of graphs. Because of the variability of the sieve elements 10 sieve elements per cross section were measured and their median was used for further analyses and graph preparation.

Another set of plants was used for the measurements of electrophysiological reactions in sieve elements of cv. Rubina and cv. Vixen, where phloem sucking aphids were used as 'bioelectrodes' (Furch et al., 2010; Salvador-Recatalà et al., 2014; Zimmermann et al., 2016). The EPG-detected EPWs were recorded in basipetal direction along a single leaf at four distances (5, 10, 15, and 20 cm) and triggered by a heat stimulus at the leaf tip (see Figure 1C [2]). The heat stimulus was applied with a lit match for 3–4 s. A replicate was composed of one leaf per plant.

A third set of plants was used to investigate the plant responses with respect to ROS and phytohormone levels. They were investigated 30 min after the heat stimulus (control plants without stimulus) by an analysis of a 4 cm leaf piece 5–9 cm

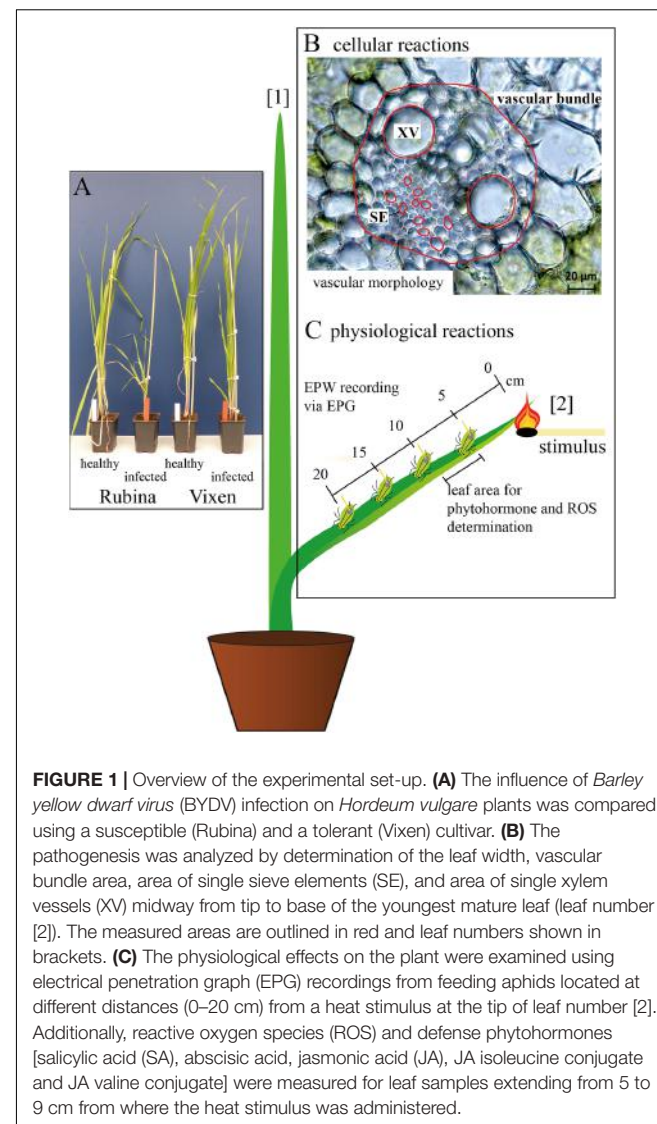


**FIGURE 1 |** Overview of the experimental set-up. **(A)** The influence of *Barley yellow dwarf virus* (BYDV) infection on *Hordeum vulgare* plants was compared using a susceptible (Rubina) and a tolerant (Vixen) cultivar. **(B)** The pathogenesis was analyzed by determination of the leaf width, vascular bundle area, area of single sieve elements (SE), and area of single xylem vessels (XV) midway from tip to base of the youngest mature leaf (leaf number [2]). The measured areas are outlined in red and leaf numbers shown in brackets. **(C)** The physiological effects on the plant were examined using electrical penetration graph (EPG) recordings from feeding aphids located at different distances (0–20 cm) from a heat stimulus at the tip of leaf number [2]. Additionally, reactive oxygen species (ROS) and defense phytohormones [salicylic acid (SA), abscisic acid, jasmonic acid (JA), JA isoleucine conjugate and JA valine conjugate] were measured for leaf samples extending from 5 to 9 cm from where the heat stimulus was administered.

from the leaf tip (leaf no. [2] Figure 1C). In rapid succession the plant samples were cut with a fresh razor blade, immediately frozen in liquid nitrogen and afterward ground to a fine powder with the use of mortar and pestle. In order to have enough plant material for the chemical analyses the material of three plants was pooled and considered as one replicate. For ROS analyses the necessary amount of plant tissue was weighed at temperatures of liquid nitrogen and stored at –80°C. For the phytohormone analyses the plant tissue was freeze dried (Alpha 1-4 LD plus; Christ, Osterode am Harz, Germany) prior to weighing.

After execution of the experiments all plants (same leaves as used for the experiments) were controlled for their infection status with the DAS-ELISA test.

### Quantification of Virus Infection by DAS-ELISA

The BYDV content was analyzed after the execution of the experiment from 50 mg leaf material coming from the same leaf

investigated in the respective experiment. DAS-ELISA (double antibody sandwich – enzyme-linked immunosorbent assay) was performed according to Clark and Adams (1977) using a polyclonal antiserum (against BYDV-PAV) produced in house at the Julius Kuehn-Institute (JKI). After 1 h of incubation with the enzyme substrate (p-nitrophenyl phosphate), extinction (EXT) was measured at 405 nm with a microtiter plate absorbance reader model Sunrise (Tecan GmbH, Grödig/Salzburg, Austria). As a threshold for a successful positive infection an EXT of  $>0.4$  was used, whereas plants that showed an EXT  $\leq 0.04$  were considered uninfected (Supplementary Figure 1, tested number of replicates see Supplementary Table 1). Plants which showed EXT between 0.04 and 0.4 were excluded from all analyses because of their indifferent infection state.

## Plant Morphology and Microscopy

Per plant one cross section was done in the middle of the 2<sup>nd</sup> leaf (midway from tip to base). Each cross section was covered with H<sub>2</sub>O<sub>dest</sub> and a cover glass and immediately observed with the light microscope (AXIO Imager.M2, Zeiss, Jena, Germany) equipped with a color camera (AXIOCAM 503 color Zeiss, Jena, Germany). Digital images were processed and measurements of the vascular bundle, xylem and phloem areas were conducted with the ZEN software (Zeiss, Jena, Germany). Per cross section two xylem vessels were measured and the mean of both was used for the statistical analyses. Because of the variability of the sieve elements 10 sieve elements per cross section were measured and their median was used for further analyses.

## Electrical Penetration Graph Recording

Randomly selected adult apterous aphids of the species *S. avenae* were prepared for EPG measurements as previously described (Will et al., 2007; Schliephake et al., 2013). Four aphids were simultaneously placed on the lower side of leaf no. [2] and their behavior was observed by continuous EPG recording. EPG recording relevant for the measurement of EPWs was started after at least one aphid had begun sieve tube penetration and ingested phloem sap (Furch et al., 2009). Afterward the leaf tip was carefully burned for 3 s to trigger EPWs. The time of burning was marked by  $-50$  mV calibration signals, triggered by the GIGA-8 EPG amplifier (EPG Systems, Wageningen, Netherlands). Induced reactions were recorded with the GIGA-8 EPG amplifier and EPG stylus software (EPG Systems, Wageningen, Netherlands) for 120 min. Data analysis was conducted using the EPG stylus analysis module in accordance with Tjallingii and Hogen Esch (1993). If an EPW amplitude was detected, the beginning of the amplitude was taken as a basis to calculate the EPW propagation speed. In case the EPW amplitude was masked by aphid behavior associated voltage changes, the observed change of behavior from ingestion (waveform E2) to secretion of watery saliva into sieve tubes (waveform E1) was taken as reference time point for EPW velocity calculation. A transition from ingestion to secretion of watery saliva was described so far in direct association with EPWs in cucurbits (Furch et al., 2010), rapeseed (Zimmermann et al., 2016) and in *Arabidopsis* (Salvador-Recatalà et al., 2014). Sieve element occlusion might act as a trigger for the observed change in aphid

behavior (Will et al., 2007, 2009; Furch et al., 2010). Propagation velocity was calculated for adjacent measuring points by the time of the detected signal and the distance between the two aphids.

Because it is not possible to distinguish between the different electrophysiological reaction types with the EPG technique, i.e., action potential, variation potential and system potential (Felle and Zimmermann, 2007; Zimmermann and Felle, 2009; Zimmermann and Mithöfer, 2013; Zimmermann et al., 2016), we term the recorded electrophysiological reactions EPW (see Furch et al., 2007).

## Analysis of Reactive Oxygen Species With DCFDA

The method employed was adapted from Jambunathan (2010). For extracting ROS from the plant tissue 0.25 mL of 10 mM Tris-HCl buffer (pH 7.2) was added to 20 mg of fresh, ground plant tissue. This mixture was gently shaken at 4°C for 5 min and then centrifuged (12000  $\times g$ , 20 min, 4°C). The supernatant was transferred into a fresh tube and stored on ice for further usage.

A 10  $\mu$ L portion of the supernatant was diluted 1:40 in 10 mM Tris-HCl buffer and added in triplicates onto a black 96 well plate (F bottom, chimney well, black Fluotrac; Greiner bio-one, Frickenhausen, Germany). Shortly before measurement, 2,7-dichlorofluorescein diacetate (DCFDA; Sigma-Aldrich, Steinheim, Germany) in dimethyl sulfoxide (DMSO) was added to the plate to achieve a final concentration of 10  $\mu$ M in a total volume of 200  $\mu$ L in each well. After gentle agitation and incubation at room temperature in the dark for about 10 min, the emitted fluorescence was measured for 10 s per well with a Tecan multi-well reader (infinite M200, Tecan Austria GmbH) using optimal gain and a total of five flashes. The fluorophore was excited with a wavelength of 485 nm and the emission recorded at 530 nm. The Tecan multi-well reader was operated with the i-control 1.5 software (Tecan Austria GmbH). Hydrogen peroxide (ACROS organics, Thermo Fischer Scientific, Geel, Belgium) was used as an external standard.

## Analysis of Phytohormones

A 1 mL portion of phytohormone extraction buffer [80% MeOH with 0.1% formic acid (FA) spiked with internal standards: 40 ng mL<sup>-1</sup> D<sub>6</sub>JA (High Purity Compounds (HPC), Cunnersdorf, Germany), D<sub>4</sub>SA (Sigma-Aldrich), D<sub>6</sub>ABA (Santa Cruz Biotechnology, Santa Cruz, CA, United States) and 8 ng mL<sup>-1</sup> D<sub>6</sub>JA-Ile (HPC)] was added to 10 mg powdered freeze dried plant tissue kept on ice. The samples were mixed for 30 s by vortexing and subsequently sonicated for 15 min at 35 kHz in a water bath at room temperature. A centrifugation step followed ( $-10^{\circ}\text{C}$  for 20 min at 4500  $\times g$ ). The supernatant was filtered through a 0.45 mm PTFE AcroPrep<sup>TM</sup> 96-well filtration plate (Pall Corporation, Port Washington, NY, United States). This filtrate (3  $\mu$ L) was analyzed by LC-MS/MS via multiple reaction monitoring (MRM) after separating the phytohormones with an Agilent HPLC system on a Zorbax Eclipse XDB-C18 column (50 mm  $\times$  4.6 mm, 1.8  $\mu\text{m}$ ; Agilent Technologies, Santa Clara, CA, United States). The column temperature was maintained at 25°C and the profile of the mobile phase set as

follows: 0.0–0.5 min, 90% of 0.05% (v/v) FA and 10% ACN; 0.5–4.0 min, 10–90% ACN; 4.0–4.5 min, 100% ACN; 4.5–7.0 min, 10% ACN. During the whole separation process the mobile phase was pumped with a flow rate of 1.1 mL min<sup>-1</sup>.

In an API 5000 tandem mass spectrometer (Applied Biosystems, Foster City, CA, United States) MRM was used to analyze parent ion → product ion fragmentation as follows: m/z 136.9 → 93.0 [collision energy (CE) –22 V; declustering potential (DP) –35 V] for SA; m/z 140.9 → 97.0 (CE –22 V; DP –35 V) for SA-D<sub>4</sub>; m/z 209.1 → 59 (CE –24 V; DP –35 V) for JA; m/z 215.1/214.1 → 59.0 (CE –24 V; DP –35 V) for JA-D<sub>5/6</sub>; m/z 322.2 → 130.1 (CE –24 V; DP –45 V) for the JA-isoleucine conjugate (JA-Ile); m/z 328.2 → 130.1 (CE –30 V; DP –50 V) for D<sub>6</sub>JA-Ile; m/z 308.19 → 116.1 (CE –30 V; DP –50 V) for the JA-valine conjugate (JA-Val); m/z 263.0 → 153.2 (CE –22 V; DP –35 V) for abscisic acid (ABA); m/z 269.0 → 159.2 (CE –22 V; DP –35 V) for ABA-D<sub>6</sub>. To achieve the mentioned MRMs a Turbospray ion source was operated in negative mode and other parameters maintained as listed below. The ion spray voltage was set to –4500 eV and the turbo gas temperature to 700°C. The nebulizing and heating gasses were adjusted to 60 psi, the curtain gas to 25 psi and the collision gas to 7 psi. The Analyst 1.6 software (Applied Biosystems) was used for data acquisition and analysis. The signals of the internal standards were used to quantify the native phytohormones.

## Statistics

In order to test whether morphological leaf characteristics were dependent on the cultivar and BYDV infection, and whether phytohormone concentrations and ROS production were influenced by infection, burning treatment, and cultivar, factorial ANOVAs followed by Tukey honest significant difference tests were used. The generalized least squares method [gls from the nlme library (Pinheiro et al., 2017)] with the varIdent variance structure was applied in case of variance heterogeneity. Whether the different variance of burning, infection, or cultivar, or a combination of factors should be incorporated into the model, was determined by comparing models with different variance structures with a likelihood ratio test and choosing the model with the smallest Akaike Information Criterion (AIC). The influence (*p*-values) of the explanatory variables was determined by sequential removal of explanatory variables starting from the full model, and comparison of the simpler with the more complex model with a likelihood ratio test (Zuur et al., 2009). Differences between factor levels were determined by factor level reduction (Crawley, 2013). If necessary to achieve normality of the residuals or variance homogeneity, data were transformed as specified in the corresponding tables (Tables 3, 4). JA-Val conjugate concentrations were only analyzed for burned plants since this jasmonate conjugate was only sporadically detected in non-burned plants. Morphological, ROS and phytohormone data were analyzed with R version 3.4.1 (R Core Team, 2017).

The presence of electrophysiological reactions at each location was categorized with “yes” and “no” and Fisher’s exact test was used for the comparison of healthy and infected plants for both cultivars. The propagation velocity was compared at each distance for the two treatments and between the barley cultivars

by using the non-parametric Steel-Dwass method. Due to the absence of any electrophysiological reactions, data points beyond 5 cm in infected plants of the cv. Rubina were not included in the test for differences of propagations velocity. These data were analyzed with jmp 12 (SAS Institute).

## RESULTS

### The Leaf and Vascular Morphology of the Cultivar Rubina Was Negatively Affected by BYDV

Since BYDV is localized in the phloem, it can be assumed to have a direct effect on this tissue. We found that the infection of the cv. Rubina significantly decreased the leaf width (–31%), vascular bundle area (–35%), sieve element area (–39%) and xylem vessel area (–29%) compared to that of uninfected plants. However, the tolerant cv. Vixen was not affected by infection (Figure 2, statistics see Table 1).

### The Electrophysiological Conductivity of the Phloem Was Impaired by BYDV Infection

The propagation of electrophysiological reactions in plants is believed to take place largely in phloem tissue (Zimmermann and Mithöfer, 2013; Hedrich et al., 2016). Since electrophysiological propagation requires coupling of the individual sieve elements, BYDV colonization of these elements may impair electrophysiological conductivity. This hypothesis was tested with EPG measurements following application of a heat stimulus (Figure 1).

The results showed that the heat stimulus triggered an unspecific electrophysiological reaction henceforward called EPW (see also Furch et al., 2007), which exhibited a decreasing velocity with increasing distance, although there is mostly no statistically significant difference between adjacent measuring points within one treatment (Figure 3A, statistical values see Table 2). Independent of the cultivar and the infection status we observed EPWs 5 cm downstream of the stimulus site (Figures 3B,C and Supplementary Figure 2). However, in the infected cv. Rubina no EPW was detected at distances from 10 to 20 cm (Figure 3C). In healthy plants of this cultivar the detection rate of EPWs decreased with distance from the site of burning, as well, but EPWs were recorded as far as 20 cm from the leaf tip. In the cv. Vixen, the detection rate of EPWs was comparable in infected and healthy plants at the respective distances (Figure 3C).

The velocity of the EPWs also diminished in healthy and infected plants of both cultivars with increasing distance from the stimulus site but mostly no statistical difference was observed between adjacent measuring points (Figure 3B and Table 2).

### The ROS Formation Was Dependent on Infection Status and Burning Treatment

The negative effect of the infection on the phloem especially in the cv. Rubina (Figures 2, 3) raised questions about

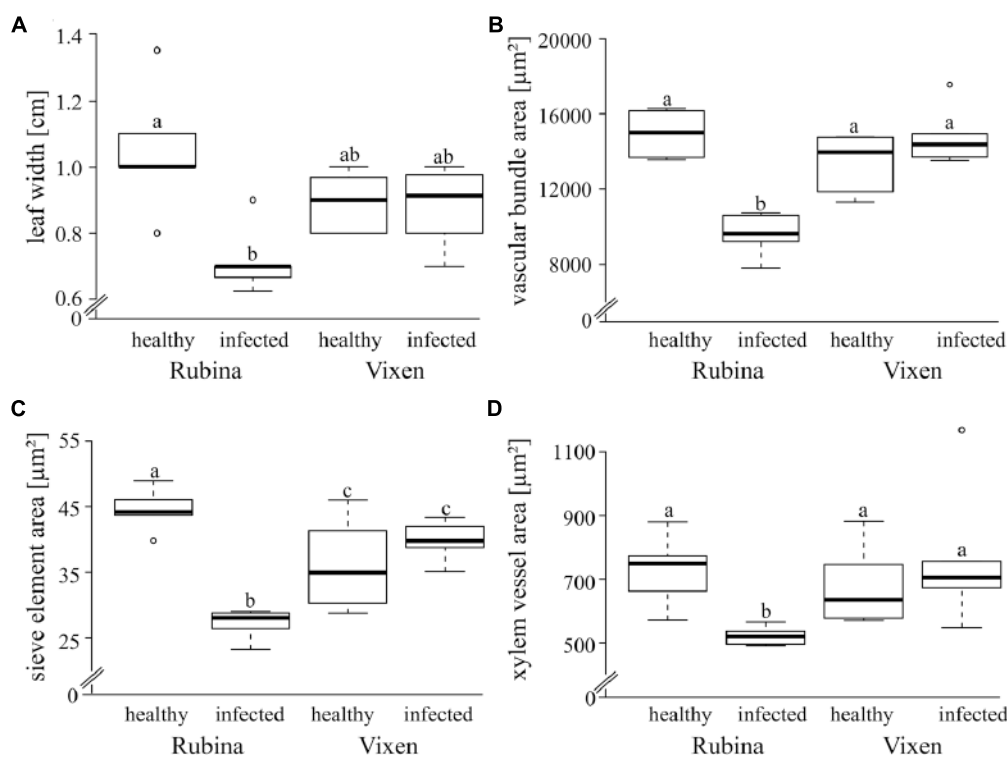


**FIGURE 2 |** Morphological comparison of healthy and BYDV infected *Hordeum vulgare* plants. The impact of BYDV infection on the morphology of a leaf and the vascular system was examined via various parameters – **(A)** leaf width (cm), **(B)** vascular bundle area ( $\mu\text{m}^2$ ), **(C)** sieve element area ( $\mu\text{m}^2$ ) and **(D)** xylem vessels area ( $\mu\text{m}^2$ ). The study included a susceptible (Rubina) and a tolerant (Vixen) cultivar. The bold horizontal line in the box illustrates the median value, boxes present the interquartile range. Note the suppressed zero at the y-axis scale! Different letters indicate statistical differences ( $p = 0.05$ ;  $N = 5-6$ ).

**TABLE 1 |** Statistics of the analysis of morphological leaf traits of the two *Hordeum vulgare* cultivars Rubina (susceptible) and Vixen (tolerant) after BYDV infection.

Morphological trait	Statistical test used	Variance structure	Factor	F/L-ratio	P-value
Leaf width	ANOVA	varIdent(form = ~1 infection)	Cultivar	0.001	0.978
			Infection	9.091	<b>0.007</b>
			Interaction	8.640	<b>0.008</b>
Vascular bundle area	ANOVA	varIdent(form = ~1 combi)	Cultivar	8.476	<b>0.009</b>
			Infection	9.867	<b>0.005</b>
			Interaction	34.115	<0.001
Sieve element area	GLS	varIdent(form = ~1 infection)	Cultivar	8.443	<b>0.004</b>
			Infection	4.682	<b>0.030</b>
			Interaction	21.235	<0.001
Xylem area	GLS	varIdent(form = ~1 combi)	Cultivar	<0.001	0.386
			Infection	13.857	<0.001
			Interaction	6.352	<b>0.012</b>

Significant P-values ( $\leq 0.05$ ) are given in bold. Depending on which statistical test was used, F-values or Likelihood ratios (L-ratio) are given. Likelihood ratios are given in italics. Interaction means the statistical interaction between cultivar and infection. Combi in the variance structure means the combination of all two main factors (cultivar, BYDV infection) i.e., each box in the boxplot of **Figure 2D** was allowed to have its own variability ( $N = 5-6$ ).

the underlying factors. One possible factor might be the general physiological stress level induced by BYDV, which might be reflected in the level of ROS. For both cultivars, we found low ROS levels in healthy plants. However, after infection ROS levels were significantly higher in plants of the cv. Rubina compared to plants of the cv. Vixen (**Figure 4** and **Table 3**). To evaluate the

magnitude of the influence of BYDV infection on the ROS formation during early signaling events in response to abiotic stresses, we applied an additional heat stimulus. Following the heat stimulus, we observed an equal significant decrease of ROS formation in a remote area ( $d = 5-9$  cm) for both cv. Rubina and cv. Vixen (**Figure 4** and **Table 3**).

## ABA and SA Were Differentially Influenced Depending on BYDV Infection and Heat Stimulus

An additional indicator of a general physiological stress is the level of the phytohormone ABA which is also associated with ROS (Gilroy et al., 2016). The ABA concentrations in healthy cv. Rubina and cv. Vixen plants were similar. Akin to the ROS formation only the cv. Rubina showed increased ABA levels after infection. The heat stimulus did not influence ABA concentrations in either cultivar, regardless of the infection status (**Figure 5** and **Table 4**).

Salicylic acid concentrations were in general slightly higher in plants of the cv. Rubina compared to plants of the cv. Vixen (**Figure 5** and **Table 4**). Whereas infection led to increased SA concentrations in both cultivars, burning did not significantly change the SA concentrations in either cultivar (**Figure 5** and **Table 4**).

## Jasmonates Were Increased After BYDV Infection

The JA pathway was also investigated to study the stress reaction to BYDV and heat stimuli. Three different jasmonates – JA, the JA-Ile and the JA-Val conjugate – were studied as representatives of the JA pathway. Similar to ABA concentrations, we found that JA, JA-Ile, and JA-Val concentrations were significantly increased in non-heat stimulated but infected cv. Rubina plants but not in infected cv. Vixen plants (**Figure 5** and **Table 4**). The jasmonate concentrations in non-heat stimulated cv. Vixen plants were either very low or not detectable (JA-Val) regardless of the infection status.

In contrast to infection, the heat stimulus led to a marked increase in jasmonate concentrations in healthy and infected plants of both cultivars (**Figure 5** and **Table 4**). However, whilst infected cv. Vixen plants showed higher jasmonate concentrations upon burning than uninfected cv. Vixen plants, infected cv. Rubina plants showed either higher (JA-Val), similar (JA) or even lower concentrations (JA-Ile) than uninfected plants. The general rise of jasmonate concentrations due to the heat stimulus was significantly stronger than that due to BYDV infection thereby showing that the maximum possible jasmonate concentration was not reached during infection.

## DISCUSSION

Susceptible barley plants like the cv. Rubina show strong symptoms such as stunted growth and yellow or red discoloration of the leaf tips whereas tolerant cultivars like the cv. Vixen with a *Ryd2* based tolerance (Schaller et al., 1964) show no or only weak symptoms.

*Barley yellow dwarf virus* is localized in the phloem and is persistently transmitted by aphids. Due to its phloem location, the virus negatively affects the integrity of the sieve elements in susceptible barley cultivars (Esau, 1957). However, despite extensive study (Schaller et al., 1964; Niks et al., 2004; Scholz et al.,

2009; Schliephake et al., 2013) the effect of BYDV on phloem parameters and plant defense responses, including changes in ROS and defense hormones, have to our knowledge not been reported.

## Phloem Infection Leads to Decreases in Vascular Development and Reduced Propagation of Electropotential Waves

With regard to development, vascular bundles develop in healthy and BYDV infected leaves in a comparable way and there is no influence on the fundamental organization of the phloem tissue (Esau, 1957). Our observations show that the phloem as well as the xylem area were both negatively affected due to BYDV infection, which could be explained by necrotic obliteration of sieve elements and xylem vessels, already occurring in differentiating vascular bundles in highly susceptible barley (Esau, 1957). Pathological degeneration and necrosis of the phloem, involving sieve elements, CCs and parenchyma cells, affects old and young vascular bundles in main and marginal veins.

*Barley yellow dwarf virus* infection affects the physiological functionality of sieve elements with regard to their propagation of EPWs as indicated by our results obtained by using aphids as bio-electrodes. EPWs show a decreasing propagation velocity along sieve tubes with increasing distance from the trigger site as previously shown in cucurbits and rapeseed (Furch et al., 2010; Zimmermann et al., 2016) and observed here for healthy plants of both cultivars and BYDV infected tolerant plants. A decrease in electrophysiological conductivity of the phloem in the BYDV infected susceptible cultivar is already indicated because of the reduced radius of single sieve elements as well as the reduced total radius of vascular bundles, combined with necrosis of single sieve elements (Esau, 1957). Moreover, there is likely to be an increase in the longitudinal (intracellular) resistance for electrophysiological signals according to the cable theory model for the calculation of the electrophysiological current along passive neurites (Taylor, 2013) and sieve tubes in plants (Hedrich et al., 2016) showing that a reduced cell radius will increase the longitudinal (intracellular) resistance for current flow. As a further effect, the lateral resistance (affecting the flow of electrophysiological current through the membrane) will decrease with decreasing cell diameter due to a relative increase of the membrane surface with regard to the cell volume. Together both parameters would negatively affect the propagation of electrophysiological current along a cable, leading to the observed loss of EPWs near to their trigger site. It can be suggested that the suppression of EPW propagation may have a negative effect on, e.g., plant defense (Trébacz et al., 2006).

The cable theory is used to explain the propagation of action potentials along neurites and was recently used for the description of electrophysiological signals in sieve tubes as mentioned above (Hedrich et al., 2016). While a neurite is part of a single cell, sieve tubes are composed out of several sieve elements, each of it a single cell with individual electrophysiological properties. Latter appears to be a strong difficulty in simply transferring the theory to

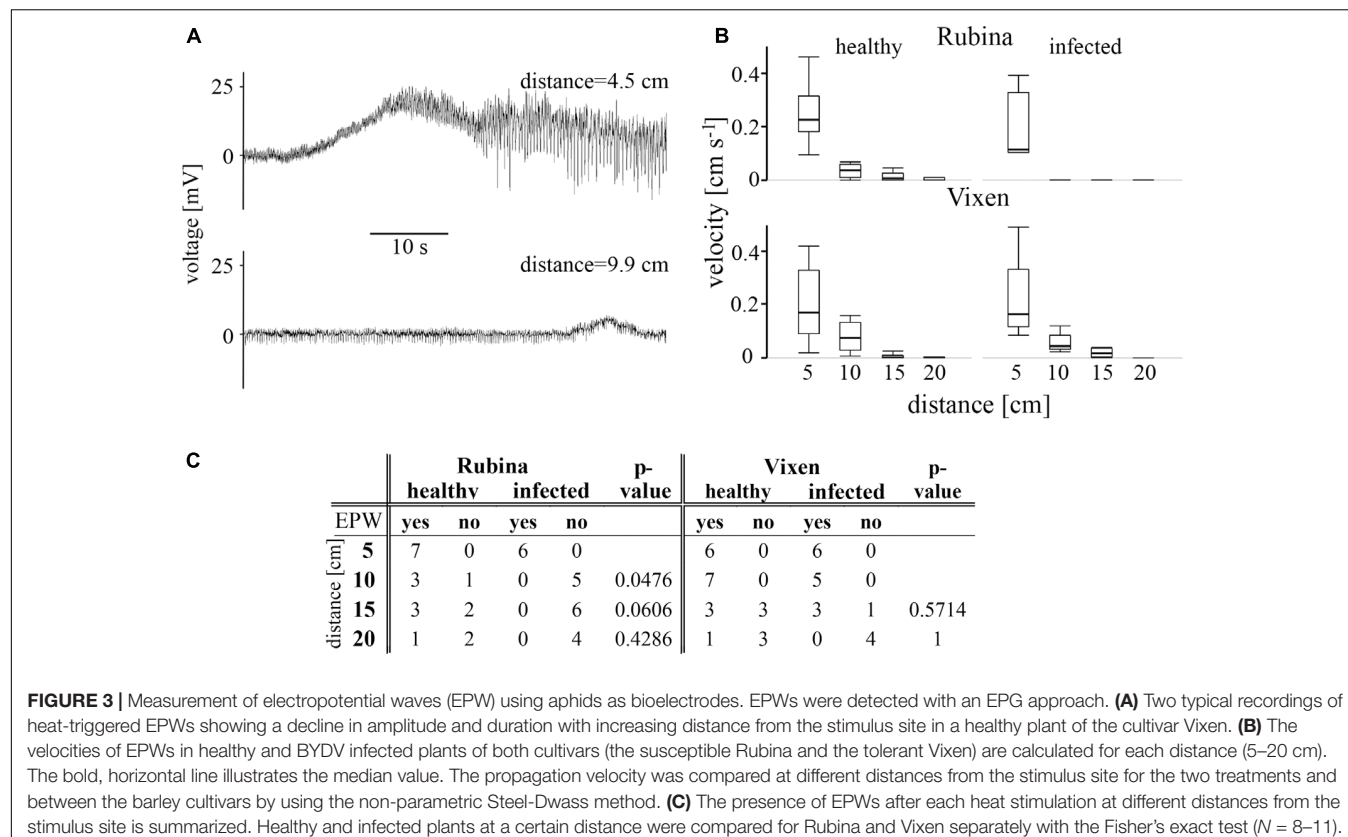


**FIGURE 3 |** Measurement of electropotential waves (EPW) using aphids as bioelectrodes. EPWs were detected with an EPG approach. **(A)** Two typical recordings of heat-triggered EPWs showing a decline in amplitude and duration with increasing distance from the stimulus site in a healthy plant of the cultivar Vixen. **(B)** The velocities of EPWs in healthy and BYDV infected plants of both cultivars (the susceptible Rubina and the tolerant Vixen) are calculated for each distance (5–20 cm). The bold, horizontal line illustrates the median value. The propagation velocity was compared at different distances from the stimulus site for the two treatments and between the barley cultivars by using the non-parametric Steel-Dwass method. **(C)** The presence of EPWs after each heat stimulation at different distances from the stimulus site is summarized. Healthy and infected plants at a certain distance were compared for Rubina and Vixen separately with the Fisher's exact test ( $N = 8–11$ ).

**TABLE 2 |** Statistical values for the analysis of EPG recording based signal velocity between adjacent measuring points of one treatment and between respective measuring points of two *Hordeum vulgare* cultivars according to BYDV infection.

Morphological trait	Statistical test used	Distance to leaf tip [cm]		N	P-value treatment	P-value healthy/inf
Rubina	Steel-Dwass	5		7	0.052	0.861
		10		4	0.819	n.t.
		15		5	n.t.	n.t.
		20		3	—	n.t.
Rubina infected	Steel-Dwass	5		6	<b>0.028</b>	
		10		5	n.t.	
		15		6	n.t.	
		20		4	—	
Vixen	Steel-Dwass	5		6	0.438	1.000
		10		7	<b>0.026</b>	0.916
		15		6	0.889	0.690
		20		4	—	0.877
Vixen infected	Steel-Dwass	5		6	0.066	
		10		5	0.256	
		15		4	0.264	
		20		4	—	

Measuring points with  $N < 4$  or where no signal was recorded were not included in a statistical comparison (n.t.). Significant P-values are given in bold.

the plant system where it does not reflect the complexity of the biological systems. Due to lacking basal experimental studies about the transfer of electrophysiological potentials in sieve tubes it is not possible to use the cable theory to fully explain our observations. A parameter that appears to be relevant for such calculations is the sieve element and

vascular bundle size (area, length) that cannot be determined without great effort when using aphids as bio-electrodes. Aphids at the different measuring points could feed from the same sieve tube or from different vascular bundles, which might have effects on the amplitude and velocity of an EPW.

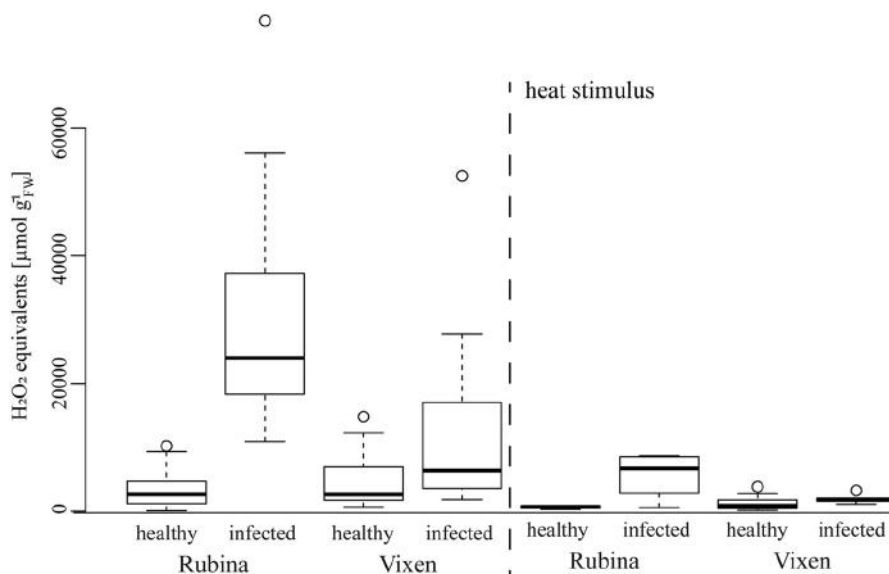


**FIGURE 4 |** Reactive oxygen species distribution in healthy and BYDV infected *H. vulgare* cultivars Rubina (susceptible) and Vixen (tolerant) with and without heat stimulus. The general defense response of BYDV susceptible (Rubina) and tolerant (Vixen) cultivars was examined by the measurement of the  $\text{H}_2\text{O}_2$  concentrations after BYDV infection and 30 min after a heat stimulus at the leaf tip. Infected Rubina plants showed a higher concentration of ROS than uninfected ones. The bold horizontal line in the box illustrates the median value, boxes represent the interquartile range.  $N = 4-19$ , exact number of replicates see Supplementary Table 2.

**TABLE 3 |** Statistics of the analysis of ROS of the two *Hordeum vulgare* cultivars Rubina (susceptible) and Vixen (tolerant) after BYDV infection and heat stimulus.

Statistical test used	Transformation/variance structure	Factor	Likelihood-ratio	P-value
gl	log varldent(form = ~1 combi)	Cultivar	1.470	0.225
		Infection	17.105	<0.001
		Heat	44.582	<0.001
		Cultivar:infection	18.209	<0.001
		Cultivar:heat	0.044	0.834
		Infection:heat	0.384	0.535
		Cultivar:infection:heat	0.620	0.431

Significant P-values are given in bold. Combi in the variance structure means the combination of all three main factors (cultivar, BYDV infection, heat stimulus) i.e., each box in the boxplot of Figure 4 was allowed to have its own variability.  $N = 4-19$ , exact number of replicates see Supplementary Table 2.

Further factors that might have an effect on the lateral and longitudinal resistance is (i) the connection to sieve elements with CCs via pore plasmodesm units (PPUs) and (ii) the connection of adjacent sieve elements via sieve pores. Plant viruses are able to modulate the opening state of plasmodesmata by using so called movement proteins (Deom et al., 1992) to help them spread (Lazarowitz and Beachy, 1999). ORF4 of BYDV encodes a 17 kDa called movement protein (Nass et al., 1998) that is required for systemic infection of the virus in barley (Chay et al., 1996). We suggest that the BYDV movement protein triggers opening of PPUs and sieve pores. The opening state of plasmodesmata is in addition also affected by plant signaling and defense compounds whereas ROS and SA trigger plasmodesmata closure (Cheval and Faulkner, 2017). Since systemic virus infection occurs in both barley cultivars tested, we suggest that PPUs and sieve pores are opened in both cultivars studied. If closure of both plasmodesmata types is not triggered by plant defense compounds, although a significant increase of ROS was

caused by BYDV infection in the two cultivars can be suggested because of systemic BYDV infection. However, this remains only speculation and has to be tested in later experiments.

### Viral Infection Induces a Greater Response of Chemical Signals in the Susceptible Than the Tolerant Cultivar

One of the reactions of plants to invasion of pathogens including viruses is the generation of ROS (Bolwell and Wojtaszek, 1997). In response to infection, we observed an increase of ROS (measured as  $\text{H}_2\text{O}_2$  equivalents; Figure 4), mainly in the susceptible cultivar similar to ROS accumulations previously reported after infection by the *Plum pox virus* (Hernandez et al., 2006; Diaz-Vivancos et al., 2008), *Cucumber mosaic virus* (Riedle-Bauer, 2000) and *Clover mosaic virus* (Clarke et al., 2002). Thus, increased ROS production seems to be a common defense response against viral infection.

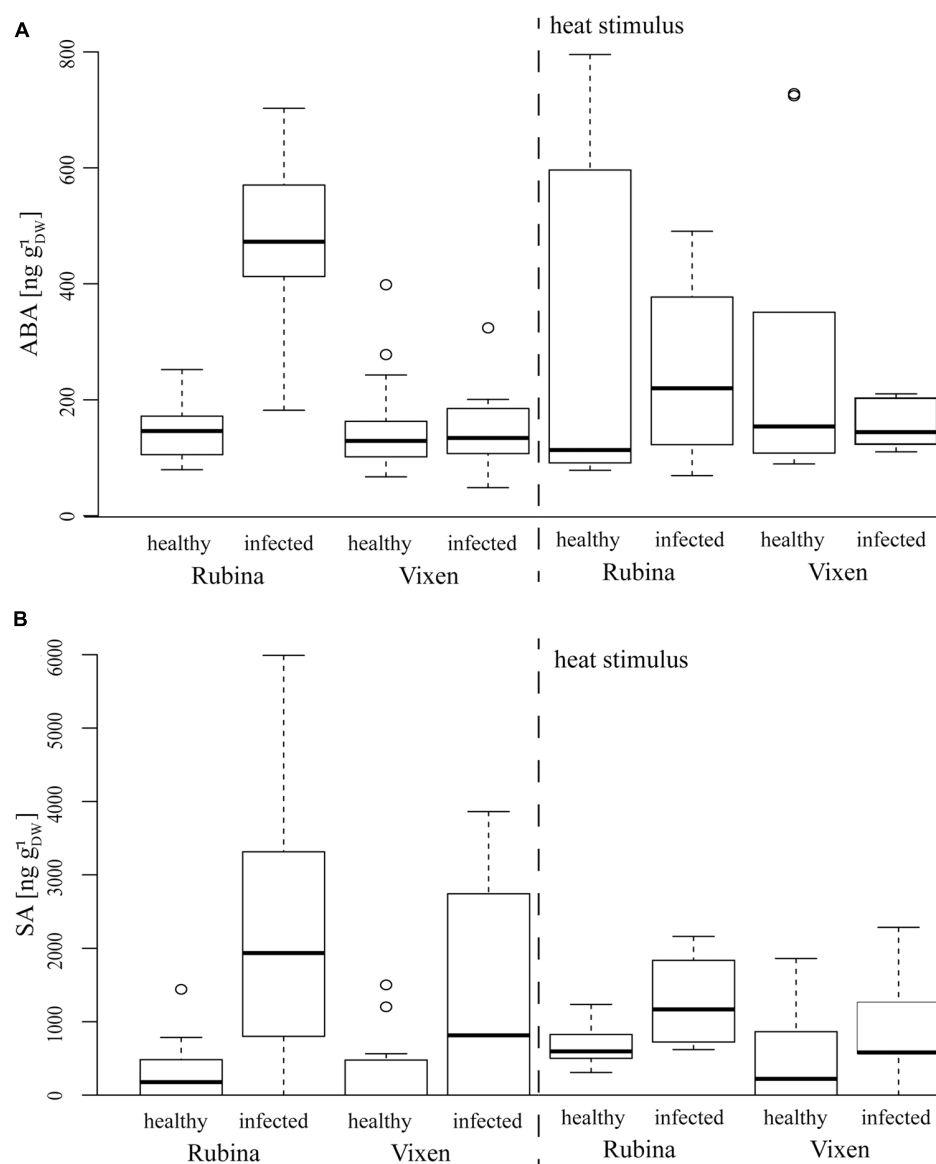


**FIGURE 5 |** Phytohormone concentrations after BYDV infection and heat stimulus in the *H. vulgare* cultivars Rubina (susceptible) and Vixen (tolerant). **(A)** Abscisic acid (ABA) levels are increased in BYDV infected plants, whereas **(B)** SA is increased in infected plants of both cultivars. Burning does not differentially influence the phytohormone levels in the different treatments. The bold horizontal line in the box illustrates the median value, boxes present the interquartile range.  $N = 4-18$ , exact number of replicates see Supplementary Table 2.

We observed a significant increase of ABA concentrations in infected cv. Rubina plants. ABA accumulation promotes closing of stomata and consequently the reduction of transpiration and, therefore, water loss. Another consequence is the decrease in gas exchange leading to the reduction of the photosynthetic activity (Cutler et al., 2010; Brandt et al., 2012; Mittler and Blumwald, 2015). The result is a reduction in organ size, vascular bundle development and growth of the whole plant, as it is shown here for infected cv. Rubina plants (Figures 1A, 2) and an early senescence (Wehner et al., 2015). The stunted growth of infected cv. Rubina plants (Figures 1A, 2) can thus be attributed to a shortage of photoassimilates due to the increased levels of both

ROS (Figure 4) and ABA (Figure 5). Further investigation of stomatal guard cells might help to evaluate this hypothesis.

Reactive oxygen species signaling in response to different stresses is also known to interfere with SA signaling (Herrera-Vasquez et al., 2015). Both infected barley cultivars showed an increase in SA concentrations compared to healthy plants, whereas the heat stimulus did not induce a response (Figure 5B). Davis et al. (2015) showed a similar increase in SA for BYDV infected wheat plants. SA promotes ROS production, on the one hand, and ROS scavenging, on the other, in a temporally dynamic way (Herrera-Vasquez et al., 2015). The increase in both ROS and SA in susceptible plants upon virus infection suggests

**TABLE 4 |** Statistical values for the analysis of phytohormone concentrations in the two *Hordeum vulgare* cultivars Rubina (susceptible) and Vixen (tolerant) according to BYDV infection and heat stimulus.

Phytohormone	Statistical test used	Transformation/variance structure	Factor	F/L-ratio	P-value
ABA	GLS	log varldent(form = ~1 combi)	Cultivar	0.959	0.327
			Infection	0.616	0.433
			Heat	2.100	0.147
			Cultivar:infection	25.053	< 0.001
			Cultivar:heat	0.834	0.361
			Infection:heat	2.710	0.100
			Cultivar:infection:heat	1.740	0.187
SA	ANOVA	square root	Cultivar	3.950	<b>0.050</b>
			Infection	25.634	< 0.001
			Heat	0.823	0.367
			Cultivar:infection	0.953	0.332
			Cultivar:heat	0.109	0.743
			Infection:heat	1.939	0.168
			Cultivar:infection:heat	0.518	0.474
JA	GLS	square root varldent(form = ~1 combi)	Cultivar	0.196	0.658
			Infection	4.032	<b>0.045</b>
			Heat	50.260	< 0.001
			Cultivar:infection	6.894	<b>0.009</b>
			Cultivar:heat	2.995	0.083
			Infection:heat	1.016	0.313
			Cultivar:infection:heat	7.542	<b>0.006</b>
JA-Ile	GLS	square root varldent(form = ~1 combi)	Cultivar	2.203	0.138
			Infection	4.833	<b>0.028</b>
			Heat	62.306	< 0.001
			Cultivar:infection	5.687	<b>0.017</b>
			Cultivar:heat	2.531	0.112
			Infection:heat	2.067	0.150
			Cultivar:infection:heat	13.375	< 0.001
JA-Val	ANOVA	log	Cultivar	0.086	0.772
			Infection	10.665	<b>0.004</b>
			Cultivar:infection	2.943	0.101

Significant P-values are given in bold. Depending on which statistical test was used F-values or Likelihood ratios (L-ratio) are given. Likelihood ratios are given in italics. Interaction means the statistical interaction between cultivar and infection. Combi in the variance structure means the combination of all three main factors (cultivar, BYDV infection, heat stimulus) i.e., each box in the boxplot of **Figures 5, 6** was allowed to have its own variability. JA-Val conjugate concentrations were only analyzed for burned plants since this jasmonate conjugate was only sporadically detected in non-burned plants. N = 4–18, exact number of replicates see Supplementary Table 2.

a concerted action of these signaling compounds. Increased SA concentrations have also been implicated in reduced growth due to an influence on the lignin content (Gallego-Giraldo et al., 2011) giving an alternative explanation for the reduced growth of infected cv. Rubina.

Infection of plants by pathogens often results in changes in the level of various phytohormones, such as SA and JA (Robert-Seilantian et al., 2007). Although, SA and JA signaling pathways are mutually antagonistic, evidences of synergistic interactions have also been reported (Mur et al., 2006). In natural environments when plants cope with multiple attackers as well as abiotic stresses, complex responses are observed (Bari and Jones, 2009), and so it is not yet known how plants prioritize one response over the other. We found marked increases of JA, JA-Ile, and JA-Val concentrations in infected cv. Rubina plants indicating the activation of JA signaling networks in this cultivar (**Figure 6**). These jasmonates also increase upon burning in all treatments keeping with previous reports (Herde et al., 1996),

however, this is the first time that JA-Val, has been implicated to be involved in this response as well. In contrast, the cv. Vixen did not display a significant increase in jasmonate levels upon viral infection. This implies a difference in this branch of the defense pathway. One may speculate that the lack of activation of the JA pathway is involved in tolerance of BYDV by Vixen. Low JA levels do not inhibit SA signaling, which may directly target anti-viral defenses. On the other hand, low jasmonate levels after infection may also be a consequence of viral tolerance if another mechanism antagonizes viral infection and so defense signaling is not induced in comparison to the susceptible cultivar.

## CONCLUSION

The susceptible barley cultivar Rubina and the tolerant cultivar Vixen were found to differ markedly after BYDV infection in

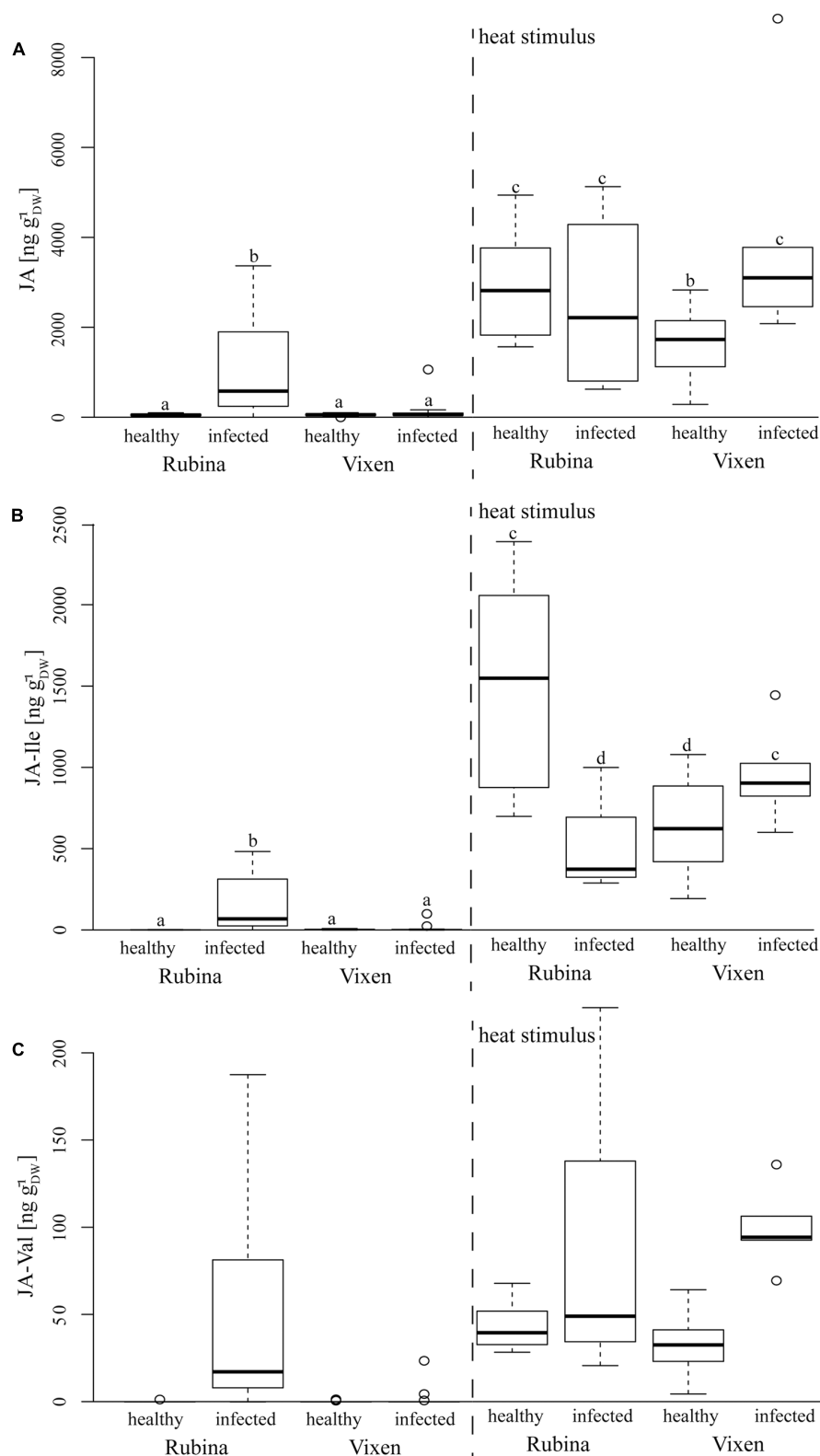


**FIGURE 6 |** Concentrations of several jasmonates in response to BYDV infection and a heat stimulus in the *Hordeum vulgare* cultivars Rubina (susceptible) and Vixen (tolerant). The jasmonates – **(A)** JA, **(B)** jasmonic acid isoleucine conjugate (JA-Ile), and **(C)** jasmonic acid valine conjugate (JA-Val) – were only detected in reaction to BYDV infection and a heat stimulus at the leaf tip. The bold horizontal line in the box illustrates the median value, boxes present the interquartile range. Different letters indicate statistical differences ( $p < 0.05$ ;  $N = 4–18$ , exact number of replicates see Supplementary Table 2).

various aspects of their phloem anatomy, electrophysiological reactions and chemical defense signaling. The reduced growth of the susceptible cultivar appears to result from increased ABA and ROS level and reductions in vascular development and suppressed long distance electrophysiological reactions. The susceptible cultivar also displayed elevated concentrations of the defense hormones ABA, SA, and jasmonates after viral infection. The superior performance of the tolerant cultivar, which carries the *Ryd2* gene, was found to be associated with low levels of hormone signaling, providing new markers for tolerance and a new context for investigating the basis of viral tolerance in barley and other plant species (Ordon et al., 2009).

## AUTHOR CONTRIBUTIONS

MKP, GK, MRZ, ACUF, and TW designed the research. MKP, GK, NT, AL, DM, ACUF, and TW performed the research. MKP, GK, MRZ, RO, JG, ACUF, and TW analyzed the data. MKP, GK, MRZ, AH, FO, ACUF, and TW wrote the paper.

## REFERENCES

- Bari, R., and Jones, J. D. G. (2009). Role of plant hormones in plant defence responses. *Plant Mol. Biol.* 69, 473–488. doi: 10.1007/s11003-008-9435-0
- Bolwell, G. P., and Wojtaszek, P. (1997). Mechanisms for the generation of reactive oxygen species in plant defence—abroad perspective. *Physiol. Mol. Plant Pathol.* 51, 347–366. doi: 10.1006/pmpp.1997.0129
- Brandt, B., Brodsky, D. E., Xue, S., Negi, J., Iba, K., Kangasjärvi, J., et al. (2012). Reconstitution of abscisic acid activation of SLAC1 anion channel by CPK6 and OST1 kinases and branched ABI1 PP2C phosphatase action. *Proc. Natl. Acad. Sci. U.S.A.* 109, 10593–10598. doi: 10.1073/pnas.1116590109
- Chay, C. A., Gunasinghe, U. B., Dinesh-Kumar, S. P., Miller, W. A., and Gray, S. M. (1996). Aphid transmission and systemic plant infection determinants of Barley yellow dwarf luteovirus -PAV are contained in the coat protein readthrough domain and 17-kDa protein, respectively. *Virology* 219, 57–65. doi: 10.1006/viro.1996.0222
- Cheval, C., and Faulkner, C. (2017). Plasmodesmal regulation during plant-pathogen interactions. *New Phytol.* 217, 62–67. doi: 10.1111/nph.14857
- Clark, M. F., and Adams, A. N. (1977). Characteristics of the microplate method enzyme-linked immunosorbent assay for the detection of plant viruses. *J. Gen. Virol.* 34, 475–483. doi: 10.1099/0022-1317-34-3-475
- Clarke, S. F., Guy, P. L., Burritt, D. J., and Jamson, P. E. (2002). Changes in the activities of antioxidant enzymes in response to virus infection and hormone treatment. *Physiol. Plant.* 114, 157–164. doi: 10.1034/j.1399-3054.2002.1140201.x
- Cooper, J. I., and Jones, A. T. (1983). Responses of plants to viruses—proposals for the use of terms. *Phytopathology* 73, 127–128. doi: 10.1094/Phyto-73-127
- Crawley, M. (2013). *The R Book*. Hoboken, NJ: John Wiley and Sons.
- Cutler, S. R., Rodriguez, P. L., Finkelstein, R. R., and Abrams, S. R. (2010). Abscisic acid: emergence of a core signaling network. *Plant Horm.* 1, 651–679. doi: 10.1146/annurev-arplant-042809-112122
- D'Arcy, C. J. (1995). "Symptomatology and host range of barley yellow dwarf" in *Barley Yellow Dwarf. 40 Years of Progress*, eds C. J. D'Arcy and P. A. Burnett (St. Paul, Minnesota: APS Press), 9–28.
- Davis, T. S., Bosque-Perez, N. A., Popova, I., and Eigenbrode, S. D. (2015). Evidence for additive effects of virus infection and water availability on phytohormone induction in a stable crop. *Front. Ecol. Evol.* 3:114. doi: 10.3389/fevo.2015.00114
- Dempsey, D. A., Vlot, A. C., Wildermuth, M. C., and Klessig, D. F. (2011). Salicylic acid biosynthesis and metabolism. *Arabidopsis Book* 9:e0156. doi: 10.1199/tab.0156
- Deom, C. M., Lapidot, M., and Beachy, R. N. (1992). Plant virus movement proteins. *Cell* 69, 221–224. doi: 10.1016/0092-8674(92)90403-Y
- Diaz-Vivancos, P., Clemente-Moreno, M. J., Rubio, M., Olmos, E., Garcia, J. A., Martinez-Gomez, P., et al. (2008). Alteration in the chloroplastic metabolism leads to ROS accumulation in pea plants in response to plum pox virus. *J. Exp. Bot.* 59, 2147–2160. doi: 10.1093/jxb/ern082
- Esau, K. (1957). Phloem degeneration in Gramineae affected by the barley yellow-dwarf virus. *Am. J. Bot.* 44, 245–251. doi: 10.2307/2438806
- Felle, H. H., and Zimmermann, M. R. (2007). Systemic signalling in barley through action potentials. *Planta* 226, 203–214. doi: 10.1007/s00425-006-0458-y
- Fromm, J., and Spanswick, R. (1993). Characteristics of action potential in willow (*Salix viminalis* L.). *J. Exp. Bot.* 44, 1119–1125. doi: 10.1093/jxb/44.7.1119
- Furch, A. C. U., Hafke, J. B., Schulz, A., and van Bel, A. J. E. (2007). Ca<sup>2+</sup>-mediated remote control of reversible sieve tube occlusion in *Vicia faba*. *J. Exp. Bot.* 58, 2827–2838. doi: 10.1093/jxb/erm143
- Furch, A. C. U., van Bel, A. J. E., Fricker, M. D., Felle, H. H., Fuchs, M., and Hafke, J. B. (2009). Sieve element Ca<sup>2+</sup> channels as relay stations between remote stimuli and sieve tube occlusion in *Vicia faba*. *Plant Cell* 21, 2118–2132. doi: 10.1105/tpc.108.063107
- Furch, A. C. U., Zimmermann, M. R., Will, T., Hafke, J. B., and van Bel, A. J. E. (2010). Remote-controlled stop of phloem mass flow by biphasic occlusion in *Cucurbita maxima*. *J. Exp. Bot.* 61, 3697–3708. doi: 10.1093/jxb/erq181
- Gallego-Giraldo, L., Escamilla-Trevino, L., Jackson, L. A., and Dixon, R. A. (2011). Salicylic acid mediates the reduced growth of lignin down-regulated plants. *Proc. Natl. Acad. Sci. U.S.A.* 108, 20814–20819. doi: 10.1073/pnas.1117873108
- Giavalisco, P., Kapitza, K., Kolasa, A., Buhtz, A., and Kehr, J. (2006). Towards the proteome of *Brassica napus* phloem sap. *Proteomics* 6, 896–909. doi: 10.1002/pmic.200500155
- Gill, S. S., and Tuteja, N. (2010). Reactive oxygen species and antioxidant machinery in abiotic stress tolerance in crop plants. *Plant Physiol. Biochem.* 48, 909–930. doi: 10.1016/j.plaphy.2010.08.016
- Gilroy, S., Bialasek, M., Suzuki, N., Gorecka, M., Devireddy, A. R., Karpinski, S., et al. (2016). ROS, calcium, and electric signals: key mediators of rapid systemic signaling in plants. *Plant Physiol.* 171, 1606–1615. doi: 10.1104/pp.16.00434
- Hafke, J. B., Furch, A. C. U., Fricker, M. D., and van Bel, A. J. E. (2009). Forosome dispersion in *Vicia faba* is triggered by Ca<sup>2+</sup> hotspots created by concerted action of diverse Ca<sup>2+</sup> channels in sieve elements. *Plant Signal. Behav.* 4, 968–972. doi: 10.4161/psb.4.10.9671

## FUNDING

This work was supported by the Deutsche Forschungsgemeinschaft (Grant No. FU 969/2-1 to ACUF and CRC1127 to RO), and partly financed by the Julius Kühn-Institut and the Max Planck Society.

## ACKNOWLEDGMENTS

We thank Riya C. Menezes (MPI-CE) for confirmation of JA-Val in *H. vulgare* by accurate MS, Michael Reichelt (MPI-CE) for help with the phytohormone measurements, Kerstin Welzel (JKI) for aphid rearing, and Evelyn Betke (JKI) for performing ELISA measurements.

## SUPPLEMENTARY MATERIAL

The Supplementary Material for this article can be found online at: <https://www.frontiersin.org/articles/10.3389/fpls.2018.00145/full#supplementary-material>

- Hedrich, R., Salvador-Recatalà, V., and Dreyer, I. (2016). Electrical wiring and long-distance plant communication. *Trends Plant Sci.* 21, 376–387. doi: 10.1016/j.tplants.2016.01.016
- Herde, O., Atzorn, R., Fisahn, J., Wasternack, C., Willmitzer, L., and Pena-Cortes, H. (1996). Localized wounding by heat initiates the accumulation of proteinase inhibitor II in abscisic acid-deficient plants by triggering jasmonic acid biosynthesis. *Plant Physiol.* 112, 853–860. doi: 10.1104/pp.112.2.853
- Hernandez, J. A., Diaz-Vivancos, P., Rubio, M., Olmos, E., Ros-Barcelo, A., and Martinez-Gomez, P. (2006). Long-term plum pox virus infection produces an oxidative stress in a susceptible apricot, *Prunus armeniaca*, cultivar but not in a resistant cultivar. *Physiol. Plant.* 126, 140–152. doi: 10.1111/j.1399-3054.2005.00581.x
- Herrera-Vasquez, A., Salinas, P., and Holguigue, L. (2015). Salicylic acid and reactive oxygen species interplay in the transcriptional control of defense genes expression. *Front. Plant Sci.* 6:171. doi: 10.3389/fpls.2015.00171
- Jambunathan, N. (2010). Determination and detection of reactive oxygen species (ROS), lipid peroxidation, and electrolyte leakage in plants. *Methods Mol. Biol.* 639, 291–297. doi: 10.1007/978-1-60761-702-0\_18
- Jensen, S. G. (1969). Occurrence of virus particles in the phloem tissue of BYDV-infected barley. *Virology* 38, 83–91. doi: 10.1016/0042-6822(69)90130-5
- Knoblauch, M., Knoblauch, J., Mullendore, D. L., Savage, J. A., Babst, B. A., Beecher, S. D., et al. (2016). Testing the Münch hypothesis of long distance transport in plants. *eLife* 5:e15341. doi: 10.7554/eLife.15341
- Koo, A. J., and Howe, G. A. (2012). Catabolism and deactivation of the lipid-derived hormone jasmonoyl-isoleucine. *Front. Plant Sci.* 3:19. doi: 10.3389/fpls.2012.00019
- Lazarowitz, S. G., and Beachy, R. N. (1999). Viral movement proteins as probes for intracellular and intercellular trafficking in plants. *Plant Cell* 11, 535–548. doi: 10.1105/tpc.11.4.535
- Mancuso, S. (1999). Hydraulic and electrical transmission of wound induced signals in *Vitis vinifera*. *Aust. J. Plant Physiol.* 26, 55–61. doi: 10.1071/PP98098
- Métraux, J. P., Signer, H., Ryals, J., Ward, E., Wyss-Benz, M., Gaudin, J., et al. (1990). Increase in salicylic acid at the onset of systemic acquired resistance in cucumber. *Science* 250, 1004–1006. doi: 10.1126/science.250.4983.1004
- Mittler, R., and Blumwald, E. (2015). The roles of ROS and ABA in systemic acquired acclimation. *Plant Cell* 27, 64–70. doi: 10.1105/tpc.114.133090
- Münch, E. (1930). *Stoffbewegungen in der Pflanze*. Jena: Gustav Fischer.
- Mur, L., Kenton, P., Atzom, R., Miersch, O., and Wasternack, C. (2006). The outcomes of concentration-specific interactions between salicylate and jasmonate signaling include synergy, antagonism, and oxidative stress leading to cell death. *Plant Physiol.* 140, 249–262. doi: 10.1104/pp.105.072348
- Nass, P. H., Domier, L. L., Jakstys, B. P., and D'Arcy, C. J. (1998). In situ localization of barley yellow dwarf virus-PAV 17-kDa protein and nucleic acids in oats. *Phytopathology* 88, 1031–1039. doi: 10.1094/PHYTO.1998.88.10.1031
- Niks, R. E., Habekuß, A., Bekele, B., and Ordon, F. (2004). A novel major gene on chromosome 6H for resistance of barley against the barley yellow dwarf virus. *Theor. Appl. Genet.* 109, 1536–1543. doi: 10.1007/s00122-004-1777-7
- Ordon, F., Habekuß, A., Kastirr, U., Rabenstein, F., and Kühne, T. (2009). Virus resistance in cereals: Source of resistance, genetics and breeding. *J. Phytopathol.* 157, 535–545. doi: 10.1111/j.1439-0434.2009.01540.x
- Parry, A. L., and Habgood, R. M. (1986). Field assessment of the effectiveness of a barley yellow dwarf virus resistance gene following its transference from spring to winter barley. *Annu. Appl. Biol.* 108, 395–401. doi: 10.1111/j.1744-7348.1986.tb07661.x
- Pel, M. J. C., and Pieterse, C. M. J. (2013). Microbial recognition and evasion of host immunity. *J. Exp. Bot.* 64, 1237–1248. doi: 10.1093/jxb/ers262
- Pinheiro, J., Bates, D., DebRoy, S., Sarkar, D., and R Core Team. (2017). *nlme: Linear and Nonlinear Mixed Effects Models. R Package Version 3.1-131*. Available at: <https://CRAN.R-project.org/package=nlme>
- R Core Team (2017). *R: A Language and Environment for Statistical Computing*. Vienna: R Foundation for Statistical Computing.
- Rhodes, J. D., Thain, J. F., and Wilson, D. C. (1996). The pathway for systemic electrical signal conduction in the wounded tomato plant. *Planta* 200, 50–57. doi: 10.1007/BF00196648
- Riedle-Bauer, M. (2000). Role of reactive oxygen species and antioxidant enzymes in systemic virus infections of plants. *J. Phytopathol.* 148, 297–302. doi: 10.1046/j.1439-0434.2000.00503.x
- Robert-Seilanian, A., Navarro, L., Bari, R., and Jones, J. D. J. (2007). Pathological hormone imbalances. *Curr. Opin. Plant Biol.* 10, 372–379. doi: 10.1016/j.pbi.2007.06.003
- Salvador-Recatalà, V., Tjallingii, W. F., and Farmer, E. E. (2014). Real-time, *in vivo* intracellular recordings of caterpillar-induced depolarization waves in sieve elements using aphid electrodes. *New Phytol.* 203, 674–684. doi: 10.1111/nph.12807
- Schaller, C. W., Qualset, C. O., and Rutger, J. N. (1964). Inheritance and linkage of the Yd2 gene conditioning resistance to the barley yellow dwarf virus disease in barley. *Crop Sci.* 4, 544–548. doi: 10.2135/cropsci1964.0011183X000400050034x
- Scheurer, K. S., Friedt, W., Huth, W., Waugh, R., and Ordon, F. (2001). QTL analysis of tolerance to a German strain of BYDV-PAV in barley (*Hordeum vulgare* L.). *Theor. Appl. Gen.* 103, 1074–1083. doi: 10.1007/s001220100632
- Schliephake, E., Habekuß, A., Scholz, M., and Ordon, F. (2013). Barley yellow dwarf virus transmission and feeding behaviour of *Ropalosiphum padi* on *Hordeum bulbosum* clones. *Entomol. Exp. Appl.* 146, 347–356. doi: 10.1111/eea.12033
- Scholz, M., Ruge-Wehling, B., Habekuß, A., Schrader, O., Pendinen, G., Fischer, K., et al. (2009). Ryd4Hb: a novel resistance gene introgressed from *Hordeum bulbosum* into barley and conferring complete and dominant resistance to the barley yellow dwarf virus. *Theor. Appl. Gen.* 119, 837–849. doi: 10.1007/s00122-009-1093-3
- Sip, V., Slrløva, L., and Chrpova, J. (2006). Screening for Barley yellow dwarf virus-resistant barley genotypes by assessment of virus content in inoculated seedlings. *J. Phytopathol.* 154, 336–342. doi: 10.1111/j.1439-0434.2006.01103.x
- Slykhuis, J. T. (1967). Methods for experimenting with mite transmission of plant viruses. *Methods Virol.* 1, 347–368.
- Taylor, R. E. (2013). Cable theory. *Phys. Tech. Biol. Res.* 6, 219–262.
- Tjallingii, W. F., and Hogendoorn, T. (1993). Fine structure of aphid stylet routes in plant tissue in correlation with EPG signals. *Physiol. Entomol.* 18, 317–328. doi: 10.1111/j.1365-3032.1993.tb00604.x
- Trębacz, K., Dziubińska, H., and Król, E. (2006). “Electrical Signals in Long-Distance Communication in Plants,” in *Communication in Plants*, eds F. Baluska, S. Mancuso, and D. Volkmann (Berlin: Springer-Verlag), 277–290.
- van Bel, A. J. E. (2003). The phloem, a miracle of ingenuity. *Plant Cell Environ.* 26, 125–149. doi: 10.1046/j.1365-3040.2003.00963.x
- Verhage, A., Vlaardingerbroek, I., Raaymakers, C., van Dam, N. M., Dicke, M., van Wees, S. C. M., et al. (2011). Rewiring of the jasmonate signalling pathway in *Arabidopsis* during insect herbivory. *Front. Plant Sci.* 2:47. doi: 10.3389/fpls.2011.00047
- Vlot, A. C., Dempsey, M. A., and Klessig, D. F. (2009). Salicylic acid, a multifaceted hormone to combat disease. *Annu. Rev. Phytopathol.* 47, 177–206. doi: 10.1146/annurev.phyto.050908.135202
- Wang, L., Halitschke, R., Kang, J.-H., Berg, A., Harnisch, F., and Baldwin, I. T. (2007). Independently silencing two JAR family members impairs levels of trypsin proteinase inhibitors but not nicotine. *Planta* 226, 159–167. doi: 10.1007/s00425-007-0477-3
- Wasternack, C., and Hause, B. (2013). Jasmonates: biosynthesis, perception, signal transduction and action in plant stress response, growth and development. An update to the 2007 review in Annals of Botany. *Ann. Bot.* 111, 1021–1058. doi: 10.1093/aob/mct067
- Wehner, G., Balko, C., Enders, M., Humbeck, K., and Odon, F. (2015). Identification of genomic regions involved in tolerance to drought stress and drought stress induced leaf senescence in juvenile barley. *BMC Plant Biol.* 15:125. doi: 10.1186/s12870-015-0524-3
- Will, T., Kornemann, S. R., Furch, A. C. U., Tjallingii, W. F., and van Bel, A. J. E. (2009). Aphid watery saliva counteracts sieve-tube occlusion: a universal phenomenon? *J. Exp. Biol.* 212, 3305–3312. doi: 10.1242/jeb.028514
- Will, T., Tjallingii, W. F., Thönen, A., and van Bel, A. J. E. (2007). Molecular sabotage of plant defense by aphid saliva. *Proc. Natl. Acad. Sci. U.S.A.* 104, 10536–10541. doi: 10.1073/pnas.0703535104
- Zimmermann, M. R., and Felle, H. H. (2009). Dissection of heat-induced systemic signals: superiority of ion fluxes to voltage changes in substomatal cavities. *Planta* 229, 539–547. doi: 10.1007/s00425-008-0850-x

- Zimmermann, M. R., and Mithöfer, A. (2013). "Electrical long-distance signaling in plants" in *Long-Distance Systemic Signaling and Communication in Plants*, ed. F. Baluska (Berlin: Springer), 291–308. doi: 10.1007/978-3-642-36470-9\_15
- Zimmermann, M. R., Mithöfer, A., Will, T., Felle, H. H., and Furch, A. C. U. (2016). Herbivore-triggered electrophysiological reactions: Candidates for systemic signals in higher plants and the challenge of their identification. *Plant Phys.* 170, 2407–2419. doi: 10.1104/pp.15.01736
- Zuur, A., Ieno, E. N., Walker, N., Saveliev, A., and Smith, G. M. (2009). *Mixed Effects Models and Extensions in Ecology With R*. New York, NY: Springer. doi: 10.1007/978-0-387-87458-6

**Conflict of Interest Statement:** The authors declare that the research was conducted in the absence of any commercial or financial relationships that could be construed as a potential conflict of interest.

Copyright © 2018 Paulmann, Kunert, Zimmermann, Theis, Ludwig, Meichsner, Oelmüller, Gershenzon, Habekuss, Ordon, Furch and Will. This is an open-access article distributed under the terms of the Creative Commons Attribution License (CC BY). The use, distribution or reproduction in other forums is permitted, provided the original author(s) and the copyright owner are credited and that the original publication in this journal is cited, in accordance with accepted academic practice. No use, distribution or reproduction is permitted which does not comply with these terms.



# High-Temperature Tolerance of Photosynthesis Can Be Linked to Local Electrical Responses in Leaves of Pea

Vladimir Sukhov\*, Vladimir Gaspirovich, Sergey Mysyagin and Vladimir Vodeneev

Department of Biophysics, N.I. Lobachevsky State University of Nizhny Novgorod, Nizhny Novgorod, Russia

## OPEN ACCESS

### Edited by:

Kazimierz Trebacz,  
Marie Curie-Sklodowska University,  
Poland

### Reviewed by:

Bratislav Stankovic,  
Loyola University Chicago,  
United States  
Joerg Fromm,  
University of Hamburg, Germany

### \*Correspondence:

Vladimir Sukhov  
vssuh@mail.ru

### Specialty section:

This article was submitted to  
Plant Physiology,  
a section of the journal  
*Frontiers in Physiology*

Received: 22 May 2017

Accepted: 19 September 2017

Published: 29 September 2017

### Citation:

Sukhov V, Gaspirovich V, Mysyagin S  
and Vodeneev V (2017)  
High-Temperature Tolerance of  
Photosynthesis Can Be Linked to  
Local Electrical Responses in Leaves  
of Pea. *Front. Physiol.* 8:763.  
doi: 10.3389/fphys.2017.00763

It is known that numerous stimuli induce electrical signals which can increase a plant's tolerance to stressors, including high temperature. However, the physiological role of local electrical responses (LERs), i.e., responses in the zone of stimulus action, in the plant's tolerance has not been sufficiently investigated. The aim of a current work is to analyze the connection between parameters of LERs with the thermal tolerance of photosynthetic processes in pea. Electrical activity and photosynthetic parameters in pea leaves were registered during transitions of air temperature in a measurement head (from 23 to 30°C, from 30 to 40°C, from 40 to 45°C, and from 45 to 23°C). This stepped heating decreased a photosynthetic assimilation of CO<sub>2</sub> and induced generation of LERs in the heated leaf. Amplitudes of LERs, quantity of responses during the heating and the number of temperature transition, which induced the first generation of LERs, varied among different pea plants. Parameters of LERs were weakly connected with the photosynthetic assimilation of CO<sub>2</sub> during the heating; however, a residual photosynthetic activity after a treatment by high temperatures increased with the growth of amplitudes and quantity of LERs and with lowering of the number of the heating transition, inducing the first electrical response. The effect was not connected with a photosynthetic activity before heating; similar dependences were also observed for effective and maximal quantum yields of photosystem II after heating. We believe that the observed effect can reflect a positive influence of LERs on the thermal tolerance of photosynthesis. It is possible that the process can participate in a plant's adaptation to stressors.

**Keywords:** heating, pea seedling, plant adaptation, thermal tolerance of photosynthesis, local electrical responses

## INTRODUCTION

The generation of local electrical responses (LERs), which are transient depolarizations of the electrical potential on the plasma membrane, is a typical electrical response in the zone of actions of numerous factors, including changes in temperature (Pyatygin et al., 1992, 1996, 1999; Krol et al., 2003, 2004, 2006; Opritov et al., 2005), increase of light intensity (Bulychev and Vredenberg, 1995; Trebacz and Sievers, 1998; Pikulenko and Bulychev, 2005), action of chemical agents (Pyatygin et al., 1996, 1999; Volkov and Ranatunga, 2006), and application electrical current (Krol et al., 2006), etc. There are several types of LERs, including receptor potentials (depolarization responses, which have low magnitude and depend stimulus strength), voltage

transients (light- and cold-induced depolarization responses, which have high magnitude, depend stimulus strength and can develop within refractory periods for action potential) and local action potentials (depolarization spikes, which have high amplitude and all-or-none characteristics) (Simons, 1981; Shimmen, 1997; Trebacz et al., 1997; Krol and Trebacz, 1999; Krol et al., 2003, 2004, 2006).

The generation of action potentials is connected with activation of  $\text{Ca}^{2+}$ ,  $\text{K}^+$ , and anion channels (Krol et al., 2006; Trebacz et al., 2006; Beilby, 2007; Felle and Zimmermann, 2007) and with transitory inactivation of  $\text{H}^+$ -ATPase in the plasma membrane (Sukhov and Vodeneev, 2009; Vodeneev et al., 2015; Sukhov, 2016). Other LERs, namely voltage transients, have  $\text{K}^+$  and anion-independent ionic mechanisms and are connected with calcium ions influxes from extra- and intracellular compartments (Krol et al., 2004); inactivation of  $\text{H}^+$ -ATPase also participate in the generation of light-induced voltage transients (Krol and Trebacz, 1999). It is probable that mechanisms of receptor potentials are not universal; in particular, touch-induced responses can be connected with  $\text{Ca}^{2+}$  and  $\text{Cl}^-$  channels (Shimmen, 1997), and cooling-induced ones can be caused by a decrease in activity of  $\text{H}^+$ -ATPase in the plasma membrane (Pyatygin et al., 1992; Pyatygin, 2004; Opritov et al., 2005).

Ionic mechanisms of LERs are similar to mechanisms of an important electrical signal—variation potential (VP). VP comprises two components: a long-term depolarization and “action potential-like” spikes (Vodeneev et al., 2015). The long-term depolarization is connected with activation of ligand-dependent and/or mechanosensitive  $\text{Ca}^{2+}$  channels and transient inactivation of  $\text{H}^+$ -ATPase in the plasma membrane (Stahlberg et al., 2006; Fromm and Lautner, 2007; Gallé et al., 2015; Katicheva et al., 2015; Vodeneev et al., 2015); i.e., this component is similar to voltage transients and, possibly, receptor potentials. Moreover, amplitude of the long-term depolarization is dependent on stimulus strength or distance from the damaged zone (Vodeneev et al., 2011; Sukhov et al., 2013); these properties support similarity of voltage transients and, possibly, receptor potentials with the long-term depolarization. In contrast, “action potential-like” spikes are rather caused by activation of voltage-dependent  $\text{Ca}^{2+}$ , anions and  $\text{K}^+$  channels (Vodeneev et al., 2011, 2015; Katicheva et al., 2014); i.e., they are similar to local action potential.

On the basis of these results we can suppose that VP has several mechanisms which are similar to those of different types of LERs; this supports the conventional hypothesis that VP is LER induced by propagation of chemical and/or hydraulic signals after local damage (Malone, 1994; Mancuso, 1999; Stahlberg et al., 2006; Fromm and Lautner, 2007; Vodeneev et al., 2015). It is known that propagating electrical signals, including VP, induce numerous physiological responses in plants (Fromm and Lautner, 2007; Gallé et al., 2015; Sukhov, 2016): changes in expression of genes (Stanković and Davies, 1996; Fisahn et al., 2004; Davies and Stankovic, 2006; Mousavi et al., 2013), production of phytohormones (Dziubinska et al., 2003; Hlavácková et al., 2006; Hlavinka et al., 2012; Mousavi et al., 2013), activation of respiration

(Filek and Kościelniak, 1997; Sukhov et al., 2014a; Surova et al., 2016a), changes in transpiration and photosynthesis (Bulychev et al., 2004; Krupenina and Bulychev, 2007; Grams et al., 2009; Pavlovic et al., 2011; Sherstneva et al., 2015; Sukhov, 2016), decrease of phloem transport (Fromm, 1991; Furch et al., 2010), etc. The important result of electrical signal propagation is an increase in a plant's tolerance to stressors (Retivin et al., 1997; Sukhov et al., 2015b). In particular, electrical signals induce the increased tolerance of photosynthetic machinery and for the entire plant to cold and heat (Retivin et al., 1999; Sukhov et al., 2014b, 2015b; Surova et al., 2016b).

In contrast, the physiological role of LERs has not been sufficiently investigated. In particular, there were only few studies (Opritov et al., 1993; Pyatygin et al., 1996; Shepherd et al., 2008; Kenderešová et al., 2012) which showed the connection between LERs and plant tolerance to stressors. Pyatygin et al. (1996) showed that plant adaptation to chilling was connected with changes in parameters of cold-induced electrical responses; moreover, fast adaptation of the plant cell to chilling was observed after generation of LERs with depolarization spikes and it was absent after electrical changes without the spikes (Opritov et al., 1993). According to the results of Shepherd et al. (2008), application of a saline medium with a low concentration of calcium induced a periodic generation of LERs, which were accompanied by viability loss in *Chara* cells; however, recurring electrical responses and viability loss were absent under application of the saline medium with a high calcium concentration. Kenderešová et al. (2012) showed that a negative relationship between amplitude of  $\text{Zn}^{2+}$ -induced LERs and tolerance of *Arabidopsis* to the high concentration of zinc was observed; however, the tolerance was investigated after several days under  $\text{Zn}^{2+}$  treatment and the connection between  $\text{Zn}^{2+}$ -induced LERs and the tolerance of *Arabidopsis* can be caused by propagation of system electrical signals.

Plant tolerance to the chilling, saline medium and zinc can thus be connected with parameters of LERs induced by these stressors. However, the possible connection with LERs was not investigated for another important stressor, namely heating. Taking into account the positive influence of VP [i.e., LER induced by chemical and (or) hydraulic signals] on the tolerance to heating of undamaged parts of the plant (Sukhov et al., 2014b, 2015b; Surova et al., 2016b), the connection between the thermotolerance and parameters of heating-induced LERs is probable. Analysis of the connection in peas was a task of the current investigation.

## MATERIALS AND METHODS

### Plant Material

Pea seedlings (14–21 days old) were used in this investigation. Seedlings were cultivated hydroponically (a half-strength Hoagland–Arnon medium) in a Binder KBW 240 plant growth chamber (Binder GmbH, Tuttlingen, Germany) at 24°C, with a 16/8-h (light/dark) photoperiod. Air humidity was not controlled.

## Electrical Measurements

The extracellular measurement of the electrical activity was performed using electrode consisting of a silver wire (0.5-mm diameter) and a pointed tip. The silver electrode ( $E_L$ ) was impaled into the mesophyll in between veins at the center of a leaflet (Figure 1A) in the closed photosynthesis-measuring

head (see below). The reference  $\text{Ag}^+/\text{AgCl}$  electrode ( $E_R$ ) (EVL-1M3.1, RUE "Gomel Measuring Equipment Plant," Gomel, Belarus) was placed in a standard solution (1 mM KCl, 0.5 mM  $\text{CaCl}_2$ , 0.1 mM NaCl) surrounding the root (about 100 ml); our previous works showed that the solution provides a stable contact between electrodes and plant (e.g.,

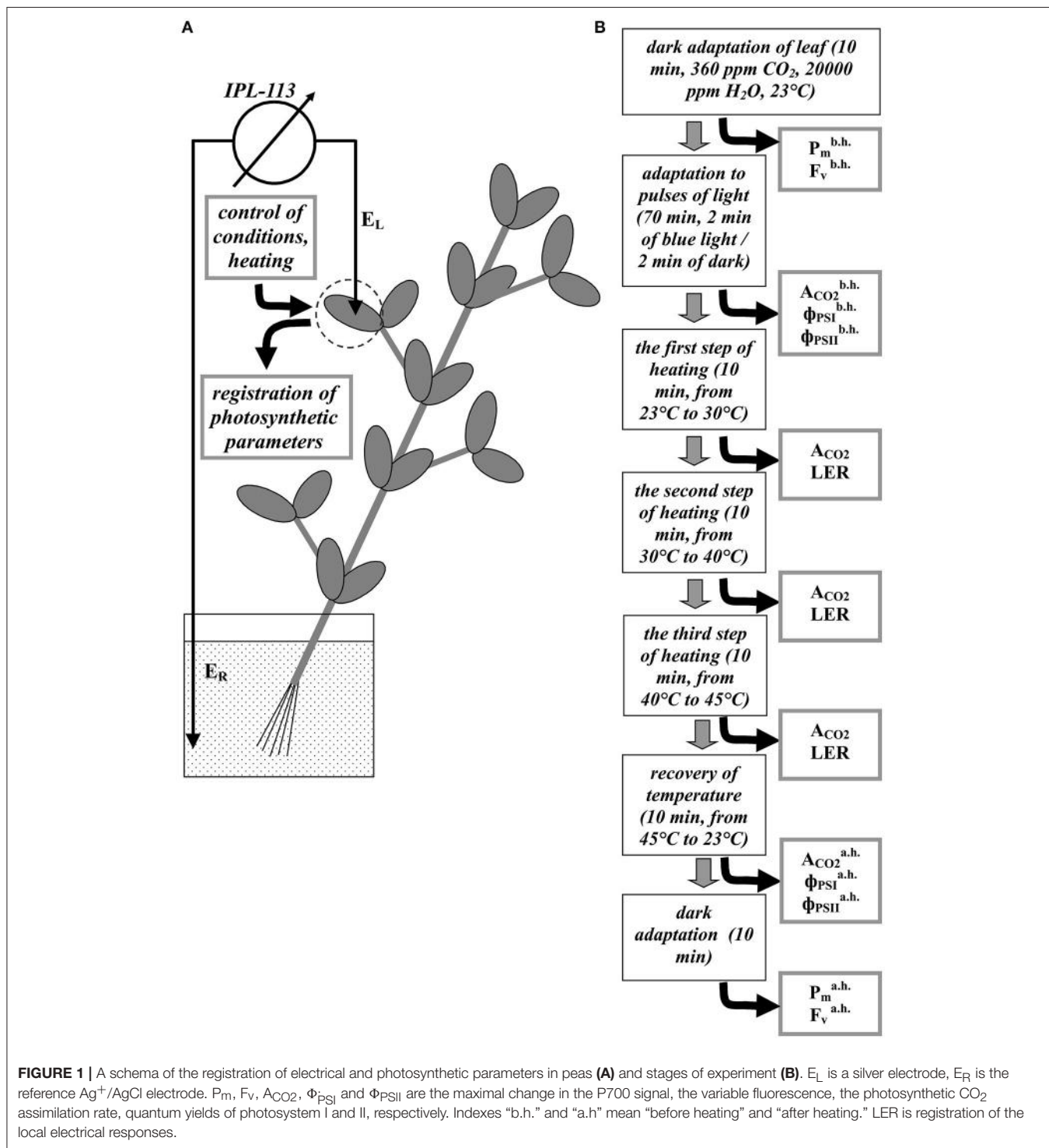


**FIGURE 1 |** A schema of the registration of electrical and photosynthetic parameters in peas (A) and stages of experiment (B).  $E_L$  is a silver electrode,  $E_R$  is the reference  $\text{Ag}^+/\text{AgCl}$  electrode.  $P_m$ ,  $F_v$ ,  $A_{\text{CO}_2}$ ,  $\Phi_{\text{PSI}}$  and  $\Phi_{\text{PSII}}$  are the maximal change in the P700 signal, the variable fluorescence, the photosynthetic  $\text{CO}_2$  assimilation rate, quantum yields of photosystem I and II, respectively. Indexes "b.h." and "a.h." mean "before heating" and "after heating." LER is registration of the local electrical responses.

Vodeneev et al., 2011, 2017). All electrodes were connected with a high-impedance ( $10^{12}$  Ohm) amplifier IPL-113 (Semico, Novosibirsk, Russia). Results of measurements were recorded (every 1 s) in a personal computer using a standard program of IPL-113 (param2). Plant adaptation before experiment was 70 min; the standard solution was not replaced.

## Measurements of Photosynthetic Parameters

A portable gas exchange measuring system GFS-3000 (Heinz Walz GmbH, Effeltrich, Germany), a measuring system for the simultaneous assessment of P700 oxidation and chlorophyll fluorescence Dual-PAM-100 (Heinz Walz GmbH), and a measuring head Cuvette 3010-Dual (Heinz Walz GmbH) were used to measure photosynthetic parameters and to control conditions in the second mature leaf (Figure 1A). The CO<sub>2</sub> concentration was 360 ppm; the relative humidity at 23°C was about 70%; temperature in the measuring head was varied (see below). We used pulses of actinic light (239  $\mu\text{mol m}^{-2} \text{s}^{-1}$ , 460 nm, 1 min); duration of dark interval between the pulses was 1 min. The durations of actinic light pulses and dark intervals were enough for stabilization of the CO<sub>2</sub> assimilation rate after transitions in the light regime.

The photosynthetic parameters were measured similarly with our previous works (Sukhov et al., 2014a,b, 2015a). The dark ( $F_0$ ) and maximal ( $F_m$ ) fluorescence yields and variable fluorescence ( $F_v$ ) (Maxwell and Johnson, 2000; Kalaji et al., 2012, 2014) were measured after the dark adaptation for 10 min (Sukhov et al., 2014b). The maximal change in the P700 signal ( $P_m$ ) of PSI, reflecting maximal P700 oxidation (Klughammer and Schreiber, 2008), was measured after the preliminary illumination by far red light for 10 s.

The steady-state ( $F$ ) and maximal ( $F'_m$ ) fluorescence yields in light (Maxwell and Johnson, 2000) and steady-state ( $P$ ) and maximal ( $P'_m$ ) P700 signals in light (Klughammer and Schreiber, 2008) were measured using saturation pulses (10,000  $\mu\text{mol m}^{-2} \text{s}^{-1}$ , 630 nm, 300 ms). The saturation pulses were generated before the end of the each pulse of actinic light. A quantum yield of PSI ( $\Phi_{\text{PSI}}$ ) was calculated using the equation  $\phi_{\text{PSI}} = (P'_m - P)/P_m$  (Klughammer and Schreiber, 2008); an effective quantum yield of PSII ( $\Phi_{\text{PSII}}$ ) was calculated using the equation  $\phi_{\text{PSII}} = (F'_m - F)/F'_m$  (Maxwell and Johnson, 2000). All parameters were programmatically calculated by software of Dual-PAM-100.

The photosynthetic CO<sub>2</sub> assimilation rate ( $\mu\text{mol CO}_2 \text{ m}^{-2} \text{ s}^{-1}$ ) was measured using the GFS-3000 system. Its software programmatically calculated the CO<sub>2</sub> assimilation rate according to Von Caemmerer and Farquhar (1981). We calculated photosynthetic CO<sub>2</sub> assimilation rate ( $A_{\text{CO}_2}$ ) as the difference between the CO<sub>2</sub> assimilation rate under light conditions and one under dark conditions for the each pulse of actinic light.

The Cuvette 3010-Dual was used for measuring of the air temperature and the leaf surface temperature in the measuring head.

## General Design of Experiment

A general design of experiment is shown in Figure 1B. First, leaves were adapted in dark, after which  $P_m^{\text{b.h.}}$  and  $F_v^{\text{b.h.}}$ , which were  $P_m$  and  $F_v$  before heating (parameters of undamaged plants), were measured. Later, after 70 min of light pulses  $A_{\text{CO}_2}^{\text{b.h.}}$ ,  $\Phi_{\text{PSI}}^{\text{b.h.}}$  and  $\Phi_{\text{PSII}}^{\text{b.h.}}$ , which were  $A_{\text{CO}_2}$ ,  $\Phi_{\text{PSI}}$ , and  $\Phi_{\text{PSII}}$  before heating (parameters of undamaged plants), were measured. Three transitions of temperature were performed after that: from 23 to 30°C, from 30 to 40°C, and from 40 to 45°C; the duration of the each transition was 10 min. Magnitudes of  $A_{\text{CO}_2}$  were measured at the end of the each step of heating. After the stepped heating, temperature was recovered to 23°C (10 min); residual  $A_{\text{CO}_2}^{\text{a.h.}}$ ,  $\Phi_{\text{PSI}}^{\text{a.h.}}$  and  $\Phi_{\text{PSII}}^{\text{a.h.}}$ , which were  $A_{\text{CO}_2}$ ,  $\Phi_{\text{PSI}}$ , and  $\Phi_{\text{PSII}}$  after heating (parameters of damaged plants), were measured after the recovery. Residual  $P_m^{\text{b.h.}}$  and  $F_v^{\text{b.h.}}$ , which were  $P_m$  and  $F_v$  after heating (parameters of damaged plants), were measured after 10 min of the dark adaptation at 23°C. LERs were registered during the each step of the heating.

It should be noted that we preliminary investigated the residual photosynthetic CO<sub>2</sub> assimilation in variants with one temperature transition (from 23 to 30°C), with two temperature transitions (from 23 to 30°C and from 30 to 40°C), and with three temperature transitions (from 23 to 30°C, from 30 to 40°C, and from 40 to 45°C). It was shown that  $A_{\text{CO}_2}^{\text{a.h.}}$  was not distinguished from  $A_{\text{CO}_2}^{\text{b.h.}}$  in variant with temperature recovery after one step of heating; decrease of this residual assimilation was not significant after two temperature transitions (the relative  $A_{\text{CO}_2}^{\text{a.h.}}$  was  $88 \pm 5\%$ ,  $n = 6$ ,  $p > 0.05$ ); significant decrease of  $A_{\text{CO}_2}^{\text{a.h.}}$  was only observed after three transitions (the relative  $A_{\text{CO}_2}^{\text{a.h.}}$  was  $65 \pm 4\%$ ,  $n = 9$ ,  $p < 0.05$ ). On basis of this result we concluded that only third temperature transition induced long-term damage of photosynthetic processes (suppression of photosynthetic assimilation was observed after the temperature recovery). This long-term damage is harmful for plant life and can decrease plant productivity; changes in magnitude of the damage reflect changes in plant thermotolerance. As a result variant with three steps of heating was only used in the subsequent work. The stepped heating was used as model of gradual changes in temperature which are observed under environmental conditions, because rate of the temperature increase by the measurement system can not be regulated.

The relative rate of the residual photosynthetic CO<sub>2</sub> assimilation and quantum yields of photosystem I and II after heating were used for estimation of a heating-induced suppression of photosynthesis. Residual relative  $P_m$ ,  $F_v$  and  $F_v/F_m$  were used for estimation of a heating-induced damage of photosystems I and II.

## Statistics

A separate seedling of pea was used for the each experiment with heating; the total number of plants was 40. Results of experiments were grouped according to different criteria (see Results). Quantities of repetitions in the groups are shown in the figures. Representative records, mean values, standard errors, scatter plots and correlation coefficients are presented in the figures.

## RESULTS

### A Heating-Induced Suppression of the Photosynthetic Assimilation of CO<sub>2</sub> in Leaves

First, we investigated suppression of the photosynthetic assimilation of CO<sub>2</sub> under stepped heating and following it (**Figure 2**). It was shown that the temperature transition from 23 to 30°C induced a slight decrease of A<sub>CO<sub>2</sub></sub> (about 11%); the transition from 30 to 40°C caused a moderate suppression of the photosynthetic CO<sub>2</sub> assimilation (about 31%); the last heating step strongly suppressed the assimilation (about 45%). A<sub>CO<sub>2</sub></sub> was increased with decrease of air temperature (about 5 min); after that it was approximately constant. After recovery of temperature (10 min) residual A<sub>CO<sub>2</sub></sub> were lower than the control value; the decrease was about 32%.

The stepped heating induced suppression of photosynthesis; moreover, the small significant decrease of photosynthetic assimilation of CO<sub>2</sub> was observed even under the heating from 23 to 30°C. As a result, each temperature transition of the stepped heating decreases photosynthetic activity; the stepped heating can thus be used in a further analysis.

### Local Electrical Responses in Leaves Induced by Stepped Heating in Peas

Analysis of the dynamics of the surface electrical potential showed that the stepped heating induced generation of LERs in most of the experiments (in 37 experiments out of 40 or 92.5%). **Figure 3** showed various dynamics of the surface potential: without LERs (**Figure 3A**) and with one (**Figure 3B**), two (**Figure 3C**) and three (**Figure 3D**) LERs. LERs were transient depolarizations; its average amplitude was 10 ± 1 mV, duration in most of the variants was more than 10 min. Amplitudes of LERs, induced by different temperature transitions, were not significantly differed. High variability of LERs amplitude

was similar with high variability of VP which is considered as LER induced by hydraulic and/or chemical signals (Vodeneev et al., 2015). In investigation of VP, variability of its parameters simplified analysis of connection between these parameters and parameters of physiological responses (Sukhov et al., 2012, 2014b; Surova et al., 2016a); as a result variability of LERs amplitude can simplify analysis of connection between the amplitude and pea thermotolerance.

It should be noted that the stepped heating also induced hyperpolarization (increase of the surface potential), which was the most expressive in peas without LERs or with one LER. In contrast, the effect was practically absent in peas with two or three LERs. It is probable that this hyperpolarization reflected temperature activation of H<sup>+</sup>-ATPase in the plasma membrane, because the maximal temperature of the leaf surface was about 40.5°C (under 45°C of air temperature in the measuring head) and optimum temperature of the H<sup>+</sup>-ATPase activity was 35–43°C (Briskin and Poole, 1983; Dupont and Mudd, 1985; Brauer et al., 1991).

**Table 1** summarizes variants of appearance of LERs at different steps of the heating. It was shown that the first temperature transition (from 23 to 30°C) induced the first LER in many experiments (45%). The second temperature transition (from 30 to 40°C) induced the first LER in 42.5% of experiments. The third temperature transition (from 40 to 45°C) induced the first LER in 5% of experiments. These results show that LER can be generated under weak or moderate heating, which is in physiological ranges and slightly suppresses photosynthesis.

**Figure 4** shows correlations (i) between the suppression of photosynthetic CO<sub>2</sub> assimilation during the first temperature transition and the amplitude of LER during this transition (**Figure 4A**), (ii) between the suppression of CO<sub>2</sub> assimilation during the second temperature transition and the amplitude of LER during this transition (**Figure 4B**), and (iii) between the suppression of CO<sub>2</sub> assimilation during the third temperature transition and the amplitude of LER during this transition (**Figure 4C**) (the method of measurement of amplitudes is shown in **Figure 3**). All correlations were weak, i.e., the photosynthetic damage throughout all time of the temperature increase was not connected with amplitudes of LERs. In particular, this result showed that photosynthetic suppression was not probable to induce LERs under heating.

### Analysis of Connection of the Residual Photosynthetic CO<sub>2</sub> Assimilation after Heating with Parameters of Local Electrical Responses in Leaves

The residual photosynthetic CO<sub>2</sub> assimilation after temperature recovery to 23°C (in 10 min after heating) can reflect a long-term damage of photosynthesis during heating, a secondary damage of photosynthesis after heating (particularly, damage induced by increased production of reactive oxygen species) and activity of fast reparation processes of photosynthesis. **Figure 5A** shows that the quantity of LERs during the stepped heating was connected with the relative rate of the residual photosynthetic CO<sub>2</sub> assimilation after heating: the small rate (60%) was in

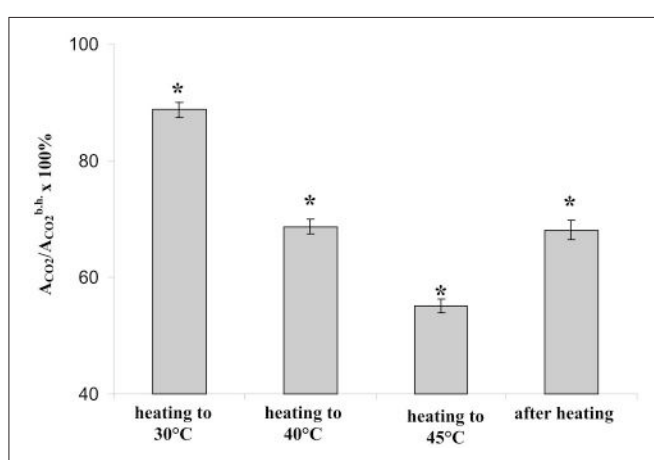


**FIGURE 2 |** The relative photosynthetic assimilation of CO<sub>2</sub> at transitions of temperature from 23 to 30°C, from 30 to 40°C, and from 40 to 45°C and after recovery of temperature from 45 to 23°C ( $n = 40$ ). Duration of steps of heating and recovery of temperature were 10 min; A<sub>CO<sub>2</sub></sub> were measured at the end of each time interval. \* $p < 0.05$  compared with 100%, Student *t*-test.

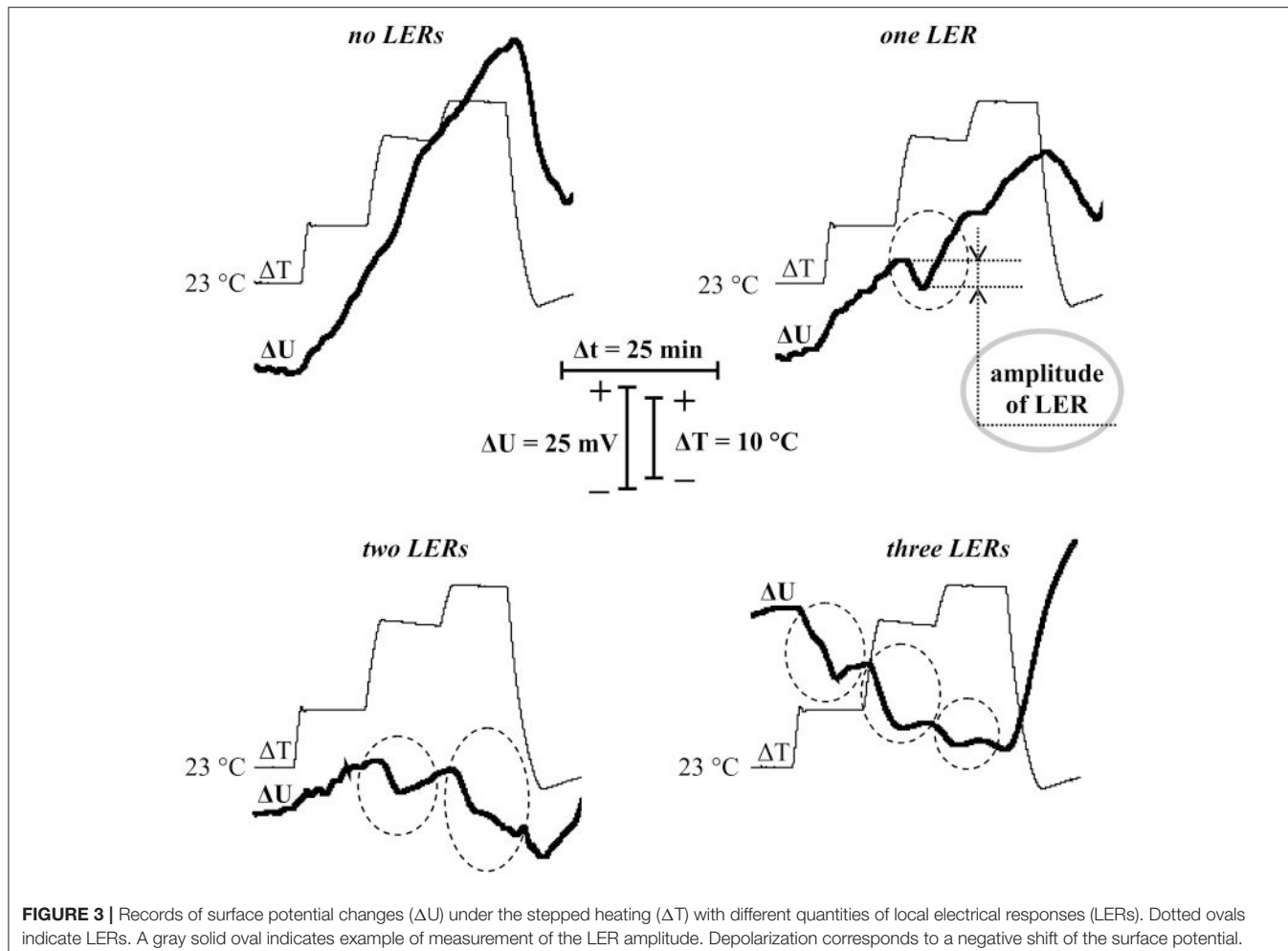


**TABLE 1 |** Distribution of LERs induced by different temperature transitions.

LERs were observed under 1st temperature transition (from 23 to 30°C)		LERs were not observed under 1st temperature transition (from 23 to 30°C)		LERs were observed under 2nd temperature transition (from 30 to 40°C)		LERs were not observed under 2nd temperature transition (from 30 to 40°C)	
LERs were observed under 2nd temperature transition (from 30 to 40°C)	LERs were not observed under 2nd temperature transition (from 30 to 40°C)	LERs were observed under 2nd temperature transition (from 30 to 40°C)	LERs were not observed under 2nd temperature transition (from 30 to 40°C)	LERs were observed under 3rd temperature transition (from 40 to 45°C)	LERs were not observed under 3rd temperature transition (from 40 to 45°C)	LERs were observed under 3rd temperature transition (from 40 to 45°C)	LERs were not observed under 3rd temperature transition (from 40 to 45°C)
10 (25%)	0 (0%)	11 (27.5%)	2 (5%)				
5 (12.5%)	3 (7.5%)	6 (15%)	3 (7.5%)				

the group without LERs or with one response, the moderate rate (70%) was in the group with two LERs, and the high rate (78%) was in the group with three LERs. Analysis of connection of the heating-induced suppression of the photosynthetic  $\text{CO}_2$  assimilation with the number of the temperature transition, which induced the first generation of LER (the number was qualitatively connected with the heating threshold for generation of the electrical response) showed a similar result (Figure 5B): the relative rate of the residual photosynthetic  $\text{CO}_2$  assimilation

after heating was maximal (71%) in the group with generation of the first LER at the first temperature transition, and it was minimal (58%) in the group with generation of the first LER at the third temperature transition or without generation of the electrical response. Figure 5C shows that the average amplitude of LER was significantly correlated with the relative rate of the residual photosynthetic  $\text{CO}_2$  assimilation after heating. It should be noted that plants without LERs were not separately analyzed because their quantity was small ( $n = 3$ ); however, the average

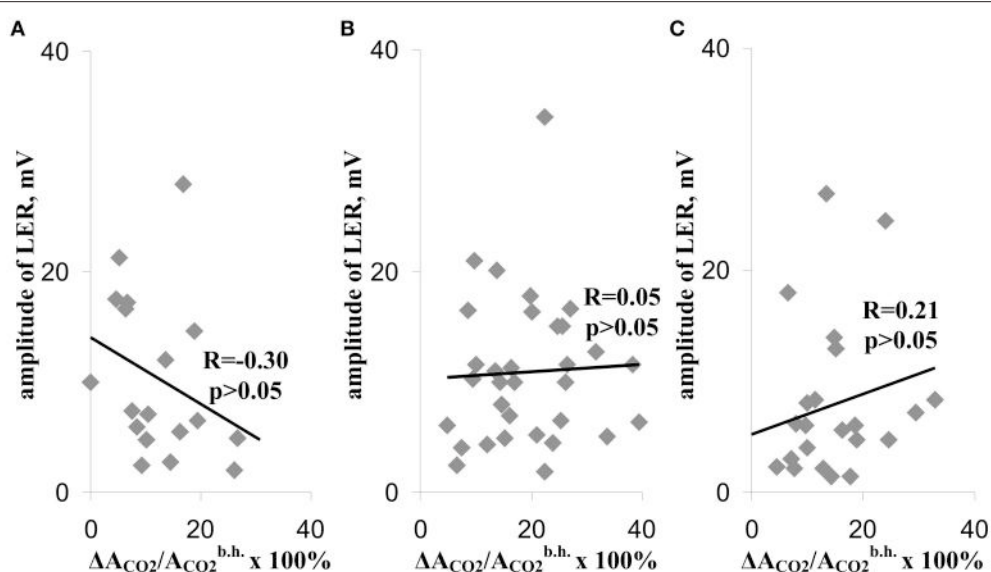


**FIGURE 4 |** Scatter plots between amplitudes of LERs and relative decreases of the photosynthetic assimilation of  $\text{CO}_2$ , which were observed during the different temperature transitions **(A–C)**. **(A)** During the temperature transition from 23 to 30°C. **(B)** During the temperature transition from 30 to 40°C. **(C)** During the temperature transition from 40 to 45°C. The group with LER observed during the 1st transition included 18 peas ( $n = 18$ ), the group with LER observed during the 2nd transition included 32 peas ( $n = 32$ ), and the group with LER observed during the 3rd transition included 23 peas ( $n = 23$ ). Individual amplitudes of LERs for each temperature transition in each plant were used. The relative decreases of the photosynthetic assimilation of  $\text{CO}_2$  ( $\Delta A_{\text{CO}_2}/A_{\text{CO}_2}^{\text{b.h.}} \times 100\%$ ) were also calculated for each temperature transition in each plant. R is Pearson's correlation coefficient.

residual photosynthetic assimilation of  $\text{CO}_2$  after heating was 55  $\pm$  3% in these plants, and it was lower than residual assimilation in plants with LERs (Figure 5).

These results show that residual photosynthetic activity after heating in pea leaves was strongly connected with parameters of heating-induced LERs. In consideration of absence of correlation between amplitudes of LERs and photosynthetic  $\text{CO}_2$  assimilation during the heating (Figure 4), parameters of LERs were strongly connected with the plant tolerance to the secondary damage of photosynthesis after heating and/or the activity of fast reparation processes of photosynthesis. Both the decreased secondary photosynthetic damage and the increased fast reparation of photosynthesis promote increased total photosynthetic thermotolerance in plant. However, the connection can be potentially caused by distinct physiological states of peas in the investigated group. As a result, in next section of work we analyzed the connection of parameters of LERs and the residual photosynthetic activity after heating in leaves with the initial rate of the photosynthetic assimilation of  $\text{CO}_2$ , i.e., with  $\text{CO}_2$  assimilation before heating.

## Analysis of the Connection of Local Electrical Response Parameters and Photosynthesis Thermotolerance with the Initial Rate of $\text{CO}_2$ Assimilation in Leaves

We used the initial rate of the photosynthetic  $\text{CO}_2$  assimilation in leaves (the assimilation before heating) as parameter which reflected the initial state of photosynthesis in different peas. Figure 6A shows that value of the initial rate of the

photosynthetic  $\text{CO}_2$  assimilation in leaves was not connected with the residual relative  $A_{\text{CO}_2}$  after heating (correlation was weak and was not significant), i.e., the thermotolerance of photosynthesis was not dependent on this initial rate of assimilation before heating. It should be additionally noted that Figure 6A shows that non-linear dependences (even, dependences with several extremes) between initial photosynthetic  $\text{CO}_2$  assimilation and the relative residual assimilation are not probable too.

In contrast, the average amplitude (Figure 6B) and the quantity of LERs during the stepped heating (Figure 6C) were significantly correlated with the initial rate of the photosynthetic  $\text{CO}_2$  assimilation. However, the correlation coefficients (0.37 and 0.44) were low; they were less than the coefficient of correlation between the average LER amplitude and the relative  $A_{\text{CO}_2}$  after heating (0.76). The connection of the initial rate of the photosynthetic  $\text{CO}_2$  assimilation with the number of the temperature transition, which induced the first LER, was not significant (Figure 6D). Thus, the photosynthesis thermotolerance in leaves was not connected with the initial photosynthetic activity; the connection of parameters of LERs with this activity was weak.

## Analysis of the Connection of Residual Parameters of Photosynthetic Light Reactions after Heating with Parameters of Local Electrical Responses in Leaves

Figure 7 shows that relative value of the residual effective ( $\Phi_{\text{PSI}}^{\text{a.h.}}/\Phi_{\text{PSI}}^{\text{b.h.}}$ ) and maximal ( $[F_v/F_m]^{\text{a.h.}}/[F_v/F_m]^{\text{b.h.}}$ ) quantum

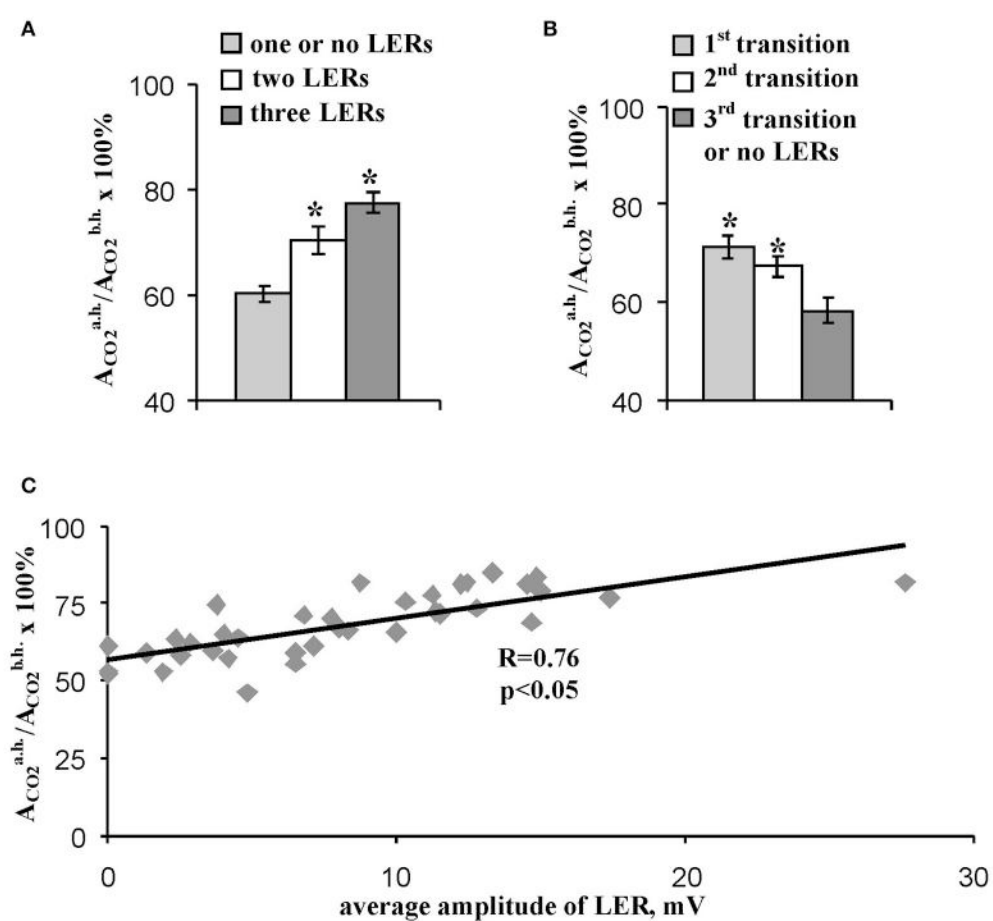


**FIGURE 5 |** Connection of the relative residual photosynthetic assimilation of  $\text{CO}_2$  after heating with parameters of LERs. **(A)** The residual  $\text{CO}_2$  assimilation after heating in peas with different quantities of LERs during stepped heating. The group with three LERs included 10 peas ( $n = 10$ ), the group with two LERs included 16 peas ( $n = 16$ ), and the group with one or no LERs included 14 peas ( $n = 14$ ). \* $p < 0.05$  compared with parameters in the group with one or no LERs, Student *t*-test. **(B)** The residual  $\text{CO}_2$  assimilation after heating in peas with different numbers of temperature transition, which induced the first generation of LER during the stepped heating. The group with the first LER induced by the 1<sup>st</sup> transition included 18 peas ( $n = 18$ ), the group with the first LER induced by the 2<sup>nd</sup> transition included 16 peas ( $n = 16$ ), and the group with the first LER induced by the 3<sup>rd</sup> transition or without LERs included 5 peas ( $n = 5$ ). \* $p < 0.05$  compared with parameters in the group with the first LER induced by the 3<sup>rd</sup> transition or without LERs, Student *t*-test. **(C)** Scatter plots between the average amplitude of LER during stepped heating and the relative residual photosynthetic assimilation of  $\text{CO}_2$  after heating ( $n = 40$ ). The average amplitude of LER was calculated for each plant. It has been assumed that the average amplitude equaled zero when LERs were absent in the plant.  $R$  is Pearson's correlation coefficient.

yields of photosystem II after heating were significantly correlated with the average amplitude of LER (0.63 and 0.49). However, the correlations were moderate; i.e., the linear connection between these parameters was not very expressive. Other investigated parameters of photosynthetic light reactions, including  $\Phi_{\text{PSI}}^{\text{a.h.}} / \Phi_{\text{PSI}}^{\text{b.h.}}$ ,  $P_m^{\text{a.h.}} / P_m^{\text{b.h.}}$ , and  $F_v^{\text{a.h.}} / F_v^{\text{b.h.}}$ , were not connected with the average amplitude of LER. **Figure 8** supports connection of the relative effective ( $\Phi_{\text{PSI}}^{\text{a.h.}} / \Phi_{\text{PSI}}^{\text{b.h.}}$ ) and maximal ( $[F_v/F_m]^{\text{a.h.}} / [F_v/F_m]^{\text{b.h.}}$ ) quantum yields of photosystem II after heating with parameters of LERs: an increase of these parameters was connected with an increase in the quantity of LERs during the stepped heating (**Figure 8A**) and with a decrease in the number of the temperature transition, which induced the first generation of LER (**Figure 8B**). The result shows that thermotolerance of photosystem II (probably, the photosystem

II tolerance to the secondary damage after heating and/or the activity of fast reparation processes in this photosystem) was connected with parameters of LERs in leaves.

### Analysis of the Connection of Residual Photosynthetic Parameters after Heating with Amplitudes of Local Electrical Responses Induced by Different Temperature Transitions

**Figure 9** shows that the relative residual photosynthetic  $\text{CO}_2$  assimilation after heating was strongly correlated with the amplitudes of LERs induced by the first and second steps of heating; however, the correlation was absent for LERs induced by the third temperature transition. Residual parameters of

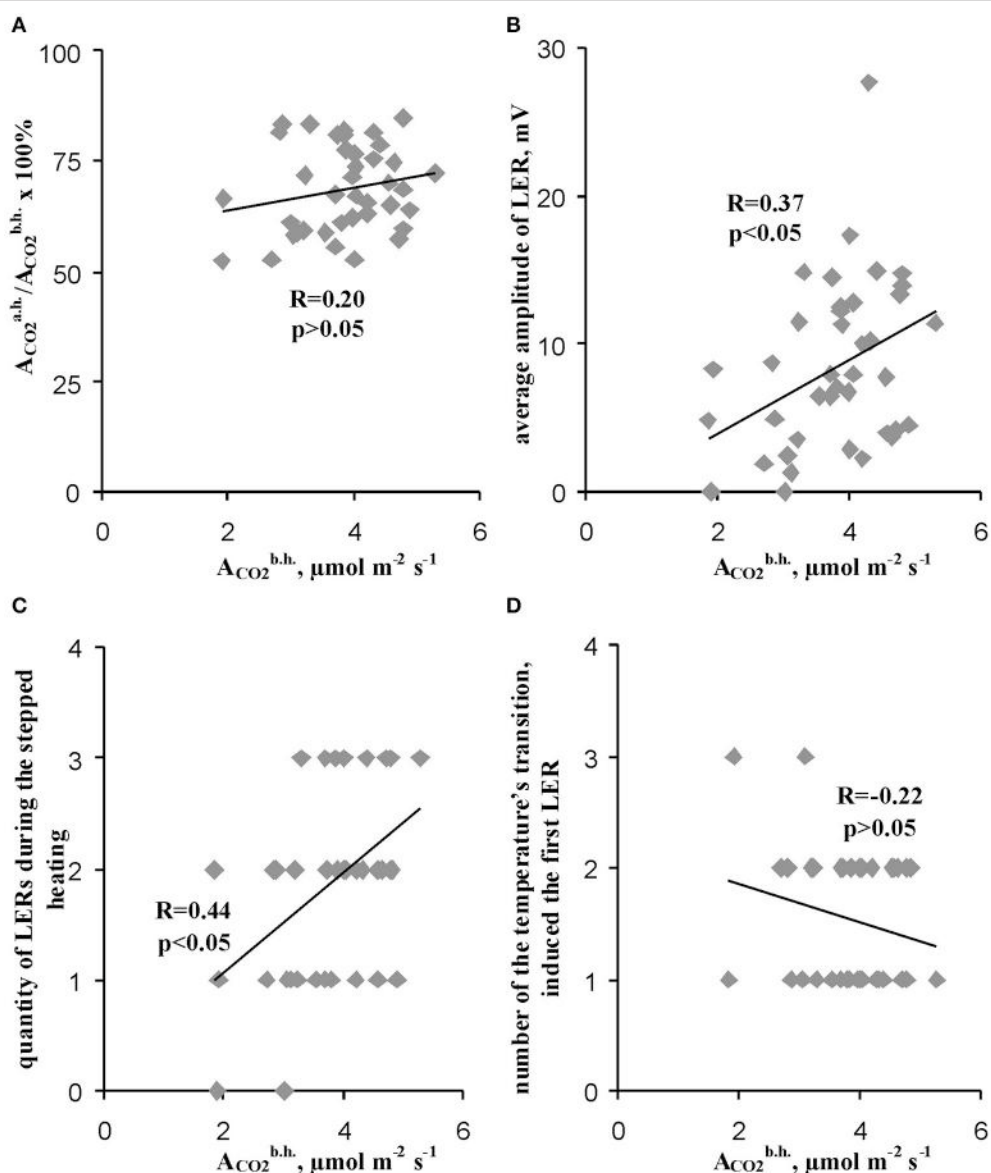


**FIGURE 6 |** Connections of the relative residual photosynthetic assimilation of CO<sub>2</sub> after heating (A) and parameters of LERs (B–D) with the rate of photosynthetic assimilation of CO<sub>2</sub> before heating. (A) Scatter plots between the relative residual photosynthetic assimilation of CO<sub>2</sub> after heating and the rate of photosynthetic assimilation of CO<sub>2</sub> before heating ( $n = 40$ ). (B) Scatter plots between the average amplitude of LER during the stepped heating and the rate of photosynthetic assimilation of CO<sub>2</sub> before heating ( $n = 40$ ). (C) Scatter plots between the quantity of LERs during the stepped heating and the rate of photosynthetic assimilation of CO<sub>2</sub> before heating ( $n = 40$ ). (D) Scatter plots between the number of temperature transition, which induced the first generation of LER during the stepped heating, and the rate of the photosynthetic assimilation of CO<sub>2</sub> before heating ( $n = 37$ , experiments without LERs were not included). The average amplitude of LER was calculated for each plant during the stepped heating. It has been assumed that the average amplitude equaled zero when LERs were absent in the plant. R is Pearson's correlation coefficient.

photosystem II after heating were maximally correlated with the amplitudes of LERs induced by the first step of heating; these correlations were weak for LERs induced by the second temperature transition; it was absent for LERs induced by the third one. The result shows that connection between LERs and photosynthetic thermotolerance (the tolerance to the secondary damage after heating and/or the activity of fast reparation

processes of photosynthesis) was stronger for early electrical responses.

## DISCUSSION

A number of studies (Retivin et al., 1997, 1999; Sukhov et al., 2014b, 2015b; Surova et al., 2016b) show a positive influence of

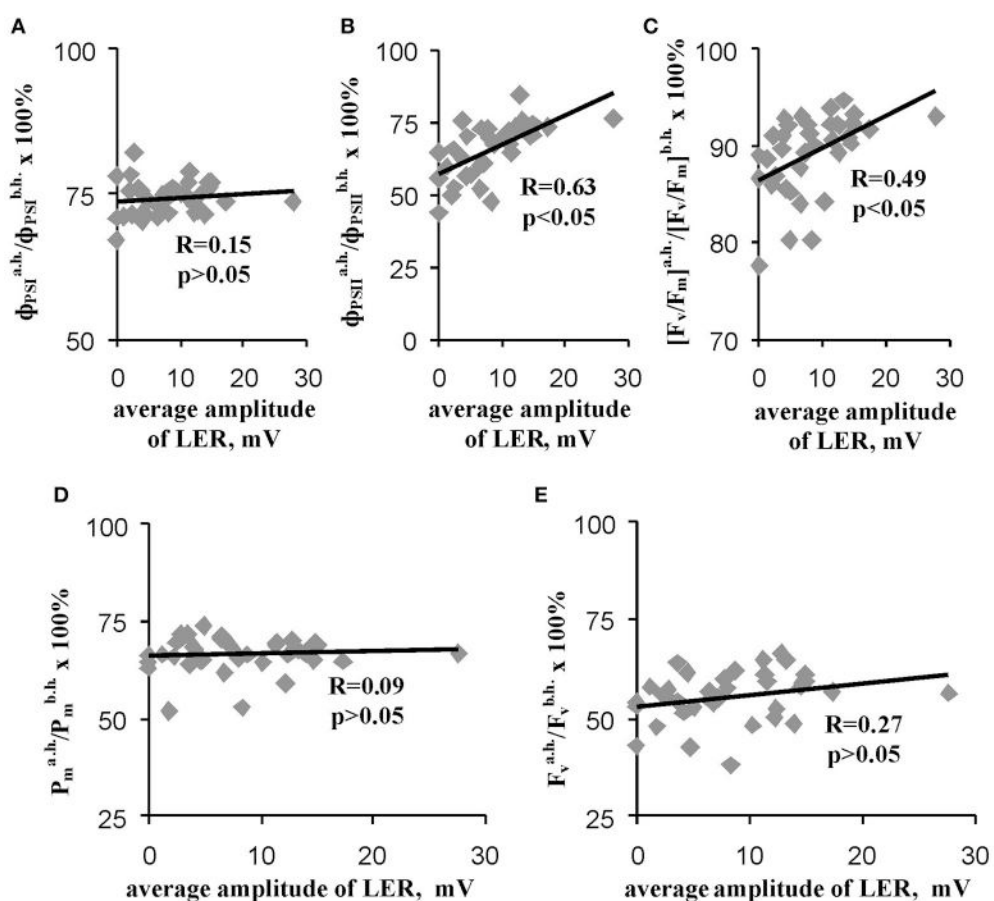


**FIGURE 7 |** Scatter plots between average amplitudes of LER and relative quantum yields of photosystems I (A) and II (B), the relative maximal quantum yield of photosystem II (C) and relative quantities of undamaged photosystems I (D) and II (E) after heating ( $n = 40$ ). The average amplitude of LER was calculated for the each plant during the stepped heating. It has been assumed that the average amplitude equaled zero when LERs were absent in the plant. R is Pearson's correlation coefficient.

electrical signals, including VP, on plant tolerance to negative changes in temperature. Considering the similarity between mechanisms of LERs and mechanisms of the generation of VP (Vodeneev et al., 2015, 2016), it can not be excluded that LERs can also influence the tolerance of plants to heating and chilling. The connection of the generation of LERs under chilling with tolerance of plants to low temperatures was shown in some studies (Opritov et al., 1993, 1994); however, the connection of parameters of heating-induced LERs with the thermotolerance of plants was not investigated.

There are two important questions in this problem. First, we previously showed that VP increased the thermotolerance of photosystem I and the whole plant (Sukhov et al., 2014b, 2015b; Surova et al., 2016b). However, VP was caused by the damaging thermal stimulus (burn), which is a standard stimulus for the induction of this electrical signal (Hlaváčková et al., 2006; Grams et al., 2009; Katicheva et al., 2014; Vodeneev et al., 2015). Thus, the first important question is “Can electrical responses be generated under physiological heating?” Our previous results (Vodeneev et al., 2017) showed that heating to 52°C induced

propagation of VP. Results of the current work showed that even the slight heating to 30°C (the temperature of the leaf surface was about 28.9°C) induced generation of electrical responses in the heated zone in 45% of peas; after second heating to 40°C (temperature of leaf surface was about 37.1°C), the first LER were observed in 42.5% of peas (Figure 3, Table 1). This result means that heating-induced LERs can be induced under slightly increased temperatures. It is unlikely that these LERs were local action potentials or voltage transients; because action potential and voltage transients have high amplitudes, additionally, action potential has an all-or-none characteristic (Krol and Trebacz, 1999). The revealed LERs were rather similar with receptor potentials with low amplitudes (Krol and Trebacz, 1999) and different mechanisms of generation (Pyatygina et al., 1992; Shimmen, 1997; Pyatygina, 2004; Opritov et al., 2005).

The mechanism of revealed LERs requires additional investigation; it is unlikely that it is connected with temperature-dependent damage of H<sup>+</sup>-ATPase in the plasma membrane because temperature optimum of the enzyme is 35–43°C (Briskin and Poole, 1983; Dupont and Mudd, 1985; Brauer et al.,

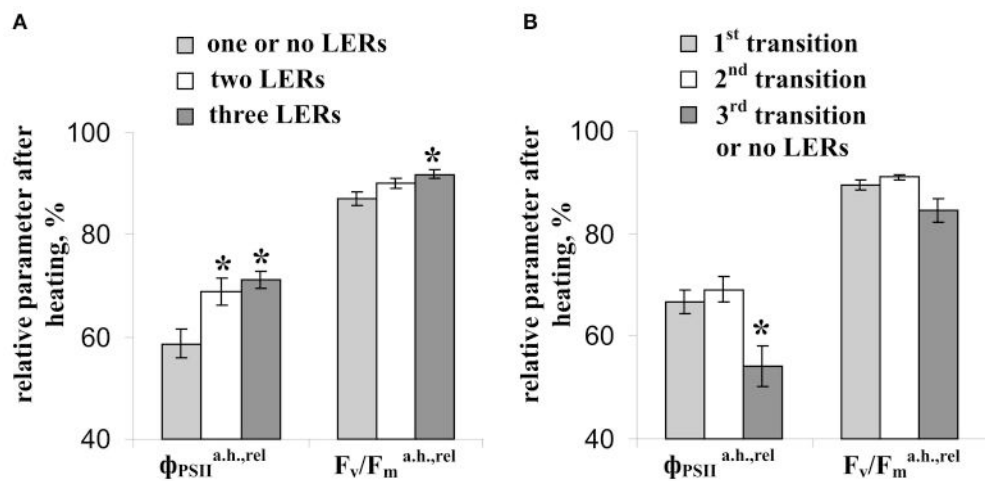


**FIGURE 8 |** Connection of the relative effective ( $\Phi_{PSII}^{a.h.,rel}$ ) and maximal ( $F_v/F_m^{a.h.,rel}$ ) quantum yields of photosystem II after heating with parameters of LERs. **(A)** The relative residual effective and maximal quantum yields of photosystem II after heating in peas with different quantities of LERs during the stepped heating. The group with three LERs included 10 peas ( $n = 10$ ), the group with two LERs included 16 peas ( $n = 16$ ), and the group with one or no LERs included 14 peas ( $n = 14$ ). \* $p < 0.05$  compared with parameters in the group with one or no LERs, Student *t*-test. **(B)** The relative residual effective and maximal quantum yields of photosystem II after heating in peas with a different number of temperature transition, which induced the first generation of LER during the stepped heating. The group with the first LER induced by the 1<sup>st</sup> transition included 18 peas ( $n = 18$ ), the group with the first LER induced by the 2<sup>nd</sup> transition included 16 peas ( $n = 16$ ), and the group with the first LER induced by the 3<sup>rd</sup> transition or without LERs included 5 peas ( $n = 5$ ). \* $p < 0.05$  compared with parameters in the group with the first LER induced by the 3<sup>rd</sup> transition or without LERs, Student *t*-test.

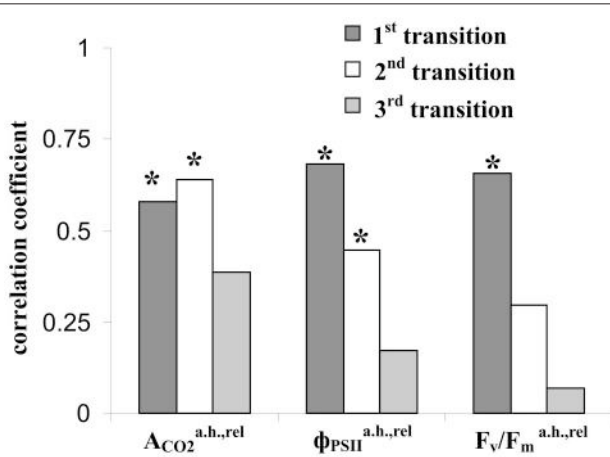


**FIGURE 9 |** Coefficients of correlation of amplitudes of LERs, induced by different temperature transitions, with the relative residual photosynthetic assimilation of  $CO_2$  ( $A_{CO_2}^{a.h.,rel}$ ), effective ( $\Phi_{PSII}^{a.h.,rel}$ ) and maximal ( $F_v/F_m^{a.h.,rel}$ ) quantum yields of photosystem II after heating. The group with LER observed during the 1<sup>st</sup> transition included 18 peas ( $n = 18$ ), the group with LER observed during the 2<sup>nd</sup> transition included 32 peas ( $n = 32$ ), and the group with LER observed during the 3<sup>rd</sup> transition included 23 peas ( $n = 23$ ). Individual amplitudes of LERs for each temperature transition in each plant were used. \*The correlation coefficient is significant.

1991). The decrease in photosynthetic  $CO_2$  assimilation, which is observed in our experiments (Figure 2), is also unlike the mechanism of generation of LERs, because their amplitudes are not correlated with magnitudes of this decrease (Figure 4). On the other hand, the influence of increased temperature can be connected with changes in the plasma membrane conductivity

(Brauer et al., 1991). In particular, Saidi et al. (2009) showed that a temperature increase to 28 and 32°C activates  $Ca^{2+}$  channels in moss plants; moreover, a temperature increase to 38°C induces transient increase of cytoplasmic  $Ca^{2+}$  concentration in the range of minutes after initiation of heating, and the response continues for at least 20 min. This long-term increase of  $Ca^{2+}$  concentration is in a good accordance with simulated dynamics of calcium ions during VP, which causes inactivation of  $H^+$ -ATPase in the plasma membrane (Sukhov et al., 2013; Sukhova et al., 2017), and with stimuli-induced propagating  $Ca^{2+}$  waves (Choi et al., 2014; Kiep et al., 2015), which is possible to be also connected with generation of VP. Thus, we can speculate that LERs, induced by the stepped heating, can be connected with  $Ca^{2+}$  influx and a decrease in  $H^+$ -ATPase activity.

The second question is “Is heating LERs connected with thermotolerance of plants?” Our results showed that parameters of heating-induced LERs (amplitudes, quantity of electrical responses, temperature threshold) were significantly connected with the residual photosynthetic  $CO_2$  assimilation (Figures 5, 9) and effective and maximal quantum yields of photosystem II (Figures 7–9) after heating; i.e., the tolerance of dark reactions of photosynthesis and light reactions in photosystem II to the increased temperature was linked to electrical responses. Probably, this increased tolerance can be connected with decrease of the secondary damage of photosynthetic processes and/or with activation of the fast photosynthetic reparation after heating because the photosynthetic  $CO_2$  assimilation during the heating, which reflected primary photosynthetic suppression, was not connected with parameters of LERs. The supposition is in a good accordance with literature data; in particular, electrical signals stimulated photosynthetic reparation processes (Retivin

et al., 1999; Surova et al., 2016b) and LERs induced recovery of the membrane potential (Opritov et al., 1993). In contrast, the thermotolerance of photosystem I was not connected with the parameters of LERs.

The connection between parameters of LERs and photosynthetic thermotolerance can be explained using three hypotheses: (i) Increase of the photosynthetic damage suppresses the generation of LERs; (ii) Generation of LERs decreases the photosynthetic damage; and (iii) Stimulation of generation of LERs and decrease of the photosynthetic damage do not interact, but they reflect a third unknown process. The first hypothesis is unlikely because correlation between suppression of photosynthesis and parameters of LERs was absent during any temperature transitions (**Figure 4**). Moreover, inactivation of photosynthesis can rather stimulate depolarization (decrease of photosynthetic activity induces depolarization of the plasma membrane potential e.g., Miedema and Prins, 1993). Thus, the connection between residual photosynthetic parameters after heating and parameters of LERs can not be caused by photosynthetic suppression during heating.

Our results definitely do not support the second or third hypothesis; however, there are some points of benefit of the second one. Firstly, the first LER was often generated during the first temperature transition from 23 to 30°C (45% of experiments, **Table 1**); i.e., their generation preceded the main thermal damage of photosynthesis (temperature transitions from 30 to 40°C and, especially, 40 to 45°C, **Figure 2**). Additionally, amplitudes of this “early” LERs induced by the first temperature transitions were significantly correlated (0.58–0.68) with the residual photosynthetic CO<sub>2</sub> assimilation and quantum yields of photosystem II after heating (**Figure 9**).

Second, the connection of the amplitudes of LERs induced by different temperature transitions with residual photosynthetic parameters after heating was decreased with the increase of the transition number (**Figure 9**); in particular, LERs induced by the third temperature transition (which mainly suppressed photosynthesis, **Figure 2**) were not connected with residual photosynthetic activity after heating. The hypothesis about the positive influence of LERs on the photosynthetic thermotolerance can explain the result in case of development for 10–20 min of LER-induced increase of the thermotolerance. Two possible chains of events can occur: (i) LERs induced by the first or the second temperature transition → development of the increased photosynthetic thermotolerance (10–20 min) → the weak damage of photosynthesis under the third transition and the active photosynthetic reparation after heating, or (ii) LERs induced by the third temperature transition → the low photosynthetic thermotolerance (it had not time to increase) and strong damage of photosynthesis under the third transition. In this connection it should be also noted that a positive effect of electrical signals on plant tolerance to gradual cooling was developed in 15–25 min after stimulation (Retivin et al., 1997); the increased of photosynthetic thermotolerance was observed in 15 min after induction of VP (Sukhov et al., 2014b, 2015b) and action potential (Retivin et al., 1999). The alternative hypothesis requires several independent mechanisms of temperature influence on parameters of LERs

and photosynthetic thermotolerance. These mechanisms should explain (i) the similar influence of temperature on the residual photosynthetic CO<sub>2</sub> assimilation after heating and LERs, induced by transitions from 23 to 30°C or from 30 to 40°C, and absence of this similarity for LERs, induced by transition from 40 to 45°C, and (ii) the similar influence of temperature on residual quantum yields of photosystem II after heating and LERs, induced by transition from 23 to 30°C, and absence of this similarity for LERs, induced by transitions from 30 to 40°C or from 40 to 45°C. We can not exclude these possible mechanisms; however, the hypothesis about influence of LERs on the photosynthetic thermotolerance seems to be simpler.

Third, **Figures 6B,C** show that the initial rate of photosynthetic CO<sub>2</sub> assimilation was significantly connected with parameters of LERs. If the initial state of a pea independently influenced LERs parameters and photosynthetic thermotolerance, then it can be expected that the initial A<sub>CO<sub>2</sub></sub> would be significantly connected with the thermotolerance. However, the initial A<sub>CO<sub>2</sub></sub> before heating was not correlated with the relative residual photosynthetic CO<sub>2</sub> assimilation after heating (**Figure 6A**).

Additionally, many potential mechanisms of LER generation can be connected with mechanisms of tolerance to stressors, including photosynthetic tolerance; in particular, the Ca<sup>2+</sup> and H<sup>+</sup> influxes can stimulate different mechanisms of protection of photosynthetic machinery (Müller et al., 2001; Hochmal et al., 2015; Sukhov, 2016), and the K<sup>+</sup> efflux can participate in protection of the plasma membrane (Opritov et al., 1994). In particular, the indirect argument, which supports the hypothesis of LER influence on photosynthetic thermotolerance, is a modification of tolerance of photosynthetic processes induced by other electrical responses—propagating electrical signals (Sukhov, 2016). It is known that action potential can increase the tolerance of photosystem II to heating and cooling (Retivin et al., 1999), and VP increases thermotolerance of photosystem I (Sukhov et al., 2014b, 2015b; Surova et al., 2016b). These changes in photosynthetic thermotolerance are connected with photosynthetic responses, induced by electrical signals (Sukhov et al., 2014b; Sukhov, 2016). In particular, an increase in thermotolerance can be caused by electrical signal-induced stimulation of the cyclic electron flow (Sukhov et al., 2015a) and the non-photochemical quenching in photosystem II (Krupenina and Bulychev, 2007; Pavlovic et al., 2011; Sukhov et al., 2012, 2014a, 2016). Both processes decrease production of reactive oxygen species and, thereby, increase tolerance to secondary photosynthetic damage (Roach and Krieger-Liszkay, 2014; Sukhov, 2016). Also, electrical signals induce an increase in ATP content in leaves and stem (Sukhov, 2016; Surova et al., 2016a), which can participate in reparation of photosystem II after damage (Allakhverdiev et al., 2005a,b, 2008). Influence of electrical signals on photosynthetic thermotolerance can be also connected with other physiological processes including changes in a stomata opening (Sukhov et al., 2015b), which can be regulated by electrical signals (Grams et al., 2009; Sukhov et al., 2012, 2015b). It should be additionally noted that time of development of VP-induced changes in cyclic electron flow, the non-photochemical quenching in photosystem II, the ATP

content and the stomata opening was about 5–10 min after propagation of VP in peas (Sukhov et al., 2014b, 2015a; Surova et al., 2016a).

There are two potential mechanisms of initiation of photosynthetic responses in plants (Sukhov, 2016), including electrical signals-induced increase of the cyclic electron flow and the non-photochemical quenching. The first is  $\text{Ca}^{2+}$  influx, which participates in the generation of action potential and VP (Sukhov and Vodeneev, 2009; Vodeneev et al., 2015), and increases the concentration of calcium ions in cytoplasm. According to a hypothesis of Krupenina and Bulychev (2007)  $\text{Ca}^{2+}$  transports to the stroma of chloroplasts and inactivates Calvin-Benson cycle enzymes. An alternative hypothesis considers the influx of  $\text{H}^+$  and changes in intra- and extracellular pH as the main mechanism of induction of photosynthetic responses (Sukhov, 2016). There are several potential ways that proton signals influence photosynthesis: (i) increased apoplastic pH can decrease  $\text{CO}_2$  flow to mesophyll cells and suppress photosynthetic dark reactions (Sherstneva et al., 2016a,b), which induces inactivation of light reactions (Pavlovic et al., 2011; Sukhov et al., 2012, 2014a); (ii) decreased pH in cytoplasm (Sukhov et al., 2014a) contributes to decreased pH in stroma and the lumen of chloroplasts (Sukhov et al., 2016), which affects photosynthetic light reactions, decreasing linear electron flow, increasing the non-photochemical quenching, and, probably, changing the location of the ferredoxin-NADP-reductase (Sukhov, 2016).

Thus, fluxes of  $\text{Ca}^{2+}$  and  $\text{H}^+$ , which are key participants in different types of LERs, including receptor potentials (Pyatygina et al., 1992; Shimmen, 1997; Pyatygina, 2004; Opritov et al.,

2005), voltage transients (Krol and Trebacz, 1999; Krol et al., 2004), and local action potentials (Krol et al., 2006; Trebacz et al., 2006; Beilby, 2007; Felle and Zimmermann, 2007), can induce responses of photosynthesis, which increases tolerance of photosynthetic machinery to increased temperatures (Sukhov et al., 2014b) and, possibly, stimulates its reparation (Surova et al., 2016a,b). Taken together, these results show that the positive influence of LERs on photosynthetic thermotolerance (the tolerance to the secondary damage after heating and/or the activity of fast reparation processes of photosynthesis) is a probably explanation of the connection between these electrical responses and tolerance to increased temperatures, which was shown in current work. However, the hypothesis requires further investigation, particularly, with using inhibitor analysis, methods of molecular biology, or genetical tools.

## AUTHOR CONTRIBUTIONS

VS: Design of experiment, analysis of data, preparation of manuscript; VG: Performance of experiments; SM: Participation in analysis of data; VV: Participation in analysis of data, participation in preparation of manuscript.

## FUNDING

This work was supported by the Ministry of Education and Science of the Russian Federation (contract no. 6.3199.2017/PCh) and the Russian Foundation for Basic Research (Project No. 16-34-00972 mol\_a).

## REFERENCES

- Allakhverdiev, S. I., Nishiyama, Y., Takahashi, S., Miyairi, S., Suzuki, I., and Murata, N. (2005a). Systematic analysis of the relation of electron transport and ATP synthesis to the photodamage and repair of photosystem II in *Synechocystis*. *Plant Physiol.* 137, 263–273. doi: 10.1104/pp.104.054478
- Allakhverdiev, S. I., Tsvetkova, N., Mohanty, P., Szalontai, B., Moon, B. Y., Debreczeny, M., et al. (2005b). Irreversible photoinhibition of photosystem II is caused by exposure of *Synechocystis* cells to strong light for a prolonged period. *Biochim. Biophys. Act.* 1708, 342–351. doi: 10.1016/j.bbabi.2005.05.006
- Allakhverdiev, S. I., Kreslavski, V. D., Klimov, V. V., Los, D. A., Carpenterier, R., and Mohanty, P. (2008). Heat stress: an overview of molecular responses in photosynthesis. *Photosyn. Res.* 98, 541–550. doi: 10.1007/s11120-008-9331-0
- Beilby, M. J. (2007). Action potential in Charophytes. *Int. Rev. Cytol.* 257, 43–82. doi: 10.1016/S0074-7696(07)57002-6
- Brauer, D., Loper, M., Schubert, C., and Tu, S. I. (1991). Effects of temperature on the coupled activities of the vanadate-sensitive proton pump from maize root microsomes. *Plant Physiol.* 96, 1114–1117. doi: 10.1104/pp.96.4.1114
- Briskin, D. P., and Poole, R. J. (1983). Characterization of a  $\text{K}^+$ -stimulated adenosine triphosphatase associated with the plasma membrane of red beet. *Plant Physiol.* 71, 350–355. doi: 10.1104/pp.71.2.350
- Bulychev, A. A., Kamzolkina, N. A., Luengviriya, J., Rubin, A. B., and Müller, S. C. (2004). Effect of a single excitation stimulus on photosynthetic activity and light-dependent pH banding in Chara cells. *J. Membr. Biol.* 202, 11–19. doi: 10.1007/s00232-004-0716-5
- Bulychev, A. A., and Vredenberg, W. J. (1995). Enhancement of the light-triggered electrical response in plant cells following their de-enegisation with uncouplers. *Physiol. Plant.* 94, 64–70. doi: 10.1111/j.1399-3054.1995.tb00785.x
- Choi, W. G., Toyota, M., Kim, S. H., Hilleary, R., and Gilroy, S. (2014). Salt stress-induced  $\text{Ca}^{2+}$  waves are associated with rapid, long-distance root-to-shoot signaling in plants. *Proc. Natl. Acad. Sci. U.S.A.* 111, 6497–6502. doi: 10.1073/pnas.1319955111
- Davies, E., and Stankovic, B. (2006). “Electrical signals, the cytoskeleton, and gene expression: a hypothesis on the coherence of the cellular responses to environmental insult,” in *Communication in Plants. Neuronal Aspects of Plant Life*, eds F. Baluška, S. Mancuso, and D. Volkman (Berlin; Heidelberg; New York, NY: Springer-Verlag), 309–320.
- Dupont, F. M., and Mudd, J. B. (1985). Acclimation to low temperature by microsomal membranes from tomato cell cultures. *Plant Physiol.* 77, 74–78. doi: 10.1104/pp.77.1.74
- Dziubinska, H., Filek, M., Koscielniak, J., and Trebacz, K. (2003). Variation and action potentials evoked by thermal stimuli accompany enhancement of ethylene emission in distant non-stimulated leaves of *Vicia faba* minor seedlings. *J. Plant Physiol.* 160, 1203–1210. doi: 10.1017/0176-1617-00914
- Felle, H. H., and Zimmermann, M. R. (2007). Systemic signaling in barley through action potentials. *Planta* 226, 203–214. doi: 10.1007/s00425-006-0458-y
- Filek, M., and Kościelniak, J. (1997). The effect of wounding the roots by high temperature on the respiration rate of the shoot and propagation of electric signal in horse bean seedlings (*Vicia faba* L. minor). *Plant Sci.* 123, 39–46. doi: 10.1016/S0168-9452(96)04567-0
- Fisahn, J., Herde, O., Willmitzer, L., and Peña-Cortés, H. (2004). Analysis of the transient increase in cytosolic  $\text{Ca}^{2+}$  during the action potential of higher plants with high temporal resolution: requirement of  $\text{Ca}^{2+}$  transients for induction of jasmonic acid biosynthesis and PINII gene expression. *Plant Cell Physiol.* 45, 456–459. doi: 10.1093/pcp/pch054
- Fromm, J. (1991). Control of phloem unloading by action potentials in Mimosa. *Physiol. Plant.* 83, 529–533. doi: 10.1111/j.1399-3054.1991.tb00130.x

- Fromm, J., and Lautner, S. (2007). Electrical signals and their physiological significance in plants. *Plant Cell Environ.* 30, 249–257. doi: 10.1111/j.1365-3040.2006.01614.x
- Furch, A. C., Zimmermann, M. R., Will, T., Hafke, J. B., and van Bel, A. J. (2010). Remote-controlled stop of phloem mass flow by biphasic occlusion in *Cucurbita maxima*. *J. Exp. Bot.* 61, 3697–3708. doi: 10.1093/jxb/erq181
- Gallé, A., Lautner, S., Flexas, J., and Fromm, J. (2015). Environmental stimuli and physiological responses: the current view on electrical signalling. *Environ. Exp. Bot.* 114, 15–21. doi: 10.1016/j.envexpbot.2014.06.013
- Grams, T. E. E., Lautner, S., Felle, H. H., Matyssek, R., and Fromm, J. (2009). Heat-induced electrical signals affect cytoplasmic and apoplastic pH as well as photosynthesis during propagation through the maize leaf. *Plant Cell Environ.* 32, 319–326. doi: 10.1111/j.1365-3040.2008.01922.x
- Hlaváčková, V., Krchnák, P., Nauš, J., Novák, O., Špundová, M., and Strnad, M. (2006). Electrical and chemical signals involved in short-term systemic photosynthetic responses of tobacco plants to local burning. *Planta* 225, 235–244. doi: 10.1007/s00425-006-0325-x
- Hlavinka, J., Nožková-Hlaváčková, V., Floková, K., Novák, O., and Nauš, J. (2012). Jasmonic acid accumulation and systemic photosynthetic and electrical changes in locally burned wild type tomato, ABA-deficient sitiens mutants and sitiens pre-treated by ABA. *Plant Physiol. Biochem.* 54, 89–96. doi: 10.1016/j.plaphy.2012.02.014
- Hochmal, A. K., Schulze, S., Trompelt, K., and Hippler, M. (2015). Calcium-dependent regulation of photosynthesis. *Biochim. Biophys. Acta* 1847, 993–1003. doi: 10.1016/j.bbabi.2015.02.010
- Kalaji, H. M., Goltsev, V., Bosa, K., Allakhverdiev, S. I., Strasser, R. J., and Govindjee. (2012). Experimental *in vivo* measurements of light emission in plants: a perspective dedicated to David Walker. *Photosyn. Res.* 114, 69–96. doi: 10.1007/s11120-012-9780-3
- Kalaji, H. M., Schansker, G., Ladle, R. J., Goltsev, V., Bosa, K., Allakhverdiev, S. I., et al. (2014). Frequently asked questions about *in vivo* chlorophyll fluorescence: practical issues. *Photosyn. Res.* 122, 121–158. doi: 10.1007/s11120-014-0024-6
- Katicheva, L., Sukhov, V., Akinchits, E., and Vodeneev, V. (2014). Ionic nature of burn-induced variation potential in wheat leaves. *Plant Cell Physiol.* 55, 1511–1519. doi: 10.1093/pcp/pcu082
- Katicheva, L., Sukhov, V., Bushueva, A., and Vodeneev, V. (2015). Evaluation of the open time of calcium channels at variation potential generation in wheat leaf cells. *Plant Signal. Behav.* 10:e993231. doi: 10.4161/15592324.2014.993231
- Kenderešová, L., Stanová, A., Pavlovkin, J., Durišová, E., Nadubinská, M., Ciamporová, M., et al. (2012). Early Zn<sup>2+</sup>-induced effects on membrane potential account for primary heavy metal susceptibility in tolerant and sensitive *Arabidopsis* species. *Ann. Bot.* 110, 445–459. doi: 10.1093/aob/mcs111
- Kiep, V., Vadassery, J., Lattke, J., Maaf, J. P., Boland, W., Peiter, E., et al. (2015). Systemic cytosolic Ca<sup>2+</sup> elevation is activated upon wounding and herbivory in *Arabidopsis*. *New Phytol.* 207, 996–1004. doi: 10.1111/nph.13493
- Klughammer, C., and Schreiber, U. (2008). Saturation pulse method for assessment of energy conversion in PS I. *PAM Appl. Notes* 1, 11–14.
- Krol, E., Dziubinska, H., Stolarz, M., and Trebacz, K. (2006). Effects of ion channel inhibitors on cold- and electrically-induced action potentials in *Dionaea muscipula*. *Biol. Plantarum.* 50, 411–416. doi: 10.1007/s10535-006-0058-5
- Krol, E., Dziubinska, H., and Trebacz, K. (2003). Low-temperature induced transmembrane potential changes in the liverwort *Conocephalum conicum*. *Plant Cell Physiol.* 44, 527–533. doi: 10.1093/pcp/pcg070
- Krol, E., Dziubinska, H., and Trebacz, K. (2004). Low-temperature-induced transmembrane potential changes in mesophyll cells of *Arabidopsis thaliana*, *Helianthus annuus* and *Vicia faba*. *Physiol. Plant.* 120, 265–270. doi: 10.1111/j.0031-9317.2004.0244.x
- Krol, E., and Trebacz, K. (1999). Calcium-dependent voltage transients evoked by illumination in the liverwort *Conocephalum conicum*. *Plant Cell Physiol.* 40, 17–24. doi: 10.1093/oxfordjournals.pcp.a029470
- Krupenina, N. A., and Bulychev, A. A. (2007). Action potential in a plant cell lowers the light requirement for non-photochemical energy-dependent quenching of chlorophyll fluorescence. *Biochim. Biophys. Acta* 1767, 781–788. doi: 10.1016/j.bbabi.2007.01.004
- Malone, M. (1994). Wound-induced hydraulic signals and stimulus transmission in *Mimosa pudica* L. *New Phytol.* 128, 49–56. doi: 10.1111/j.1469-8137.1994.tb03985.x
- Mancuso, S. (1999). Hydraulic and electrical transmission of wound-induced signals in *Vitis vinifera*. *Aust. J. Plant Physiol.* 26, 55–61. doi: 10.1071/PP98098
- Maxwell, K., and Johnson, G. N. (2000). Chlorophyll fluorescence—a practical guide. *J. Exp. Bot.* 51, 659–668. doi: 10.1093/jexbot/51.345.659
- Miedema, H., and Prins, H. B. (1993). Simulation of the light-induced oscillations of the membrane potential in *Potamogeton* leaf cells. *J. Membr. Biol.* 133, 107–117. doi: 10.1007/BF00233792
- Mousavi, S. A. R., Chauvin, A., Pascaud, F., Kellenberger, S., and Farmer, E. E. (2013). GLUTAMATE RECEPTOR-LIKE genes mediate leaf-to-leaf wound signaling. *Nature* 500, 422–426. doi: 10.1038/nature12478
- Müller, P., Li, X.-P., and Niyogi, K. K. (2001). Non-photochemical quenching: A response to excess light energy. *Plant Physiol.* 125, 1558–1566. doi: 10.1104/pp.125.4.1558
- Opritov, V. A., Lobov, S. A., Pyatygina, S. S., and Mysyagin, S. A. (2005). Analysis of possible involvement of local bioelectric responses in chilling perception by higher plants exemplified by *Cucurbita pepo*. *Russ. J. Plant Physiol.* 52, 801–808. doi: 10.1007/s11183-005-0118-2
- Opritov, V. A., Pyatygina, S. S., and Krauz, V. O. (1993). Role of electrical activity in cooling-induced development of adaptation syndrome in higher plant cells. *Russ. J. Plant Physiol.* 40, 537–542.
- Opritov, V. A., Pyatygina, S. S., Krauz, V. O., Khudyakov, V. A., and Abramova, N. N. (1994). Activation of the electrogenic plasmalemma H<sup>+</sup>-pump in the adaptation of higher plants to moderate low-temperature stress. *Russ. J. Plant Physiol.* 41, 428–432.
- Pavlovic, A., Slováková, L., Pandolfi, C., and Mancuso, S. (2011). On the mechanism underlying photosynthetic limitation upon trigger hair irritation in the carnivorous plant Venus flytrap (*Dionaea muscipula* Ellis). *J. Exp. Bot.* 62, 1991–2000. doi: 10.1093/jxb/erq404
- Pikulenko, M. M., and Bulychev, A. A. (2005). Light-triggered action potentials and changes in quantum efficiency of photosystem II in *Anthoceros* cells. *Russ. J. Plant Physiol.* 52, 584–590. doi: 10.1007/s11183-005-0087-5
- Pyatygina, S. S. (2004). Role of plasma membrane in cold action perception in plant cells. *Biol. Membr. (Moscow)* 21, 442–449.
- Pyatygina, S. S., Opritov, V. A., Abramova, N. N., and Vodeneev, V. A. (1999). Primary bioelectric response of higher plant cells to the combined action of stress factors. *Russ. J. Plant Physiol.* 46, 530–536.
- Pyatygina, S. S., Opritov, V. A., and Khudyakov, V. A. (1992). Subthreshold changes in excitable membranes of *Cucurbita pepo* L. stem cells during cooling-induced action-potential generation. *Planta* 186, 161–165. doi: 10.1007/BF00196244
- Pyatygina, S. S., Opritov, V. A., Krauz, V. O., and Polovinkin, A. V. (1996). Increase in cold resistance of electrogenesis as a basis for adaptive repolarization in higher plant cells during chilling. *Russ. J. Plant Physiol.* 43, 223–227.
- Retivin, V. G., Opritov, V. A., and Fedulina, S. B. (1997). Generation of action potential induces preadaptation of *Cucurbita pepo* L. stem tissues to freezing injury. *Russ. J. Plant Physiol.* 44, 432–442.
- Retivin, V. G., Opritov, V. A., Lobov, S. A., Tarakanov, S. A., and Khudyakov, V. A. (1999). Changes in the resistance of photosynthesizing cotyledon cells of pumpkin seedlings to cooling and heating, as induced by the stimulation of the root system with KCl solution. *Russ. J. Plant Physiol.* 46, 689–696.
- Roach, T., and Krieger-Liszkay, A. (2014). Regulation of photosynthetic electron transport and photoinhibition. *Curr. Protein Pept. Sci.* 15, 351–362. doi: 10.2174/1389203715666140327105143
- Saidi, Y., Finka, A., Muriset, M., Bromberg, Z., Weiss, Y. G., Maathuis, F. J., et al. (2009). The heat shock response in moss plants is regulated by specific calcium-permeable channels in the plasma membrane. *Plant Cell* 21, 2829–2843. doi: 10.1105/tpc.108.065318
- Shepherd, V. A., Beilby, M. J., Al Khazaaly, S. A., and Shimmen, T. (2008). Mechano-perception in Chara cells: the influence of salinity and calcium on touch-activated receptor potentials, action potentials and ion transport. *Plant Cell Environ.* 31, 1575–1591. doi: 10.1111/j.1365-3040.2008.01866.x
- Sherstneva, O. N., Surova, L. M., Vodeneev, V. A., Plotnikova, Y. I., Bushueva, A. V., and Sukhov, V. S. (2016a). The role of the intra- and extracellular protons in the photosynthetic response induced by the variation potential in pea seedlings. *Biochem. (Moscow) Suppl. Ser. A* 10, 60–67. doi: 10.1134/S1990747815050116
- Sherstneva, O. N., Vodeneev, V. A., Katicheva, L. A., Surova, L. M., and Sukhov, V. S. (2015). Participation of intracellular and extracellular pH changes in photosynthetic response development induced by variation

- potential in pumpkin seedlings. *Biochemistry (Moscow)* 80, 776–784. doi: 10.1134/S0006297915060139
- Sherstneva, O. N., Vodeneev, V. A., Surova, L. M., Novikova, E. M., and Sukhov, V. S. (2016b). Application of a mathematical model of variation potential for analysis of its influence on photosynthesis in higher plants. *Biochem. Moscow Suppl. Ser. A* 10, 269–277. doi: 10.1134/S1990747816030089
- Shimmen, T. (1997). Studies on mechano-perception in characeae: effects of external  $\text{Ca}^{2+}$  and  $\text{Cl}^-$ . *Plant Cell Physiol.* 38, 691–697. doi: 10.1093/oxfordjournals.pcp.a029222
- Simons, P. J. (1981). The role of electricity in plant movements. *New Phytol.* 87, 11–37. doi: 10.1111/j.1469-8137.1981.tb01687.x
- Stahlberg, R., Cleland, R. E., and van Volkenburgh, E. (2006). “Slow wave potentials – a propagating electrical signal unique to higher plants,” in *Communication in Plants. Neuronal Aspects of Plant Life*, eds F. Baluška, S. Mancuso, and D. Volkmann (Berlin; Heidelberg; New York, NY: Springer-Verlag), 291–308.
- Stanković, B., and Davies, E. (1996). Both action potentials and variation potentials induce proteinase inhibitor gene expression in tomato. *FEBS Lett.* 390, 275–279. doi: 10.1016/0014-5793(96)00672-2
- Sukhov, V. (2016). Electrical signals as mechanism of photosynthesis regulation in plants. *Photosyn. Res.* 130, 373–387. doi: 10.1007/s11120-016-0270-x
- Sukhov, V., Akinchits, E., Katicheva, L., and Vodeneev, V. (2013). Simulation of variation potential in higher plant cells. *J. Membrane Biol.* 246, 287–296. doi: 10.1007/s00232-013-9529-8
- Sukhov, V., Orlova, L., Mysyagin, S., Sinitcina, J., and Vodeneev, V. (2012). Analysis of the photosynthetic response induced by variation potential in geranium. *Planta* 235, 703–712. doi: 10.1007/s00425-011-1529-2
- Sukhov, V., Sherstneva, O., Surova, L., Katicheva, L., and Vodeneev, V. (2014a). Proton cellular influx as a probable mechanism of variation potential influence on photosynthesis in pea. *Plant Cell Environ.* 37, 2532–2541. doi: 10.1111/pce.12321
- Sukhov, V., Surova, L., Morozova, E., Sherstneva, O., and Vodeneev, V. (2016). Changes in  $\text{H}^+$ -ATP synthase activity, proton electrochemical gradient, and pH in pea chloroplast can be connected with variation potential. *Front. Plant Sci.* 7:1092. doi: 10.3389/fpls.2016.01092
- Sukhov, V., Surova, L., Sherstneva, O., Katicheva, L., and Vodeneev, V. (2015a). Variation potential influence on photosynthetic cyclic electron flow in pea. *Front. Plant Sci.* 5:766. doi: 10.3389/fpls.2014.00766
- Sukhov, V., Surova, L., Sherstneva, O., Bushueva, A., and Vodeneev, V. (2015b). Variation potential induces decreased PSI damage and increased PSII damage under high external temperatures in pea. *Funct. Plant Biol.* 42, 727–736. doi: 10.1071/FP15052
- Sukhov, V., Surova, L., Sherstneva, O., and Vodeneev, V. (2014b). Influence of variation potential on resistance of the photosynthetic machinery to heating in pea. *Physiol. Plant.* 152, 773–783. doi: 10.1111/ppl.12208
- Sukhov, V., and Vodeneev, V. (2009). A mathematical model of action potential in cells of vascular plants. *J. Membrane Biol.* 232, 59–67. doi: 10.1007/s00232-009-9218-9
- Sukhova, E., Akinchits, E., and Sukhov, V. (2017). Mathematical models of electrical activity in plants. *J. Membrane Biol.* 250, 407–423. doi: 10.1007/s00232-017-9969-7
- Surova, L., Sherstneva, O., Vodeneev, V., Katicheva, L., Semina, M., and Sukhov, V. (2016a). Variation potential-induced photosynthetic and respiratory changes increase ATP content in pea leaves. *J. Plant Physiol.* 202, 57–64. doi: 10.1016/j.jplph.2016.05.024
- Surova, L., Sherstneva, O., Vodeneev, V., and Sukhov, V. (2016b). Variation potential propagation decreases heat-related damage of pea photosystem I by 2 different pathways. *Plant Signal. Behav.* 11:e1145334. doi: 10.1080/15592324.2016.1145334
- Trebacz, K., Dziubinska, H., and Krol, E. (2006). “Electrical signals in long-distance communication in plants,” in *Communication in Plants. Neuronal Aspects of Plant Life*, eds F. Baluška, S. Mancuso, and D. Volkmann (Berlin; Heidelberg: Springer-Verlag), 277–290.
- Trebacz, K., and Sievers, A. (1998). Action potentials evoked by light in traps of *Dionaea muscipula* Ellis. *Plant Cell Physiol.* 39, 369–372. doi: 10.1093/oxfordjournals.pcp.a029379
- Trebacz, K., Simonis, W., and Schöönknecht, G. (1997). Effects of anion channel inhibitors on light-induced potential changes in the liverwort *Conocephalum conicum*. *Plant Cell Physiol.* 38, 550–557. doi: 10.1093/oxfordjournals.pcp.a029204
- Vodeneev, V. A., Akinchits, E. K., Orlova, L. A., and Sukhov, V. S. (2011). The role of  $\text{Ca}^{2+}$ ,  $\text{H}^+$ , and  $\text{Cl}^-$  ions in generation of variation potential in pumpkin plants. *Russ. J. Plant Physiol.* 58, 974–981. doi: 10.1134/S1021443711050256
- Vodeneev, V. A., Katicheva, L. A., and Sukhov, V. S. (2016). Electrical signals in higher plants: mechanisms of generation and propagation. *Biophysics* 61, 505–512. doi: 10.1134/S0006350916030209
- Vodeneev, V., Akinchits, E., and Sukhov, V. (2015). Variation potential in higher plants: mechanisms of generation and propagation. *Plant Signal. Behav.* 10:e1057365. doi: 10.1080/15592324.2015.1057365
- Vodeneev, V., Mudrilov, M., Akinchits, E., Balalaeva, I., and Sukhov, V. (2017). Parameters of electrical signals and photosynthetic responses induced by them in pea seedlings depend on the nature of stimulus. *Funct. Plant Biol.* doi: 10.1071/FP16342
- Volkov, A. G., and Ranatunga, D. R. A. (2006). Plants as environmental biosensors. *Plant Signal Behav.* 1, 105–115. doi: 10.4161/psb.1.3.3000
- Von Caemmerer, S., and Farquhar, G. D. (1981). Some relationships between the biochemistry of photosynthesis and the gas exchange of leaves. *Planta* 153, 376–387. doi: 10.1007/BF00384257

**Conflict of Interest Statement:** The authors declare that the research was conducted in the absence of any commercial or financial relationships that could be construed as a potential conflict of interest.

Copyright © 2017 Sukhov, Gaspirovich, Mysyagin and Vodeneev. This is an open-access article distributed under the terms of the Creative Commons Attribution License (CC BY). The use, distribution or reproduction in other forums is permitted, provided the original author(s) or licensor are credited and that the original publication in this journal is cited, in accordance with accepted academic practice. No use, distribution or reproduction is permitted which does not comply with these terms.



# Calcium and Calmodulin Are Involved in Nitric Oxide-Induced Adventitious Rooting of Cucumber under Simulated Osmotic Stress

Lijuan Niu<sup>1†</sup>, Jian Yu<sup>1†</sup>, Weibiao Liao<sup>1\*</sup>, Jihua Yu<sup>1</sup>, Meiling Zhang<sup>2</sup> and Mohammed M. Dawuda<sup>1,3</sup>

<sup>1</sup> College of Horticulture, Gansu Agricultural University, Lanzhou, China, <sup>2</sup> College of Science, Gansu Agricultural University, Lanzhou, China, <sup>3</sup> Department of Horticulture, Faculty of Agriculture, University for Development Studies, Tamale, Ghana

## OPEN ACCESS

### Edited by:

Kazimierz Trebacz,  
Maria Curie-Skłodowska University,  
Poland

### Reviewed by:

Vladimir Vodeneev,  
N. I. Lobachevsky State University  
of Nizhny Novgorod, Russia  
Rafael Ribeiro,  
Universidade Estadual de Campinas,  
Brazil

### \*Correspondence:

Weibiao Liao  
liaowb@gau.edu.cn

<sup>†</sup>These authors have contributed  
equally to this work.

### Specialty section:

This article was submitted to  
Plant Physiology,  
a section of the journal  
*Frontiers in Plant Science*

Received: 13 June 2017

Accepted: 13 September 2017

Published: 27 September 2017

### Citation:

Niu L, Yu J, Liao W, Yu J, Zhang M  
and Dawuda MM (2017) Calcium  
and Calmodulin Are Involved in Nitric  
Oxide-Induced Adventitious Rooting  
of Cucumber under Simulated  
Osmotic Stress.  
*Front. Plant Sci.* 8:1684.  
doi: 10.3389/fpls.2017.01684

Osmotic stress is a major form of abiotic stress that adversely affects growth and development of plants and subsequently reduces yield and quality of crops. In this study, the effect of nitric oxide (NO) and calcium ( $\text{Ca}^{2+}$ ) on the process of adventitious rooting in cucumber (*Cucumis sativus* L.) under simulated osmotic stress was investigated. The results revealed that the effect of exogenous NO and  $\text{Ca}^{2+}$  in promoting the development of adventitious roots in cucumber seedlings under simulated osmotic stress was dose-dependent, with a maximal biological response at 10  $\mu\text{M}$  NO donor nitroprusside (SNP) or 200  $\mu\text{M}$   $\text{Ca}^{2+}$ . The application of  $\text{Ca}^{2+}$  chelators or channel inhibitors and calmodulin (CaM) antagonists significantly reversed NO-induced adventitious rooting, implying that endogenous  $\text{Ca}^{2+}$ /CaM might be involved in NO-induced adventitious rooting under osmotic stress. Moreover, intracellular Ca amount was also increased by NO in cucumber hypocotyls during the development of adventitious roots under osmotic stress. This increase of endogenous  $\text{Ca}^{2+}$  was inhibited by NO specific scavenger 2-(4-carboxyphenyl)-4,4,5,5-tetramethylimidazoline-1-oxyl-3-oxide potassium salt (cPTIO), nitrate reductase inhibitors tungstate ( $\text{Na}_2\text{WO}_4$ ) and sodium azide ( $\text{NaN}_3$ ). This gives an indication that  $\text{Ca}^{2+}$  might be a downstream signaling molecule in the adventitious root development by NO under osmotic condition. The results also show that NO or  $\text{Ca}^{2+}$  play a positive role in improving plant water status and photosynthetic system by increasing chlorophyll content and photochemical activity in leaves. Furthermore, NO and  $\text{Ca}^{2+}$  treatment might alleviate the negative effects of osmotic stress by decreasing membrane damage and reactive oxygen species (ROS) production by enhancing the activities of superoxide dismutase (SOD), catalase (CAT) and ascorbate peroxidase (APX). Therefore,  $\text{Ca}^{2+}$ /CaM may act as a downstream signaling molecule in NO-induced development of adventitious root under simulated osmotic stress through improving the photosynthetic performance of leaves and activating antioxidative system in plants.

**Keywords:** abiotic stress, adventitious rooting, nitric oxide, calcium, chlorophyll fluorescence, antioxidant system

## INTRODUCTION

Nitric oxide (NO), as a free radical gas, has been synthesized enzymatically or non-enzymatically (Skiba et al., 1993; Rockel et al., 2002). Previous reports have indicated that NO might regulate the growth and physiological processes in plants, including seed germination (Beligni and Lamattina, 2000; Wang et al., 2015), root growth and development (Liao et al., 2011; Zhao et al., 2015), senescence (Liao et al., 2013), stomatal closure (Neill et al., 2002; Shi C. et al., 2015) and the growth of pollen tube (Wang et al., 2009). It has also been reported that NO plays an essential role in response to various abiotic stresses (Garcia-Mata and Lamattina, 2001; Salgado et al., 2013; Kaur et al., 2015; Liu W. et al., 2015). Besides, an increasing body of evidence indicated that NO served as a regulator in plant response to osmotic stress. Liao et al. (2012a) found that exogenous NO improved the development of adventitious roots in marigold explants under drought stress conditions by improving photosynthesis and carbohydrate and nitrogen contents. Shan et al. (2015) have reported that jasmonic acid (JA) alleviated drought stress by inducing endogenous NO, which could up-regulate the activity of ASA-GSH cycle. In addition, Jday et al. (2016) found that exogenous application of NO increased drought tolerance and mitigated damage by regulating proline metabolism and reducing oxidative damage by increasing the activities of superoxide dismutase (SOD) and catalase (CAT) in *Cakile maritima*.

Increasing evidence pointed out that the change of intracellular  $\text{Ca}^{2+}$  concentration is a mark of signaling transduction to mediate various cellular processes in plants (Kong et al., 2015; Tang et al., 2015). Recently, it has been reported that  $\text{Ca}^{2+}$  regulates the processes of growth and development in plants including seed germination (Kong et al., 2015), pollen tube growth (Zhou et al., 2014), and root growth (Liao et al., 2012b). Some studies have indicated that variations in cytosolic free  $\text{Ca}^{2+}$  concentration might be involved in plant response to different kinds of abiotic stresses (Zou et al., 2015; Li et al., 2016).  $\text{Ca}^{2+}$  plays a role in mediating plant adaptation to drought stress condition. For instance, Zou et al. (2010) found that  $\text{Ca}^{2+}$  could mediate stomatal movements in *Arabidopsis* plants under drought stress through calcium-dependent protein kinases (CDPKs). Application of  $\text{Ca}^{2+}$  also reduced drought-induced proline accumulation, which implied that  $\text{Ca}^{2+}$  played a role in response to drought stress in *Triticum aestivum* L. (Sadiqov et al., 2002). However, the mechanism of  $\text{Ca}^{2+}$  signaling in regulating plant growth and response to abiotic stress still needs further investigation.

The interaction of NO and  $\text{Ca}^{2+}$  has been regarded as a critical regulator in plant growth and development and in response to abiotic stress. For example, Lanteri et al. (2006) reported that  $\text{Ca}^{2+}$  is involved in NO-induced adventitious root formation in cucumber. Chen and Kao (2012) found that  $\text{Ca}^{2+}$  was involved in NO-induced formation of lateral roots (LR) in rice. Excluding endogenous  $\text{Ca}^{2+}$  inhibited the NO-induced LR formation. However, the authors did not find any relationship between  $\text{Ca}^{2+}$  and endogenous NO during LR

formation. A crosstalk between NO and  $\text{Ca}^{2+}$  in inducing adventitious rooting in marigold under normal condition has been reported (Liao et al., 2012b). In addition,  $\text{Ca}^{2+}$  signaling induced endogenous NO accumulation by inducing hydrogen peroxide ( $\text{H}_2\text{O}_2$ ) generation during stomatal closure in *Arabidopsis* guard cells (Wang et al., 2012). Xu et al. (2016) also found an interaction between NO and  $\text{Ca}^{2+}$  under high irradiance in tall fescue leaves. The occurrence of a crosstalk between NO and  $\text{Ca}^{2+}$  under copper stress was also found in *Ulva compressa* (González et al., 2012). NO generation under copper stress might be dependent on  $\text{Ca}^{2+}$  release through various  $\text{Ca}^{2+}$  channels, which were also activated by NO (González et al., 2012). Cellular responses to NO and  $\text{Ca}^{2+}$  signaling are complicated, therefore, further research to deepen our understanding of the crosstalk between NO and  $\text{Ca}^{2+}$  in plants is needed.

Osmotic stress as a situation which might prevent plants from absorbing enough water induces the inhibition of plant growth and oxidative damage (Jiang et al., 1993). The common osmotic stresses include drought, salt and cold stresses. It has been reported that osmotic stress significantly reduced the fresh weight and water content in leaf blade and leaf petiole of sugar beet (*Beta vulgaris* L.) (Wu et al., 2016). Osmotic stress interfered with various metabolic processes (Búfalo et al., 2016) in plants such as photosynthesis (Bündig et al., 2016) and respiration (Zorrilla-Fontanesi et al., 2016). Previous study has shown that  $\text{Ca}^{2+}$  and CDPK could be involved in adventitious rooting, which was induced by NO in cucumber (Lanteri et al., 2006). However, Liao et al. (2012b) indicated that NO induced adventitious root development in marigold through enhancing endogenous  $\text{Ca}^{2+}$  and CaM level under stress-free conditions. The role of NO and  $\text{Ca}^{2+}$  in adventitious rooting under abiotic stress is unknown. We conduct this experiment with the hypothesis that NO,  $\text{Ca}^{2+}$  and their crosstalk may affect adventitious development in plants under abiotic stress. The objective of this study was to elucidate the potential role of NO and  $\text{Ca}^{2+}$  in adventitious rooting process under osmotic stress condition. In this study, we provide evidence that  $\text{Ca}^{2+}/\text{CaM}$  are required for NO-induced adventitious root development in cucumber under osmotic stress and this improves our understanding of the mechanism of NO signaling transduction under abiotic stress.

## MATERIALS AND METHODS

### Plant Materials

Cucumber (*Cucumis sativus* 'Xinchun 4') seeds were germinated in petri dishes on filter papers moistened with distilled water and maintained at  $25 \pm 1^\circ\text{C}$  for 6 days with a 14 h photoperiod (photosynthetically active radiation =  $200 \mu\text{mol s}^{-1} \text{ m}^{-2}$ ). Primary roots of 6 days old seedlings were removed and the cucumber explants were then maintained under the same conditions of temperature and photoperiod for another 6 days in the presence of different media as indicated below. These media were changed every day in order to keep the solution fresh. Root number and length per explant were counted and measured.

## Treatments of Explants

Experiment 1: Polyethylene glycol 6000 (PEG 6000, Shanghai Chemical Reagent Co. Ltd., Shanghai, China) was used to simulate osmotic stress. Explants were placed in Petri dishes containing filter paper moistened with distilled water (control) and different concentrations of PEG 6000, sodium nitroprusside (SNP, a donor of NO, Merck, Darmstadt, Germany) and calcium chloride ( $\text{CaCl}_2$ , Solarbio, Beijing, China) and kept at  $25 \pm 1^\circ\text{C}$ . The following chemicals were added with suitable concentration of PEG, SNP, or  $\text{CaCl}_2$ : $50 \mu\text{M}$  S-nitroso-*N*-acetylpenicillamine (SNAP, a donor of NO, Sigma, United States),  $50 \mu\text{M}$   $\text{K}_4\text{Fe}(\text{CN})_6$  (SNP analog, Solarbio, Beijing, China),  $100 \mu\text{M}$  sodium nitrate ( $\text{NaNO}_3$ , degradation product of SNP, Solarbio, Beijing, China).

Experiment 2: Ca chelators and channel inhibitors and CaM antagonists: (1)  $100 \mu\text{M}$  ethylene glycol-*bis* (2-aminoethyl ether)-*N,N,N',N'*-tetraacetic acid (EGTA, Sigma, United States): a  $\text{Ca}^{2+}$  chelator (Liao et al., 2012b); (2)  $30 \mu\text{M}$  1,2-*bis* (o-aminophenoxy)ethane-*N,N,N',N'*-tetraacetic acid tetra (acetoxymethyl) ester (BAPTA/AM, Santa Cruz, CA, United States; BAPTA-AM was prepared for 15 min at  $-20^\circ\text{C}$  before the experiment): a membrane permeable  $\text{Ca}^{2+}$  chelator (Liao et al., 2012b); (3)  $80 \mu\text{M}$  *N*-(6-aminohexyl)-5-chloro-1-naphthalenesulfonamide hydrochloride (W-7, Santa Cruz, CA, United States): a CaM antagonist (González et al., 2012); (4)  $80 \mu\text{M}$  *N*-(6-aminohexyl)-1-naphthalenesulfonamide (W-5, Santa Cruz, CA, United States): a CaM antagonist (Liao et al., 2012b); (5)  $100 \mu\text{M}$  trifluoperazine dihydrochloride (TFP, Santa Cruz, CA, United States): a CaM antagonist (Lanteri et al., 2006); (6)  $500 \mu\text{M}$  lanthanum chloride ( $\text{LaCl}_3$ , Solarbio, Beijing, China): a  $\text{Ca}^{2+}$  channel blocker (Lanteri et al., 2006); (7)  $150 \mu\text{M}$  nifedipine (Solarbio, Beijing, China): a  $\text{Ca}^{2+}$  channel blocker (Reiss and Herth, 1985).

Experiment 3: NO scavengers and nitrate reductase inhibitors: (1)  $200 \mu\text{M}$  2-(4-carboxy-2-phenyl)-4, 4, 5, 5-tetramethylimidazoline-1-oxy-3-oxide (cPTIO, Sigma, United States): a NO specific scavenger (Liao et al., 2012b); (2)  $10 \mu\text{M}$  sodium azide ( $\text{NaN}_3$ , Solarbio, Beijing, China): a nitrate reductase inhibitor (Liao et al., 2013); (3)  $100 \mu\text{M}$  sodium tungstate ( $\text{Na}_2\text{WO}_4$ , Solarbio, Beijing, China): a nitrate reductase inhibitor (Tian et al., 2007). The concentrations of these chemicals were based on the results of a preliminary experiment.

## Cytosolic Free $\text{Ca}^{2+}$ Observation

Fluo-3/AM (Sigma, United States) as molecular probes was utilized to determine intracellular Ca level in plant.  $20 \mu\text{M}$  Fluo-3/AM was loaded into cucumber hypocotyls (about  $100 - 200 \text{ mm}$  long) at  $4^\circ\text{C}$  in the dark (Zhang et al., 1998). After 2 h of incubation, the hypocotyls were washed three times with distilled water to remove the excess of fluorescence and place under  $20^\circ\text{C}$  for 1 h. The Fluo-3 fluorescence of the hypocotyls after 48 h of treatments was visualized via fluorescence microscope (Leica 400  $\times$ , Planapo, Wetzlar, Germany), for an excitation wavelength of 488 nm and an emission wavelength of 520–530 nm. After that, the fluorescence intensity of endogenous  $\text{Ca}^{2+}$  at 48 h was measured via Image Pro software (Media Cybernetics, United States).

## Determination of Endogenous NO Production

Fluorescent probe 4-amino-5-methylamino-2',7'-diamino-fluoresceindiacetate (DAF-FM DA) was utilized to measure the level of endogenous NO in cucumber hypocotyls after 48 h of treatments. The hypocotyls were loaded with  $10 \mu\text{M}$  DAF-FM DA (Graziano and Lamattina, 2007) in  $50 \text{ mM}$  Tris-HCl (pH 7.4) for 2 h in the dark. Then, the samples were washed three times with fresh buffer for 15 min. DAF-FM DA fluorescence was visualized via fluorescence microscope (Leica 400  $\times$ , Planapo, Wetzlar, Germany), for excitation with the 488 nm, and emission with 500 – 530 nm.

## Measurement of Water Potential

The water potential of cucumber leaves was directly determined using a dew-point water potential meter WP4T (Decagon Devices, United States). The measurements of water potential in cucumber leaves after 48 h of treatment were made at 9:00 – 10:00 am.

## Determination of TBARS, $\text{H}_2\text{O}_2$ and $\text{O}_2^-$ Content

TBARS content was determined as described by Cakmak and Horst (1991).  $0.2 \text{ g}$  fresh explant was grounded with  $3 \text{ mL}$  of  $0.1\% (\text{w/v})$  trichloroacetic acid (TCA). The homogenate was centrifuged at  $12000 \text{ g}$  for 5 min,  $1 \text{ mL}$  supernatant was added to  $4 \text{ mL}$  of  $20\% (\text{w/v})$  TCA which included  $0.5\% (\text{w/v})$  TBA. Then, samples were incubated in a water-bath (30 min) at  $90^\circ\text{C}$ . After that, the reaction was incubated in ice bath. After  $10000 \text{ g}$  centrifugation for 5 min, the absorbance of the supernatant was recorded at 532 and  $600 \text{ nm}$ .

$\text{H}_2\text{O}_2$  content was determined the method of Velikova et al. (2000).  $0.2 \text{ g}$  sample was homogenized with  $4 \text{ mL}$  of  $0.1\% (\text{w/v})$  trichloroacetic acid in an ice bath. After  $12000 \text{ g}$  centrifugation at  $4^\circ\text{C}$  for 15 min, the absorbance of the mixture reaction which includes  $0.5 \text{ mL}$  of the supernatant,  $0.5 \text{ mL}$  of  $10 \text{ mM}$  potassium phosphate buffer (pH 7.0) and  $1 \text{ mL}$  of  $1 \text{ M}$  potassium iodide was recorded at  $390 \text{ nm}$ .

The rate of superoxide production ( $\text{O}_2^-$ ) was measured according to Chaitanya and Naithani (1994). Fresh cucumber explant ( $0.2 \text{ g}$ ) was homogenized with  $100 \text{ mM}$  sodium-phosphate buffer (pH 7.8) in an ice bath. The centrifugation was performed for 20 min at  $4^\circ\text{C}$ . The mixture includes  $0.5 \text{ mL}$  of  $100 \text{ mM}$  sodium phosphate buffer (pH 7.8),  $0.5 \text{ mL}$  of  $1 \text{ mM}$  hydroxylammonium chloride and  $0.5 \text{ mL}$  of supernatant. Then,  $1 \text{ mL}$  of  $17 \text{ mM}$  sulfanilic acid and  $1 \text{ mL}$  of  $7 \text{ mM}$   $\alpha$ -naphthylamine were added in the reaction which was maintained at  $25^\circ\text{C}$  for 20 min. The absorbance of sample was measured at  $540 \text{ nm}$ . ROS production was measured after 48 h of treatments.

## Determination of Chlorophyll Content

About  $0.2 \text{ g}$  leaves were ground to a fine powder and extracted with  $5 \text{ mL}$  of  $80\% (\text{v/v})$  acetone. The amounts of Chlorophyll a, b, or a + b after 48 h of treatments were determined by spectrophotometer, measuring the absorbance at  $645$  and  $663 \text{ nm}$

and the chlorophyll concentration (mg/g DW) was calculated by using the equations according to Arnon (1949).

## Measurement of Chlorophyll Fluorescence

This was measured as described by Genty et al. (1989). Fluorescence parameters of cucumber leaves after 48 h were measured using chlorophyll fluorescence imaging system (MAXI Imaging-PAM, Walz, Effeltrich, Germany) at 25°C. The intensities of the modulated measuring beam, actinic light and saturating light were 0.1  $\mu\text{mol m}^{-2} \text{s}^{-1}$ , 81  $\mu\text{mol m}^{-2} \text{s}^{-1}$  and 2700  $\mu\text{mol m}^{-2} \text{s}^{-1}$  PFD, respectively. The duration of saturation pulses was 0.8 s. Meanwhile, the duration of actinic light was set to 5 min to obtain chlorophyll fluorescence under the steady state condition. After putting the plant samples to 30 min dark period adaptation, the initial fluorescence yield ( $F_0$ ) was obtained. The maximum fluorescence yield ( $F_m$ ) was measured with the application of a saturation pulse. Variable chlorophyll fluorescence ( $F_v$ ) was evaluated as  $F_v = F_m - F_0$ . The maximum quantum yield of PSII ( $F_v / F_m$ ) were calculated as  $F_v / F_m = (F_m - F_0) / F_m$ . Maximum fluorescence yield of the light adapted leaf ( $F_m'$ ) were obtained after the application of a saturation pulse and  $F_s$  represented steady-state chlorophyll fluorescence. Effective quantum yield of PSII ( $\Phi_{PSII}$ ) =  $(F_m' - F_s)/F_m'$ . After turning off action light, far red light (10  $\mu\text{mol m}^{-2} \text{s}^{-1}$ ) was illuminated immediately obtaining the minimum fluorescence yield in light-adapted state ( $F_0'$ ). Photochemical quenching ( $qP = [F_m' - F_s]/[F_m' - F_0']$ ) and non-photochemical (NPQ =  $[F_m - F_m']/F_m'$ ) quenching coefficients were calculated (Liu Z. et al., 2015).

## Antioxidant Enzyme Assays

Frozen explant (approximately 200 mg) were homogenized in 5 mL of 50 mM sodium phosphate buffer (pH 7.8) containing 5 mM ethylenediaminetetraacetic acid and 2% polyvinylpyrrolidone for SOD and CAT assay or the combination with the addition of 2 mM ascorbic acid (ASC) for ascorbate peroxidase (APX) assay. The homogenate was centrifuged at 12000 g for 20 min at 4°C and the supernatant was used as the crude enzyme extract. Total SOD activity was measured according to Dhindsa et al. (1981). The definition of one unit of SOD was the amount of crude enzyme extract required to inhibit the reduction rate of Nitrotetrazolium Blue chloride (NBT) by 50%. APX activity was evaluated by measuring the decrease in absorbance at 290 nm of a reaction mixture including 25 mM sodium phosphate buffer containing 0.1 mM ethylenediaminetetraacetic acid (pH 7.0), 20 mM H<sub>2</sub>O<sub>2</sub>, 5 mM ASC and 0.1 mL enzyme extract as previously described by Nakano and Asada (1981). According to Aebi (1984), CAT activity was evaluated by monitoring the consumption of H<sub>2</sub>O<sub>2</sub> at 240 nm by a reaction mixture including 25 mM sodium phosphate buffer, 0.1 mM ethylenediaminetetraacetic acid (pH 7.0), 100 mM H<sub>2</sub>O<sub>2</sub> and 0.1 mL enzyme extract. The activities of antioxidant enzymes were measured after 48 h of treatments.

## Statistical Analysis of the Data

All the results in the figures and table were expressed as the mean values  $\pm$  SE from three independent replicates (10 samples per replication). Data was analyzed using the Statistical Package for Social Sciences for Windows (version 13.00; SPSS, Inc., Chicago, IL, United States). Analysis of Variance (ANOVA) was done and statistical differences among treatments were analyzed through Duncan's multiple range test ( $P < 0.05$ ).

## RESULTS

### Effect of Exogenous SNP and CaCl<sub>2</sub> on Adventitious Rooting under Osmotic Stress

To assess the effect of PEG on adventitious rooting in cucumber, we performed a dose-response experiment with PEG. When different concentrations of PEG solution were applied, the amount of adventitious roots and root length decreased significantly (Figure 1). As shown in Figure 1, root number and root length under 0.05% PEG decreased to about half that of the control treatment. Therefore, 0.05% PEG was utilized to simulate osmotic stress in the following experiments.

In order to investigate the effects of NO on the development of adventitious root under osmotic stress, cucumber explants were treated with different concentrations of SNP (a donor of NO). As shown in Figure 2, lower concentrations of SNP (1, 10, and 50  $\mu\text{M}$ ) treatments significantly increased the number

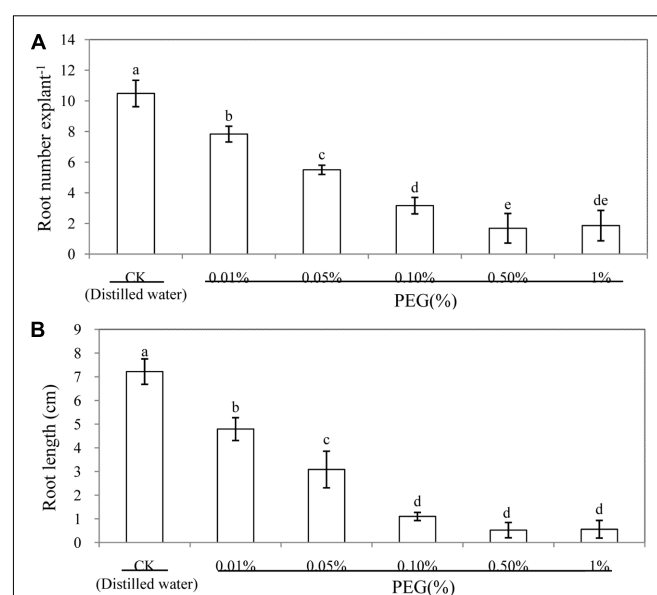
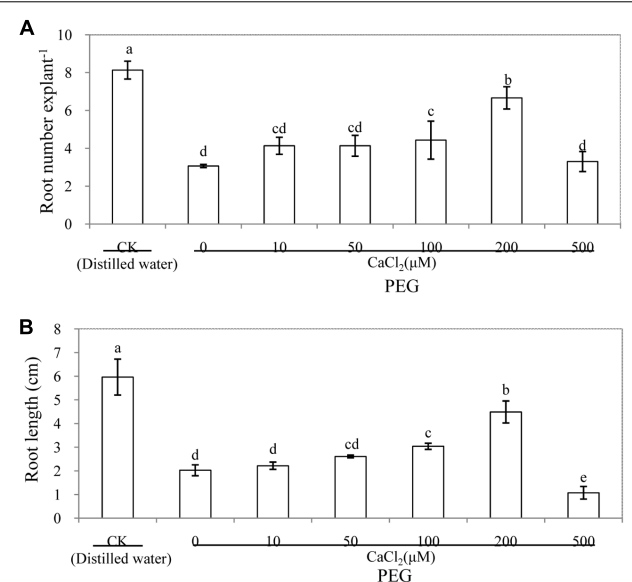
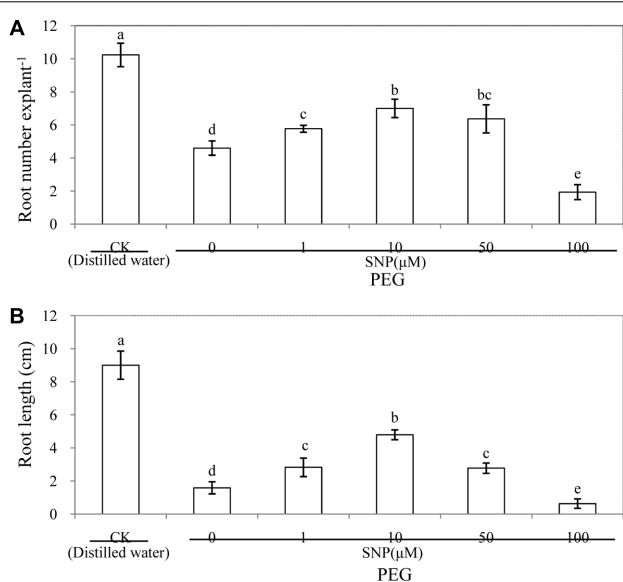


**FIGURE 1 |** Effect of different concentrations of PEG on adventitious root development in cucumber explants. The primary roots were removed from hypocotyl of 6-day-old seedlings. Explants were incubated for 6 days with different concentrations of PEG 6000. The numbers (A) and root length (B) of adventitious root were expressed as mean  $\pm$  SE ( $n = 3$ , 10 explants were used per replicate). Bars with different lower case letters were significantly different by Duncan's multiple range test ( $p < 0.05$ ).



of adventitious roots and root length under osmotic stress. However, a higher dose (100  $\mu\text{M}$  SNP) significantly decreased the root number and root length, which indicates that the effect of NO on root number of adventitious roots was dose-dependent under osmotic stress, with a maximal biological response at 10  $\mu\text{M}$  SNP (Figure 2 and Supplementary Figure S1). Additionally, root numbers and root length of 10  $\mu\text{M}$  SNP treatment increased by 52.2 and 201.9%, respectively, compared with those of PEG treatment. These results indicate that 10  $\mu\text{M}$  SNP might significantly reverse the adverse effect of osmotic stress and promote the development of adventitious roots. Thus, 10  $\mu\text{M}$  SNP was utilized for further experiments to study the processes of adventitious rooting under osmotic stress.

As shown in Figure 3, the number and length of adventitious roots were significantly affected by different concentrations of  $\text{CaCl}_2$  treatments under osmotic stress. Exogenous  $\text{CaCl}_2$  treatments showed a concentration-dependent effect on adventitious rooting. There was no marked difference between 0, 10, and 50  $\mu\text{M}$   $\text{CaCl}_2$ . Meanwhile, root number from 100 and 200  $\mu\text{M}$   $\text{CaCl}_2$ -treated explants increased by 44.3 and 117.3%, respectively, compared with those of the PEG treatment. In addition, application of 200  $\mu\text{M}$   $\text{CaCl}_2$  significantly increased the root length by 121.2% in comparison with the PEG treatment alone. The number and length of adventitious roots decreased greatly at  $\text{CaCl}_2$  concentration of 500  $\mu\text{M}$  (Figure 3 and Supplementary Figure S2). Among the different concentrations of  $\text{CaCl}_2$  treatments, 200  $\mu\text{M}$   $\text{CaCl}_2$  significantly increased the root number and root length and had the greatest effect in

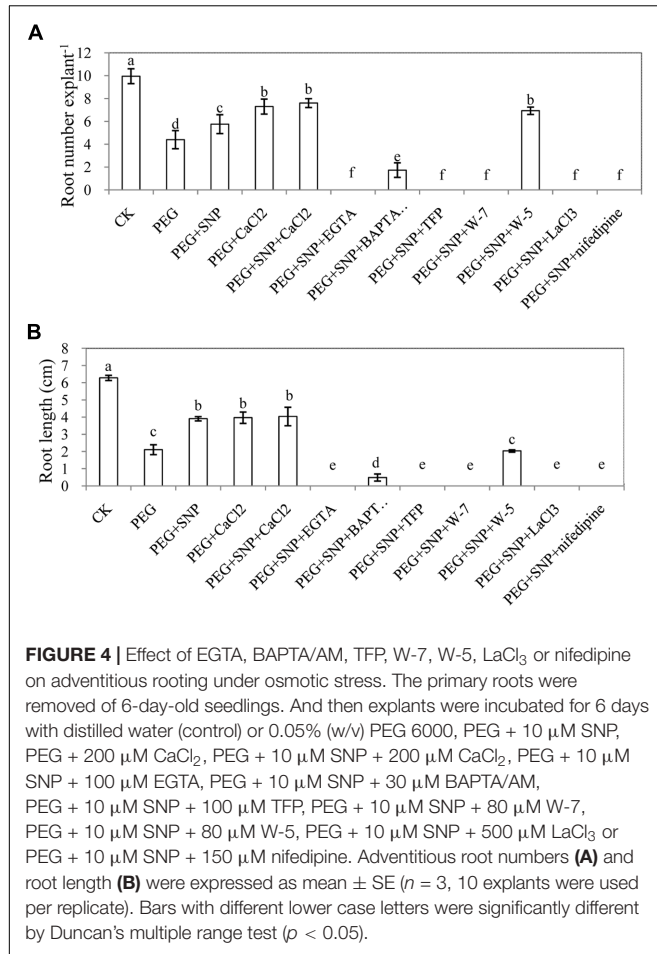
promoting the development of adventitious root under osmotic stress. Therefore, we utilized 200  $\mu\text{M}$   $\text{CaCl}_2$  in the following experiments.

## Effect of $\text{Ca}^{2+}$ Chelators, Channel Inhibitors and CaM Antagonists on Adventitious Rooting under Osmotic Stress

In order to further investigate the requirement of  $\text{Ca}^{2+}/\text{CaM}$  for NO-induced adventitious rooting,  $\text{Ca}^{2+}$  chelators (EGTA, BAPTA/AM),  $\text{Ca}^{2+}$  channel inhibitors ( $\text{LaCl}_3$  or nifedipine) and CaM antagonist (TFP, W-7 and W-5) were applied in this study (Figure 4). The results showed that EGTA, BAPTA/AM,  $\text{LaCl}_3$  and nifedipine significantly inhibited the development of adventitious roots under osmotic stress. Similarly, TFP and W-7 treatments also had a significant reduction in adventitious rooting. However, W-5, acting as a CaM antagonist, hardly reduced adventitious root number and length. SNP,  $\text{CaCl}_2$  and SNP +  $\text{CaCl}_2$  treatments obviously alleviated osmotic stress and promoted the development of adventitious roots (Figure 4 and Supplementary Figure S3).

## Effect of $\text{K}_4\text{Fe}(\text{CN})_6$ , SNAP and cPTIO on Adventitious Rooting under Osmotic Stress

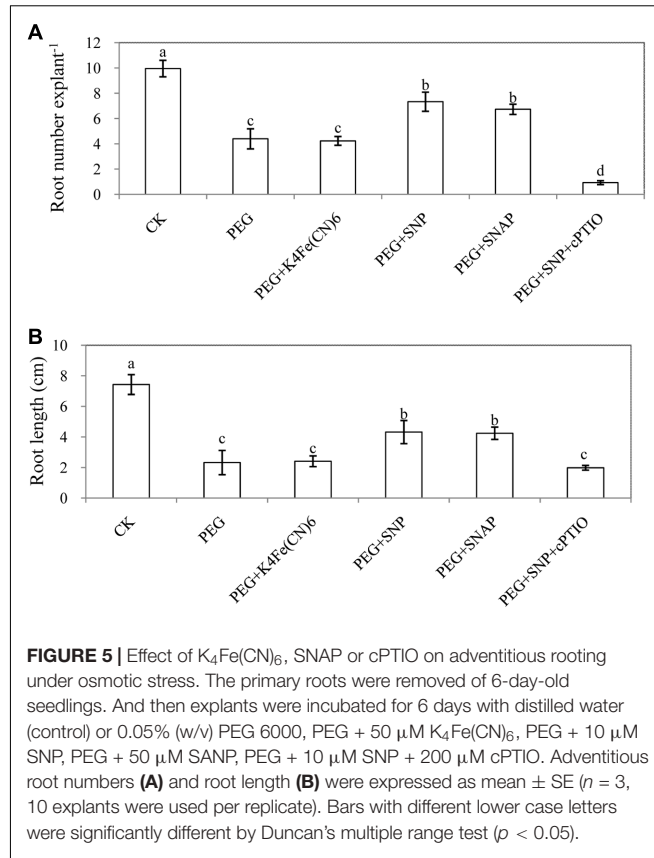
Here,  $\text{K}_4\text{Fe}(\text{CN})_6$  and SNAP were used to further confirm that the formation of adventitious root is mediated by NO. Obviously,



SNAP treatment promoted adventitious rooting under osmotic stress. These results implied that NO released from SNP or SNAP might be responsible for the enhancement of adventitious rooting under osmotic stress. In addition, cPTIO significantly reversed the promotive effects of NO on adventitious rooting (Figure 5 and Supplementary Figure S4).

### Fluorescence Intensity of Ca<sup>2+</sup> in Hypocotyls during Adventitious Rooting under Osmotic Stress as Affected by SNP

To investigate whether there is a link between NO and Ca<sup>2+</sup> during adventitious rooting under osmotic stress, changes in fluorescence intensity of Ca<sup>2+</sup> in hypocotyls were analyzed (Figures 6A,B and Supplementary Figures S5, S7). At 48 h, treatment with PEG + CaCl<sub>2</sub> in Ca<sup>2+</sup> fluorescence intensity was significantly higher than that of PEG treatment alone. However, cPTIO, NaNO<sub>3</sub> or Na<sub>2</sub>WO<sub>4</sub> treatments which may inhibit NO generation significantly impaired the fluorescence intensity of intracellular Ca<sup>2+</sup> in cucumber hypocotyl at 48 h. Besides, there was no significant difference between PEG treatment and PEG + NaNO<sub>3</sub> treatment. This gives an indication that NO plays a crucial role in increasing intracellular Ca<sup>2+</sup> presence. Removing



endogenous NO decreased the level of intracellular Ca<sup>2+</sup> which implied NO was responsible for the changes in intracellular Ca<sup>2+</sup> during adventitious rooting under osmotic stress.

### Changes in Fluorescence Intensity of NO in Hypocotyls of Cucumber during Adventitious Rooting under Osmotic Stress

In order to investigated the connection between NO and Ca<sup>2+</sup> during adventitious rooting under osmotic stress, the level of NO fluorescent intensity was studied (Supplementary Figure S6). As shown in Figure 6C, at 48 h, PEG + SNP treatment enhanced the fluorescent intensity of NO production, compared to the control or PEG treatment. Meanwhile, the application of CaCl<sub>2</sub> relatively increased the accumulation of endogenous NO in cucumber hypocotyl during the development of adventitious root under osmotic stress. The NO scavenger or inhibitor remarkably resulted in a reduction in fluorescence intensity of NO in cucumber. These results implied that there could be a relationship between the amount of endogenous NO and the process of adventitious rooting under osmotic stress.

### Effects of NO and CaCl<sub>2</sub> on Leaf Water of Cucumber under Osmotic Stress

Figure 7 showed that the value of leaf  $\Psi_w$  in PEG treatment is significantly lower than that of the control during adventitious

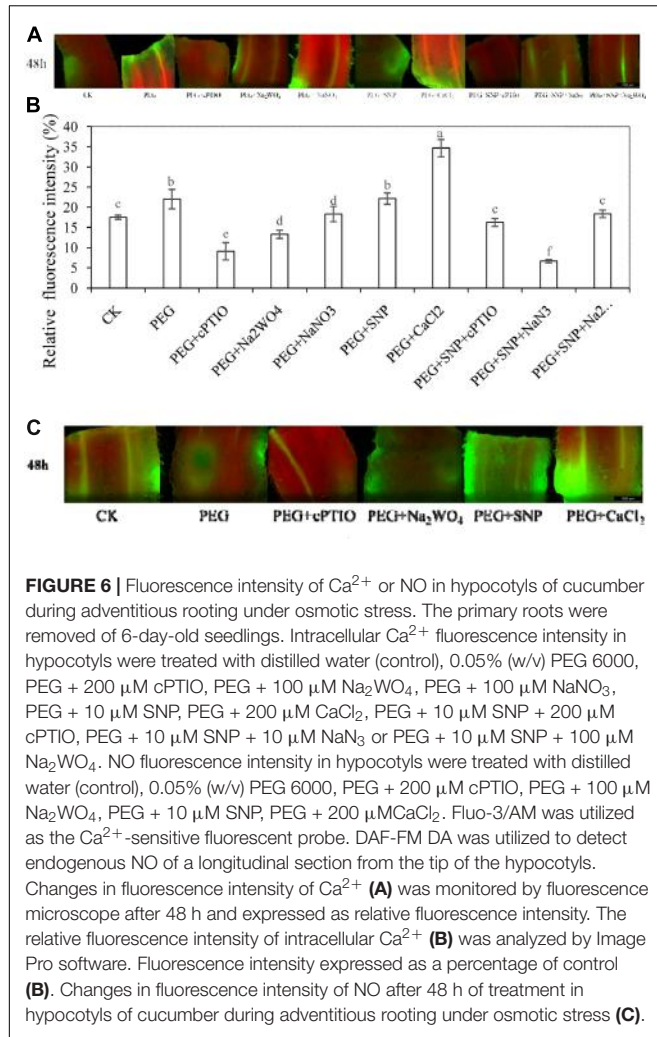


**FIGURE 6 |** Fluorescence intensity of  $\text{Ca}^{2+}$  or NO in hypocotyls of cucumber during adventitious rooting under osmotic stress. The primary roots were removed of 6-day-old seedlings. Intracellular  $\text{Ca}^{2+}$  fluorescence intensity in hypocotyls were treated with distilled water (control), 0.05% (w/v) PEG 6000, PEG + 200  $\mu\text{M}$  cPTIO, PEG + 100  $\mu\text{M}$  Na<sub>2</sub>WO<sub>4</sub>, PEG + 100  $\mu\text{M}$  NaNO<sub>3</sub>, PEG + 10  $\mu\text{M}$  SNP, PEG + 200  $\mu\text{M}$  CaCl<sub>2</sub>, PEG + 10  $\mu\text{M}$  SNP + 200  $\mu\text{M}$  cPTIO, PEG + 10  $\mu\text{M}$  SNP + 10  $\mu\text{M}$  Na<sub>3</sub>N or PEG + 10  $\mu\text{M}$  SNP + 100  $\mu\text{M}$  Na<sub>2</sub>WO<sub>4</sub>. NO fluorescence intensity in hypocotyls were treated with distilled water (control), 0.05% (w/v) PEG 6000, PEG + 200  $\mu\text{M}$  cPTIO, PEG + 100  $\mu\text{M}$  Na<sub>2</sub>WO<sub>4</sub>, PEG + 10  $\mu\text{M}$  SNP, PEG + 200  $\mu\text{M}$  CaCl<sub>2</sub>. Fluo-3/AM was utilized as the  $\text{Ca}^{2+}$ -sensitive fluorescent probe. DAF-FM DA was utilized to detect endogenous NO of a longitudinal section from the tip of the hypocotyls. Changes in fluorescence intensity of  $\text{Ca}^{2+}$  (**A**) was monitored by fluorescence microscope after 48 h and expressed as relative fluorescence intensity. The relative fluorescence intensity of intracellular  $\text{Ca}^{2+}$  (**B**) was analyzed by Image Pro software. Fluorescence intensity expressed as a percentage of control (**B**). Changes in fluorescence intensity of NO after 48 h of treatment in hypocotyls of cucumber during adventitious rooting under osmotic stress (**C**).

rooting at 48 h. In addition, PEG + SNP or PEG + CaCl<sub>2</sub> treatment significantly increased leaf  $\Psi_w$  in comparison to PEG-treated leaves only. At 48 h, leaf  $\Psi_w$  of explants treated with PEG increased by 31.8% compared with the control. Application of SNP or CaCl<sub>2</sub> remarkably increased the  $\Psi_w$  by 10.4%, 55.0% in cucumber leaf, respectively, compared to that of PEG treatment alone. However, EGTA, BAPTA/AM, TFP, W-7, LaCl<sub>3</sub> or nifedipine treatments resulted in a significant reduction in leaf  $\Psi_w$  during adventitious rooting under osmotic stress. This indicates that  $\text{Ca}^{2+}$  might be responsible for NO-mediated stress response during adventitious rooting in cucumber under osmotic stress.

## Effects of NO and CaCl<sub>2</sub> on TBARS, H<sub>2</sub>O<sub>2</sub> and O<sub>2</sub><sup>−</sup> of Cucumber Leaf under Osmotic Stress

As shown in Figure 8, PEG treatment significantly increased the concentration of TBARS, H<sub>2</sub>O<sub>2</sub> and O<sub>2</sub><sup>−</sup>. The level of reactive oxygen species (ROS) in  $\text{Ca}^{2+}$  chelators,  $\text{Ca}^{2+}$  channel inhibitors or CaM antagonist were significantly higher than those

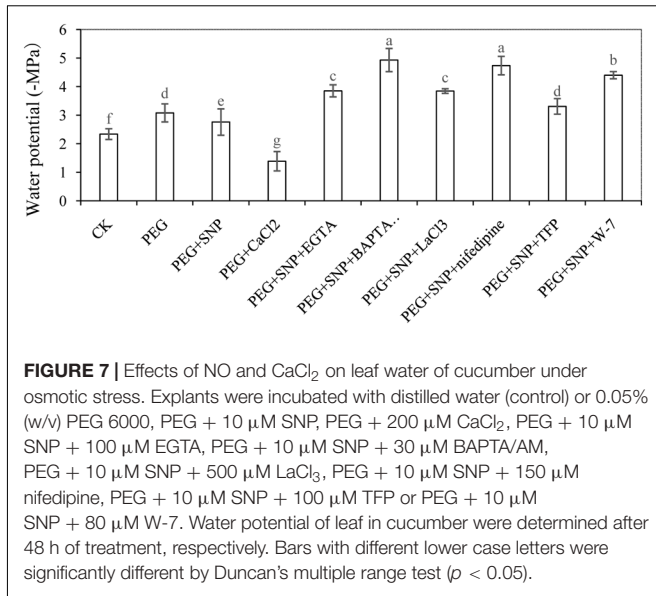


**FIGURE 7 |** Effects of NO and  $\text{CaCl}_2$  on leaf water of cucumber under osmotic stress. Explants were incubated with distilled water (control) or 0.05% (w/v) PEG 6000, PEG + 10  $\mu\text{M}$  SNP, PEG + 200  $\mu\text{M}$  CaCl<sub>2</sub>, PEG + 10  $\mu\text{M}$  SNP + 100  $\mu\text{M}$  EGTA, PEG + 10  $\mu\text{M}$  SNP + 30  $\mu\text{M}$  BAPTA/AM, PEG + 10  $\mu\text{M}$  SNP + 500  $\mu\text{M}$  LaCl<sub>3</sub>, PEG + 10  $\mu\text{M}$  SNP + 150  $\mu\text{M}$  nifedipine, PEG + 10  $\mu\text{M}$  SNP + 100  $\mu\text{M}$  TFP or PEG + 10  $\mu\text{M}$  SNP + 80  $\mu\text{M}$  W-7. Water potential of leaf in cucumber were determined after 48 h of treatment, respectively. Bars with different lower case letters were significantly different by Duncan's multiple range test ( $p < 0.05$ ).

of PEG + SNP and PEG + CaCl<sub>2</sub> treatments. At 48 h, TBARS concentration with PEG treatment was 135.7% higher than that of control (Figure 8A). However, the concentration of TBARS in PEG + SNP and PEG + CaCl<sub>2</sub> treatments was significantly reduced by 66.9 and 48.2% compared to PEG treatment.

Figure 8B showed that H<sub>2</sub>O<sub>2</sub> concentration with PEG + SNP and PEG + CaCl<sub>2</sub> treatments reduced by 23.3 and 36.6% at 48 h, respectively, compared to PEG-treated explants. Conversely, the level of H<sub>2</sub>O<sub>2</sub> in EGTA, BAPTA/AM, TFP, W-7, LaCl<sub>3</sub> or nifedipine treatments was expressed at a higher level in comparison with PEG + SNP and PEG + CaCl<sub>2</sub> treatments at 48 h. The level of O<sub>2</sub><sup>−</sup> treated with PEG was significantly enhanced with respect to the control (Figure 8C). In addition, a reduction of O<sub>2</sub><sup>−</sup> content was observed under PEG + SNP and PEG + CaCl<sub>2</sub> treatments at 48 h, compared to that of PEG treatment. However, the accumulation of O<sub>2</sub><sup>−</sup> content in  $\text{Ca}^{2+}$  chelators,  $\text{Ca}^{2+}$  channel inhibitors or CaM antagonist treatment remarkably increased at 48 h.

## Effect of SNP and CaCl<sub>2</sub> on the Activities of Antioxidant Enzymes during Adventitious Rooting under Osmotic Stress

To further assess whether alleviation of osmotic stress is related to NO- or CaCl<sub>2</sub>-induced antioxidant defense, we measured the activity of antioxidant enzymes in cucumber explants during adventitious rooting under osmotic stress. The SOD activity in PEG + SNP or PEG + CaCl<sub>2</sub> was increased by 28.3 and 26.4%, respectively, compared to PEG treatment at 48 h (Figure 9A). Meanwhile, the CAT activity in PEG + SNP or PEG + CaCl<sub>2</sub> treatment at 48 h was 31.5 and 32.3% higher than that in osmotic stress alone (Figure 9B). Meanwhile, SNP, CaCl<sub>2</sub> or SNP + CaCl<sub>2</sub> treatments resulted in a significant increase of APX activity under osmotic stress (Figure 9C). However, during the

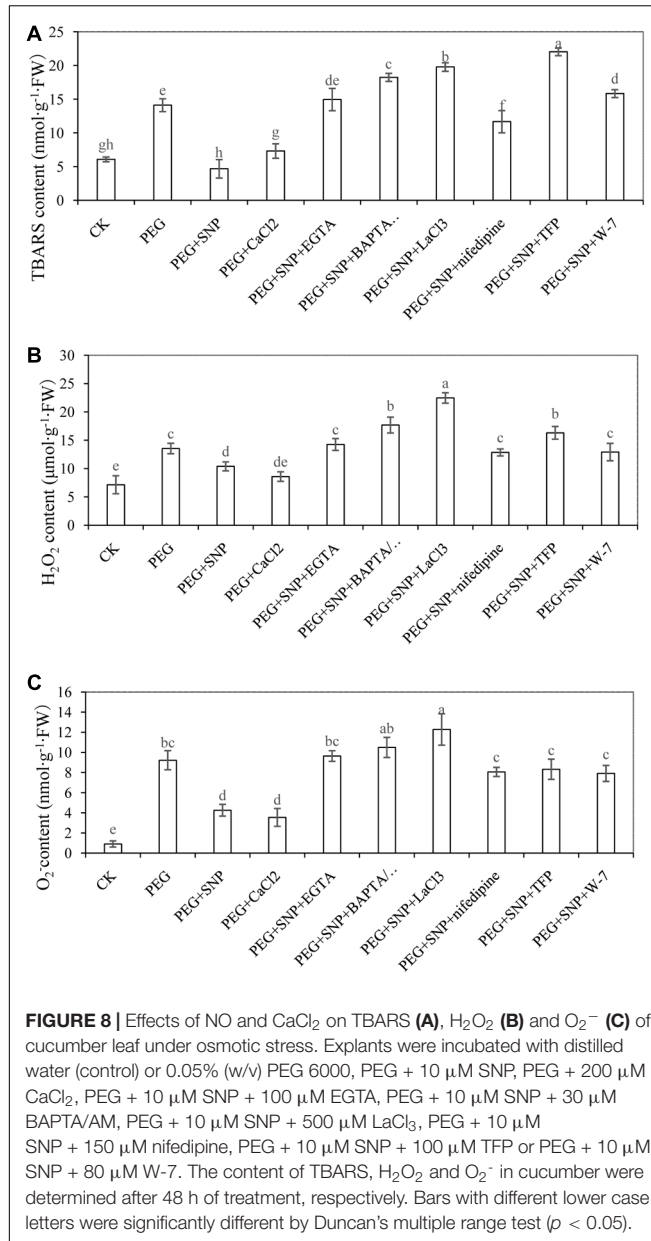


**FIGURE 8 |** Effects of NO and CaCl<sub>2</sub> on TBARS (**A**), H<sub>2</sub>O<sub>2</sub> (**B**) and O<sub>2</sub><sup>−</sup> (**C**) of cucumber leaf under osmotic stress. Explants were incubated with distilled water (control) or 0.05% (w/v) PEG 6000, PEG + 10 μM SNP, PEG + 200 μM CaCl<sub>2</sub>, PEG + 10 μM SNP + 100 μM EGTA, PEG + 10 μM SNP + 30 μM BAPTA/AM, PEG + 10 μM SNP + 500 μM LaCl<sub>3</sub>, PEG + 10 μM SNP + 150 μM nifedipine, PEG + 10 μM SNP + 100 μM TFP or PEG + 10 μM SNP + 80 μM W-7. The content of TBARS, H<sub>2</sub>O<sub>2</sub> and O<sub>2</sub><sup>−</sup> in cucumber were determined after 48 h of treatment, respectively. Bars with different lower case letters were significantly different by Duncan's multiple range test ( $p < 0.05$ ).

development of adventitious root, EGTA, BAPTA/AM, TFP, W-7, LaCl<sub>3</sub> or nifedipine treatments significantly suppressed these antioxidant enzyme activities to levels lower than that of PEG treatment.

## Effects of SNP and CaCl<sub>2</sub> on Photosynthetic System during Adventitious Rooting under Osmotic Stress

### Chlorophyll Content

Osmotic stress decreased chlorophyll content in our experiment (**Figure 10**). The chl a, chl b, chl (a + b) concentration in cucumber leaves from explants that were treated with in

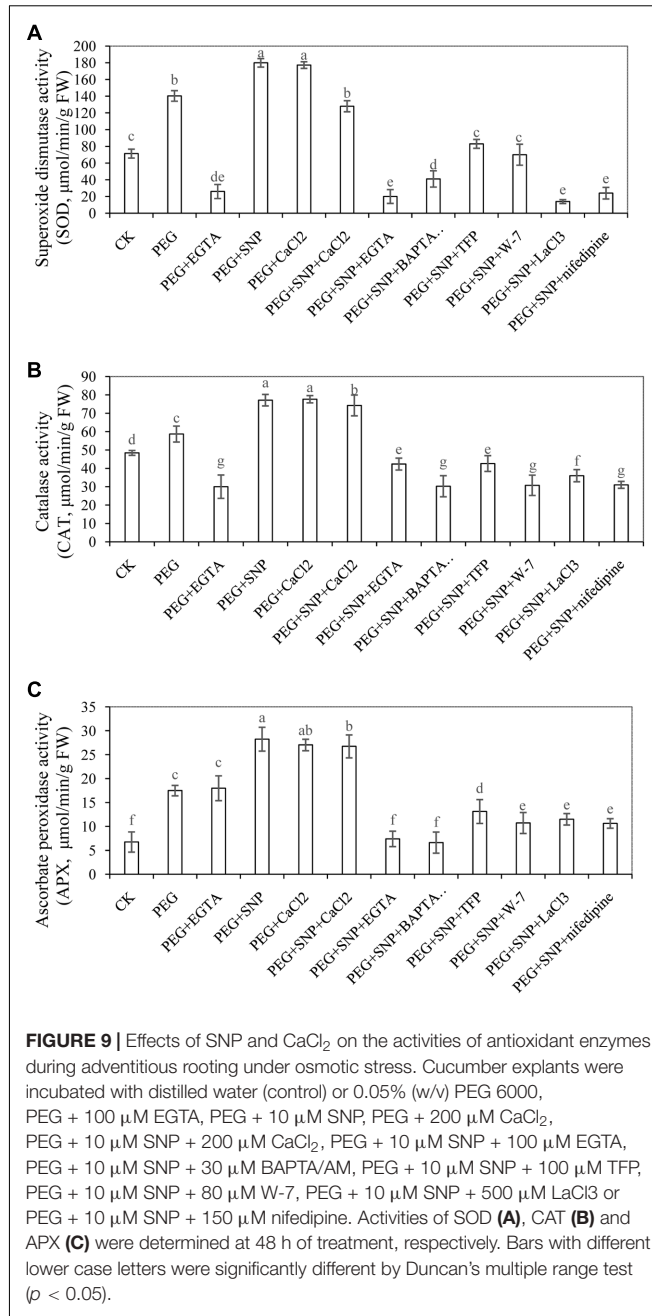


**FIGURE 9 |** Effects of SNP and CaCl<sub>2</sub> on the activities of antioxidant enzymes during adventitious rooting under osmotic stress. Cucumber explants were incubated with distilled water (control) or 0.05% (w/v) PEG 6000, PEG + 100 μM EGTA, PEG + 10 μM SNP, PEG + 200 μM CaCl<sub>2</sub>, PEG + 10 μM SNP + 200 μM CaCl<sub>2</sub>, PEG + 10 μM SNP + 100 μM EGTA, PEG + 10 μM SNP + 30 μM BAPTA/AM, PEG + 10 μM SNP + 100 μM TFP, PEG + 10 μM SNP + 80 μM W-7, PEG + 10 μM SNP + 500 μM LaCl<sub>3</sub> or PEG + 10 μM SNP + 150 μM nifedipine. Activities of SOD (**A**), CAT (**B**) and APX (**C**) were determined at 48 h of treatment, respectively. Bars with different lower case letters were significantly different by Duncan's multiple range test ( $p < 0.05$ ).

SNP, Ca<sup>2+</sup> or SNP + CaCl<sub>2</sub> treatments significantly increased, compared with those from PEG and PEG + EGTA treatment. These results suggested that application of NO or CaCl<sub>2</sub> was more effective in retarding the loss of chlorophyll and in improving photochemistry under osmotic stress. However, EGTA, BAPTA/AM, TFP, W-7, LaCl<sub>3</sub> and nifedipine treatments decreased the level of chl a, chl b and chl (a + b), compared to explant exposed to SNP, CaCl<sub>2</sub> or SNP + CaCl<sub>2</sub> treatments. Meanwhile, the concentrations of chl a, chl b, chl (a + b) in explants treated with EGTA, BAPTA/AM, TFP, W-7, LaCl<sub>3</sub> and nifedipine were significantly lower than those of PEG treatment which indicated that Ca<sup>2+</sup>/CaM might

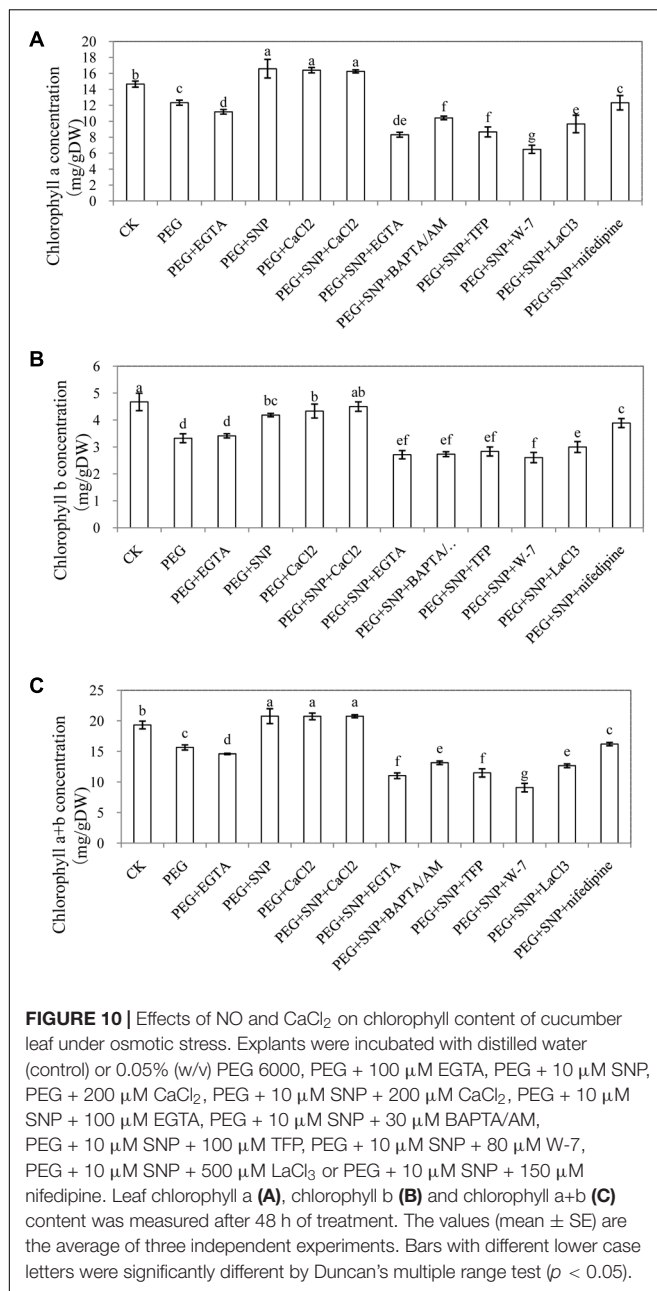


**FIGURE 10 |** Effects of NO and CaCl<sub>2</sub> on chlorophyll content of cucumber leaf under osmotic stress. Explants were incubated with distilled water (control) or 0.05% (w/v) PEG 6000, PEG + 100 μM EGTA, PEG + 10 μM SNP, PEG + 200 μM CaCl<sub>2</sub>, PEG + 10 μM SNP + 200 μM CaCl<sub>2</sub>, PEG + 10 μM SNP + 100 μM EGTA, PEG + 10 μM SNP + 30 μM BAPTA/AM, PEG + 10 μM SNP + 100 μM TFP, PEG + 10 μM SNP + 80 μM W-7, PEG + 10 μM SNP + 500 μM LaCl<sub>3</sub> or PEG + 10 μM SNP + 150 μM nifedipine. Leaf chlorophyll a (**A**), chlorophyll b (**B**) and chlorophyll a+b (**C**) content was measured after 48 h of treatment. The values (mean ± SE) are the average of three independent experiments. Bars with different lower case letters were significantly different by Duncan's multiple range test ( $p < 0.05$ ).

be involved in NO-regulating the increases in chlorophyll content.

### Effect of SNP or CaCl<sub>2</sub> on Photochemistry under Osmotic Stress

Compared to the control, PEG and PEG + EGTA treatment decreased the value of Fv/Fm (**Table 1**). However, SNP treatment or CaCl<sub>2</sub> treatment increased Fv/Fm by 9.2 and 8.2% higher than that of control, respectively. Moreover, EGTA, BAPTA/AM, TFP or W-7 treatments resulted in 12.6, 15.5, 14.1, and 14.6% reduction in Fv/Fm, respectively, compared to osmotic stress. LaCl<sub>3</sub> and nifedipine treatment significantly reduced Fv/Fm by 46.4 and 37.9%, respectively, compared to that of PEG + SNP

treatment. In addition, the effect of different treatments on ΦPSII and qP were similar to that of Fv/Fm (**Table 1**). PEG treatment significantly increased NPQ compared with control. However, PEG + SNP or PEG + CaCl<sub>2</sub> treatments significantly decreased NPQ. There was a significant increase in NPQ level after removing the endogenous Ca<sup>2+</sup>/CaM. These results implied that NO or Ca<sup>2+</sup> had a positive role in improving the development of adventitious root by regulating chlorophyll fluorescent parameters.

## DISCUSSION

Previous studies have indicated that NO and Ca<sup>2+</sup>, as signaling molecules, might be involved in plants response to abiotic stress (Shan et al., 2015; Zou et al., 2015; Silveira et al., 2017a). However, whether there is a relationship between NO and Ca<sup>2+</sup>/CaM in the development of adventitious root under osmotic stress has not received the needed research attention. In this study, we have found that Ca<sup>2+</sup>/CaM interactions were involved in NO-induced adventitious rooting process in cucumber under osmotic stress.

### Actions and Relationships between NO and Ca<sup>2+</sup> on Promoting Adventitious Rooting under Osmotic Stress

The number and length of adventitious roots in cucumber was retarded by different concentrations of PEG treatment. However, when exogenous SNP or CaCl<sub>2</sub> were applied under osmotic stress, root number and length was significantly increased to levels higher than those of PEG treatment (**Figures 2, 3**). According to previous report, NO promoted adventitious root formation in marigold under drought stress (Liao et al., 2012a). Ca<sup>2+</sup> was also found to have induced the adventitious rooting

**TABLE 1 |** Effects of SNP or CaCl<sub>2</sub> on photochemistry under osmotic stress.

Treatments	Fv/Fm	ΦPSII	qP	NPQ
CK	0.783d	0.597c	0.647i	0.467l
PEG	0.683e	0.533d	0.583e	0.713f
PEG + EGTA	0.630f	0.452g	0.498j	0.668h
PEG + SNP	0.855a	0.667a	0.723a	0.527i
PEG + CaCl <sub>2</sub>	0.847b	0.653b	0.717b	0.520j
PEG + SNP + CaCl <sub>2</sub>	0.827c	0.653b	0.703c	0.517k
PEG + SNP + EGTA	0.597g	0.463e	0.503d	0.757b
PEG + SNP + BAPTA/AM	0.577k	0.447h	0.513f	0.767a
PEG + SNP + TFP	0.587i	0.453f	0.507h	0.747e
PEG + SNP + W-7	0.583j	0.437i	0.508g	0.750d
PEG + SNP + LaCl <sub>3</sub>	0.558l	0.350k	0.396k	0.671g
PEG + SNP + nifedipine	0.591h	0.413j	0.304l	0.755c

Explants were incubated with distilled water (control) or 0.05% (w/v) PEG 6000, PEG + 100 μM EGTA, PEG + 10 μM SNP, PEG + 200 μM CaCl<sub>2</sub>, PEG + 10 μM SNP + 200 μM CaCl<sub>2</sub>, PEG + 10 μM SNP + 30 μM BAPTA/AM, PEG + 10 μM SNP + 100 μM TFP, PEG + 10 μM SNP + 80 μM W-7, PEG + 10 μM SNP + 500 μM LaCl<sub>3</sub> or PEG + 10 μM SNP + 150 μM nifedipine. Parameters of chlorophyll fluorescence with different treatments were conducted after 48 h of treatment. Values followed by a different lower-case letter in the same column were significantly different by Duncan's multiple range test at  $p < 0.05$ .

process in marigold explants under normal condition (Liao et al., 2012b). According to our results (**Figures 2, 3**), SNP or  $\text{Ca}^{2+}$  had the dose-dependent effect on induction of adventitious rooting in cucumber under osmotic stress. In addition, results from PEG +  $\text{K}_4\text{Fe}(\text{CN})_6$ , PEG + SNAP and PEG + SNP + cPTIO treatments further confirmed the role of NO released from SNP and SNAP (**Figure 5**). These results indicated that suitable dosages of NO or  $\text{Ca}^{2+}$  might alleviate the injury due to osmotic stress on adventitious rooting. Previous researches have suggested that NO or  $\text{Ca}^{2+}$  played critical roles in enhancing stress resistance through mediating antioxidant defense system, protecting the structure of cell membrane and chlorophyll function as well as maintaining ion homeostasis in plants (Shan et al., 2015; Zou et al., 2015; Li et al., 2016). Recently, the crosstalk between NO and  $\text{Ca}^{2+}$  under abiotic stress in plants was reported. For example, NO might mediate  $\text{Ca}^{2+}$ -regulated antioxidant enzymes activities to respond against high irradiance-induced oxidative stress (Xu et al., 2016). Similarly, Lang et al. (2014) investigated the functional relationship between NO and  $\text{Ca}^{2+}$  mediating root ion fluxes under salt stress. In another experiment with explants treated with EGTA, BAPTM/AM,  $\text{LaCl}_3$ , nifedipine, TFP and W-7, the formation of NO-induced adventitious root was significantly retarded under osmotic stress (**Figure 4**). These results revealed that inhibition of endogenous  $\text{Ca}^{2+}/\text{CaM}$  might completely inhibit the NO-induced adventitious rooting under osmotic condition. Previous study on rice indicated that  $\text{Ca}^{2+}$  was involved in NO-induced lateral root formation (Chen and Kao, 2012) and  $\text{Ca}^{2+}$  inhibitors (EGTA and BAPTA/AM) or CaM antagonists (TFP and W-7) were found to have suppressed the positive effects of NO and  $\text{H}_2\text{O}_2$  on adventitious rooting of marigold under stress-free condition (Liao et al., 2012a). Additionally, Lanteri et al. (2006) also found that  $\text{Ca}^{2+}$  might be involved in NO- or auxin-induced adventitious root formation through activating CDPK activity and the application of  $\text{Ca}^{2+}$  channel inhibitors significantly suppressed NO- and IAA-induced development of adventitious rooting which indicated that  $\text{Ca}^{2+}$  is required for the adventitious rooting process. Our results further revealed that  $\text{Ca}^{2+}/\text{CaM}$  played an essential role in NO-induced adventitious rooting under abiotic stress.  $\text{Ca}^{2+}/\text{CaM}$  might be a downstream signaling in the NO-induced adventitious rooting under osmotic stress.

The application of SNP elevated intracellular  $\text{Ca}^{2+}$  in cucumber hypocotyls under osmotic stress which indicated that the promotive effect of NO under osmotic stress was dependent on increasing the production of  $\text{Ca}^{2+}$  in plant cell. Abdul-Awal et al. (2016) reported that NO could mediate increases of  $[\text{Ca}^{2+}]_{\text{cyt}}$  through activity of ADP-Ribosyl Cyclase in *Arabidopsis*. Ma et al. (2008) also suggested that NO synthesis might be activated by  $\text{Ca}^{2+}$  through CaMs in *Arabidopsis*. These studies suggested that NO and  $\text{Ca}^{2+}$  may modulate each other's level to regulate the plant developmental and physiological processes. In our study, SNP + cPTIO, SNP +  $\text{NaN}_3$  and SNP +  $\text{Na}_2\text{WO}_4$  significantly inhibited the level of endogenous  $\text{Ca}^{2+}$  during adventitious root formation (**Figures 6A,B**). In addition, treatment with PEG + cPTIO or PEG +  $\text{Na}_2\text{WO}_4$  significantly decreased the production of endogenous  $\text{Ca}^{2+}$  in

hypocotyl as well. Therefore,  $\text{Ca}^{2+}$  might be as downstream of NO in the development of adventitious root under osmotic stress. In previous studies, hydrogen gas ( $\text{H}_2$ ) (Zhu et al., 2016), carbon monoxide (CO) (Chen et al., 2017) and  $\text{H}_2\text{O}_2$  (Xuan et al., 2008; Yang et al., 2013) were also suggested to be involved in plants adventitious rooting. These signaling molecules may mediate each other through activation of receptors or targeted protein to affect the process of adventitious rooting in plants. Additionally, Endogenous NO might accumulate during the development of adventitious root (**Figure 6C**). Previous studies showed that NO could be an essential signaling molecule to regulate the development and growth of adventitious roots in plants (Lanteri et al., 2008; Liao et al., 2012a). Pagnussat et al. (2002) also suggested that NO might be involved in auxin-induced adventitious root formation through transient NO accumulation in cucumber explants. These results indicated that NO is responsible for the adventitious root organogenesis. Silveira et al. (2017a) found that drought-tolerant sugarcane genotype could accumulate more NO than the sensitive one, suggesting that there might exist an association between drought-tolerance and NO production and metabolism. Interestingly,  $\text{CaCl}_2$  treatment also increased the content of endogenous NO as well which implied that there might be a close interplay between NO and  $\text{Ca}^{2+}$  during the development of adventitious roots in cucumber under stress condition.

## Activation of Antioxidative Response during Adventitious Rooting under Osmotic Stress

An increase in the ROS level might induce membrane lipid peroxidation in cells (Panyuta et al., 2016). In order to investigate the effects of SNP and  $\text{CaCl}_2$  on the development of adventitious root under osmotic stress, the changes in TBARS in cucumber explants were analyzed. At 48 h, PEG treatment significantly enhanced the concentration of TBARS in comparison with the control (**Figure 8A**), which implied that osmotic stress might induce the accumulation of TBARS (Jaleel et al., 2007). In addition, PEG + SNP and PEG +  $\text{CaCl}_2$  treatments significantly reduced the content of TBARS compared to PEG treatment (**Figure 8A**). Previous study showed NO could protect sunflower leaves under Cd-induced oxidative stress by decreasing TBARS content (Laspina et al., 2005). Besides, Larkindale and Knight (2002) also suggested that inhibiting the endogenous  $\text{Ca}^{2+}$  content could increase the oxidative damage under heat stress by increasing the TBARS content in *Arabidopsis*. Our results showed that the application of SNP or  $\text{CaCl}_2$  significantly decrease TBARS content in cucumber explant under osmotic stress (**Figure 8A**). However, the TBARS content of EGTA, BAPTA/AM, TFP, W-7,  $\text{LaCl}_3$  or nifedipine treatments were significantly higher than those of SNP or  $\text{CaCl}_2$  treatments. These results indicated that removal of endogenous  $\text{Ca}^{2+}$  during NO-induced adventitious rooting under osmotic stress probably increased the level of membrane lipid peroxidation, hence, aggravated oxidative stress and caused cell death or the decrease of relative antioxidant enzymes activities (Liu et al., 2013; Chen et al., 2015).

$\text{H}_2\text{O}_2$  or  $\text{O}_2^-$ , which was a form of ROS, also caused oxidative damage in plants under stressful condition (Romero-Puertas et al., 2004; Cho and Seo, 2005). Wang and Yang (2005) found that SNP pre-treatment significantly inhibited the generation of  $\text{O}_2^-$  and  $\text{H}_2\text{O}_2$  in the roots of *Cassia tora* L under Aluminum (Al) stress. Another research also found that there is a reduction in the content of  $\text{H}_2\text{O}_2$ , TBARS and other ROS in  $\text{CaCl}_2$  treatment in soybean seedlings under salt stress (Arshi et al., 2010). Our results showed that SNP or  $\text{CaCl}_2$  treatments under osmotic stress significantly reduced the production of  $\text{H}_2\text{O}_2$  or  $\text{O}_2^-$  during the process of adventitious root development (**Figures 8B,C**). However, the application of  $\text{Ca}^{2+}$  chelators,  $\text{Ca}^{2+}$  channel inhibitors or CaM antagonist might keep a higher level  $\text{H}_2\text{O}_2$  or  $\text{O}_2^-$  content than those of SNP or  $\text{CaCl}_2$  treatment. These findings also suggest that NO or  $\text{Ca}^{2+}$  might reverse the damage of osmotic stress during adventitious rooting by blocking the generation of ROS in cucumber explants.

There are several reports that NO or  $\text{Ca}^{2+}$  might have the capacity to regulate the antioxidant system by increasing the activities of antioxidant enzymes under various stresses (Shi K. et al., 2015; Zou et al., 2015; Silveira et al., 2017b). Our results showed that SNP,  $\text{CaCl}_2$  or SNP +  $\text{CaCl}_2$  treatment significantly increased the activities of antioxidant enzymes during the development of adventitious root under osmotic stress. SOD, CAT and APX activities in cucumbers treated with SNP,  $\text{CaCl}_2$  or SNP +  $\text{CaCl}_2$  were higher than those of PEG treatment (**Figure 9**). Li et al. (2016) suggested that  $\text{Ca}^{2+}$  could alleviate the inhibition of Cd on the root growth by reducing oxidative injuries which indicated that there could be a relationship between the root growth and oxidative system. Moreover, El-Shabrawi et al. (2010) also found that there was a positive relationship between increased antioxidant defense mechanism and the reduction of oxidative damage. The increased activities of antioxidant enzymes increased oxidation resistance by decreasing ROS generation rate during adventitious rooting process.

## Enhancement of Water Retention and Photosynthetic Activity under Osmotic Stress

In order to confirm the influence of PEG-induced osmotic stress, leaf  $\Psi_w$  in cucumber was determined in our experiment (**Figure 7**). Previous study found that Cd might decrease leaf  $\Psi_w$  and relative water content (RWC) in bean plants (Barcelo et al., 1986). Wilson et al. (2014) also suggested that plastid osmotic stress might significantly decreased water potential in *Arabidopsis*. In our study, greater reduction in leaf  $\Psi_w$  was observed with PEG treatment compared to the control (**Figure 7**). The leaf  $\Psi_w$  was significantly increased by exogenous supplied SNP or  $\text{CaCl}_2$  under osmotic stress. Recent research suggested NO might alleviate water deficit stress through increasing leaf  $\Psi_w$  and RWC in *Cakile maritima* (Jday et al., 2016). Our results indicated that application of exogenous NO might increase the water potential in cucumber under stress condition to alleviate the damage of osmotic stress during adventitious rooting. Meanwhile, inhibition of

endogenous  $\text{Ca}^{2+}$  accumulation might reverse the positive effect of NO on alleviating the osmotic damage during the development of adventitious root in cucumber.

Górnik et al. (2008) found that drought stress reduced chlorophyll content in the leaves during rooting of grapevine cuttings. In addition, Humphries and Thorne (1964) suggested that photosynthesis was retarded when root growth was restricted by application of kinetin. These results imply that there is a link between photosynthesis and rooting. Uchida et al. (2002) found that suitable concentration of NO restored the chlorophyll levels in rice leaves and protected photosystem II (PSII) to maintain a relatively high activity under salt and heat stresses. Also, Silveira et al. (2016) indicated that exogenous NO might improve photosynthesis under water deficit and Tiwari et al. (2016) noticed that  $\text{Ca}^{2+}$  application alleviated the reduction of chl a under heat stress. The application of  $\text{CaCl}_2$  enhanced photosynthesis by increasing the contents of chl a, chl b, and chl (a + b) in *Zoysia japonica* under drought stress (Xu et al., 2013). In our study, the content of chl a, chl b, or chl (a + b) in cucumbers treated with PEG was significantly lower than those of control, while application of SNP or  $\text{CaCl}_2$  under osmotic stress increased the concentrations of chl a, chl b, or chl (a + b) to levels higher than PEG treatment alone (**Figure 10**). These findings indicated that NO or  $\text{CaCl}_2$  treatment might significantly prevent the degradation of chlorophyll in cucumber in order to promote photosynthesis during adventitious rooting under osmotic stress. The EGTA, BAPTA/AM, TFP, W-7,  $\text{LaCl}_3$  and nifedipine, however, caused significant degradation of chlorophyll content in the leaves. It has been reported that abiotic stress led to decreases in photosynthetic rates by affecting chlorophyll fluorescence parameters in plants (Hou et al., 2016). In our study, PEG treatment significantly decreased the value of Fv/Fm,  $\Phi_{\text{PSII}}$  or qP but increased NPQ. However, SNP or  $\text{CaCl}_2$  treatment increased Fv/Fm,  $\Phi_{\text{PSII}}$  or qP which implied that NO or  $\text{CaCl}_2$  could reduce damage to photosynthesis under osmotic stress, maintaining the photochemical activity. Zhang et al. (2012) found that NO alleviated iron-deficiency in peanut leaves via increasing Fv/Fm and  $\Phi_{\text{PSII}}$  which suggested that NO had a protective effect on photosystem II (PSII) in plants. In addition, Zhao and Tan (2005) reported that exogenous  $\text{Ca}^{2+}$  also played a crucial role in protecting photochemistry in wheat plants under heat and high irradiance stresses. However, EGTA or  $\text{LaCl}_3$  treatment had the opposite effect which indicated that endogenous  $\text{Ca}^{2+}$  might be involved in mediating photosynthesis in wheat. These results indicated that there might be a positive relationship between adventitious rooting and photosynthetic level. Besides,  $\text{Ca}^{2+}$  might be a downstream molecule involved in NO-induced formation of photosynthetic pigments and increases of photochemical activity in order to promote adventitious rooting under osmotic stress.

## CONCLUSION

The results of our experiments have shown that exogenous application of NO and  $\text{CaCl}_2$  alleviated osmotic stress and

promoted the development of adventitious roots in cucumber under stressful conditions. Our data also revealed that  $\text{Ca}^{2+}/\text{CaM}$  might be downstream molecules of NO signaling pathway, protecting photosynthetic system and stimulating the antioxidant defense system. As there is a complex interaction between NO and  $\text{Ca}^{2+}/\text{CaM}$  in the adventitious rooting process under abiotic stress, further work should focus on the molecular mechanism of the crosstalk between NO and  $\text{Ca}^{2+}/\text{CaM}$  during signaling transduction under various stresses.

## AUTHOR CONTRIBUTIONS

WL designed the experiments; LN and JY performed the experiments; WL, LN, and MZ performed data analysis; WL, LN, and JY wrote the manuscript; WL, JhY, and MD edited the manuscript.

## REFERENCES

- Abdul-Awal, S. M., Hotta, C. T., Davey, M. P., Dodd, A. N., Smith, A. G., and Webb, A. A. (2016). NO-mediated  $[\text{Ca}^{2+}]_{\text{cyt}}$  increases depend on ADP-ribosyl cyclase activity in *Arabidopsis*. *Plant Physiol.* 171, 623–631. doi: 10.1104/pp.15.01965
- Aebi, H. (1984). Catalase *in vitro*. *Methods Enzymol.* 105, 121–126. doi: 10.1016/S0076-6879(84)05016-3
- Arnon, D. I. (1949). Copper enzymes in isolated chloroplasts. Polyphenol oxidase in *Beta vulgaris*. *Plant Physiol.* 24, 1–15. doi: 10.1104/pp.24.1.1
- Arshi, A., Ahmad, A., Aref, I. M., and Iqbal, M. (2010). Calcium interaction with salinity-induced effects on growth and metabolism of soybean (*Glycine max* L.) cultivars. *J. Environ. Biol.* 31, 795–801.
- Barcelo, J., Poschenrieder, C., Andreu, I., and Gunse, B. (1986). Cadmium-induced decrease of water stress resistance in bush bean plants (*Phaseolus vulgaris* L. cv. Contender) I. Effects of Cd on water potential, relative water content, and cell wall elasticity. *J. Plant Physiol.* 125, 17–25. doi: 10.1016/S0176-1617(86)80239-5
- Beligni, M. V., and Lamattina, L. (2000). Nitric oxide stimulates seed germination and de-etiolation, and inhibits hypocotyl elongation, three light-inducible responses in plants. *Planta* 210, 215–221. doi: 10.1007/PL00008128
- Búfalo, J., Rodrigues, T. M., de Almeida, L. F. R., dos Santos Tozin, L. R., Marques, M. O. M., and Boaro, C. S. F. (2016). PEG-induced osmotic stress in *Mentha x piperita* L.: structural features and metabolic responses. *Plant Physiol. Biochem.* 105, 174–184. doi: 10.1016/j.plaphy.2016.04.009
- Bündig, C., Jozefowicz, A. M., Mock, H. P., and Winkelmann, T. (2016). Proteomic analysis of two divergently responding potato genotypes (*Solanum tuberosum* L.) following osmotic stress treatment *in vitro*. *J. Proteomics* 143, 227–241. doi: 10.1016/j.jprot.2016.04.048
- Cakmak, I., and Horst, W. J. (1991). Effect of aluminium on lipid peroxidation, superoxide dismutase, catalase, and peroxidase activities in root tips of soybean (*Glycine max*). *Physiol. Plant.* 83, 463–468. doi: 10.1111/j.1399-3054.1991.tb00121.x
- Chaitanya, K. K., and Naithani, S. C. (1994). Role of superoxide, lipid peroxidation and superoxide dismutase in membrane perturbation during loss of viability in seeds of *Shorea robusta* Gaertn. f. *New Phytol.* 126, 623–627. doi: 10.1111/j.1469-8137.1994.tb02957.x
- Chen, H., Gao, H., Fang, X., Ye, L., Zhou, Y., and Yang, H. (2015). Effects of allyl isothiocyanate treatment on postharvest quality and the activities of antioxidant enzymes of mulberry fruit. *Postharvest Biol. Technol.* 108, 61–67. doi: 10.1016/j.postharvbio.2015.05.011
- Chen, Y., Wang, M., Hu, L., Liao, W., Dawuda, M. M., and Li, C. (2017). Carbon monoxide is involved in hydrogen gas-induced adventitious root development in cucumber under simulated drought stress. *Front. Plant Sci.* 8:128. doi: 10.3389/fpls.2017.00128
- Chen, Y. H., and Kao, C. H. (2012). Calcium is involved in nitric oxide- and auxin-induced lateral root formation in rice. *Protoplasma* 249, 187–195. doi: 10.1007/s00709-011-0277-2
- Cho, U. H., and Seo, N. H. (2005). Oxidative stress in *Arabidopsis thaliana* exposed to cadmium is due to hydrogen peroxide accumulation. *Plant Sci.* 168, 113–120. doi: 10.1016/j.plantsci.2004.07.021
- Dhindsa, R. S., Plumb-Dhindsa, P., and Thorpe, T. A. (1981). Leaf senescence: correlated with increased levels of membrane permeability and lipid peroxidation, and decreased levels of superoxide dismutase and catalase. *J. Exp. Bot.* 32, 93–101. doi: 10.1093/jxb/32.1.93
- El-Shabrawi, H., Kumar, B., Kaul, T., Reddy, M. K., Singla-Pareek, S. L., and Sopory, S. K. (2010). Redox homeostasis, antioxidant defense, and methylglyoxal detoxification as markers for salt tolerance in Pokkali rice. *Protoplasma* 245, 85–96. doi: 10.1007/s00709-010-0144-6
- Garcia-Mata, C., and Lamattina, L. (2001). Nitric oxide induces stomatal closure and enhances the adaptive plant responses against drought stress. *Plant Physiol.* 126, 1196–1204. doi: 10.1104/pp.126.3.1196
- Genty, B., Briantais, J. M., and Baker, N. R. (1989). The relationship between the quantum yield of photosynthetic electron transport and quenching of chlorophyll fluorescence. *Biochim. Biophys. Acta* 990, 87–92. doi: 10.1016/S0304-4165(89)80016-9
- González, A., de los Ángeles Cabrera, M., Henríquez, M. J., Contreras, R. A., Morales, B., and Moenne, A. (2012). Cross talk among calcium, hydrogen peroxide, and nitric oxide and activation of gene expression involving calmodulins and calcium-dependent protein kinases in *Ulva compressa* exposed to copper excess. *Plant Physiol.* 158, 1451–1462. doi: 10.1104/pp.111.191759
- Górnik, K., Grzesik, M., and Romanowska-Duda, B. (2008). The effect of chitosan on rooting of grapevine cuttings and on subsequent plant growth under drought and temperature stress. *J. Fruit Ornam. Plant Res.* 16, 333–343.
- Graziano, M., and Lamattina, L. (2007). Nitric oxide accumulation is required for molecular and physiological responses to iron deficiency in tomato roots. *Plant J.* 52, 949–960. doi: 10.1111/j.1365-313X.2007.03283.x
- Hou, W., Sun, A. H., Chen, H. L., Yang, F. S., Pan, J. L., and Guan, M. Y. (2016). Effects of chilling and high temperatures on photosynthesis and chlorophyll fluorescence in leaves of watermelon seedlings. *Biol. Plant.* 60, 148–154. doi: 10.1007/s10535-015-0575-1
- Humphries, E. C., and Thorne, G. N. (1964). The effect of root formation on photosynthesis of detached leaves. *Ann. Bot.* 28, 391–400. doi: 10.1111/j.1438-8677.2008.00104.x
- Jaleel, C. A., Gopi, R., Sankar, B., Manivannan, P., Kishorekumar, A., Sridharan, R., et al. (2007). Studies on germination, seedling vigour, lipid peroxidation and

## ACKNOWLEDGMENTS

We thank the reviewers for their valuable comments. This work was supported by the National Natural Science Foundation of China (Nos. 31160398 and 31560563), the Post Doctoral Foundation of China (Nos. 20100470887 and 2012T50828), the Key Project of Chinese Ministry of Education (No. 211182), the Research Fund for the Doctoral Program of Higher Education (No. 20116202120005), the Natural Science Foundation of Gansu References Province, China (Nos. 1308RJZA179, 1308RJZA262, 1606RJZA073, and 1606RJZA077), and Feitian and Fuxi Excellent Talents in Gansu Agricultural University in Lanzhou, China.

## SUPPLEMENTARY MATERIAL

The Supplementary Material for this article can be found online at: <http://journal.frontiersin.org/article/10.3389/fpls.2017.01684/full#supplementary-material>

- proline metabolism in *Catharanthus roseus* seedlings under salt stress. *S. Afr. J. Bot.* 73, 190–195. doi: 10.1016/j.sajb.2006.11.001
- Jday, A., Rejeb, K. B., Slama, I., Saadallah, K., Bordenave, M., Planchais, S., et al. (2016). Effects of exogenous nitric oxide on growth, proline accumulation and antioxidant capacity in cakile maritima seedlings subjected to water deficit stress. *Funct. Plant Biol.* 43, 939–948. doi: 10.1071/FP15363
- Jiang, M., Yang, W., Xu, J., and Chen, Q. (1993). Active oxygen damage effect of chlorophyll degradation in rice seedlings under osmotic stress. *Acta Bot. Sin.* 36, 289–295.
- Kaur, G., Singh, H. P., Batish, D. R., Mahajan, P., Kohli, R. K., and Rishi, V. (2015). Exogenous nitric oxide (NO) interferes with lead (Pb)-induced toxicity by detoxifying reactive oxygen species in hydroponically grown wheat (*Triticum aestivum*) roots. *PLOS ONE* 10:e0138713. doi: 10.1371/journal.pone.0138713
- Kong, D. J., Ju, C. L., Parihar, A., Kim, S., Cho, D., and Kwak, J. M. (2015). *Arabidopsis* glutamate receptor homolog3.5 modulates cytosolic Ca<sup>2+</sup> level to counteract effect of abscisic acid in seed germination. *Plant Physiol.* 167, 1630–1642. doi: 10.1104/pp.114.251298
- Lang, T., Sun, H. M., Li, N. Y., Lu, Y. J., Shen, Z. D., Jing, X. S., et al. (2014). Multiple signaling networks of extracellular ATP, hydrogen peroxide, calcium, and nitric oxide in the mediation of root ion fluxes in secretor and non-secretor mangroves under salt stress. *Aquat. Bot.* 119, 33–43. doi: 10.1016/j.aquabot.2014.06.009
- Lanteri, M. L., Laxalt, A. M., and Lamattina, L. (2008). Nitric oxide triggers phosphatidic acid accumulation via phospholipase D during auxin-induced adventitious root formation in cucumber. *Plant Physiol.* 147, 188–198. doi: 10.1104/pp.107.111815
- Lanteri, M. L., Pagnussat, G. C., and Lamattina, L. (2006). Calcium and calcium-dependent protein kinases are involved in nitric oxide-and auxin-induced adventitious root formation in cucumber. *J. Exp. Bot.* 57, 1341–1351. doi: 10.1093/jxb/erj109
- Larkindale, J., and Knight, M. R. (2002). Protection against heat stress-induced oxidative damage in *Arabidopsis* involves calcium, abscisic acid, ethylene, and salicylic acid. *Plant Physiol.* 128, 682–695. doi: 10.1104/pp.010320
- Laspina, N. V., Groppa, M. D., Tomaro, M. L., and Benavides, M. P. (2005). Nitric oxide protects sunflower leaves against Cd-induced oxidative stress. *Plant Sci.* 169, 323–330. doi: 10.1016/j.plantsci.2005.02.007
- Li, P., Zhao, C. Z., Zhang, Y. Q., Wang, X. M., Wang, X. Y., Wang, J. F., et al. (2016). Calcium alleviates cadmium-induced inhibition on root growth by maintaining auxin homeostasis in *Arabidopsis* seedlings. *Protoplasma* 253, 185–200. doi: 10.1007/s00709-015-0810-9
- Liao, W. B., Huang, G. B., Yu, J. H., and Zhang, M. L. (2012a). Nitric oxide and hydrogen peroxide alleviate drought stress in marigold explants and promote its adventitious root development. *Plant Physiol. Biochem.* 58, 6–15. doi: 10.1016/j.plaphy.2012.06.012
- Liao, W. B., Huang, G. B., Yu, J. H., Zhang, M. L., and Shi, X. L. (2011). Nitric oxide and hydrogen peroxide are involved in indole-3-butryric acid-induced adventitious root development in marigold. *J. Hortic. Sci. Biotechnol.* 86, 159–165. doi: 10.1080/14620316.2011.11512742
- Liao, W. B., Zhang, M. L., Huang, G. B., and Yu, J. H. (2012b). Ca<sup>2+</sup> and CaM are involved in NO- and H<sub>2</sub>O<sub>2</sub>-induced adventitious root development in marigold. *J. Plant Growth Regul.* 31, 253–264. doi: 10.1007/s00344-011-9235-7
- Liao, W. B., Zhang, M. L., and Yu, J. H. (2013). Role of nitric oxide in delaying senescence of cut rose flowers and its interaction with ethylene. *Sci. Hortic.* 155, 30–38. doi: 10.1016/j.scientia.2013.03.005
- Liu, J., Macarisin, D., Wisniewski, M., Sui, Y., Drobys, S., Norelli, J., et al. (2013). Production of hydrogen peroxide and expression of ROS-generating genes in peach flower petals in response to host and non-host fungal pathogens. *Plant Pathol.* 62, 820–828. doi: 10.1111/j.1365-3059.2012.02683.x
- Liu, W., Li, R. J., Han, T. T., Cai, W., Fu, Z. W., and Lu, Y. T. (2015). Salt stress reduces root meristem size by nitric oxide-mediated modulation of auxin accumulation and signaling in *Arabidopsis*. *Plant Physiol.* 168, 343–356. doi: 10.1104/pp.15.00030
- Liu, Z., Chen, W., and He, X. (2015). Influence of Cd<sup>2+</sup> on growth and chlorophyll fluorescence in a hyperaccumulator: *Lonicera japonica* Thunb. *J. Plant Growth Regul.* 34, 672–676. doi: 10.1007/s00344-015-9483-z
- Ma, W., Smigel, A., Tsai, Y. C., Braam, J., and Berkowitz, G. A. (2008). Innate immunity signaling: cytosolic Ca<sup>2+</sup> elevation is linked to downstream nitric oxide generation through the action of calmodulin or a calmodulin-like protein. *Plant Physiol.* 148, 818–828. doi: 10.1104/pp.108.125104
- Nakano, Y., and Asada, K. (1981). Hydrogen peroxide is scavenged by ascorbate-specific peroxidase in spinach chloroplasts. *Plant Cell Physiol.* 22, 867–880.
- Neill, S. J., Desikan, R., Clarke, A., and Hancock, J. T. (2002). Nitric oxide is a novel component of abscisic acid signaling in stomatal guard cells. *Plant Physiol.* 128, 13–16. doi: 10.1104/pp.010707
- Pagnussat, G. C., Simontacchi, M., Puntarulo, S., and Lamattina, L. (2002). Nitric oxide is required for root organogenesis. *Plant Physiol.* 129, 954–956. doi: 10.1104/pp.004036
- Panyuta, O., Belava, V., Fomaidi, S., Kalinichenko, O., Volkogon, M., and Taran, N. (2016). The effect of pre-sowing seed treatment with metal nanoparticles on the formation of the defensive reaction of wheat seedlings infected with the eyespot causal agent. *Nanoscale Res. Lett.* 11, 92. doi: 10.1186/s11671-016-1305-0
- Reiss, H. D., and Herth, W. (1985). Nifedipine-sensitive calcium channels are involved in polar growth of lily pollen tubes. *J. Cell Sci.* 76, 247–254.
- Rockel, P., Strube, F., Rockel, A., Wildt, J., and Kaiser, W. M. (2002). Regulation of nitric oxide (NO) production by plant nitrate reductase *in vivo* and *in vitro*. *J. Exp. Bot.* 53, 103–110. doi: 10.1093/jxb/53.366.103
- Romero-Puertas, M. C., Rodríguez-Serrano, M., Corpas, F. J., Gomez, M. D., and Del Rio, L. A. (2004). Cadmium-induced subcellular accumulation of O<sub>2</sub>- and H<sub>2</sub>O<sub>2</sub> in pea leaves. *Plant Cell Environ.* 27, 1122–1134. doi: 10.1111/j.1365-3040.2004.01217.x
- Sadiqov, S. T., Akbulut, M., and Ehmedov, V. (2002). Role of Ca<sup>2+</sup> in drought stress signaling in wheat seedlings. *Biochemistry (Moscow)* 67, 491–497. doi: 10.1023/A:1015298309888
- Salgado, I., Martínez, M. C., Oliveira, H. C., and Frungillo, L. (2013). Nitric oxide signaling and homeostasis in plants: a focus on nitrate reductase and S-nitrosoglutathione reductase in stress-related responses. *Braz. J. Bot.* 36, 89–98. doi: 10.1007/s40415-013-0013-6
- Shan, C. J., Zhou, Y., and Liu, M. J. (2015). Nitric oxide participates in the regulation of the ascorbate-glutathione cycle by exogenous jasmonic acid in the leaves of wheat seedlings under drought stress. *Protoplasma* 252, 1397–1405. doi: 10.1007/s00709-015-0756-y
- Shi, C., Qi, C., Ren, H., Huang, A., Hei, S., and She, X. (2015). Ethylene mediates brassinosteroid-induced stomatal closure via Gα protein-activated hydrogen peroxide and nitric oxide production in *Arabidopsis*. *Plant J.* 82, 280–301. doi: 10.1111/tpj.12815
- Shi, K., Li, X., Zhang, H., Zhang, G. Q., Liu, Y. R., Zhou, Y. H., et al. (2015). Guard cell hydrogen peroxide and nitric oxide mediate elevated CO<sub>2</sub>-induced stomatal movement in tomato. *New Phytol.* 208, 342–353. doi: 10.1111/nph.13621
- Silveira, N. M., Frungillo, L., Marcos, F. C., Pelegrino, M. T., Miranda, M. T., Seabra, A. B., et al. (2016). Exogenous nitric oxide improves sugarcane growth and photosynthesis under water deficit. *Planta* 244, 181–190. doi: 10.1007/s00425-016-2501-y
- Silveira, N. M., Hancock, J. T., Frungillo, L., Siasou, E., Marcos, F. C., Salgado, I., et al. (2017a). Evidence towards the involvement of nitric oxide in drought tolerance of sugarcane. *Plant Physiol. Biochem.* 115, 354–359. doi: 10.1016/j.plaphy.2017.04.011
- Silveira, N. M., Marcos, F. C., Frungillo, L., Moura, B. B., Seabra, A. B., Salgado, I., et al. (2017b). S-nitrosoglutathione spraying improves stomatal conductance, Rubisco activity and antioxidant defense in both leaves and roots of sugarcane plants under water deficit. *Physiol. Plant.* 160, 383–395. doi: 10.1111/ppl.12575
- Skiba, U., Smith, K. A., and Fowler, D. (1993). Nitrification and denitrification as sources of nitric oxide and nitrous oxide in a sandy loam soil. *Soil Biol. Biochem.* 25, 1527–1536. doi: 10.1016/0038-0717(93)90007-X
- Tang, R. J., Zhao, F. G., Garcia, V. J., Kleist, T. J., Yang, L., Zhang, H. X., et al. (2015). Tonoplast CBL-CIPK calcium signaling network regulates magnesium homeostasis in *Arabidopsis*. *Proc. Natl. Acad. Sci. U.S.A.* 112, 3134–3139. doi: 10.1073/pnas.1420944112
- Tian, Q. Y., Sun, D. H., Zhao, M. G., and Zhang, W. H. (2007). Inhibition of nitric oxide synthase (NOS) underlies aluminum-induced inhibition of root elongation in *Hibiscus moscheutos*. *New Phytol.* 174, 322–331. doi: 10.1111/j.1469-8137.2007.02005.x
- Tiwari, A., Singh, P., and Asthana, R. K. (2016). Role of calcium in the mitigation of heat stress in the cyanobacterium *Anabaena* PCC 7120. *J. Plant Physiol.* 199, 67–75. doi: 10.1016/j.jplph.2016.05.012

- Uchida, A., Jagendorf, A. T., Hibino, T., Takabe, T., and Takabe, T. (2002). Effects of hydrogen peroxide and nitric oxide on both salt and heat stress tolerance in rice. *Plant Sci.* 163, 515–523. doi: 10.1016/S0168-9452(02)00159-0
- Velikova, V., Yordanov, I., and Edreva, A. (2000). Oxidative stress and some antioxidant systems in acid rain-treated bean plants: protective role of exogenous polyamines. *Plant Sci.* 151, 59–66. doi: 10.1016/S0168-9452(99)00197-1
- Wang, P., Zhu, J. K., and Lang, Z. (2015). Nitric oxide suppresses the inhibitory effect of abscisic acid on seed germination by S-nitrosylation of SnRK2 proteins. *Plant Signal. Behav.* 10:e1031939. doi: 10.1080/15592324.2015.1031939
- Wang, W. H., Yi, X. Q., Han, A. D., Liu, T. W., Chen, J., Wu, F. H., et al. (2012). Calcium-sensing receptor regulates stomatal closure through hydrogen peroxide and nitric oxide in response to extracellular calcium in *Arabidopsis*. *J. Exp. Bot.* 63, 177–190. doi: 10.1093/jxb/err259
- Wang, Y. H., Chen, T., Zhang, C. Y., Hao, H. Q., Liu, P., Zheng, M. Z., et al. (2009). Nitric oxide modulates the influx of extracellular Ca<sup>2+</sup> and actin filament organization during cell wall construction in *Pinus bungeana* pollen tubes. *New Phytol.* 182, 851–862. doi: 10.1111/j.1469-8137.2009.02820.x
- Wang, Y. S., and Yang, Z. M. (2005). Nitric oxide reduces aluminum toxicity by preventing oxidative stress in the roots of *Cassia tora* L. *Plant Cell Physiol.* 46, 1915–1923. doi: 10.1093/pcp/pci202
- Wilson, M. E., Basu, M. R., Bhaskara, G. B., Verslues, P. E., and Haswell, E. S. (2014). Plastid osmotic stress activates cellular stress responses in *Arabidopsis*. *Plant Physiol.* 165, 119–128. doi: 10.1104/pp.114.236620
- Wu, G. Q., Feng, R. J., and Shui, Q. Z. (2016). Effect of osmotic stress on growth and osmolytes accumulation in sugar beet (*Beta vulgaris* L.) plants. *Plant Soil Environ.* 62, 189–194. doi: 10.17221/101/2016-PSE
- Xu, C., Li, X., and Zhang, L. (2013). The effect of calcium chloride on growth, photosynthesis, and antioxidant responses of *Zoysia japonica* under drought conditions. *PLOS ONE* 8:e68214. doi: 10.1371/journal.pone.0068214
- Xu, Y. F., Chu, X. T., Fu, J. J., Yang, L. Y., and Hu, T. M. (2016). Crosstalk of nitric oxide with calcium induced tolerance of tall fescue leaves to high irradiance. *Biol. Plant.* 60, 376–384. doi: 10.1007/s10535-016-0597-3
- Xuan, W., Zhu, F. Y., Xu, S., Huang, B. K., Ling, T. F., Qi, J. Y., et al. (2008). The heme oxygenase/carbon monoxide system is involved in the auxin-induced cucumber adventitious rooting process. *Plant Physiol.* 148, 881–893. doi: 10.1104/pp.108.125567
- Yang, W., Zhu, C., Ma, X., Li, G., Gan, L., Ng, D., et al. (2013). Hydrogen peroxide is a second messenger in the salicylic acid-triggered adventitious rooting process in mung bean seedlings. *PLOS ONE* 8:e84580. doi: 10.1371/journal.pone.0084580
- Zhang, W. H., Rengel, Z., and Kuo, J. (1998). Determination of intracellular Ca<sup>2+</sup> in cells of intact wheat roots: loading of acetoxymethyl ester of Fluo-3 under low temperature. *Plant J.* 15, 147–151. doi: 10.1046/j.1365-313X.1998.00188.x
- Zhang, X. W., Dong, Y. J., Qiu, X. K., Hu, G. Q., Wang, Y. H., and Wang, Q. H. (2012). Exogenous nitric oxide alleviates iron-deficiency chlorosis in peanut growing on calcareous soil. *Plant Soil Environ.* 58, 111–120.
- Zhao, H. J., and Tan, J. F. (2005). Role of calcium ion in protection against heat and high irradiance stress-induced oxidative damage to photosynthesis of wheat leaves. *Photosynthetica* 43, 473–476. doi: 10.1007/s11099-005-0076-0
- Zhao, X., Wang, J., Yuan, J., Wang, X. L., Zhao, Q. P., Kong, P. T., et al. (2015). Nitric Oxide-Associated Protein1 (AtNOA1) is essential for salicylic acid-induced root waving in *Arabidopsis thaliana*. *New Phytol.* 207, 211–224. doi: 10.1111/nph.13327
- Zhou, L. M., Lan, W. Z., Jiang, Y. Q., Fang, W., and Luan, S. (2014). A calcium-dependent protein kinase interacts with and activates a calcium channel to regulate pollen tube growth. *Mol. Plant* 7, 369–376. doi: 10.1093/mp/sst125
- Zhu, Y. C., Liao, W. B., Niu, L. J., Wang, M., and Ma, Z. J. (2016). Nitric oxide is involved in hydrogen gas-induced cell cycle activation during adventitious root formation in cucumber. *BMC Plant Biol.* 16:146. doi: 10.1186/s12870-016-0834-0
- Zorrilla-Fontanesi, Y., Rouard, M., Cenci, A., Kissel, E., Do, H., Dubois, E., et al. (2016). Differential root transcriptomics in a polyploid non-model crop: the importance of respiration during osmotic stress. *Sci. Rep.* 6:22583. doi: 10.1038/srep22583
- Zou, J. J., Li, X. D., Ratnasekera, D., Wang, C., Liu, W. X., Song, L. F., et al. (2015). *Arabidopsis* Calcium-Dependent Protein Kinase8 and Catalase3 function in abscisic acid-mediated signaling and H<sub>2</sub>O<sub>2</sub> homeostasis in stomatal guard cells under drought stress. *Plant Cell* 27, 1445–1460. doi: 10.1105/tpc.15.00144
- Zou, J. J., Wei, F. J., Wang, C., Wu, J. J., Ratnasekera, D., Liu, W. X., et al. (2010). *Arabidopsis* calcium-dependent protein kinase CPK10 functions in abscisic acid- and Ca<sup>2+</sup>-mediated stomatal regulation in response to drought stress. *Plant Physiol.* 154, 1232–1243. doi: 10.1104/pp.110.157545
- Conflict of Interest Statement:** The authors declare that the research was conducted in the absence of any commercial or financial relationships that could be construed as a potential conflict of interest.
- Copyright © 2017 Niu, Yu, Liao, Yu, Zhang and Dawuda. This is an open-access article distributed under the terms of the Creative Commons Attribution License (CC BY). The use, distribution or reproduction in other forums is permitted, provided the original author(s) or licensor are credited and that the original publication in this journal is cited, in accordance with accepted academic practice. No use, distribution or reproduction is permitted which does not comply with these terms.



# Cytosolic and Nucleosolic Calcium Signaling in Response to Osmotic and Salt Stresses Are Independent of Each Other in Roots of *Arabidopsis* Seedlings

Feifei Huang, Jin Luo, Tingting Ning, Wenhan Cao, Xi Jin, Heping Zhao, Yingdian Wang and Shengcheng Han\*

Beijing Key Laboratory of Gene Resource and Molecular Development, College of Life Sciences, Beijing Normal University, Beijing, China

## OPEN ACCESS

### Edited by:

Simon Gilroy,  
University of Wisconsin-Madison,  
United States

### Reviewed by:

Melanie Krebs,  
Centre for Organismal Studies,  
University of Heidelberg, Germany  
Yule Liu,  
Tsinghua University, China

### \*Correspondence:

Shengcheng Han  
schan@bnu.edu.cn

### Specialty section:

This article was submitted to  
Plant Cell Biology,  
a section of the journal  
*Frontiers in Plant Science*

Received: 13 July 2017

Accepted: 07 September 2017

Published: 21 September 2017

### Citation:

Huang F, Luo J, Ning T, Cao W, Jin X, Zhao H, Wang Y and Han S (2017) Cytosolic and Nucleosolic Calcium Signaling in Response to Osmotic and Salt Stresses Are Independent of Each Other in Roots of *Arabidopsis* Seedlings. *Front. Plant Sci.* 8:1648.  
doi: 10.3389/fpls.2017.01648

Calcium acts as a universal second messenger in both developmental processes and responses to environmental stresses. Previous research has shown that a number of stimuli can induce  $[Ca^{2+}]$  increases in both the cytoplasm and nucleus in plants. However, the relationship between cytosolic and nucleosolic calcium signaling remains obscure. Here, we generated transgenic plants containing a fusion protein, comprising rat parvalbumin (PV) with either a nuclear export sequence (PV-NES) or a nuclear localization sequence (NLS-PV), to selectively buffer the cytosolic or nucleosolic calcium. Firstly, we found that the osmotic stress-induced cytosolic  $[Ca^{2+}]$  increase ( $OICl_{cyt}$ ) and the salt stress-induced cytosolic  $[Ca^{2+}]$  increase ( $SICl_{cyt}$ ) were impaired in the PV-NES lines compared with the *Arabidopsis* wildtype (WT). Similarly, the osmotic stress-induced nucleosolic  $[Ca^{2+}]$  increase ( $OICl_{nuc}$ ) and salt stress-induced nucleosolic  $[Ca^{2+}]$  increase ( $SICl_{nuc}$ ) were also disrupted in the NLS-PV lines. These results indicate that PV can effectively buffer the increase of  $[Ca^{2+}]$  in response to various stimuli in *Arabidopsis*. However, the  $OICl_{cyt}$  and  $SICl_{cyt}$  in the NLS-PV plants were similar to those in the WT, and the  $OICl_{nuc}$  and  $SICl_{nuc}$  in the PV-NES plants were also same as those in the WT, suggesting that the cytosolic and nucleosolic calcium dynamics are mutually independent. Furthermore, we found that osmotic stress- and salt stress-inhibited root growth was reduced dramatically in the PV-NES and NLS-PV lines, while the osmotic stress-induced increase of the lateral root primordia was higher in the PV-NES plants than either the WT or NLS-PV plants. In addition, several stress-responsive genes, namely *CML37*, *DREB2A*, *MYB2*, *RD29A*, and *RD29B*, displayed diverse expression patterns in response to osmotic and salt stress in the PV-NES and NLS-PV lines when compared with the WT. Together, these results imply that the cytosolic and nucleosolic calcium signaling coexist to play the pivotal roles in the growth and development of plants and their responses to environment stresses.

**Keywords:** *Arabidopsis*, calcium dynamics, cytosolic calcium, nucleosolic calcium, parvalbumin, subcellular localization

## INTRODUCTION

Calcium is commonly accepted as a ubiquitous second messenger in eukaryotic organisms in which it regulates diverse biological processes, such as fertilization, pollen tube elongation, proliferation, neural signaling, and learning (Berridge et al., 2000; Bootman et al., 2001; Cullen and Lockyer, 2002). The cytosolic  $\text{Ca}^{2+}$  ( $[\text{Ca}^{2+}]_{\text{cyt}}$ ) increases or oscillations arise from an external  $\text{Ca}^{2+}$  influx, which is primarily mediated by the plasma membrane  $\text{Ca}^{2+}$  channels, such as CNGCs (DeFalco et al., 2016), GLRs (Davenport, 2002), annexins (Laohavisit et al., 2009) and hyperosmolarity-gated calcium-permeable channel (OSCas) (Yuan et al., 2014), and/or internal store  $\text{Ca}^{2+}$  release, which is mediated by endomembrane-localized  $\text{Ca}^{2+}$  channels, such as the vacuolar  $\text{Ca}^{2+}$ -activated two-pore channel 1 (TPC1) (Peiter et al., 2005). Although the voltage-dependent  $\text{Ca}^{2+}$  channels and ligand-gated  $\text{Ca}^{2+}$  channels, such as inositol 1,4,5-trisphosphate- and cyclic ADP ribose-activated channels (Muir and Sanders, 1997; Navazio et al., 2001), have been well characterized via electrophysiological approaches, no molecular identity has been found for these channels in plants to date. In addition, the efflux of  $[\text{Ca}^{2+}]_{\text{cyt}}$  is achieved by  $\text{Ca}^{2+}$ -ATPases and/or  $\text{Ca}^{2+}/\text{H}^+$  anti-porter systems (Kudla et al., 2010), which are responsible for the restoration of  $[\text{Ca}^{2+}]_{\text{cyt}}$  to pre-stimulus levels. Therefore, a given  $\text{Ca}^{2+}$  signal is generated by balancing, in a strictly regulated way, the activation of  $\text{Ca}^{2+}$  channels, the subsequent inactivation of channels, and the activation of efflux transporters to meet wide-ranging needs in plant growth and development.

Stimulus-specific  $\text{Ca}^{2+}$  signals, when viewed in terms of the spatial and temporal dynamics of the stimulus-induced changes in  $[\text{Ca}^{2+}]_{\text{cyt}}$ , have been called the ‘ $\text{Ca}^{2+}$  signature’ which is characterized by the duration, frequency, amplitude, and spatial location of  $[\text{Ca}^{2+}]$  (McAinsh and Pittman, 2009). The  $\text{Ca}^{2+}$  signature in plants has two basic patterns: the first is the circadian  $\text{Ca}^{2+}$  oscillation that occurs at the whole-tissue level (Johnson et al., 1995), which is mainly regulated by the CAS-IP<sub>3</sub> pathway in *Arabidopsis* (Tang et al., 2007) and is measured by an aequorin-based calcium indicator (Knight et al., 1991); the second is those short-term  $\text{Ca}^{2+}$  increases or spikes which respond to various abiotic and biotic stimuli, namely light, high and low temperatures, touch, salt and drought, osmotic stress, plant hormones, fungal elicitors, and nodulation factors (Sanders et al., 1999), which can be measured by aequorin and fluorescence resonance energy transfer (FRET)-based yellow

cameleon indicators (Miyawaki et al., 1997). In addition, the  $[\text{Ca}^{2+}]_{\text{cyt}}$  signals can form a signaling cassette with the reactive oxygen species (ROS) in order to facilitate long-distance systemic responses in each plant, which may provide the feed-forward mechanisms to amplify and transmit the stimuli signals (Choi et al., 2016).

$\text{Ca}^{2+}$  is a core regulator in many cellular signal-transduction cascades that modulates gene transcription, which happens in the cell nucleus. It is a dual-membrane organelle bound by the inner and outer nuclear membranes and fused at the nuclear pores. The contiguous perinuclear space within the lumen of the endoplasmic reticulum plays the role of  $\text{Ca}^{2+}$  storage in signal transduction. So the interesting question is whether nucleosolic  $\text{Ca}^{2+}$  ( $[\text{Ca}^{2+}]_{\text{nuc}}$ ) is as important as  $[\text{Ca}^{2+}]_{\text{cyt}}$  to be involved in gene expression. Analyzing gene transcription in the hippocampal neurons, Hardingham et al. (1997) demonstrated that  $[\text{Ca}^{2+}]_{\text{nuc}}$  activates gene transcription by a mechanism distinct from gene regulation as driven by  $[\text{Ca}^{2+}]_{\text{cyt}}$ . Previous study showed that EGF triggered the  $[\text{Ca}^{2+}]$  increases in both the nucleus and cytosol. However, EGF-induced transactivation of the ternary complex factor, Elk-1, required  $[\text{Ca}^{2+}]_{\text{nuc}}$  but not  $[\text{Ca}^{2+}]_{\text{cyt}}$  in HepG2 or HEK293 cells (Pusl et al., 2002). Therefore,  $[\text{Ca}^{2+}]_{\text{nuc}}$  signaling is generated autonomously or just caused by the passive diffusion from cytoplasm has raised tremendous attention. Mazars and colleagues clearly showed that the delay between  $[\text{Ca}^{2+}]_{\text{cyt}}$  peak and  $[\text{Ca}^{2+}]_{\text{nuc}}$  in tobacco suspension cells could range from seconds in response to mastoparan (Pauly et al., 2000) to minutes in response to osmotic shocks (Pauly et al., 2001), elicitors (Lecourieux et al., 2005) and sphingolipids (Xiong et al., 2008; Lachaud et al., 2010). In the legume symbiosis signaling pathway, both the rhizobial bacteria nodulation factor and the arbuscular mycorrhizal fungi Myc factor can induce  $[\text{Ca}^{2+}]_{\text{nuc}}$  oscillations (Sieberer et al., 2009; Genre et al., 2013), which are sensed by a nuclear-localized CCaMK that activates the different transcriptional regulators required for nodulation and mycorrhization, respectively (Charpentier and Oldroyd, 2013). Previous research has shown that the potassium-permeable channel, DMI1, and the SERCA MCA8 are localized to the nuclear membranes, and they are essential for the nucleosolic  $\text{Ca}^{2+}$  spiking that occurs in *Medicago truncatula* (Capoen et al., 2011). Furthermore, Charpentier et al. (2016) showed that the three cyclic nucleotide-gated ion channels, CNGC15a/b/c, are located at the nuclear envelope where they form a complex with DMI1, which mediates nuclear  $\text{Ca}^{2+}$  release and subsequent symbiotic responses in *M. truncatula*. These results highlight the potential of the nucleus to independently generate the  $\text{Ca}^{2+}$  signals in both plant and animal cells (Bootman et al., 2009; Mazars et al., 2011).

Using tagged versions of Cameleon YC 3.6 (Nagai et al., 2004) that were separately targeted to the cytoplasm, with a nuclear export sequence (NES-YC), and to the nucleoplasm, with a nuclear localization sequence (NLS-YC), Krebs et al. (2012) found that external ATP induced the  $[\text{Ca}^{2+}]_{\text{nuc}}$  and  $[\text{Ca}^{2+}]_{\text{cyt}}$  increases in the *Arabidopsis* root cells and the Nod factor induced the  $[\text{Ca}^{2+}]_{\text{nuc}}$  and  $[\text{Ca}^{2+}]_{\text{cyt}}$  spiking in *Lotus japonicus* root hair cells. These results suggested that stimuli could simultaneously induce the  $\text{Ca}^{2+}$  signaling in the cytosol

**Abbreviations:** CAS-IP<sub>3</sub>,  $\text{Ca}^{2+}$ -sensing receptor-inositol trisphosphate; CCaMK,  $\text{Ca}^{2+}$ /calmodulin-dependent Ser/Thr protein kinase; CFP, cyan fluorescent protein; CNGC15, cyclic nucleotide-gated channel 15; DMI1, does not Make Infections 1; DTT, dithiothreitol; EGF, epidermal growth factor; eYFP, enhanced yellow fluorescent protein; GLRs, glutamate receptor-like channels; LRP, lateral root primordium; MKK, mitogen-activated protein kinase kinase; NES, nuclear export signal; NLS, nuclear localized signal; OICl<sub>cyt</sub>, osmotic stress-induced cytosolic  $[\text{Ca}^{2+}]$  increase; OICl<sub>nuc</sub>, osmotic stress-induced nucleosolic  $[\text{Ca}^{2+}]$  increase; OPDA, 12-oxophytodienoic acid; PV, parvalbumin; PVDF, polyvinylidene fluoride; SDS, sodium dodecyl sulfate; SERCA, sarko/endoplasmic reticulum  $\text{Ca}^{2+}$ -ATPase; SICI<sub>cyt</sub>, salt stress-induced cytosolic  $[\text{Ca}^{2+}]$  increase; SICI<sub>nuc</sub>, salt stress-induced nucleosolic  $[\text{Ca}^{2+}]$  increase; WT, wild type; YC, Cameleon YC 3.6.

and nucleus. However, the relationship between cytosolic  $\text{Ca}^{2+}$  signaling and nucleosolic  $\text{Ca}^{2+}$  signaling in plants is still not clear. PV is a  $\text{Ca}^{2+}$ -binding protein with three EF hand motifs, one of them is inactive owing to a two amino-acid deletion in the loop region (Cates et al., 2002), and functions as calcium buffer in fast-contracting muscles, brain and some endocrine tissues (Berchtold et al., 1984; Cowan et al., 1990). Prior studies showed that the expression of PV, when selectively targeted to the nucleus (PV-NLS) or cytoplasm (PV-NES), is able to locally attenuate  $[\text{Ca}^{2+}]_{\text{nuc}}$  and  $[\text{Ca}^{2+}]_{\text{cyt}}$  by 50%, respectively, in response to stimulation with ATP in HepG2 cells (Pusl et al., 2002) or vasopressin in SKHep1 cells (Rodrigues et al., 2007). In the present study, we first generated transgenic *Arabidopsis* plants that selectively expressed PV targeted to the cytoplasm (PV-NES) or nucleus (NLS-PV). Then we crossed the *PV*-NES and NLS-PV lines with those of *NES-YC* and *NLS-YC*, respectively, to yield four double-transgenic lines, *NES-YC/PV-NES*, *NLS-YC/NLS-PV*, *NES-YC/NLS-PV*, and *NLS-YC/PV-NES*, for measuring  $[\text{Ca}^{2+}]_{\text{cyt}}$  and  $[\text{Ca}^{2+}]_{\text{nuc}}$  in the plant response to hyperosmolarity and salt stresses. Using this toolkit, we deciphered the temporal and spatial characteristics of  $\text{Ca}^{2+}$  signatures in the nucleus and the cytosol in *Arabidopsis* root cells.

## MATERIALS AND METHODS

### Plant Material and Growth Conditions

*Arabidopsis thaliana* (Col-0 ecotype) plants were grown under 16 h light ( $120 \mu\text{mol m}^{-2} \text{s}^{-1}$ )/8 h dark at  $22^\circ\text{C}$  and 60% relative humidity. Seeds of *Arabidopsis* were surface-sterilized by 75% ethanol and plated on Murashige and Skoog (MS) salts, 1% sucrose, 0.8% (w/v) agar, pH 5.8. After stratification at  $4^\circ\text{C}$  in the dark for 3 days, the dishes were transferred to a growth chamber for germination and seedling growth of 7 days. About 15–20 seedlings were planted into pots for continued growth and monitored during the experiment. Transgenic plants were generated using the floral-dip method (Clough and Bent, 1998) and screened using the MS medium containing 50  $\mu\text{g/mL}$  Hygromycin. To detect whether the PV buffers the calcium increase in cytoplasm or nucleus, we generated the *Arabidopsis* plants to co-express PV and the calcium indicator Cameleon YC3.6 (YC) by separately crossing three transgenic plants which had nuclear-localized PV (NLS-PV) or cytosolic-localized PV (NES-PV) with either *NES-YC* or *NLS-YC* transgenic *Arabidopsis* (Krebs et al., 2012), the latter kindly gifted to us from Dr. Jörg Kudla. For each construct, the independent transgenic lines were selected, and the three lines were used for the following experiments.

### DNA Constructs

The CDS of the *PV* gene was cloned from rat muscle tissue. The NLS segment was cloned from the *Arabidopsis BRI1-EMS-SUPPRESSOR 1* (BES1, AT1G19350) gene (Yin et al., 2005) and the NES from the human MKK gene (Tolwinski et al., 1999). The NLS was fused to the N-terminal of PV via PCR, digested by *BamHI* and *NotI*, and cloned into pE2c and pE6c plasmids (Addgene, Cambridge, MA, United States). The NES was fused

to the C-terminal of PV, digested by *BamHI* and *NotI*, and cloned into pE2n and pE6n. The primers used to clone these gene fragments are listed in Supplementary Table S1.

The pE2n, pE2c, pE6n, and pE6c constructs containing different PV fragments were used in combination with the destination vector pMDC32<sup>1</sup> with the Gateway LR II kit (Invitrogen, Carlsbad, CA, United States) to generate all of the plant expression vectors. These were introduced into the *Agrobacterium tumefaciens* strain, GV3101, for the *Arabidopsis* transformation. Construct maps containing both *PV*-NES and NLS-PV are shown in Supplementary Figure S1. All vectors were confirmed by sequencing.

### Subcellular Localization of NLS-PV and PV-NES in the *Arabidopsis* Mesophyll Protoplasts

The vectors containing either *eYFP-PV-NES* or *NLS-PV-eYFP* and the nuclear marker gene were co-transformed and transiently expressed in the *Arabidopsis* mesophyll protoplasts, as described before (Liang et al., 2015). After incubation for 16 h at  $22^\circ\text{C}$  in the dark, fluorescence was visualized by using a Zeiss LSM 700 confocal microscope (Zeiss, Oberkochen, Germany). Observations were made using a  $63\times$  objective under oil immersion. The eYFP fluorescence was excited at 488 nm and collected at shortpass 550 infrared (IR). The chloroplast autofluorescence was also excited at 488 nm, but it was collected at longpass 640 IR. The mCherry fluorescence was excited at 555 nm and collected at shortpass 630 IR. The pinhole was approximately 1.0 unit and the thickness of optical section was approximately 0.5  $\mu\text{m}$ . The nuclear marker labeled by mCherry served as the control.

### Protein Extraction and Western Blot Analyses

Four-week-old transgenic *Arabidopsis* leaves were frozen in liquid nitrogen and ground using a mortar and pestle. The samples were incubated on ice for 2 h in an extraction buffer I that contained 50 mM Tris-HCl, pH 8.0, 50 mM NaCl, 5 mM MgCl<sub>2</sub>, 0.1% Triton X-100, 5 mM DTT, and the appropriate protease inhibitor cocktail (Roche, Basel Switzerland), and then centrifuged at 80 000 g, at  $4^\circ\text{C}$ , for 30 min. The ensuing supernatants were centrifuged again under the same conditions and collected as the cytosolic compartment. The pellet was re-suspended with an extraction buffer II that contained 50 mM Tris-HCl, pH 8.0, 150 mM NaCl, 10% glycerol, 0.1% Triton X-100, 0.1% NP-40, 2 mM MgCl<sub>2</sub>, 5 mM DTT, and 1x protease inhibitor cocktail, and centrifuged again under same conditions as above. The nuclear proteins are in the pellet and were re-suspended with the buffer II in equal volume. In addition, 6-day-old *Arabidopsis* seedlings were collected, ground in liquid nitrogen, and used for the total protein extraction with a buffer (50 mM Tris-HCl, pH 6.8, 2% SDS, 10% glycerin, and 1%  $\beta$ -mercaptoethanol).

Protein extracts were resolved on 12%-SDS-polyacrylamide gels and electro-blotted onto Bio-Rad Immun-Blot PVDF

<sup>1</sup><http://www.arabidopsis.org/>

membranes (Bio-Rad, Hercules, CA, United States). After this transfer, the PVDF membranes were blocked in Tris-buffered saline-Tween 20 (TBST; containing 10 mM Tris-HCl, pH 8.0, 150 mM NaCl, and 0.05% Tween 20), which contained 5% bovine serum albumin (Sigma-Aldrich, St. Louis, MO, United States), for 1 h at room temperature and then incubated overnight with a primary antibody at 4°C. The membranes were washed of 10 min for three times in the TBST and incubated with the secondary antibody—anti-rabbit immunoglobulin G, dilution 1:2000 or anti-mouse immunoglobulin G, dilution 1:3000—for 30 min. Next, the membranes were washed of 10 min for three times in the TBST. To examine the alkaline phosphatase activity, the Chemiluminescent Substrate (Roche) was used according to the manufacturer's protocol. The primary anti-PV antibody (Abcam, dilution 1:2000) was used to detect the expression of PV in the transgenic plants. The non-specific band after blotted with anti-PV antibody was used as the loading control of the cytosolic proteins and the anti-histone antibody (Sigma-Aldrich, dilution 1:10000) was used as the loading control of the nuclear proteins.

## Arabidopsis Seedling Preparation for Ca<sup>2+</sup> Imaging

After germination, the *Arabidopsis* seedlings were grown vertically on the half-strength MS medium for 5–7 days and their roots were prepared for Ca<sup>2+</sup> imaging following Krebs et al. (2012), with some modifications. The roots were immobilized by overlaying them with 1% (w/v) low-melting-point agarose (Amresco) in the Attofluor® Cell Chambers (Invitrogen). After digging a small tunnel in the agarose to expose the root, we gently applied 200 µl bathing solution buffer [0.5x MS salt, 1% sucrose, 10 mM 2-(*N*-morpholino)ethanesulfonic acid [MES]-KOH, pH 5.8] to the chamber. The shoot was not submerged in the solution. High concentrations of NaCl and sorbitol in the same solution were separately perfused as the stimulus into the chamber. The mature zone of the *Arabidopsis* roots was selected for the subsequent Ca<sup>2+</sup> measurements.

## FRET Measurements

To examine the FRET signals of the transgenic plants, we used an inverted fluorescence microscope (Axio Observer A1; Zeiss) equipped with an iXon3 EMCCD camera (Oxford Instruments, Abingdon, United Kingdom), a Lambda DG4 fluorescent light source (Sutter Instruments, Novato, CA, United States), and Bright Line filter sets (Semrock Inc., Rochester, NY, United States). Images captured with the CFP (438Ex/483Em), CpVenus (500Ex/542Em), and FRET filters (FCFP, FCpVenus and Fraw (438Ex/542Em), respectively, were collected every 3 s at room temperature by using a 40× oil objective (N.A.1.30; Zeiss) and processed in Slidebook v.5.0 software (Intelligent Imaging Innovations, Denver, CO, United States).

The FRET signal was calculated using a previously described formula (Ma et al., 2015):  $\text{FRETc} = \text{Fraw} - \text{Fd/Dd} * \text{FCFP} - \text{Fa/Da} * \text{FCpVenus}$ , where FRETc represents the corrected energy transfer, Fd/Dd represents the measured bleed-through of CFP through the FRET filter (0.826), and Fa/Da is the measured bleed-through of CpVenus through the FRET filter (0.048).

To reduce the variation caused by different expression levels in the transgenic plants, the FRETc values were normalized against donor fluorescence (FCFP) to generate an N-FRET (i.e., normalized FRET) signal.

To eliminate the influences of instrument-dependent factors, the apparent FRET efficiency, or Eapp, was calculated using the following equation:  $Eapp = N\text{-FRET}/(N\text{-FRET} \pm G)$  (Zal and Gascoigne, 2004), where G (4.59) is the system-dependent factor. It is obtained through a partial CpVenus photo-bleaching method:  $G = (\text{FRETc} - \text{FRETc}_{\text{post}})/(\text{FCFP}_{\text{post}} - \text{FCFP})$ , where FRETc<sub>post</sub> and FCFP<sub>post</sub> are the corresponding FRETc and FCFP values after the partial photo-bleach of CpVenus. The intensity of the light used to bleach CpVenus was carefully chosen so that would not also bleach CFP. All of the fluorescence images were collected and briefly processed in MetaFluor software (Molecular Devices, Sunnyvale, CA, United States); the data were further analyzed with Matlab R2014a and plotted by using GraphPad Prism v.5.0 software. The average FRET measurements in response to the different stimuli represent the value of 20–30 root cells from at least nine independent seedlings, each of which included 3 to 6 root cells. Analysis of statistical significance was performed with the unpaired Student's *t*-test in the GraphPad Prism 5.0 software. The results are presented as means ± SD.

## Abiotic Treatment, Total RNA Isolation, and Quantitative Real-Time (qRT)-PCR Analysis

*Arabidopsis* seeds of the wildtype (WT), NES-PV, and NLS-PV lines were sowed onto a sterile plate containing 1/2 MS salts, 1% sucrose, 0.8% (w/v) agar, and pH 5.8, and stratified at 4°C in the dark for 3 days. Then, the dishes were transferred to the growth chamber for the germination over 6 days. The seedlings were transferred onto 1/2 MS plates or 1/2 MS medium supplemented with either 150 mM of NaCl or 250 mM of sorbitol, and cultivated for 11 days to observe their root growth or for 6 h to perform qRT-PCR.

Total RNA was isolated from seedling samples by using the Eastep® Super (Promega, Fitchburg, United States) according to the protocols. Approximately 2 µg of total RNA was reverse transcribed into first-strand cDNA by using the First-Strand cDNA Synthesis SuperMix (TransScript, Beijing China). The qRT-PCR was performed on the 7500 Fast Real-Time PCR System (Applied Biosystems, Foster City, CA, United States) which used a Power SYBR® Green PCR Master Mix (TransStart, Beijing China). The *Arabidopsis Actin2* served as an internal control. The stress-responsive genes selected for detecting their expression are listed in Supplementary Table S2. All primers used in this study are listed in Supplementary Table S3. At least three independent biological replicates were performed for the qRT-PCR analysis. Value changes of more than twofold, >2 or <0.5, were considered to, respectively, indicate the induction or repression of gene expression. The data analysis was carried out using the Data Processing System, and a two-way analysis of variance (ANOVA) followed by Tukey's multiple range test were conducted to determine any significant differences among the group means (Tang and Zhang, 2013).

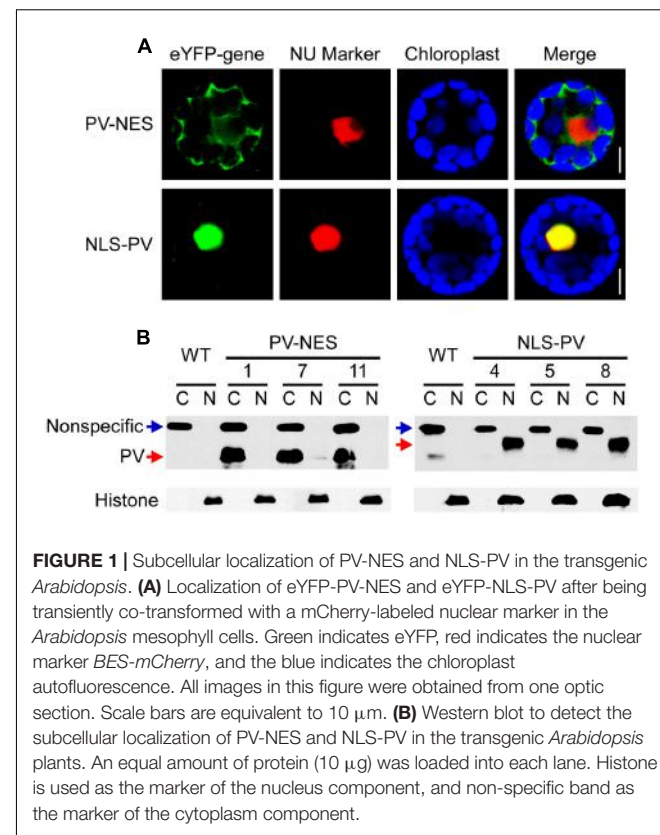
## RESULTS

### Expression of the $\text{Ca}^{2+}$ Binding Protein PV in *Arabidopsis*

To study the relationship between cytosolic and nucleosolic calcium signaling in plants, we constructed binary vectors targeting the  $\text{Ca}^{2+}$ -binding protein PV to either the nucleus or cytoplasm, by fusing it with a NLS (NLS-PV) or a NES (PV-NES), and transducing the vectors into *Arabidopsis* WT via *Agrobacterium*. Meanwhile, to verify the localization signal, two vectors with the indicated PV fused with yellow fluorescent protein—eYFP-PV-NES and eYFP-NLS-PV (**Supplementary Figure S1**)—were generated and transiently co-transformed with the mCherry-labeled nuclear marker into the *Arabidopsis* mesophyll protoplasts. We found that eYFP-PV-NES was restricted to the cytoplasm, whereas eYFP-NLS-PV was co-localized with the nuclear marker (**Figure 1A**). Through resistance screening and the reverse transcription (RT)-PCR assay (data not shown), we firstly discarded the transgenic lines which has different growth phenotype with WT in whole life cycle, then obtained the single-insertion,  $T_3$  homozygous NLS-PV and PV-NES transgenic lines. So, the proteins extracted from the cytoplasm and nucleus of the three independent lines were isolated and detected by immunoblotting, revealing that the PV was distributed only in the nuclear compartment in the NLS-PV lines and in the cytoplasm compartment in the PV-NES lines (**Figure 1B**, the original images of **Figure 1B** is shown in (**Supplementary Figure S3**)). These results proved that the subcellular localization of PV-NES or NLS-PV is specific to the cytoplasm or nucleus in the transgenic plants, which lay the foundation for its selective buffering of  $[\text{Ca}^{2+}]_{\text{cyt}}$  or  $[\text{Ca}^{2+}]_{\text{nuc}}$ .

### PV-NES Attenuates the Osmotic Stress-Induced $[\text{Ca}^{2+}]_{\text{cyt}}$ Increase ( $\text{OICl}_{\text{cyt}}$ ) and Salt Stress-Induced $[\text{Ca}^{2+}]_{\text{cyt}}$ Increase ( $\text{SICl}_{\text{cyt}}$ )

To explore the effect of PV on the cellular  $[\text{Ca}^{2+}]$  elevations, we crossed the PV-NES lines with those *Arabidopsis* plants containing the cytoplasm-localized Yellow Cameleon 3.6 Indicator (NES-YC), and thus obtained the homozygous NES-YC/PV-NES lines with resistance screening. Then, the  $[\text{Ca}^{2+}]_{\text{cyt}}$  was monitored in response to different stimuli in the root cells of *Arabidopsis* plants either expressing NES-YC or co-expressing NES-YC/PV-NES. Firstly, we found that 250 mM of sorbitol, when used as an osmotic stress stimulus, can trigger a rapid increase of  $[\text{Ca}^{2+}]_{\text{cyt}}$  in the root cells of the NES-YC plants; the value of  $\Delta E_{\text{app}}/E_{\text{app,rest}}$  reached 0.16, which is similar to that of a previous study (Krebs et al., 2012). However,  $\text{OICl}_{\text{cyt}}$  was disrupted in the NES-YC/PV-NES lines, with a  $\Delta E_{\text{app}}/E_{\text{app,rest}}$  value that was approximately 0.05 (**Figures 2A–C**). Similarly, 125 mM NaCl was also able to induce a single peak of  $[\text{Ca}^{2+}]_{\text{cyt}}$  increase in the root cells of the NES-YC plants, but it was impaired in the NES-YC/PV-NES lines (**Figures 2D–F**). The increased FRET fluorescence and decreased CFP fluorescence after adding the 250 mM of sorbitol or 125 mM of NaCl to the



root cells of the NES-YC plants are shown in (**Supplementary Figures S2A,B**). Together, these results demonstrated that the cytosolic-localized PV can effectively buffer the change of  $[\text{Ca}^{2+}]_{\text{cyt}}$  and thereby inhibit  $\text{OICl}_{\text{cyt}}$  and  $\text{SICl}_{\text{cyt}}$  in the *Arabidopsis* root cells.

### NLS-PV Impaired the Osmotic Stress-Induced $[\text{Ca}^{2+}]_{\text{nuc}}$ Increase ( $\text{OICl}_{\text{nuc}}$ ) and Salt Stress-Induced $[\text{Ca}^{2+}]_{\text{nuc}}$ Increase ( $\text{SICl}_{\text{nuc}}$ )

We also obtained the homozygous NLS-YC/NLS-PV lines and used these plants to monitor the calcium elevations in the nucleus after adding 250 mM sorbitol or 125 mM NaCl. Firstly, we found that  $\text{OICl}_{\text{nuc}}$  in the root cells of NLS-YC plants rapidly increased and oscillated, with a peak value for  $\Delta E_{\text{app}}/E_{\text{app,rest}}$  of approximately 0.82. However,  $\text{OICl}_{\text{nuc}}$  was disrupted in the NLS-YC/NLS-PV lines for which the value of  $\Delta E_{\text{app}}/E_{\text{app,rest}}$  was approximately 0.28 (**Figures 3A–C**). In addition, the calcium oscillation pattern of  $\text{SICl}_{\text{nuc}}$  was also impaired in the NLS-YC/NLS-PV lines compared with that of the NLS-YC plants, and the  $\Delta E_{\text{app}}/E_{\text{app,rest}}$  values had decreased from 0.8 to 0.2 (**Figures 3D–F**). (**Supplementary Figures S2C,D**) show the increased FRET fluorescence and decreased CFP fluorescence in the root cells of the NLS-YC plants after adding 250 mM sorbitol or 125 mM NaCl treatments. These results showed that nuclear-localized PV could also buffer  $\text{OICl}_{\text{nuc}}$  and  $\text{SICl}_{\text{nuc}}$  in *Arabidopsis*.

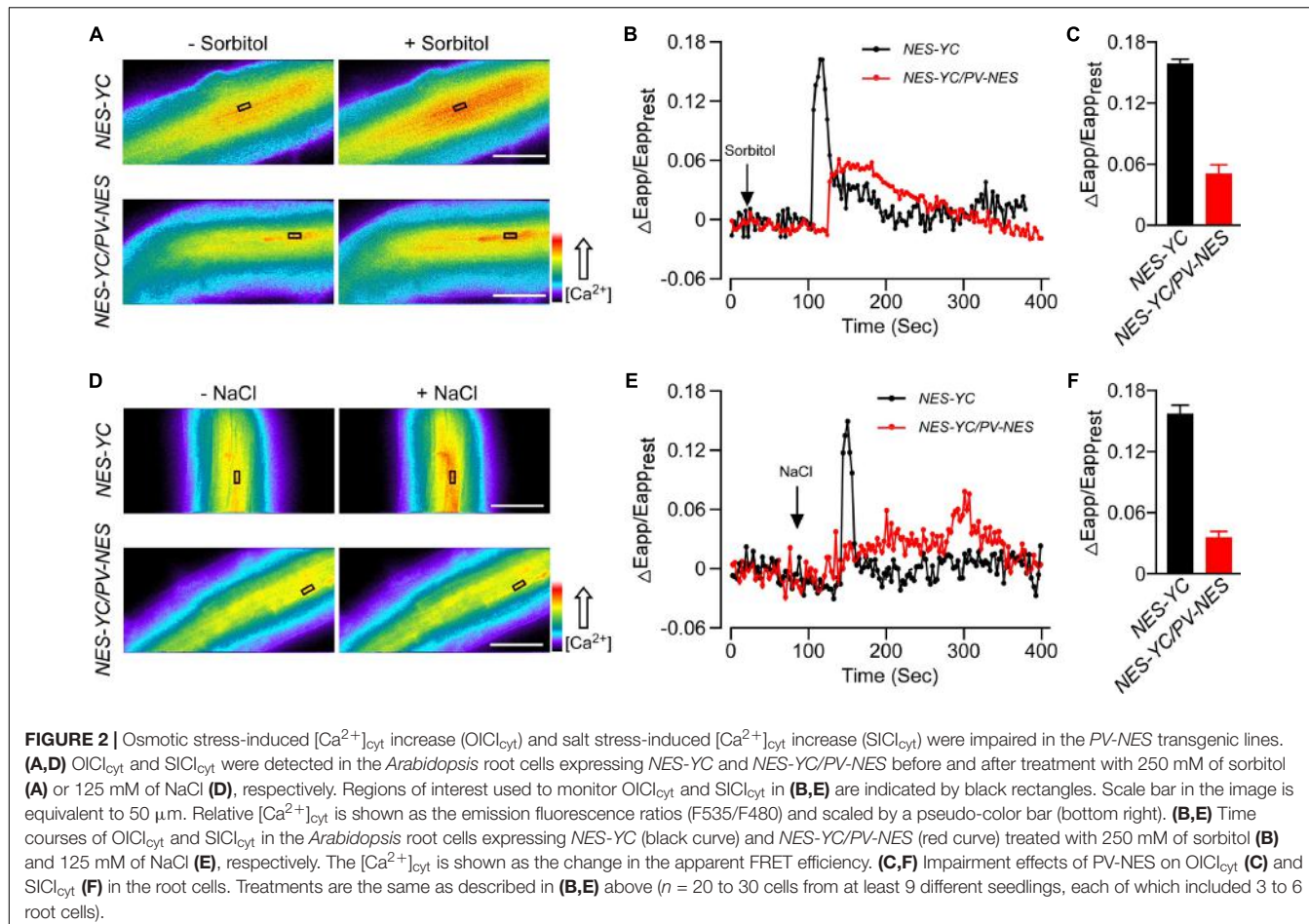


**FIGURE 2 |** Osmotic stress-induced  $[Ca^{2+}]_{cyt}$  increase ( $OICl_{cyt}$ ) and salt stress-induced  $[Ca^{2+}]_{cyt}$  increase ( $SICI_{cyt}$ ) were impaired in the PV-NES transgenic lines. **(A,D)**  $OICl_{cyt}$  and  $SICI_{cyt}$  were detected in the *Arabidopsis* root cells expressing NES-YC and NES-YC/PV-NES before and after treatment with 250 mM of sorbitol **(A)** or 125 mM of NaCl **(D)**, respectively. Regions of interest used to monitor  $OICl_{cyt}$  and  $SICI_{cyt}$  in **(B,E)** are indicated by black rectangles. Scale bar in the image is equivalent to 50  $\mu$ m. Relative  $[Ca^{2+}]_{cyt}$  is shown as the emission fluorescence ratios (F535/F480) and scaled by a pseudo-color bar (bottom right). **(B,E)** Time courses of  $OICl_{cyt}$  and  $SICI_{cyt}$  in the *Arabidopsis* root cells expressing NES-YC (black curve) and NES-YC/PV-NES (red curve) treated with 250 mM of sorbitol **(B)** and 125 mM of NaCl **(E)**, respectively. The  $[Ca^{2+}]_{cyt}$  is shown as the change in the apparent FRET efficiency. **(C,F)** Impairment effects of PV-NES on  $OICl_{cyt}$  **(C)** and  $SICI_{cyt}$  **(F)** in the root cells. Treatments are the same as described in **(B,E)** above ( $n = 20$  to 30 cells from at least 9 different seedlings, each of which included 3 to 6 root cells).

## Changes in $[Ca^{2+}]_{cyt}$ Triggered by Osmotic or Salt Stresses Are Independent of Those for $[Ca^{2+}]_{nuc}$ in *Arabidopsis*, and Vice Versa

To further reveal the inter-relationship between  $[Ca^{2+}]_{cyt}$  and  $[Ca^{2+}]_{nuc}$ , we intercrossed *NEC-YC* with *NLS-PV* and *NLS-YC* with *PV-NES* plants. Doing so gave us the homozygous *NEC-YC/NLS-PV* and *NLS-YC/PV-NES* double-transgenic lines for detecting the  $OICl$  and  $SICI$  in the cytoplasm and nucleus, respectively. Firstly, the responses, in terms of the pattern and  $\Delta E_{app}/E_{app,rest}$ , for the cytoplasm calcium dynamics in the root cells of the *NEC-YC/NLS-PV* plants were similar to those seen in the *NES-YC* plants when they received 250 mM of sorbitol or 125 mM of NaCl (Figures 4A–D). This shows that blocking nuclear calcium has no effect on  $OICl_{cyt}$  and  $SICI_{cyt}$ . Likewise, we separately measured the change of  $[Ca^{2+}]_{nuc}$  in response to the 250-mM sorbitol or 125-mM NaCl treatments in the root cells of the *NLS-YC* and *NLS-YC/PV-NES* lines and found that blocking the cytosolic calcium with PV-NES did not affect  $OICl_{nuc}$  and  $SICI_{nuc}$  (Figures 4E–H). Interestingly, we want to show that the increase of  $[Ca^{2+}]_{nuc}$  in response to osmotic or salt stresses showed two kinds of patterns in the different cells of the root mature zone: one is a rapid increase following

by oscillations (Figures 3B,E), while the other is just a single peak (Figures 4E,F). Each pattern accounted for approximately 50%. In addition, blocking the cytosolic calcium signal with PV-NES had no effect on these two patterns of  $[Ca^{2+}]_{nuc}$ . Via the Western blot, we also confirmed that PV is expressed in all these intercrossed lines (Supplementary Figure S4). In order to rule out any bias about the increases of  $[Ca^{2+}]_{cyt}$  and  $[Ca^{2+}]_{nuc}$  due to stimulus application in this study, we perform the control experiment where only MS medium is added to the seedlings and show that the medium cannot trigger any change of  $\Delta E_{app}/E_{app,rest}$  (Supplementary Figure S5). These results proved that cytosolic and nucleosolic calcium dynamics are independent of each other in *Arabidopsis*.

## Both Cytosolic and Nucleosolic Calcium Are Involved in Root Growth and the Transcription of Several Abiotic Stress-Induced Genes in *Arabidopsis*

To better distinguish the respective roles of cytosolic and nucleosolic calcium signaling in plant growth and development, we detected the root growth of WT, PV-NES, and NLS-PV plants under conditions of abiotic stress. As expected, we showed that NLS-PV and PV-NES have no effects on normal root growth in

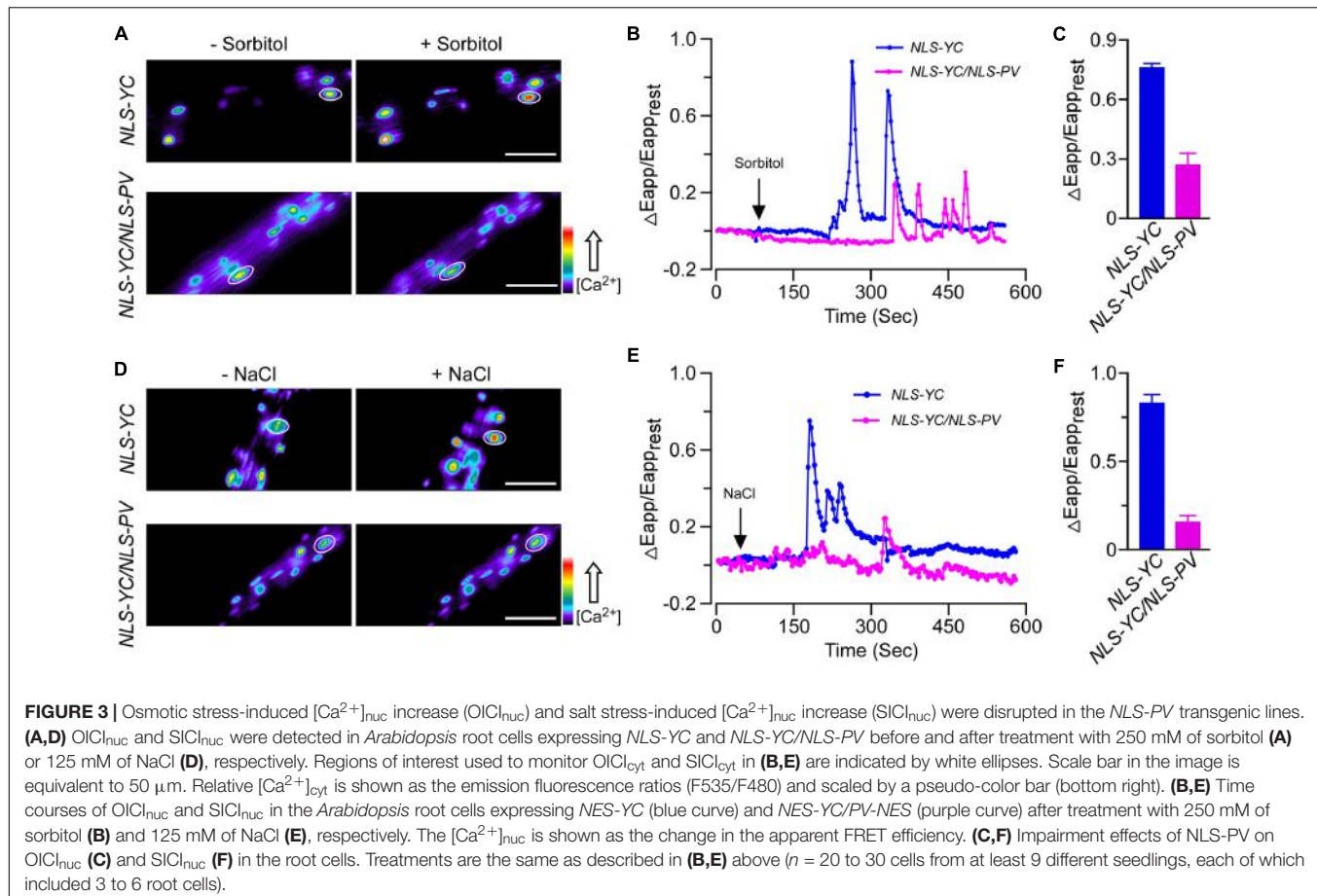


**FIGURE 3 |** Osmotic stress-induced  $[Ca^{2+}]_{nuc}$  increase ( $OICl_{nuc}$ ) and salt stress-induced  $[Ca^{2+}]_{nuc}$  increase ( $SiCl_{nuc}$ ) were disrupted in the *NLS-PV* transgenic lines. (**A, D**)  $OICl_{nuc}$  and  $SiCl_{nuc}$  were detected in *Arabidopsis* root cells expressing *NLS-YC* and *NLS-YC/NLS-PV* before and after treatment with 250 mM of sorbitol (**A**) or 125 mM of NaCl (**D**), respectively. Regions of interest used to monitor  $OICl_{cyt}$  and  $SiCl_{cyt}$  in (**B, E**) are indicated by white ellipses. Scale bar in the image is equivalent to 50  $\mu$ m. Relative  $[Ca^{2+}]_{cyt}$  is shown as the emission fluorescence ratios (F535/F480) and scaled by a pseudo-color bar (bottom right). (**B, E**) Time courses of  $OICl_{nuc}$  and  $SiCl_{nuc}$  in the *Arabidopsis* root cells expressing *NES-YC* (blue curve) and *NES-YC/PV-NES* (purple curve) after treatment with 250 mM of sorbitol (**B**) and 125 mM of NaCl (**E**), respectively. The  $[Ca^{2+}]_{nuc}$  is shown as the change in the apparent FRET efficiency. (**C, F**) Impairment effects of NLS-PV on  $OICl_{nuc}$  (**C**) and  $SiCl_{nuc}$  (**F**) in the root cells. Treatments are the same as described in (**B, E**) above ( $n = 20$  to 30 cells from at least 9 different seedlings, each of which included 3 to 6 root cells).

the 1/2 MS medium, and that both the treatments of 125 mM NaCl and 250 mM sorbitol can inhibit the root growth of the WT, *PV-NES*, and *NLS-PV* plants. However, the root length of both the *PV-NES* and *NLS-PV* plants were markedly longer than that of the WT plants when the medium contained 125 mM of NaCl, but not 250 mM of sorbitol. This indicated that the cytosolic and nucleosolic calcium signaling participated in the response to salt stress regulating the root growth in *Arabidopsis* (**Figures 5A, B**). In addition, treatment with 250 mM sorbitol induced the development of lateral root primordia at a high density in the WT roots, while the lateral primordia density of *PV-NES* plants was greater than that of either the WT or *NLS-PV* plants. Nevertheless, the 125-mM NaCl treatment led to no obvious differences in the development of lateral primordia among the WT, *PV-NES*, and *NLS-PV* plants (**Figures 5A, C**). Together, these results suggested that cytosolic calcium, but not nucleosolic calcium, is involved in the osmotic stress response regulating the growth of lateral root primordia in *Arabidopsis*.

Previous studies revealed that several genes, such as *CML37* (Scholz et al., 2015), *DREB2A* (Sakuma et al., 2006), *MYB2* (Abe, 2002), *RD29A* (Msanne et al., 2011), *RD29B* (Msanne et al., 2011; Virlouvet et al., 2014) and *RD22* (Harshavardhan et al., 2014), are stress-responsive genes in *Arabidopsis*; so, here we performed qRT-PCR to detect whether their expression was related to cytosolic and/or nucleosolic calcium. Compared with

the expression of the genes up-regulated by the sorbitol or NaCl treatment in WT, we found that the up-regulated level of *CML37* and *MYB2* were inhibited in both *PV-NES* and *NLS-PV* plants, whereas that of *DREB2A* was inhibited only in the *PV-NES* plants and that of *RD29A* only in *NLS-PV* plants after receiving the 125-mM NaCl treatment. However, the up-regulated levels of *RD29A* and *RD29B* were higher in the *PV-NES* than in WT plants after treatment with 125 mM of NaCl. More interestingly, the sorbitol treatment-induced expression of *CML37* and *DREB2A* was higher in the *NLS-PV* lines than for the WT and *PV-NES* plants, and the transcription of *MYB2*, *RD29A*, and *RD29B* were greater in both *PV-NES* and *NLS-PV* lines than those in WT (**Figure 6**). We also found the expression pattern of *RD22* after treatment with osmotic or salt stresses stayed the same in the *PV-NES* and *NLS-PV* plants as in WT (**Supplementary Figure S6**). These results suggested that  $[Ca^{2+}]_{cyt}$  and  $[Ca^{2+}]_{nuc}$  both participate in the various transcription of stress-related plant genes.

## DISCUSSION

Drought and salt stress are major abiotic constraints that are capable of impairing plant growth and development and inflicting severe crop losses worldwide (Munns and

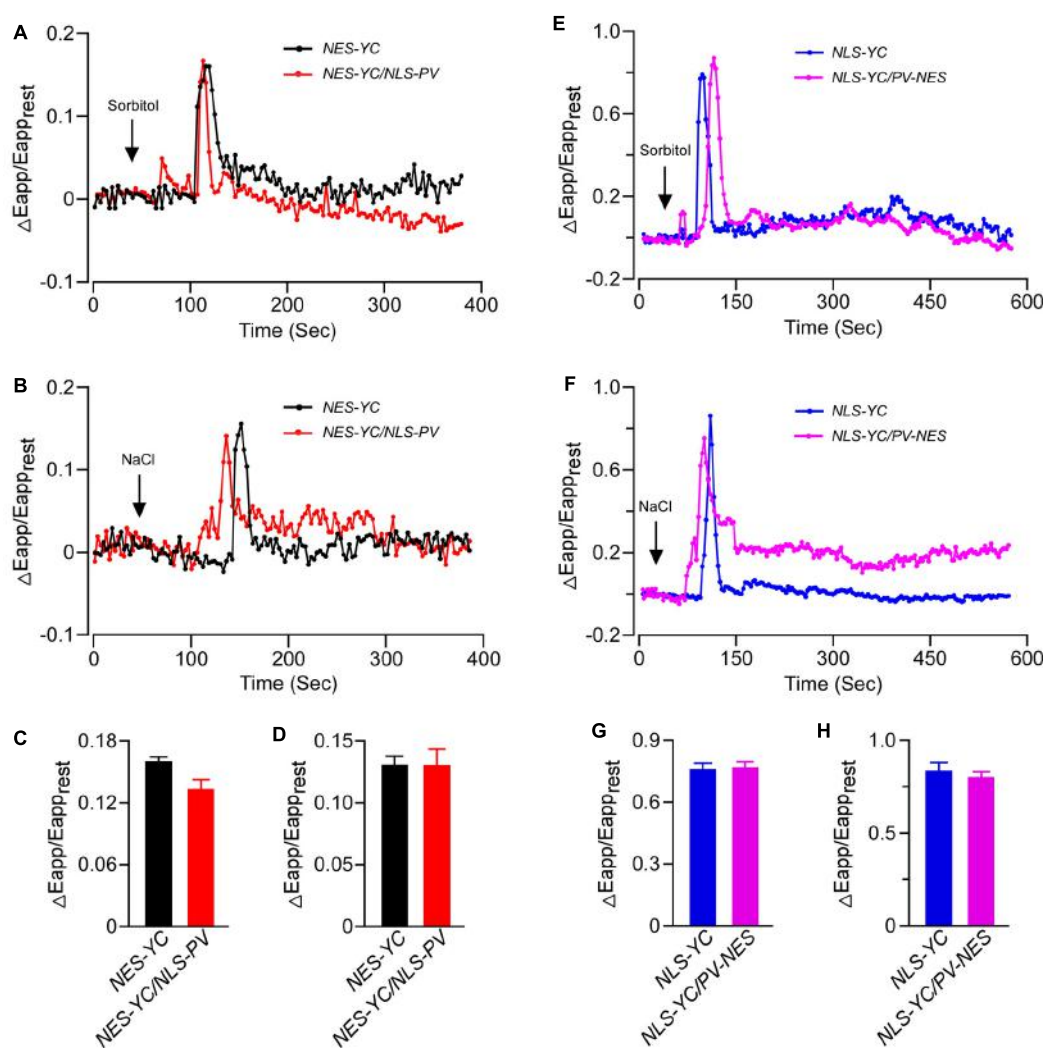
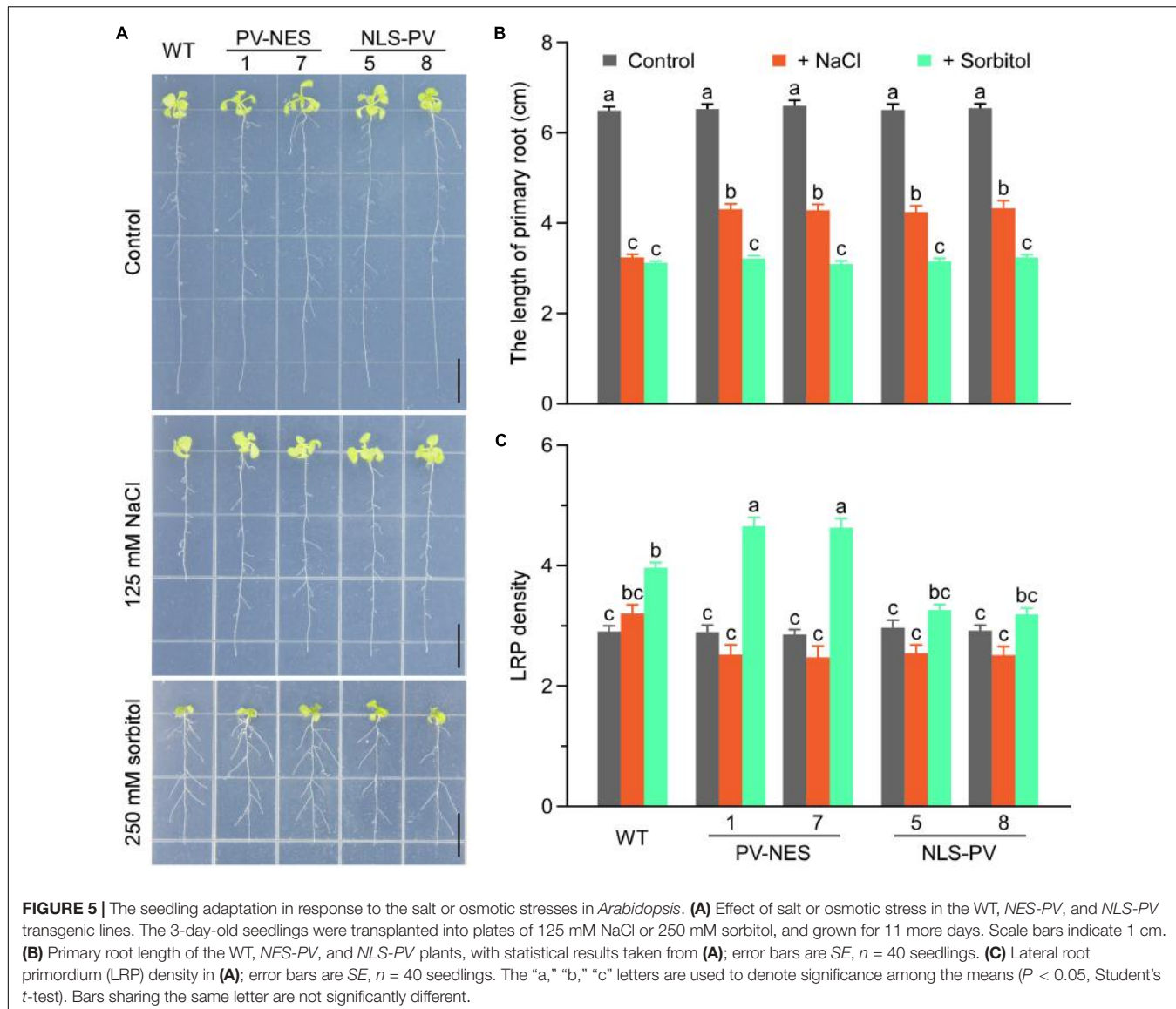


**FIGURE 4 |** The increases of  $[Ca^{2+}]_{cyt}$  and  $[Ca^{2+}]_{nuc}$  triggered by osmotic stress or salt stress were independent of each other. **(A,B)** Time courses of OICl<sub>cyt</sub> and SICl<sub>cyt</sub> detected in the *Arabidopsis* root cells expressing NES-YC (black curve) and NES-YC/NLS-PV (red curve) after treatment with 250 mM of sorbitol (**A**) or 125 mM of NaCl (**B**), respectively. The  $[Ca^{2+}]_{cyt}$  is shown as the change in the apparent FRET efficiency. **(C,D)** Impairment effects of NLS-PV on OICl<sub>cyt</sub> (**C**) and SICl<sub>cyt</sub> (**D**) in the root cells. The values are means  $\pm$  SD ( $n = 20$  to 30 cells). **(E,F)** Time courses of OICl<sub>nuc</sub> and SICl<sub>nuc</sub> detected in the *Arabidopsis* root cells expressing NLS-YC (blue curve) and NLS-YC/PV-NES (purple curve) after treatment with 250 mM of sorbitol (**E**) or 125 mM of NaCl (**F**), respectively. The  $[Ca^{2+}]_{cyt}$  is shown as the change in the apparent FRET efficiency. **(G,H)** Impairment effects of PV-NES on OICl<sub>nuc</sub> (**G**) and SICl<sub>nuc</sub> (**H**) in the root cells. The values are means  $\pm$  SD ( $n = 20$  to 30 cells from at least 9 different seedlings, each of which included 3 to 6 root cells).

(Tester, 2008). The first phase common to both drought and salt stress is characterized by osmotic stress (Shavrukov, 2013). Here, we demonstrated that osmotic and salt stresses induced  $[Ca^{2+}]_{nuc}$  and  $[Ca^{2+}]_{cyt}$  increases in *Arabidopsis* root cells. These results suggested that both cytosolic and nucleosolic calcium serve as the secondary messengers involved with plant responses to various environmental stresses and developmental processes. In agreement with studies of animal cells (Pusl et al., 2002; Rodrigues et al., 2007), we further proved that when PV is targeted to the cytoplasm or nucleoplasm it could buffer OICl<sub>cyt</sub> and SICl<sub>cyt</sub>, or OICl<sub>nuc</sub> and SICl<sub>nuc</sub>, respectively. This approach could be established in plants for the first time to study how  $Ca^{2+}$

operates and functions for different stimuli in different plant tissues/organs.

Using the organelle-targeted  $Ca^{2+}$  indicator, Cameleon YC3.6, to produce stably transformed *Arabidopsis* plants lets us monitor organelle-specific  $Ca^{2+}$  dynamics and compare the  $[Ca^{2+}]$  kinetics between different organelles in *planta* (Krebs et al., 2012; Loro et al., 2012; Stael et al., 2012; Bonza et al., 2013). For example, Loro et al. (2012) showed that mitochondrial  $Ca^{2+}$  accumulation is strictly related to the intensity of the cytosolic  $Ca^{2+}$  increase, demonstrating a tight association between mitochondrial and cytosolic  $Ca^{2+}$  dynamics. Generally, the endoplasmic reticulum (ER) acts as a  $Ca^{2+}$  store that releases  $Ca^{2+}$  for stimulus-induced  $[Ca^{2+}]_{cyt}$  increases; however, Bonza



et al. (2013) showed that  $\text{Ca}^{2+}$  elevations in ER are followed by various stimuli-induced  $[\text{Ca}^{2+}]_{\text{cyt}}$  increases in *Arabidopsis* root-tip cells, with distinct dynamics, which does not support a significant role of ER  $[\text{Ca}^{2+}]$  as a source of  $\text{Ca}^{2+}$  release that contributes to the formation of cytosolic  $\text{Ca}^{2+}$  signatures. In this study, we investigated the triggering of OICI<sub>cyt</sub> by 250 mM of sorbitol and that of SICI<sub>cyt</sub> by 125 mM of NaCl in the root cells of the NES-YC transgenic lines. We found a similar pattern of OICI<sub>cyt</sub> and SICI<sub>cyt</sub>, featuring a single peak of  $[\text{Ca}^{2+}]$  elevation—consistent with findings for the root cells of aequorin-transgenic *Arabidopsis* seedlings (Kiegle et al., 2000; Tracy et al., 2008)—and a sustained and peak-decreased OICI<sub>cyt</sub> and SICI<sub>cyt</sub> pattern in the NEC-YC/PV-NES root cells (Figures 2B,E). More interestingly, OICI<sub>nuc</sub> and SICI<sub>nuc</sub> in the root cells of the NLS-YC lines showed two distinct patterns: the transient increases and oscillation of  $[\text{Ca}^{2+}]$ , with each pattern about approximately 50% in the different cells of the mature root zone (Figures 3B,E, 4E,F).

In addition, we found that the targeted PV in the nucleus can block OICI<sub>nuc</sub> and SICI<sub>nuc</sub> in the root cells of NLS-YC/NLS-PV lines. However, Loro et al. (2012) showed that osmotic stress-induced  $\text{Ca}^{2+}$  transients in the nucleoplasm are kinetically similar to those in the cytoplasm of *Arabidopsis* guard cells. These results indicated that the temporal and spatial characteristics of calcium signatures present in different plant organs in response to various stimuli.

Extensive studies show that the same stimuli—such as osmotic shocks triggered by high concentration of sorbitol or NaCl (Mithöfer and Mazars, 2002), jasmonic acid (JA) and its biosynthetic precursor OPDA (Walter et al., 2007), ATP or Nod factor (Krebs et al., 2012)—may trigger increases of both  $[\text{Ca}^{2+}]_{\text{nuc}}$  and  $[\text{Ca}^{2+}]_{\text{cyt}}$  yet this has diverse patterns in different plants. In addition, the outer nuclear membrane is bordered by the endoplasmic reticulum, so they share a common  $\text{Ca}^{2+}$  pool,  $\text{Ca}^{2+}$ -permeable channels, and  $\text{Ca}^{2+}$ -ATPase carriers to produce

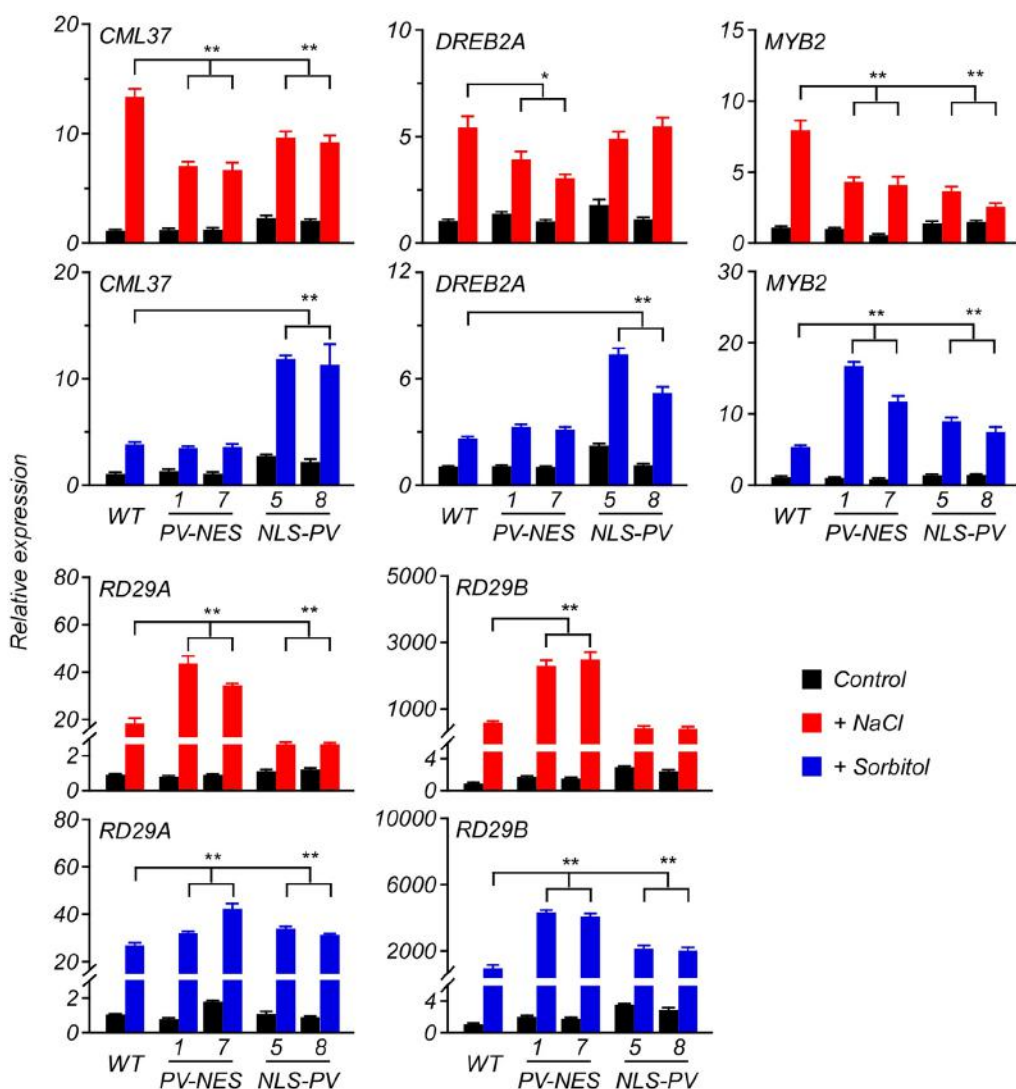


**FIGURE 6 |** Expression of several genes in response to the salt or osmotic stresses in the 6-day-old *Arabidopsis* seedlings. The qRT-PCR analyses were performed to detect the transcript abundance of *CML37*, *DREB2A*, *MYB2*, *RD29A*, and *RD29B* responding to 125 mM of NaCl or 250 mM of sorbitol applied to the seedlings. Error bars are SD,  $n = 3$  biological replicates. \* $P < 0.05$ , \*\* $P < 0.001$  (two-way ANOVA followed by a Tukey's multiple comparisons test), which represent the significant difference of gene expression in transgenic lines compared with WT after the stresses treatment.

$\text{Ca}^{2+}$  signaling in plants. In this study, we first used the PV-NES fusion protein to buffer the  $[\text{Ca}^{2+}]_{\text{cyt}}$  increases to demonstrate a stimulus-induced  $[\text{Ca}^{2+}]_{\text{nuc}}$  that was independent of  $[\text{Ca}^{2+}]_{\text{cyt}}$  with distinct dynamics. Similarly, blocking  $[\text{Ca}^{2+}]_{\text{nuc}}$  with NLS-PV has no effect on the stimulus-induced  $[\text{Ca}^{2+}]_{\text{cyt}}$  increases in the *Arabidopsis* root cells. These results show that cytosolic and nucleosolic calcium signaling are independent of each other in *Arabidopsis*, which raises two interesting questions: (i) how do plants sense and transduce extracellular stimuli to simultaneously induce the  $[\text{Ca}^{2+}]$  increases in the cytoplasm and nucleoplasm, and (ii) what is the physiological extent and function of organelle-specific calcium signaling?

Osmotic and salt stress inhibition of plant growth and development is a general phenomenon, and a pressing and

interesting scientific issue. Here, we revealed that PV-NES and NLS-PV plants exhibit a reduced salt stress-mediated inhibition of root growth, but not of osmotic stress-mediated inhibition of root growth; this suggests that salt stress-induced  $[\text{Ca}^{2+}]$  increases in both the cytoplasm and nucleoplasm mediate the salt stress-induced growth inhibition in *Arabidopsis*. Another interesting result we found is the lateral root primordia density of PV-NES plants exceeding those of WT and NLS-PV plants, but only when treated with 250 mM of sorbitol; this indicates that the OICL<sub>cyt</sub> is somehow involved in the osmotic-stress mediated development of lateral roots. Prior studies have found that calcium signaling is crucial for plant adaptation to various stresses and that it participates in rapid changes in gene expression (Dodd et al., 2010; Reddy et al., 2011).

Compared with the up-regulated expression of key stress-responsive genes, *CML37* (Scholz et al., 2015), *DREB2A* (Sakuma et al., 2006), *MYB2* (Abe, 2002), *RD29A* (Msanne et al., 2011), *RD29B* (Msanne et al., 2011; Virlouvet et al., 2014) in the WT, they were expressed differently in the *PV-NES* and *NLS-PV* plants after the NaCl and sorbitol treatments, respectively (Figure 6). These results further implied that cytosolic calcium signaling and nuclear calcium signaling function independently in the stress response pathways of plants. We also found that the expression of some genes, for instance *RD22*, is related neither to cytosolic or nucleosolic calcium in response to osmotic or salt stresses in *Arabidopsis*. This indicates that one or more calcium-independent signaling pathway(s) participated in the expression regulation of *RD22* in *Arabidopsis* plants. It is also possible that overexpression of *PV-NES* or *NLS-PV* themselves could affect the gene expression in a  $[Ca^{2+}]$ -independent pathway in the transgenic *Arabidopsis* plants. Further experiments are needed to address this issue. For example, we can generate transgenic plants overexpressing  $Ca^{2+}$ -binding deficient mutants of PV (Pusl et al., 2002), and demonstrate that these PV mutants cause changes in gene expression in a calcium-independent manner. Recently, high-throughput sequencing approaches have become available, capable of generating large expression data profiles which provides a useful tool for characterizing the stress-responsive gene(s) mediated by different calcium signaling pathways using the *PV-NES* and *NLS-PV* plants. In sum, our study is the first to show that cytosolic and nucleosolic calcium dynamics are mutually independent in plants, yet play coexisting roles critical in regulating gene expression for plant adaptation to various environmental stresses.

## AUTHOR CONTRIBUTIONS

Conceived and designed the experiments: SH, FH, and JL. Performed the experiments: FH, JL, TN, WC, and XJ. Analyzed the data: FH, JL, HZ, YW, and SH. Contributed reagents/materials/analysis tools: YW and SH. Wrote the paper: FH, HZ, YW, and SH.

## FUNDING

This work was co-supported by the National Natural Science Foundation of China (Grant No. 31070250), the Program for New Century Excellent Talents in University (No. NCET-08-005), and the Fundamental Research Funds for the Central Universities (No. 2009SD-16).

## REFERENCES

- Abe, H. (2002). *Arabidopsis* AtMYC2 (bHLH) and AtMYB2 (MYB) function as transcriptional activators in abscisic acid signaling. *Plant Cell* 15, 63–78. doi: 10.1105/tpc.006130
- Berchtold, M. W., Celio, M. R., and Heizmann, C. W. (1984). Parvalbumin in non-muscle tissues of the rat. Quantitation and immunohistochemical localization. *J. Biol. Chem.* 259, 5189–5196.

## ACKNOWLEDGMENTS

We thank Jörg Kudla (Institute of Plant Biology and Biotechnology, Westfälische Wilhelms-Universität Münster, Germany) for providing the NES-YC3.6 and NLS-YC3.6 *Arabidopsis* plants. We thank Youjun Wang for critically reading the manuscript and for technical support in the calcium imaging.

## SUPPLEMENTARY MATERIAL

The Supplementary Material for this article can be found online at: <http://journal.frontiersin.org/article/10.3389/fpls.2017.01648/full#supplementary-material>

**FIGURE S1** | Schematics of the different PV constructs. Fusion proteins were constructed, consisting of PV with NES fused to the C-terminal region (i.e., PV-NES) and NLS to the N-terminal region (i.e., NLS-PV), and eYFP fused to the N-terminal of these two fusion proteins (i.e., eYFP-PV-NES and eYFP-NLS-PV). The 35S promoter sequence is indicated by the light-blue arrow, the 3XHA tag by the purple rectangular box, the PV by the yellow rectangular box, the NLS by the deep blue rectangular box, the NES by the green rectangular box, the eYFP by the light-green rectangular box, the NOS terminator by the red arrow, Hygromycin is the plant selection marker (denoted by the gray rectangle box), and the T-DNA border is depicted as an empty rectangle box. The line bar is the length of 200 base pairs (bp).

**FIGURE S2** | The changes in CFP and CpVenus intensities that were used to calculate the apparent FRET efficiency. (A) 250-mM sorbitol treatment of the NES-YC transgenic lines shown in Figure 2B. (B) 125-mM NaCl treatment of the NES-YC transgenic lines shown in Figure 2D. (C) 250-mM sorbitol treatment of the NLS-YC transgenic lines shown in Figure 3B. (D) 125-mM NaCl treatment of the NLS-YC transgenic lines shown in Figure 3D.

**FIGURE S3** | The original image of Figure 1B: Western blot to detect the subcellular localization of PV-NES and NLS-PV in the transgenic *Arabidopsis* plants. An equal amount of protein (10  $\mu$ g) was loaded into each lane. Histone is used as the marker of the nucleus component, and non-specific band as the marker of the cytoplasm component.

**FIGURE S4** | Western blot to detect the PV levels in the WT and different transgenic plants. An equal amount of protein (10  $\mu$ g) was loaded into each lane. The non-specific band is used as the marker of the loading control.

**FIGURE S5** | The change of  $[Ca^{2+}]_{cyt}$  or  $[Ca^{2+}]_{nuc}$  response to bathing medium as the stimuli in transgenic plants roots. (A) NES-YC transgenic lines. (B) NES-YC/PV-NES transgenic lines. (C) NES-YC/NLS-PV transgenic lines. (D) NLS-YC transgenic lines. (E) NLS-YC/NLS-PV transgenic lines. (F) NLS-YC/NES-PV transgenic lines. Each measurement was examined at about six individual seedling roots, which include 3~6 cells for every root.

**FIGURE S6** | The transcription level of *RD22* in response to the treatment with a high concentration of sorbitol and NaCl in 6-day-old seedlings of the WT, *NES-PV*, and *NLS-PV* plants, as detected via qRT-PCR. Error bars are SD,  $n = 3$  biological replicates. \* $P < 0.05$ , \*\* $P < 0.001$  (two-way ANOVA followed by Tukey's multiple comparisons test).

Berridge, M. J., Lipp, P., and Bootman, M. D. (2000). The versatility and universality of calcium signalling. *Nat. Rev. Mol. Cell Biol.* 1, 11–21. doi: 10.1038/35036035

Bonza, M. C., Loro, G., Behera, S., Wong, A., Kudla, J., and Costa, A. (2013). Analyses of  $Ca^{2+}$  accumulation and dynamics in the endoplasmic reticulum of *Arabidopsis* root cells using a genetically encoded Cameleon sensor. *Plant Physiol.* 163, 1230–1241. doi: 10.1104/pp.113.226050

- Bootman, M. D., Fearnley, C., Smyrnias, I., MacDonald, F., and Roderick, H. L. (2009). An update on nuclear calcium signalling. *J. Cell Sci.* 122, 2337–2350. doi: 10.1242/jcs.028100
- Bootman, M. D., Lipp, P., and Berridge, M. J. (2001). The organisation and functions of local  $\text{Ca}^{2+}$  signals. *J. Cell Sci.* 114(Pt 12), 2213–2222.
- Capoen, W., Sun, J., Wysham, D., Otegui, M. S., Venkateshwaran, M., Hirsch, S., et al. (2011). Nuclear membranes control symbiotic calcium signaling of legumes. *Proc. Natl. Acad. Sci. U.S.A.* 108, 14348–14353. doi: 10.1073/pnas.1107912108
- Cates, M. S., Teodoro, M. L., and Phillips, G. N. (2002). Molecular mechanisms of calcium and magnesium binding to parvalbumin. *Biophys. J.* 82, 1133–1146. doi: 10.1016/s0006-3495(02)75472-6
- Charpentier, M., and Oldroyd, G. E. (2013). Nuclear calcium signaling in plants. *Plant Physiol.* 163, 496–503. doi: 10.1104/pp.113.220863
- Charpentier, M., Sun, J., Vaz Martins, T., Radhakrishnan, G. V., Findlay, K., Soumpourou, E., et al. (2016). Nuclear-localized cyclic nucleotide-gated channels mediate symbiotic calcium oscillations. *Science* 352, 1102–1105. doi: 10.1126/science.aae0109
- Choi, W. G., Hilleary, R., Swanson, S. J., Kim, S. H., and Gilroy, S. (2016). Rapid, long-distance electrical and calcium signaling in plants. *Annu. Rev. Plant Biol.* 67, 287–307. doi: 10.1146/annurev-applant-043015-112130
- Clough, S. J., and Bent, A. F. (1998). Floral dip: a simplified method for *Agrobacterium*-mediated transformation of *Arabidopsis thaliana*. *Plant J.* 16, 735–743. doi: 10.1046/j.1365-313x.1998.00343.x
- Cowan, R. L., Wilson, C. J., Emson, P. C., and Heizmann, C. W. (1990). Parvalbumin-containing GABAergic interneurons in the rat neostriatum. *J. Comp. Neurol.* 302, 197–205. doi: 10.1002/cne.903020202
- Cullen, P. J., and Lockyer, P. J. (2002). Integration of calcium and Ras signalling. *Nat. Rev. Mol. Cell Biol.* 3, 339–348. doi: 10.1038/nrm808
- Davenport, R. (2002). Glutamate receptors in plants. *Ann. Bot.* 90, 549–557. doi: 10.1093/aob/mcf228
- DeFalco, T. A., Moeder, W., and Yoshioka, K. (2016). Opening the gates: insights into cyclic nucleotide-gated channel-mediated signaling. *Trends Plant Sci.* 21, 903–906. doi: 10.1016/j.tplants.2016.08.011
- Dodd, A. N., Kudla, J., and Sanders, D. (2010). The language of calcium signaling. *Annu. Rev. Plant Biol.* 61, 593–620. doi: 10.1146/annurev-applant-070109-104628
- Genre, A., Chabaud, M., Balzergue, C., Puech-Pages, V., Novero, M., Rey, T., et al. (2013). Short-chain chitin oligomers from arbuscular mycorrhizal fungi trigger nuclear  $\text{Ca}^{2+}$  spiking in *Medicago truncatula* roots and their production is enhanced by strigolactone. *New Phytol.* 198, 190–202. doi: 10.1111/nph.12146
- Hardingham, G. E., Chawla, S., Johnson, C. M., and Bading, H. (1997). Distinct functions of nuclear and cytoplasmic calcium in the control of gene expression. *Nature* 385, 260–265. doi: 10.1038/385260a0
- Harshavardhan, V. T., Van Son, L., Seiler, C., Junker, A., Weigelt-Fischer, K., Klukas, C., et al. (2014). AtRD22 and AtUSPL1, members of the plant-specific BURP domain family involved in *Arabidopsis thaliana* drought tolerance. *PLOS ONE* 9:e110065. doi: 10.1371/journal.pone.0110065
- Johnson, C. H., Knight, M. R., Kondo, T., Masson, P., Sedbrook, J., Haley, A., et al. (1995). Circadian oscillations of cytosolic and chloroplastic free calcium in plants. *Science* 269, 1863–1865. doi: 10.1126/science.7569925
- Kiegle, E., Moore, C. A., Haseloff, J., Tester, M. A., and Knight, M. R. (2000). Cell-type-specific calcium responses to drought, salt and cold in the *Arabidopsis* root. *Plant J.* 23, 267–278. doi: 10.1046/j.1365-313x.2000.00786.x
- Knight, M. R., Campbell, A. K., Smith, S. M., and Trewavas, A. J. (1991). Transgenic plant aequorin reports the effects of touch and cold-shock and elicitors on cytoplasmic calcium. *Nature* 352, 524–526. doi: 10.1038/352524a0
- Krebs, M., Held, K., Binder, A., Hashimoto, K., Den Herder, G., Parniske, M., et al. (2012). FRET-based genetically encoded sensors allow high-resolution live cell imaging of  $\text{Ca}^{2+}$  dynamics. *Plant J.* 69, 181–192. doi: 10.1111/j.1365-313X.2011.04780.x
- Kudla, J., Batistic, O., and Hashimoto, K. (2010). Calcium signals: the lead currency of plant information processing. *Plant Cell* 22, 541–563. doi: 10.1105/tpc.109.072686
- Lachaud, C., Da Silva, D., Cotelle, V., Thuleau, P., Xiong, T. C., Jauneau, A., et al. (2010). Nuclear calcium controls the apoptotic-like cell death induced by d-erythro-sphinganine in tobacco cells. *Cell Calcium* 47, 92–100. doi: 10.1016/j.ceca.2009.11.011
- Laohavisit, A., Mortimer, J. C., Demidchik, V., Coxon, K. M., Stancombe, M. A., Macpherson, N., et al. (2009). *Zea mays* annexins modulate cytosolic free  $\text{Ca}^{2+}$  and generate a  $\text{Ca}^{2+}$ -permeable conductance. *Plant Cell* 21, 479–493. doi: 10.1105/tpc.108.059550
- Lecourieux, D., Lamotte, O., Bourque, S., Wendehenne, D., Mazars, C., Ranjeva, R., et al. (2005). Proteinaceous and oligosaccharidic elicitors induce different calcium signatures in the nucleus of tobacco cells. *Cell Calcium* 38, 527–538. doi: 10.1016/j.ceca.2005.06.036
- Liang, M., Li, H., Zhou, F., Li, H., Liu, J., Hao, Y., et al. (2015). Subcellular distribution of NTL transcription factors in *Arabidopsis thaliana*. *Traffic* 16, 1062–1074. doi: 10.1111/tra.12311
- Loro, G., Drago, I., Pozzan, T., Schiavo, F. L., Zottini, M., and Costa, A. (2012). Targeting of Cameleons to various subcellular compartments reveals a strict cytoplasmic/mitochondrial  $\text{Ca}^{2+}$  handling relationship in plant cells. *Plant J.* 71, 1–13. doi: 10.1111/j.1365-313X.2012.04968.x
- Ma, G., Wei, M., He, L., Liu, C., Wu, B., Zhang, S. L., et al. (2015). Inside-out  $\text{Ca}^{2+}$  signalling prompted by STIM1 conformational switch. *Nat. Commun.* 6:7826. doi: 10.1038/ncomms8826
- Mazars, C., Briere, C., Bourque, S., and Thuleau, P. (2011). Nuclear calcium signaling: an emerging topic in plants. *Biochimie* 93, 2068–2074. doi: 10.1016/j.biochi.2011.05.039
- McAinsh, M. R., and Pittman, J. K. (2009). Shaping the calcium signature. *New Phytol.* 181, 275–294. doi: 10.1111/j.1469-8137.2008.02682.x
- Mithöfer, A., and Mazars, C. (2002). Aequorin-based measurements of intracellular  $\text{Ca}^{2+}$  signatures in plant cells. *Biol. Proced. Online* 4, 105–118. doi: 10.1251/bpo40
- Miyawaki, A., Llopis, J., Heim, R., McCaffery, J. M., Adams, J. A., Ikura, M., et al. (1997). Fluorescent indicators for  $\text{Ca}^{2+}$  based on green fluorescent proteins and calmodulin. *Nature* 388, 882–887. doi: 10.1038/42264
- Msanne, J., Lin, J., Stone, J. M., and Awada, T. (2011). Characterization of abiotic stress-responsive *Arabidopsis thaliana* RD29A and RD29B genes and evaluation of transgenes. *Planta* 234, 97–107. doi: 10.1007/s00425-011-1387-y
- Muir, S. R., and Sanders, D. (1997). Inositol 1,4,5-Trisphosphate-sensitive  $\text{Ca}^{2+}$  release across nonvacuolar membranes in cauliflower. *Plant Physiol.* 114, 1511–1521. doi: 10.1104/pp.114.4.1511
- Munns, R., and Tester, M. (2008). Mechanisms of salinity tolerance. *Annu. Rev. Plant Biol.* 59, 651–681. doi: 10.1146/annurev.applant.59.032607.092911
- Nagai, T., Yamada, S., Tominaga, T., Ichikawa, M., and Miyawaki, A. (2004). Expanded dynamic range of fluorescent indicators for  $\text{Ca}^{2+}$  by circularly permuted yellow fluorescent proteins. *Proc. Natl. Acad. Sci. U.S.A.* 101, 10554–10559. doi: 10.1073/pnas.0400417101
- Navazio, L., Mariani, P., and Sanders, D. (2001). Mobilization of  $\text{Ca}^{2+}$  by cyclic ADP-ribose from the endoplasmic reticulum of cauliflower florets. *Plant Physiol.* 125, 2129–2138. doi: 10.1104/pp.125.4.2129
- Pauly, N., Knight, M. R., Thuleau, P., Graziana, A., Muto, S., Ranjeva, R., et al. (2001). The nucleus together with the cytosol generates patterns of specific cellular calcium signatures in tobacco suspension culture cells. *Cell Calcium* 30, 413–421. doi: 10.1054/ceca.2001.0250
- Pauly, N., Knight, M. R., Thuleau, P., van der Luit, A. H., Moreau, M., Trewavas, A. J., et al. (2000). Cell signalling: control of free calcium in plant cell nuclei. *Nature* 405, 754–755. doi: 10.1038/35015671
- Peiter, E., Maathuis, F. J. M., Mills, L. N., Knight, H., Pelloux, J., Hetherington, A. M., et al. (2005). The vacuolar  $\text{Ca}^{2+}$ -activated channel TPC1 regulates germination and stomatal movement. *Nature* 434, 404–408. doi: 10.1038/nature03381
- Pusl, T., Wu, J. J., Zimmerman, T. L., Zhang, L., Ehrlich, B. E., Berchtold, M. W., et al. (2002). Epidermal growth factor-mediated activation of the ETS domain transcription factor Elk-1 requires nuclear calcium. *J. Biol. Chem.* 277, 27517–27527. doi: 10.1074/jbc.M203002200
- Reddy, A. S., Ali, G. S., Celesnik, H., and Day, I. S. (2011). Coping with stresses: roles of calcium- and calcium/calmodulin-regulated gene expression. *Plant Cell* 23, 2010–2032. doi: 10.1105/tpc.111.084988
- Rodrigues, M. A., Gomes, D. A., Leite, M. F., Grant, W., Zhang, L., Lam, W., et al. (2007). Nucleoplasmic calcium is required for cell proliferation. *J. Biol. Chem.* 282, 17061–17068. doi: 10.1074/jbc.M700490200
- Sakuma, Y., Maruyama, K., Osakabe, Y., Qin, F., Seki, M., Shinozaki, K., et al. (2006). Functional analysis of an *Arabidopsis* transcription factor, DREB2A,

- involved in drought-responsive gene expression. *Plant Cell* 18, 1292–1309. doi: 10.1105/tpc.105.035881
- Sanders, D., Brownlee, C., and Harper, J. F. (1999). Communicating with calcium. *Plant Cell* 11, 691–706. doi: 10.1105/tpc.11.4.691
- Scholz, S. S., Reichelt, M., Vadassery, J., and Mithofer, A. (2015). Calmodulin-like protein CML37 is a positive regulator of ABA during drought stress in *Arabidopsis*. *Plant Signal. Behav.* 10:e1011951. doi: 10.1080/15592324.2015.1011951
- Shavrukov, Y. (2013). Salt stress or salt shock: Which genes are we studying? *J. Exp. Bot.* 64, 119–127. doi: 10.1093/jxb/ers316
- Sieberer, B. J., Chabaud, M., Timmers, A. C., Monin, A., Fournier, J., and Barker, D. G. (2009). A nuclear-targeted cameleon demonstrates intranuclear  $\text{Ca}^{2+}$  spiking in *Medicago truncatula* root hairs in response to rhizobial nodulation factors. *Plant Physiol.* 151, 1197–1206. doi: 10.1104/pp.109.142851
- Stael, S., Wurzinger, B., Mair, A., Mehlmer, N., Vothknecht, U. C., and Teige, M. (2012). Plant organellar calcium signalling: an emerging field. *J. Exp. Bot.* 63, 1525–1542. doi: 10.1093/jxb/err394
- Tang, Q.-Y., and Zhang, C.-X. (2013). Data Processing System (DPS) software with experimental design, statistical analysis and data mining developed for use in entomological research. *Insect Sci.* 20, 254–260. doi: 10.1111/j.1744-7917.2012.01519.x
- Tang, R.-H., Han, S., Zheng, H., Cook, C. W., Choi, C. S., Woerner, T. E., et al. (2007). Coupling diurnal cytosolic  $\text{Ca}^{2+}$  oscillations to the CAS-IP3 pathway in *Arabidopsis*. *Science* 315, 1423–1426. doi: 10.1126/science.1134457
- Tolwinski, N. S., Shapiro, P. S., Goueli, S., and Ahn, N. G. (1999). Nuclear localization of mitogen-activated protein kinase kinase 1 (MKK1) is promoted by serum stimulation and G2-M progression: requirement for phosphorylation at the activation lip and signaling downstream of MKK. *J. Biol. Chem.* 274, 6168–6174. doi: 10.1074/jbc.274.10.6168
- Tracy, F. E., Gillham, M., Dodd, A. N., Webb, A. A. R., and Tester, M. (2008). NaCl-induced changes in cytosolic free  $\text{Ca}^{2+}$  in *Arabidopsis thaliana* are heterogeneous and modified by external ionic composition. *Plant Cell Environ.* 31, 1063–1073. doi: 10.1111/j.1365-3040.2008.01817.x
- Virlouvet, L., Ding, Y., Fujii, H., Avramova, Z., and Fromm, M. (2014). ABA signaling is necessary but not sufficient for RD29B transcriptional memory during successive dehydration stresses in *Arabidopsis thaliana*. *Plant J.* 79, 150–161. doi: 10.1111/tpj.12548
- Walter, A., Mazars, C., Maitrejean, M., Hopke, J., Ranjeva, R., Boland, W., et al. (2007). Structural requirements of jasmonates and synthetic analogues as inducers of  $\text{Ca}^{2+}$  signals in the nucleus and the cytosol of plant cells. *Angew. Chem. Int. Ed. Engl.* 46, 4783–4785. doi: 10.1002/anie.200604989
- Xiong, T. C., Coursol, S., Grat, S., Ranjeva, R., and Mazars, C. (2008). Sphingolipid metabolites selectively elicit increases in nuclear calcium concentration in cell suspension cultures and in isolated nuclei of tobacco. *Cell Calcium* 43, 29–37. doi: 10.1016/j.ceca.2007.02.005
- Yin, Y., Vafeados, D., Tao, Y., Yoshida, S., Asami, T., and Chory, J. (2005). A new class of transcription factors mediates brassinosteroid-regulated gene expression in *Arabidopsis*. *Cell* 120, 249–259. doi: 10.1016/j.cell.2004.11.044
- Yuan, F., Yang, H., Xue, Y., Kong, D., Ye, R., Li, C., et al. (2014). OSCA1 mediates osmotic-stress-evoked  $\text{Ca}^{2+}$  increases vital for osmosensing in *Arabidopsis*. *Nature* 514, 367–371. doi: 10.1038/nature13593
- Zal, T., and Gascoigne, N. R. (2004). Photobleaching-corrected FRET efficiency imaging of live cells. *Biophys. J.* 86, 3923–3939. doi: 10.1529/biophysj.103.022087

**Conflict of Interest Statement:** The authors declare that the research was conducted in the absence of any commercial or financial relationships that could be construed as a potential conflict of interest.

Copyright © 2017 Huang, Luo, Ning, Cao, Jin, Zhao, Wang and Han. This is an open-access article distributed under the terms of the Creative Commons Attribution License (CC BY). The use, distribution or reproduction in other forums is permitted, provided the original author(s) or licensor are credited and that the original publication in this journal is cited, in accordance with accepted academic practice. No use, distribution or reproduction is permitted which does not comply with these terms.

# Advantages of publishing in Frontiers



## OPEN ACCESS

Articles are free to read for greatest visibility and readership



## FAST PUBLICATION

Around 90 days from submission to decision



## HIGH QUALITY PEER-REVIEW

Rigorous, collaborative, and constructive peer-review



## TRANSPARENT PEER-REVIEW

Editors and reviewers acknowledged by name on published articles



## REPRODUCIBILITY OF RESEARCH

Support open data and methods to enhance research reproducibility



## DIGITAL PUBLISHING

Articles designed for optimal readership across devices



FOLLOW US  
@frontiersin



IMPACT METRICS  
Advanced article metrics track visibility across digital media



EXTENSIVE PROMOTION  
Marketing and promotion of impactful research



LOOP RESEARCH NETWORK  
Our network increases your article's readership